# Kryoimmunelektronenmikroskopische Lokalisierung synaptischer Proteine in Nervenendigungen und astrozytären Zellen

Dissertation
zur Erlangung des Doktorgrades
der Naturwissenschaften

vorgelegt beim Fachbereich Biologie
der Johann Wolfgang Goethe Universität
in Frankfurt am Main
Germany

von
Lixia ZHANG
aus Qingdao, VR China

Frankfurt am Main 2004

Vom Fachbereich Biologie der
Johann Wolfgang Goethe-Universität als Dissertation angenommen.

Dekan: Prof. Dr. B. Streit

Gutachter: Prof. Dr. H. Zimmermann
Prof. Dr. W. Volknandt

Datum der Disputation: 15.01.2004

# Cryoimmunoelectron microscopic localization of synaptic proteins in nerve terminals and astrocytic cells

Dissertation for
the degree of doctor of
Natural Sciences

Presented
to the Faculty of Biology of
the Johann Wolfgang Goethe University
Frankfurt am Main
Germany

by
Lixia ZHANG
From Qingdao, P. R. China

Frankfurt am Main 2004

Accepted as dissertation by Faculty of Biology of the Johann Wolfgang Goethe University, Frankfurt am Main, Germany

Dean: Prof. Dr. B. Streit

Referee: Prof. Dr. H. Zimmermann
Prof. Dr. W. Volknandt

Date of the Disputation: 15.01.2004

## Acknowledgement

I would like to thank Prof. Dr. Herbert Zimmermann sincerely for his agreement of the realization of my dissertation in his laboratory and, especially, for his kind guidance and valuable discussion in the research, which contribute substantially to the success of the work.

I would also present my thanks to Prof. Dr. Walter Volknandt for his great interest, helpful discussion and constant support during the course of experiments.

I thank PD Dr. Nobert Braun for his helpful advices, valuable instruction and assistance in various laboratory techniques.

I am grateful to Dipl. Biol. Markus Marxen for introducing the technique of electron microscopy, Dr Alexander Wilhelm for methods of molecular biology and cell culture, Andea Hellwig (university of Heidelberg) for the cryo-ultrathin-section technique, Dr. Sybille Winkelhaus for the LR Gold postembedding method, also to Mr. Klaus Hammer and Mr. Heinz Schewe for the helpful technical assistance.

I am greatly indebted to all the colleagues in our laboratory for their helps and supports.

Special thanks to my husband Qian for his great patience and assistance in preparation of the photographic plates and text-correction of my dissertation.

Finally, I would like to thank the Deutsche Forschungsgemeinschaft for the financing of my dissertation (SFB 474).

# Table of Contents

# Abbreviations

| | |
|---|---|
| AVP | arginine vasopressin |
| BSA | bovine serum albumin |
| CAPS | $Ca^{2+}$-dependent activator proteins |
| CNS | central nervous system |
| csps | cysteine string proteins |
| DAB | diaminobenzidine |
| DMEM | Dulbecco´s Modified Eagle Medium |
| EAA | excitatory amino acid |
| EDTA | ethylenediaminetetraacetic acid |
| EGTA | ethylene glycol bis (β-aminoethyl ether)-N,N,N´,N´-tetraacetate |
| ER | endoplasmic reticulum |
| FCS | fetal calf serum |
| FIFC | fluorescein isothiocyanate |
| GABA | γ-aminobutyric acid |
| GDI | GDP dissociation inhibitor |
| GFAP | glial fibrillary acidic protein |
| GFP | green fluorescent protein |
| HA | hemagglutinin |
| HRP | horseradish peroxidase |
| LDCV | large dense-core vesicle |
| MV | microvesicle |
| NGF | nerve growth factor |
| NMDA | N-methyl-D-aspartate |
| NSF | N-ethylmaleimide-sensitive factor |
| NSG | neurosecretory granule |
| OD | optical density |
| OT | oxytocin |
| PB | phosphate buffer |
| PBS | phosphate buffered saline |
| PVP | polyvinyl pyrrolidon |
| RFP | red fluorescent protein |
| SDS | sodium dodecyl sulfate |
| SNAP-25 | synaptosomal associated protein of 25 kDa |
| SNAPs | soluble NSF attachment proteins |
| SNARE | soluble N-ethylmaleimide-sensitive factor attachment protein receptor |
| t-SNARE | target membrane SNARE |
| v-SNARE | vesicle membrane SNARE |
| SV2 | synaptic vesicle protein 2 |
| SV | synaptic vesicle |
| TBS | tris-buffered saline |
| TGN | trans-Golgi network |
| VAMP | vesicle-associated membrane protein |
| VOCC | voltage-operated $Ca^{2+}$ channel |
| VSVG | vesicular stomatitis virus glycoprotein |

# 1. Introduction

## 1.1. Release of messenger substances from synaptic nerve terminals and neurosecretory endings

The messenger substances in nerve endings are packaged in two types of secretory vesicles. Upon stimulation, they are released via calcium-dependent regulated exocytosis. The synaptic nerve terminals are equipped with morphologically specialized release sites, the active zones. In contrast, neurosecretory endings lack active zones. A number of synaptic proteins have been identified to be involved in the regulated exocytosis.

### 1.1.1. Two primary classes of secretory vesicles

The release of messenger substances is the fundamental form of intercellular communication in the nervous system. Two primary classes of secretory vesicles, synaptic vesicles (SVs) and neurosecretory granules (NSGs), have been known to be involved in the transmission of messengers in neuronal and neuroendocrine cells (De Camilli and Jahn, 1990; Zimmermann, 1990). Synaptic vesicles in fast synapses are responsible for the fast information transfer. They are highly homogeneous in size, with an average diameter of ~50 nm. Synaptic vesicles are electron-lucent and contain some classical low-molecular weight messengers, such as glutamate, acetylcholine, glycine, and GABA. They are continuously regenerated by local exo-endocytotic recycling in nerve terminals (Regnier-Vigouroux and Huttner, 1993). By contrast, neuropeptide transmitters and hormones are packaged in larger, more heterogeneous granules. The granules possess an electron dense core and are also called large dense-core vesicles (LDCVs). They have a widespread distribution in the nervous tissue but are highly enriched in neuroendocrine cells (Thureson-Klein et al., 1986). The neurosecretory granules originate from the trans-Golgi network (TGN, Burgess and Kelly, 1987; Bauerfeind and Huttner, 1993). After exocytosis, they cannot be reloaded in the cell periphery. Their membrane constituents must ultimately return to the TGN for regeneration.

Both synaptic vesicles and neurosecretory granules release their messenger molecules via depolarization-induced, $Ca^{2+}$-dependent regulated exocytosis, but two distinct release modes occur in the nervous system. Docked synaptic vesicles release their contents extremely rapidly, within one millisecond of the influx of calcium (Sabatini and Regehr, 1996). However, the latency for exocytosis of peptides is much higher (Leenders et al., 2002; Martin,

1994; Thomas et al., 1993). High frequency of stimulation favors peptide secretion (Jahn et al., 1990). The ratio of LDCVs/SVs increases with the enhancement of stimulation frequency. Remarkably, the types and the regulation of $Ca^{2+}$ channels and the $Ca^{2+}$ dependence of synaptic vesicle secretion differ clearly from those of the neurosecretory granules. A localized submembranous $Ca^{2+}$ increase is much more effective in evoking release of synaptic vesicles. The local increase in the $Ca^{2+}$ concentration at the active zone from the basal level of 100-200 mM results in the release of docked synaptic vesicles (Mochida, 2000). In contrast, uniform elevation of $Ca^{2+}$ favors predominantly granule release (Burgoyne, 1991; Verhage et al., 1991). Moreover, the neurotransmitter release is directly regulated by the different $Ca^{2+}$ channel types, whereas the cooperativity of multiple $Ca^{2+}$ channels in raising the intracellular $Ca^{2+}$ concentration above release threshold appears to be required for the release regulation of secretory granules (Leenders et al., 1999). Correspondingly, the release site for synaptic vesicles and granules is obviously different. The exocytosis of the synaptic vesicles occurs only at the active zones, the specialized release site of the presynaptic plasma membrane. By contrast, the exocytosis of peptide-containing secretory granules appears to take place laterally to the active zone (Thureson-Klein and Klein, 1990), more widely at nerve terminals and dendrites (Zhu et al., 1986; Morris and Pow, 1988). Evidently, the exocytosis process of these two types of secretory vesicles is differentially controlled (Mochida et al., 1998; Leenders et al., 1999; De Camilli and Jahn, 1990; Zimmermann, 1997).

### 1.1.2. Synaptic proteins in the regulated exocytosis of synaptic vesicles

In the central nervous system, the presynaptic terminals of the fast synapses are filled predominantly with numerous small electron-lucent synaptic vesicles and a few larger electron dense granules. Synaptic vesicles are organized into two distinct functional pools, a large reserve pool and a quantitatively smaller releasable pool (Pieribone et al., 1995; Kuromi and Kidokoro, 1998). The releasable vesicles approach the active zone, where they are eventually released through fusion with the membrane upon stimulation. The less abundant granules have a more diffuse distribution in the neuronal cytoplasm. They release their contents preferentially lateral to the active zones (Zhu et al., 1986). The release of the fast-acting low-molecular weight neurotransmitter from small synaptic vesicles is the main characteristics of fast synapse. It depends on the coordinated action of many relative proteins(Jahn et al., 2003)**.** A number of the synaptic proteins have been found to play a crucial role in the regulated exocytosis of the synaptic vesicles.

**SNARE hypothesis and the relative proteins**

The synaptic vesicle cycle at the nerve terminals consists of a number of distinct steps, including the vesicle release from reserve pool, targeting to the active zone, docking, priming, exocytosis and endocytotic retrieval of synaptic vesicles (Sudhof, 1995; Benfenati et al., 1999). Among them, the exocytosis via membrane fusion is the key event. It has been known that the molecular mechanism for vesicular exocytosis is conserved in all eukaryotic organisms ranging from yeast to human (Morgan, 1995; Ferro-Novick and Jahn, 1994; Bennett and Scheller, 1993). A number of proteins that are involved in vesicle docking and fusion have been identified. The attractive SNARE (soluble N-ethylmaleimide-sensitive factor attachment protein receptor) hypothesis has been proposed to derive a generalized model for the regulation of vesicle exocytosis (Sollner et al., 1993a; Rothman, 1994a). The family of SNARE proteins whose members are found either on the target membranes, the t-SNARES, or on vesicles, the v-SNAREs, is considered to provide the primary apparatus necessary for vesicle exocytosis. They are distinguished by the SNARE motif, heptad repeats of 60-70 amino acids (Jahn and Sudhof, 1999; Jahn et al., 2003; Rizo and Sudhof, 2002). In mammalian brain the 18 kDa vesicle-associated membrane protein (VAMP II, also known as synaptobrevin II), the major v-SNARE, combines specifically at the synaptic active zone with the plasma membrane proteins syntaxin I (35 kDa) and synaptosomal associated protein (25 kDa, SNAP-25), the major t-SNAREs, to form a 7S core complex between the opposing vesicle membrane and the plasma membrane (Sollner et al., 1993b). VAMP II and syntaxin I are C-terminally anchored integral membrane proteins. To the contrary, the plasma membrane protein SNAP-25 does not contain transmembrane domains, but associates with the plasma membrane via palmitoylation on cysteine residues at the center of the protein (Zheng and Bobich, 1998). Structural analyses showed that the α-helical regions corresponding to the SNARE motifs of the v- and t-SNAREs assemble into four-stranded helical bundles that span opposing membranes, to which VAMP II and syntaxin I contribute one α-helix, respectively, but SNAP-25 provides two helices (Sutton et al., 1998; Fasshauer et al., 1998). Three SNARE proteins bind in parallel within the core complex that brings the membranes into very close contact (Hanson et al., 1997; Lin and Scheller, 1997; Poirier et al., 1998). The intermolecular interactions via coiled-coil structures were thought to be involved in complex formation (Chapman et al., 1994; Fasshauer et al., 1997a). This complex is very stable. It is resistant to heat (Fasshauer et al., 1997b) and sodium dodecyl sulfate (SDS), the denaturing detergent (Hayashi et al., 1994a; Pellegrini et al., 1995). Formation of this extremely stable trans

(opposing membranes) SNARE complex brings the synaptic vesicles and cell membrane into close opposition and presumably provides the essential driving force for membrane fusion (Jahn and Sudhof, 1999; Robinson and Martin, 1998; Fasshauer et al., 2002).

The functional involvement of the SNARE proteins VAMP II, SNAP-25 and syntaxin I in regulated exocytosis is evidenced strongly by the observation that they are substrates of some neurotoxin proteases (Rossetto et al., 2001; Montecucco and Schiavo, 1995; Link et al., 1994). These neurotoxins are produced by anaerobic bacteria of genus *Clostridium*, including tetanus toxin (TeTx, with one single type) and the bolulinum neurotoxins (with seven distinct types, designated BoNT/A to BoNT/G). VAMP II is known to be cleaved by tetanus toxin and the botulinum toxins B, D, F and G. SNAP-25 is the target of botulinum toxins A and E. Syntaxin I is cleaved by botulinum toxin C (Ahnert-Hilger and Bigalke, 1995; Montecucco et al., 1996; Schiavo et al., 2000). All of these toxins are the severe inhibitors of neural transmission. Although the poisoned presynaptic nerve terminals reveal no morphological injury and the synaptic vesicles still appear docked to the presynaptic membrane (Pallanck et al., 1995; Sudhof, 1995), the selective proteolysis of these toxins prevents the assembly of the core complex and results in a blockade of vesicle exocytosis. This implies that the assembly of the core complex is essential for membrane fusion (Jahn and Sudhof, 1999; Rizo and Sudhof, 2002).

Although the core complex resists dissociation by SDS denaturation and clostridial neurotoxin cleavage (Hayashi et al., 1994a; Pellegrini et al., 1994), it can be disassembled by the ATPase NSF (N-ethylmaleimide-sensitive factor) together with its adaptor proteins SNAPs (Hayashi et al., 1995; soluble NSF attachment proteins, Sollner et al., 1993a). The NSF and SNAPs are two structurally and functionally conserved proteins in the evolution of eukaryotic cells (Jahn and Sudhof, 1999). The formation of the SNARE complex provides a high affinity binding site for α-SNAP (McMahon and Sudhof, 1995), which in turn forms a NSF binding site. The 7S SNARE complex recruits NSF and SNAPs from the cytoplasm to form so-called 20S particles (Hanson et al., 1997). The ATPase activity of NSF is stimulated upon binding to α-SNAP (Barnard et al., 1997). NSF dissociates the SNARE complex under ATP hydrolysis. Then the components of the complex can participate in another round of membrane fusion. However, although the SNARE proteins VAMP II, SNAP-25 and syntaxin I have been demonstrated to be essential components of the neurotransmitter release process and the assembly and disassembly of the core complex tightly associated with membrane fusion, the precise mechanism remains to be further elucidated.

Except for participating in the formation of the core complex, SNARE proteins are also found to interact with the other proteins in the nerve terminals that may play a regulatory role in SNARE function. The bindings of synaptophysin, a 38 kDa synaptic vesicle protein, to VAMP II (Edelmann et al., 1995), the ATPase Hrs-2 to SNAP-25 (Bean et al., 1997; Bean et al., 1997; Tsujimoto and Bean, 2000) as well as the mammalian neuronal proteins munc-18 and munc-13 to syntaxin I (Hata et al., 1993; Betz et al., 1997; Margittai et al., 2003; Yang et al., 2000) have been proposed to prevent inappropriate formation of docking and fusion complex before docking. Munc-18 has recently been found to be essential factors for membrane fusion (Gallwitz and Jahn, 2003; Jahn et al., 2003; Toonen and Verhage, 2003). In addition, the SNARE complex can also interact with the 65-kDa vesicle-associated protein synaptotagmin I that is displaced by α-SNAP during the disassembly of the core complex (Sollner et al., 1993a). Synaptotagmin I is thought to function as a calcium sensor and a fusion clamp, preventing the release of neurotransmitter from docked vesicles in the absence of a signal (Sollner et al., 1993a; Volknandt, 1995). The hydrophilic complexins compete with α-SNAP, but not with synaptotagmin I, for binding to the core complex (McMahon et al., 1995; Pabst et al., 2000). Complexins stabilize the fully assembled SNARE complex and modulate neuroexocytosis (Chen et al., 2002; Rizo and Sudhof, 2002; Pabst et al., 2002). Thus, by regulating assembly or disassembly of the SNARE complex these proteins play essential roles in synaptic vesicle exocytosis.

## SV2 - an abundant vesicle-associated protein

Synaptic vesicle protein 2 (SV2), a widespread membrane glycoprotein in neurons and endocrine cells, is specifically integral to the synaptic vesicle membrane but does not participate in the SNARE complex. SV2 is expressed in two major isoforms, SV2A and SV2B, and one minor isoform SV2C with a restricted cellular distribution (Janz and Sudhof, 1999; Bajjalieh et al., 1994). As a ubiquitous vesicle protein, SV2 is used extensively as a general marker for the synaptic vesicles (Volknandt, 1995). SV2 contains 12 transmembrane domains: Its six N-terminal and six C-terminal transmembrane domains are highly homologous to glucose and neurotransmitter transporters in the plasma membrane (Feany et al., 1992; Bajjalieh et al., 1992). However, despite its homology to transporter proteins, the function of SV2 remains to be established. A $Ca^{2+}$-regulated direct interaction between SV2A and synaptotagmin has been reported (Schivell et al., 1996). Recently, it has been revealed by electrophysiological studies that SV2s are probably $Ca^{2+}$ dependent inhibitors of neurotransmitter release. They function as redundant $Ca^{2+}$ regulators in neurotransmitter

release (Janz et al., 1999). However, by direct measuring the exocytosis in adrenal chromaffin cells, it has also been proposed recently that SV2 is required to modulate the readily releasable pool of secretory vesicles. Loss of SV2A has been found to be associated with fewer SDS-resistant SNARE complexes. SV2 may modulate directly the formation of fusion complexes (Xu and Bajjalieh, 2001).

**The role of Rab3A in the regulation of neurotransmitter release**

Rab3A belongs to the family of the small GTP-binding Rab proteins (20-25kDa). Members of the Rab family have a distinct subcellular localization among various cellular compartments (Jahn and Sudhof, 1999; Simons and Zerial, 1993; Olkkonen and Stenmark, 1997). They play important roles in vesicle transport, tethering with target membranes and exocytosis (Zerial and McBride, 2001; Novick and Zerial, 1997; Schimmoller et al., 1998; Jahn et al., 2003). Although they are not involved in the components of the core complex, Rab proteins are considered to function in facilitating the formation of SNARE complexes (Sogaard et al., 1994; Schimmoller et al., 1998) and modulate the activity of SNAREs (Novick and Zerial, 1997; Johannes et al., 1996).

The Rab3 subfamily comprises Rab3A-D. Rab3A is the most abundant Rab protein in the brain and play an essential role in the regulation of neurotransmitter release (Fischer et al., 1990). As the other Rab proteins, Rab3A is able to cycle between the active GTP-bound Rab3A on the membrane and the inactive GDP-bound form in the cytoplasm. This process is controlled by the specific regulatory protein GDP dissociation inhibitor (GDI, Chou and Jahn, 2000; Ullrich et al., 1993; Pfeffer, 1994). The cycle of Rab3A is closely linked to the recycling of synaptic vesicles. Triggering of synaptic vesicle exocytosis leads to the dissociation of Rab3A from synaptic vesicles and dramatically increases the GDP/GTP ratio of Rab3A (Fischer et al., 1991; Stahl et al., 1994; Fischer et al., 1994a). Rab3A is thought to to play a role in the recruitment of synaptic vesicles for exocytosis (Geppert et al., 1994). In addition, there is also evidence that Rab3A acts as a negative modulator of exocytosis and limits the extent of $Ca^{2+}$-triggered vesicle fusion (Johannes et al., 1994; Holz et al., 1994; Lledo et al., 1994). Recently, a post-docking role for Rab3A has been proposed. Rab3A has been shown to regulate a late step in exocytosis, associated with the fusion reaction (Schluter et al., 2002; Geppert et al., 1997; Geppert and Sudhof, 1998). The GTP-bound form of Rab3 interacts with at least two effector proteins, Rabphilin and Rim (Bean and Scheller, 1997). Rabphilin is a vesicle-associated protein (Mizoguchi et al., 1994) which is recruited to synaptic vesicles by Rab3A and is dissociated from synaptic vesicles after GTP hydrolysis

(Stahl et al., 1996; McKiernan et al., 1996; Li et al., 1994). Rabphilin has been revealed to have a positive effect on secretion (Chung et al., 1995). Rim proteins exclusively localize to the presynaptic active zones in synapses (Wang et al., 1997b). The interaction between Rim and Rab3A occurs only when synaptic vesicles approach the presynaptic membrane which can play an important role in maintaining docking specificity (Zheng and Bobich, 1998; Benfenati et al., 1999). In addition, recent study has indicated that Rab3A also has a classical transport role in the trafficking of synaptic vesicles to their target at the active zone in mouse brain nerve terminals (Leenders et al., 2001).

**Participation of N-type and P/Q-type $Ca^{2+}$ channels in fast neurotransmitter release**

Exocytosis in synaptic nerve terminals is rapidly triggered by the influx of $Ca^{2+}$ through voltage-operated $Ca^{2+}$ channels (Trimble et al., 1991; VOCC, Zimmermann, 1990). Neural $Ca^{2+}$ channels are heteromeric proteins constituted by a α1 subunit, which forms the transmembrane ion-conducting pore. Depolarization of the nerve terminal by an action potential results in the opening of VOCC. By controlling the entry of $Ca^{2+}$ necessary for exocytosis, $Ca^{2+}$ channels can regulate excitation-secretion coupling. Under physiological conditions, multiple types of $Ca^{2+}$ channels with different biophysical and pharmacological properties are involved in the regulation of neurotransmitter release in the mammalian central nervous system (Dunlap et al., 1995). Different $Ca^{2+}$ channel subtypes serve distinct roles in neuronal excitation and transmission of signals (Elliott et al., 1995). The presence of various types of $Ca^{2+}$ channels in different regulatory sites would permit a high degree of flexibility of regulation under diverse conditions of stimulation and modulation (Turner et al., 1993). N- and P/Q-type $Ca^{2+}$ channels, containing the pore-forming α1B or α1A subunits, respectively, are preferentially coupled to the exocytosis of rapid neurotransmitters in fast synapses. Pharmacological evidence suggests that N-type $Ca^{2+}$ channels are selectively blocked by the marine snail-derived toxins ω-conotoxin GVIA or MVIIA (Ellinor et al., 1994; Woppmann et al., 1994). P/Q-type $Ca^{2+}$ channels are inhibited by ω-conotoxin MVIIC and spider toxin ω-agatoxin IVA (Takahashi and Momiyama, 1993; Sather et al., 1993; Stea et al., 1994).

The short latency between $Ca^{2+}$ influx and exocytosis of synaptic vesicles in fast synapses suggests that $Ca^{2+}$ channels are positioned in close proximity to the synaptic release sites (Goda and Sudhof, 1997; Llinas et al., 1992). Furthermore, biochemical experiments demonstrate that $Ca^{2+}$ channels are closely associated with the exocytotic apparatus at synaptic terminals (Seagar and Takahashi, 1998; Martin-Moutot et al., 1996; Rettig et al., 1996). Both N- and P/Q-type $Ca^{2+}$ channels have been purified from brain with SNARE

proteins as a stable complex (Sheng et al., 1998; Martin-Moutot et al., 1996). This assures the exposure of the docking complex to inflowing extracellular $Ca^{2+}$. Moreover, at the molecular level N- or P/Q-type $Ca^{2+}$ channels have been revealed to bind directly to syntaxin I, SNAP-25, and synaptotagmin I through a synaptic protein interaction (synprint) site in the intracellular loop domains II and III of both the α1B and α1A subunits (Sheng et al., 1994; Kim and Catterall, 1997). By altering SNARE protein function, the interaction of the synprint site of N-type $Ca^{2+}$ channels with SNARE proteins has been demonstrated to enhance neurotransmitter release (Mochida et al., 1998). In addition, this interaction also contributes to excitation-secretion coupling by optimally locating the calcium sensors to allow a close temporal relationship between $Ca^{2+}$ influx and evoked release. On the other hand, direct interactions between $Ca^{2+}$ channel proteins and the exocytic machinery may have important effects on the behavior of the presynaptic $Ca^{2+}$ channels themselves by regulating their function in response to depolarization. Therefore, $Ca^{2+}$ channels play a crucial role in the nerve terminal, not only by mediating the entry of calcium across the plasma membrane to initiate transmitter release but also by providing structural elements that are integral to vesicle release processes (Sheng et al., 1998; Stanley, 1997).

**The active zone and the related protein Bassoon**

The active zone in the presynaptic nerve terminals constitutes the principal site for regulated neurotransmitter release from nerve cells (Landis et al., 1988; Zhai et al., 2001). It is the specialized region of the presynaptic plasma membrane situated exactly opposite to the postsynaptic neurotransmitter reception apparatus (Hirokawa et al., 1989). At the active zone, a small pool of synaptic vesicles docks and fuses with the presynaptic plasma membrane in a highly coordinated way (Betz and Angleson, 1998; Dresbach et al., 2001). The active zone material has been thought to help the docking of the vesicles and the anchoring of the channels (Harlow et al., 2001; Burns and Augustine, 1995). At the ultrastructural level, it has been recognized that the presynaptic active zone carries highly organized electron dense structures on the cytoplasmic side of the presynaptic membrane (Gray and Guillery, 1966; Pfenninger et al., 1969). Moreover, a regularly arranged hexagonal array is located at the active zone plasma membrane that is referred to as the presynaptic dense projection (Peters et al., 1991; Akert, 1972; Pfenninger et al., 1972). Until now, its protein composition is essentially unknown. However, this structure plays a critical role in synaptic vesicle attachment and the release of the neurotransmitters (Zimmermann, 1993).

Bassoon has recently been identified as a novel 420-kDa protein of the presynaptic nerve terminals (tom et al., 1998). It was found extensively in both excitatory glutamatergic synapses and inhibitory GABAergic synapses throughout the brain (Richter et al., 1999). Strikingly, Bassoon has a very restricted distribution, mainly interspersing between clear synaptic vesicles in the vicinity of the active zone (tom et al., 1998). Biochemical studies suggest that it has a tight association with the cytomatrix. Thus, as a scaffold protein of the presynaptic cytomatrix at the active zone, Bassoon may play a fundamental role in neurotransmitter release and therefore potentially be involved in the regulation of the synaptic vesicle cycle (Gundelfinger and tom, 2000; Dresbach et al., 2001).

### 1.1.3. Secretion of messenger substances in neurosecretory endings of the neurohypophysis

Like all other terminals, the neurosecretory endings of the neurohypophysis contain two types of vesicular organelles. However, in contrast to fast synapses, a large number of electron dense neurosecretory granules occurs in the neurohypophysis (Russell, 1981). These granules, with a diameter of 150-230 nm, contain arginine vasopressin (AVP) or oxytocin (OT) (Van Leeuwen and Swaab, 1977) that are secreted directly into the blood stream (Morris et al., 1978). In addition, there is a considerable number of electron-lucent microvesicles (MVs) among the granule populations (Tweedle, 1983). These microvesicles are ~50 nm in diameter and indistinguishable in morphology from synaptic vesicles. Under normal physiological conditions, microvesicles segregate into a morphologically separate population from the granules. Short linking strands of 30-60 nm are found specifically between microvesicles that make them clustered to each other (Hayashi et al., 1994b).

So far, little is known concerning the role of the microvesicles in the neurohypophysis. Microvesicles were first postulated to be vesicles formed during membrane recycling of neurosecretory granules (Douglas et al., 1971; Nagasawa et al., 1971). Later, it was evidenced that they were functionally independent of the neurosecretory granules and under high potassium stimulation they were redistributed towards the plasma membrane facing the basal lamina (Morris and Nordmann, 1980). Moreover, after electrical stimulation microvesicles showed a scattered distribution over the neurosecretory terminals and some labels of synaptophysin were found near the plasma membrane (Hayashi et al., 1994b). This implied that microvesicles might perform regulated exocytosis upon stimulation. Microvesicles were revealed to be able to store glutamate (Meeker et al., 1991) as well as norepinephrine

(Moriyama et al., 1995). Furthermore, many synaptic vesicle proteins have been demonstrated to be associated with microvesicles (Navone et al., 1989; Jurgutis et al., 1996). Recently, it has been demonstrated by capacitance measurements that microvesicles can undergo $Ca^{2+}$-triggered exocytosis in response to membrane depolarization in the neurohypophysis (Klyachko and Jackson, 2002).

The terminals of the neurohypophysis possess no structurally defined release sites. However, similar to the secretion of peptides from typical synapses, the release of the neurohypophysial hormones vasopressin and oxytocin from the granules into the blood stream has been known to be also $Ca^{2+}$-dependent and to require enhanced axonal action potentials (Legendre and Poulain, 1992). The release process is much slower, reflecting the integration of $Ca^{2+}$ influx over many action potentials. Patch-clamp experiments in isolated neurohypophysial terminals have identified multiple types of $Ca^{2+}$ channels, containing N-, L-, P/Q- and R-type $Ca^{2+}$ channels (Fisher and Bourque, 1995; Wang et al., 1997a; Wang et al., 1999). It has been revealed that N- and L- type $Ca^{2+}$ channels may control the secretion of both vasopressin and oxytocin (Wang et al., 1993; Wang et al., 1999). The N-type $Ca^{2+}$ channel blocker ω-conotoxin GVIA is able to block 50-70% of electrically evoked release (Obaid et al., 1989). P/Q- and R-type $Ca^{2+}$ channels appear to be selectively involved in vasopressin and oxytocin release, respectively (Wang et al., 1997a; Wang et al., 1999). Up to now, little is known about the exocytosis of microvesicles.

## 1.2. Release of messenger substances from astrocytes

In the mammalian central nervous system (CNS), the neurons are surrounded by a 10-fold higher number of glial cells. According to the classical view of the nervous system, glial cells are incapable of conducting action potentials and have only an inferior role in neural cell function, in that they support the physiology of associated neurons. However, in the recent years, it has been shown that glial cells are dynamic and have more complicated functions in intercellular signaling processes of the nervous system.

### 1.2.1. Involvement of astrocytes in the synaptic transmission

Astrocytes represent a major sub-type of glial cell. They make up nearly forty percent of the cell composition of the total CNS and fill most of the spaces between neurons. They are intimately associated with neurons in the brain to form a connected network. Their processes intermingle with neuronal processes and closely enwrap the synapses. It has been well

established that astrocytes serve multiple homeostatic function in the brain including maintaining extracelluar pH and ionic composition at a low physiological level, taking up and degrading neurotransmitters that are released from neurons into the extracellular space, such as excitatory amino acids (EAAs) glutamate and aspartate. They were thought to be responsible mainly for maintenance of an ideal environment for neural cell function and for regulation of interactions among neurons or between neurons and the blood stream.

However, more recently increasing evidence suggests that astrocytes are able to actively participate in the processing of brain information other than simply providing structural, metabolic and trophic support (Araque et al., 2001; Haydon, 2001; Bezzi and Volterra, 2001; Volknandt, 2002). The proximity to neuronal synapses makes them in an advantageous position to receive the released neurotransmitters from the synaptic cleft. Astrocytes have been indicated to possess not only a number of transporters for the neurotransmitters, but also voltage-gated ionic channels (Carmignoto, 2000; Latour et al., 2003) and a variety of membrane receptors for different classical neurotransmitter substances and peptides, such as receptors for glutamate, ATP, GABA, noradrenaline, or neuropeptides (Porter and McCarthy, 1997). Their membrane-bound receptors can be activated during synaptic activity. Astrocytes have been reported to be able to respond directly to various synaptically released neurotransmitters, leading to an increase of their intracellular $Ca^{2+}$ concentration.

Astrocytes have been indicated to be able to synthesize and release many neuroactive substances containing different neurotransmitters, neuropeptides and growth factors. $Ca^{2+}$ elevation in astrocytes has been demonstrated to lead to receptor-mediated release of these signaling substances, for example, the release of glutamate and aspartate by the neuroligand bradykinin or by glutamate receptor agonists (Parpura et al., 1994; Bezzi et al., 1998; Jeftinija et al., 1996), of ATP by glutamate receptor agonists (Queiroz et al., 1999) and of secretogranin II, a typical marker for regulated secretory granules, by several secretagogues (Calegari et al., 1999). Similar to neurons, astrocytes contain a dual secretory pathway for the release of both the low molecular substances and the peptide constituents (Volknandt et al., 2002).

Interestingly, the released messenger substances from astrocytes can in turn act as a signaling substance and feedback to the surrounding neurons to produce functional changes. Studies performed in both cell culture and isolated hippocampal slices in situ (Bezzi et al., 1998; Parpura et al., 1994; Bezzi et al., 1998) have indicated that a $Ca^{2+}$-dependent glutamate-release pathway from astrocytes can signal to neighbouring neurons to elevate their

intracellular $Ca^{2+}$ levels and modulate neuronal activity. In addition, GABA has also been revealed to be able to enhance $Ca^{2+}$ levels in astrocytes and start back signaling to neurons (Kang et al., 1998). Therefore, a continuous bi-directional signal communications between neurons and astrocytes takes place during synaptic activity (Vesce et al., 1999; Carmignoto, 2000). Furthermore, recent experiments have also demonstrated the presence of an astrocyte-to-astrocyte signaling system through the astrocyte network. The neuron-induced elevation of $Ca^{2+}$ levels in astrocytes can spread as astrocytic excitation to adjacent astrocytes in the form of slow $Ca^{2+}$ waves which are likely to be mediated by the release ATP from astrocytes (Haydon, 2001; Guthrie et al., 1999; Cotrina et al., 1998). Moreover, a distal response away from the original stimulus is generated by affecting synapses located at a distance, leading to lateral signal transfer between synapses. Thus, by way of an astrocytic propagating circuit of $Ca^{2+}$ wave, astrocytes may communicate extensively with neurons. Evidently, through the $Ca^{2+}$-dependent transmitter release, astrocytes play an active role in regulating neuronal activity and in modulating synaptic transmission, which provide the additional spatial and temporal complexity in the information processing in the brain and should have significant effects on the function of the nervous system.

### 1.2.2. Regulated exocytosis as the possible astrocytic release pathway

Up to now, little is known about the underlying molecular mechanisms responsible for this receptor-mediated astrocytic messenger release. It has been evidenced that the cellular release of glutamate from astrocytes is not mediated by the reverse operation of glutamate transporters, because transport inhibitors fail to affect $Ca^{2+}$-dependent glutamate release (Araque et al., 2000). Astrocytes have been reported to have a developed endocytic vesicular system that is mainly composed of caveolae, clathrin-coated pits and vesicles, a variety of endosomal structures and lysosome (Megias et al., 2000). Proliferating astrocytes reveal a large number of vacuoles and vesicles of different size and shape (Lindo et al., 1993). Despite the fact that astrocytes neither exhibit a large number of small clustered vesicles nor form apparent synapses with special organized release site as neural cells do, there is increasing evidence demonstrating that the astrocytic release process of messenger substance shares some common properties with the neurotransmitter release from synaptic terminals as given in the following:

At first, similar to the neuronal exocytosis, the cellular release of low molecular glutamate and the secretory granule protein secretogranin II from cultured astrocytes has been indicated

to occur in a $Ca^{2+}$-dependent manner (Calegari et al., 1999; Parpura et al., 1994). Moreover, it has been recently shown that the $Ca^{2+}$-regulated astrocytic glutamate release pathway is engaged at physiological $Ca^{2+}$ levels (Parpura and Haydon, 2000).

In addition, it has been demonstrated in various experiments that the released messenger substances from astrocytes are probably stored in a vesicular compartment and that a vesicular exocytotic pathway underlies $Ca^{2+}$-dependent release: 1) In the presence of extracellular calcium, the vertebrate neurotoxin α-latrotoxin was found to cause sustained release of glutamate from cultured astrocytes (Parpura et al., 1995b). α-Latrotoxin is an active component of black widow spider venom and has been known to induce massive vesicle exocytosis of transmitters from nerve terminals (Petrenko et al., 1991). 2) Bafilomicin A1, a well-known vacuolar ATPase inhibitor, was indicated to reduce the release of glutamate from astrocytes by dissipating a vesicular electrochemical proton gradient necessary for transmitter uptake into vesicles (Araque et al., 2000). 3) At the ultrastructural level the granule protein secretogrnin II was found to be stored in dense core vesicles and released in response to secretagogues (Calegari et al., 1999).

Moreover, the release of messenger substances in astrocytes has been shown to be impaired by some clostridial neurotoxins that cleave specific protein components of the synaptic vesicle fusion machinery, just as their blocking function in neurons. Botulinum toxin B and tetanus neurotoxin, which selectively cleave the v-SNARE VAMP II and thereby block exocytosis in neurons, result in a decrease in VAMP II immunoreactivity and abolish $Ca^{2+}$-dependent bradykinin-induced glutamate release in astrocytes (Jeftinija et al., 1997). Botulinum B has also been demonstrated to inhibit strongly the astrocyte-induced glutamate response in neurons (Araque et al., 2000); Pretreatment of astrocytes with botulinum neurotoxin A and C, which cleave t-SNARE SNAP-25 and syntaxin I in neurons, respectively, diminish or abolish bradykinin-induced release of glutamate from astrocytes (Jeftinija et al., 1997). Additionally, tetanus toxin and botulinum toxins were found to cleave the ubiquitous v-SNARE cellubrevin, a homologue of synaptobrevin in astrocytes (Parpura et al., 1995a; Verderio et al., 1999). These results implicate that SNARE proteins are involved in the $Ca^{2+}$-dependent astrocytic release process of messenger substances.

Cultured astrocytes were also found to express some members of the SNARE proteins such as the v-SNAREs VAMP II and cellubrevin, and the t-SNAREs syntaxin I (Parpura et al., 1995a) and SNAP-23, a analogue of the neuronal SNAP-25 (Hepp et al., 1999). In our laboratory, a variety of other synaptic proteins were identified in primary astrocyte cultures

from cerebral cortices of newborn rats (Maienschein et al., 1999). They are the synaptic vesicle proteins SV2, synaptophysin, synaptotagmin I, synapsin I, Rab3A, and the t-SNARE SNAP-25. Thus, almost all of the proteins thought to be essential for the synaptic transmission have been identified in cultured astrocytes.

In conclusion, a large body of experimental work implicates that astrocytes may release their messenger substances in a similar way as neurons. Moreover, the SNARE protein-regulated vesicular exocytosis is probably involved also in the astrocytic secretory process.

## 1.3. Aims of the study

### 1.3.1. Localization of synaptic proteins in the hippocampal mossy fiber terminals and the neurohypophysial endings

Although members of the SNARE family have been implicated in the process of vesicle docking and fusion by means of a combination of genetic and biochemical approaches, strong morphological evidence for a preferential association of SNARE proteins with release sites at synapses in situ is lacking. In addition, even though numbers of proteins that are involved in synaptic vesicle exocytosis have been identified, the accurate molecular mechanism restricting the fusion of synaptic vesicles to the active zone remains unclear. The function of the proteins is dependent on their precise subcellular localization. Elucidation of the ultrastructural localization of these proteins should provide invaluable information for a thorough understanding of their roles in vesicular exocytosis.

In the present study, using the immunogold labeling method on frozen ultrathin sections, the localization of SNARE and other exocytosis-relevant synaptic proteins would be investigated in two different types of nerve terminals. One is the identifiable type of central synapse, the mossy fiber synapse with multiple special release sites in the hippocampal CA3 subfield; the other is the neurosecretory endings of the neurohypophysis that are not provided with special release sites. The purpose is to compare the distribution of synaptic proteins in two different types of nerve terminals and particularly to address the question whether SNARE proteins are preferentially associated with active zones in fast synapses and to what extent the localization of these proteins in terminals lacking defined release sites is different from that in synaptic terminals.

### 1.3.2. Localization of synaptic proteins in primary astrocyte culture

A large number of data have indicated that astrocytes may release messenger substance using a mechanism resembling the neuronal secretory process. The regulated vesicular exocytosis and, especially, the classical SNARE mechanism are probably involved in their secretory process. However, alternative hypotheses for this $Ca^{2+}$-dependent release way cannot be rule out. Further studies are required to elucidate thoroughly the molecular mechanism in this process. Ultrastructural studies can exhibit the precise localization of the proteins responsible for regulated exocytosis at their functional site, providing further evidence for biochemical and physiological studies. The aim of the present study is to investigate the subcellular localization of synaptic proteins on the endogenous vesicular organelles and the stimulation-induced endocytotic compartments using electron microscopy, so as to verify their function in the astrocytic vesicle cycle.

### 1.3.3. Expression and localization of the transfected synaptic proteins in the astrocytoma cell line U373 MG

In the studies of regulated exo- and endocytosis of neural cells the rat pheochromocytoma-derived PC12 cell line has been evidenced to be a very effective experimental tool. Obviously, a permanent cell line with astrocytic secretory properties would play an important role in the investigation of the molecular mechanisms of astrocytic messenger release. The cell line U373 MG derives from a human astrocytoma. It was revealed to express glial fibrillary acidic protein (GFAP), the most specific marker for cells of astrocytic origin, and has been widely applied in a variety of studies of astrocytic functional properties. Interestingly, U373 has also been shown to be able to release nerve growth factor NGF (Emmett et al., 1997), glutamate (Ye and Sontheimer, 1999) and GABA (Soria-Jasso and Arias-Montano, 1996). However, it remains unknown whether the secretion of these substances in U373 MG possess the same characteristic as that in astrocytes, and particularly, whether regulated vesicular exocytosis is also involved in the secretory processes of U373 MG as in astrocytes and neurons.

To clarify the secretory characteristics of permanent U373 cells and to determine whether the U373 MG cell line can be used as an effective experimental tool for further studies of the astrocytic exocytosis mechanism, this part of the study focused on the expression and localization of several important proteins responsible for regulated exocytosis and intercellular membrane fusion in U373 cells. Multiple engineered constructs coding for these

proteins as well as relevant additional tags would be transiently transfected into these cells and the expressed recombinant proteins would be immunolocalized by means of fluorescence and cryo-electron microscopy.

# 2. Materials and Methods

## 2.1. Localization of synaptic proteins in the hippocampus and neurohypophysis using the cryo-immunogold technique

In the present study, an improved cryo-immunogold technique, which combines the Tokuyasu thawed cryosection technique (Tokuyasu, 1973) with the immunogold method, was adapted to localize various synaptic proteins in mossy fiber terminals of the hippocampus and neurosecretory endings of the neurohypophysis. With the aid of the cryo-protectant and the special contrasting and drying method, the Tokuyasu thawed cryosection technique has been demonstrated as a excellent method for preservation of the ultrastructural details and high resolution of the fine structure. Moreover, cryosections prepared according to this technique have been evidenced to be a good substrate for immunolabeling (Griffiths et al., 1984).

### 2.1.1. Experimental animals and perfusion fixation

Adult wistar rats (Charles River, Sulzfeld Germany) between 200 g and 300 g in body weight were used for the experiments. They were anaesthetized lightly by inhalation of $CO_2$, then injected with Nembutal (60 mg/kg) intraperitoneally. After several minutes, when animals were deeply anaesthetized, transcardial perfusion that ensured rapid access and even distribution of fixative into the tissue was immediately performed.

Because formaldehyde is a toxic and hazardous chemical by inhalation and skin contact, perfusion was carried out in a well-ventilated hood. At first, the lines were checked for absence of air bubbles that would seriously impair the perfusion. Then the thorax was opened with scissors. The cannula that was connected to the perfusion apparatus was inserted into the left ventricle of the heart and clamped in place with a pair of hemostats. The right atrium was severed immediately. The animal was first preperfused with 50 ml phosphate buffered saline (PBS) containing heparin (0.5 mg /ml) to flush the blood from the vascular system. Heparin prevented clotting of the blood that would impede the distribution of fixative. Then the two-way-tap was turned and the animal was perfused with 200 ml freshly prepared fixative solution. Once the perfusion was completed, hippocampus and neurohypophysis were immediately dissected out and immersed in the same fixative for 2 hours at room temperature.

Phosphate buffered saline (PBS)

137 mM NaCl, 3 mM KCl, 100 mM $Na_2HPO_4$, 18 mM $KH_2PO_4$, pH 7.4.

Fixative solution

4% paraformaldehyde, 0.05% glutaraldehyde and 0.2% picric acid in PBS, made up freshly every time.

For 200 ml fixative: dissolve 8 g of paraformaldehyde powder in 150 ml of distilled water while heating on a stir plate to ~60°C in a well-ventilated area. Add several drops of 1 N NaOH until the solution becomes clear. Cool the solution and then filter. Add 20 ml 10x PBS and 0.4 ml saturated aqueous picric acid and bring the total volume to 200 ml. Adjust the pH with 1 N HCl to 7.4. Before use, add 400 µl EM-grade 25% aqueous glutaraldehyde and mix.

## 2.1.2. Cryoprotection and freezing

After rinsing the fixed specimens in PBS three times, each for 5 min, to remove unbound fixative, small pieces of tissue (~2 $mm^3$) containing the CA3 region were carefully cut out in a drop of PBS, avoiding any mechanical squeezing or pulling that might damage the subcellular morphology of the tissue. Then these small tissue blocks were infiltrated with the cryoprotectant, 2.3 M sucrose in PBS or a mixture of 1.8 M sucrose and 20% PVP (polyvinyl pyrrolidon), for ~3 hours. Infiltration with cryoprotectant permits rapid freezing and prevents the formation of ice crystals within the tissue (Tokuyasu and Singer, 1976). It is essential for vitrification of the tissue pieces during freezing. The cryoprotectant solution was changed several times during infiltration. Cryo-protected tissue blocks were embedded in a droplet of fresh solution, and then quickly mounted onto specimen pins. They were orientated under a stereo microscope and frozen by rapid plunging into liquid nitrogen. The blocks were solidified so that sections could be cut thin enough for examination under the electron microscope. The specimens should be mounted and frozen as quickly as possible to avoid dehydration. The frozen specimens were placed into a small plastic storage container individually and kept in liquid nitrogen. They could be repeatedly sectioned and stored without problem.

A mixture of 1.8 M sucrose and 20% (w/v) PVP (for 10 ml)

2 g PVP (MW 10000, Sigma)
8 ml of 2.3 M sucrose in PBS
0.4 ml of 1.1M $Na_2CO_3$ in PBS

stirred at the room temperature for at least 1 hour. Air bubbles were then removed in a desiccator under vacuum at 25 mbar for ~15 minutes.

### 2.1.3. Preparation of support films

Because the cryo-sections were somewhat unstable under the electron beam, the grids were covered with a thin film beforehand to support the specimen and to avoid serious damage. The film should be strong enough to remain attached to the grids throughout all manipulations. In this study, grids were coated with pioloform as a support film.

The preparation was carried out under a ventilated hood. 70-80 ml of a 1.8% pioloform solution dissolved in chloroform was poured into a glass cylinder, which had a tap at the bottom. All glass slides were wiped with a tissue to remove the dust before use. A clean glass slide was placed into the solution, the cap of the glass cylinder was covered and the tap was opened. The solution was allowed to drain slowly into the stock bottle under the cylinder. The draining speed greatly affected the film thickness. Rapid draining made the film too thick. When the solution was completely drained out of the cylinder, the slide was taken out and allowed to dry in the air in vertical position. Scores were made with a scalpel blade ~1.5 mm off the edge of the slide to define the limits of film. The slide should be dipped carefully at an angle of 45° into a deep glass trough filled with distilled water, letting the film float slowly off the slide. The interference color of the pioloform film should be silver, gray or gold. Other colors indicated that the film was too thick. Thereafter hexagonal 200 mesh nickel grids were placed orderly with the matte side down in contact with the film onto the pioloform film floating on the water surface. A piece of parafilm was placed carefully onto the pioloform film with the attached grids and the pioloform film was adhering to the parafilm. The grids were now sandwiched between the parafilm and the pioloform. The parafilm together with the pioloform film and the grids was lifted slowly off the surface of the water and placed with the pioloform film lying on the parafilm in a dry Petri dish to exclude dust. The filmed grids were allowed to dry at room temperature and before use they were coated with carbon and glow-discharged for 60 seconds using a vacuum coating device (BAL-TEC, MED 020 coating system, Leica, Germany). The carbon coating was used for stabilizing the pioloform film under the electron beam and the glow discharge for improving the hydrophilicity of the grid surface that facilitated the spreading of the sections more evenly over the grid.

### 2.1.4. Trimming and sectioning

Cryosectioning was performed with an ultramicrotome (Reichert Ultracut) equipped with a FCS cryo-attachment system (Leica, Germany). The system consisted of a cryochamber, a 25-liter Dewar flask with an automatic pump and a control device. The cryochamber was

mounted onto the knife support of the ultramicrotome and cooled by constantly flooding liquid nitrogen from the Dewar flask via an automatic pump (Fig.1A).

Prior to sectioning, the cryochamber was precooled to the operating temperature (–100°C or –110°C). Then the specimen pin with the attached specimen was quickly transferred with precooled forceps from the liquid nitrogen into the cryochamber, keeping the specimen still under liquid nitrogen in its small storage container. The specimen pin was taken out and inserted into the sample holder. Then the sample holder was tightened to lock the specimen pin in place. The specimen was at first trimmed carefully with the metal trimming knife, which was advanced in 1 μm steps. The specimen was moved up and down manually to result in a approx. 0.5 x 0.8 mm rectangular sectioning surface that included the area of interest, such as hippocampus or neurohypophysis. Then this front sectioning face of the block was trimmed smooth with a 45° glass knife. At last, the ultra thin sections were cut automatically with a dry cryodiamond knife (Diatome, Switzerland) at a clearance angle of 6°. The sectioning speed was set at 1 mm/s. The thickness setting was adjusted to section at 85 or 90 nm. Good sections yielded gold, purple, or blue interference colors.

Because the cryo-sectioning was performed dry in the cryochamber, the static electricity built up by friction in the dry nitrogen atmosphere made the sectioning and manipulating of sections difficult. Therefore, an anti-static device, Static Line Ionisator (Diatom Company, Switzerland) was used during sectioning. The static charges could be neutralized by the small electric current emitted from the anti-static device to facilitate sectioning. Serial sections were usually obtained with this device.

The sections were manipulated with an eyelash mounted on a stick and collected in small groups on the knife surface under the binocular microscope. 4-6 Sections from the ribbon of sections were picked up with a platinum loop containing a droplet of pick-up solution, a mixture with 2.3 M sucrose in PBS and 2% methylcellulose in distilled water (1:1 volume ratio) which resulted in improved preservation of ultrastructure (Liou et al., 1996). The picking-up of the sections should be finished before freezing of the droplet. The loop with frozen droplet and sections was removed from the cryochamber. The droplet and sections were allowed to thaw at room temperature for a while. Then the sections that were situated on the lower surface of the droplet were attached directly to a 200 mesh nickel grid. The grids were covered with pioloform film beforehand and prior to use coated with carbon and glow-discharged. The grids were placed section-side down on the surface of PBS. The pick-up solution was allowed to diffuse out of the sections in the PBS. (Fig.1B).

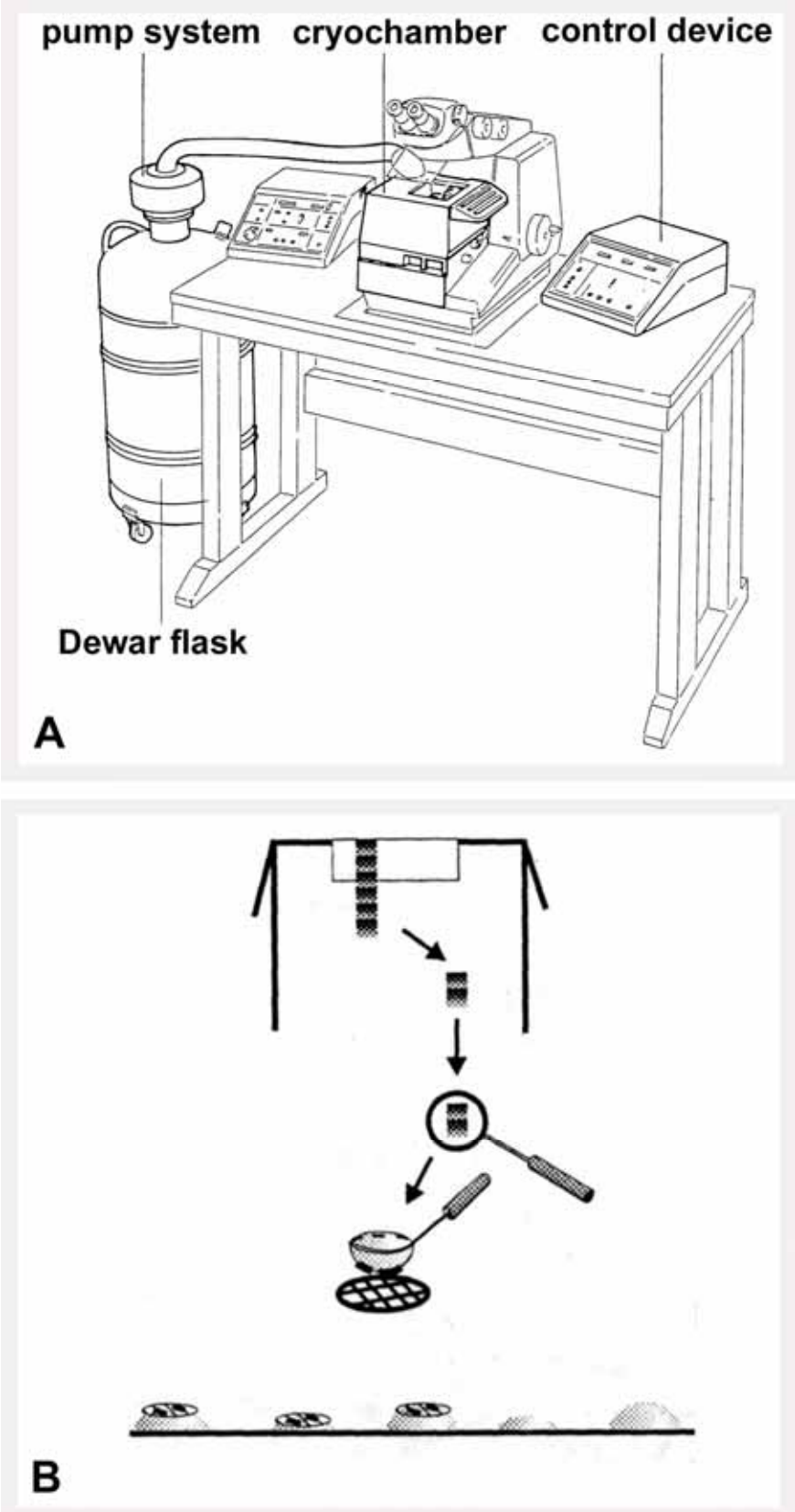


Fig.1. (A) The FCS cryo-ultramicrotome system. The FCS cryoattachment consists of a cryochamber, a control device and a 25 liter Dewar flask with an automatic pump system (Leica, 1997). The cryo-chamber is mounted onto the knife support of the ultramicrotome.
(B) Schematic diagram of the sectioning and picking-up of the sections in the cryoimmunogold technique (from Liou. et al, 1996).

### 2.1.5. Immunolabeling for electron microscopy

An immunogold procedure modified from Griffiths (1993) was used in this study for immunolabeling of the synaptic proteins in nerve terminals. The grids with ultrathin sections were floated sequentially on droplets of the various solutions at the surface of a piece of parafilm, keeping the section side of the grid down in the liquid and the back side of the grid up and dry. The entire labeling process was performed at room temperature unless it is specifically mentioned.

At first, the sections were incubated in droplets of 50 mM glycine in PBS for 10 minutes to quench the remaining free aldehyde groups. The amino group of the glycine would bind to free aldehyde groups left on the specimens and prevent them from binding to the antibody, reducing the nonspecific background. Then they were floated in 5% bovine serum albumin (BSA) in PBS for 20 minutes to block non-specific binding sites. The immunolabeling was carried out by incubating the sections on the droplets of the immunoreagents inside a Petri dish, which ensured a dust-free moist environment. Because of the small volume of the antibody solution, a piece of water-soaked tissue paper was placed within the petri dish to minimize evaporation of the immunoreagents. The grids were placed directly from 5% BSA onto the droplets of primary antibody diluted appropriately in PBS containing 1% BSA in a moist Petri dish and incubated for 2 hours or overnight at 4°C to locate the protein of interest. After washing intensively in PBS (6 times for 30 minutes) to remove the unbound primary antibodies, sections were incubated with colloidal gold-conjugated (10 nm, in some cases also 5 nm) secondary antibody diluted 1:20 with 1% BSA for 2 hours or overnight at 4°C in a moist petri dish. Thereafter the sections were washed in PBS buffer 6 times for 30 minutes to remove the unbound secondary antibodies and postfixed in 2.5% glutaraldehyde in PBS for 10 minutes. The glutaraldehyde was washed out in PBS for 3 x 5 minutes. Then the grids were rinsed in double-distilled water for 4 x 2 minutes to remove the phosphate. Phosphate in the sections would precipitate the uranyl ions during the following staining.

***Control experiments***

Control experiments were always performed with sections adjacent to those showing a positive reaction with the normal immunocytochemical staining. These sections were processed precisely as described above, with the only exception that the primary antibody was replaced by 1% BSA in PBS. The sections were incubated with 10 nm colloidal gold-conjugated secondary antibody, goat anti-mouse IgG or goat anti-rabbit IgG, in order to analyse for nonspecific binding of secondary antibodies.

***Double immunolabeling***

The double immunolabeling method was applied to compare the localization of two synaptic proteins of interest on the same tissue section. Two primary antibodies raised in different donor species and directed against different synaptic proteins were applied. The monoclonal antibody (from mouse) and the polyclonal antibody (from rabbit) used in the present study bound to the corresponding secondary antibodies that were conjugated to two differentially sized gold particles markers (5 nm or 10 nm). The availability of different-sized gold particles makes the immunogold method particularly suitable for the ultrastructural demonstration of various proteins in the same preparation.

Immunostaining for the two antibodies was performed sequentially on the cryo-sections. After blockade of the non-specific binding sites with 5% BSA for 20 minutes, the first primary antibody, washing buffer PBS and the corresponding immunogold-conjugated secondary antibody were used one after another as described above. Then the sections were washed intensively with PBS and blocked again with 5% BSA for 20 minutes. The immunolabeling procedure was repeated by sequential application of the second primary antibody, washing buffer PBS and the corresponding immunogold-conjugated secondary antibody. Thereafter, the specimens were treated as mentioned above.

***Immunolabeling with 1.4-nm Nanogold and silver enhancement***

In order to improve the density of immunolabeling, 1.4 nm Nanogold with Fab fragments and silver enhancement were employed in the localization of synaptic proteins in the CA3 region of the hippocampus. The small 1.4 nm Nanogold with Fab fragments reveal excellent penetration into the tissue (Sun et al., 1995) and have been shown to be able to pass easily through 1-2 µm thick cryosections (Takizawa and Robinson, 1994). Therefore, they would be expected to penetrate completely through the 90 nm thick ultra-thin cryosections used in the present study. These immunogold particles are too small to be resolved in thin sections by normal observation with electron microscopy, but can be visualized after silver enhancement (Danscher, 1981b; Burry et al., 1992). Silver enhancement is a process in which gold catalyzes the silver reduction that leads to the deposition of silver around the gold particles, such that the small gold particle can be grown to a useful size for electron microscopic observation (Danscher, 1981c). The silver enhancement procedure does not deteriorate ultrastructural detail.

The practical experimental procedure in the present study is as following: the cryosections were at first treated as described above. After the incubation with the primary antibody anti-VAMP II, the sections were washed intensively with PBS and incubated in 1.4 nm gold particles with covalently attached goat anti-mouse Fab. The 1.4-nm gold probes were diluted 1:200 in PBS containing 1% BSA. After washing with PBS six times in 30 minutes, the sections were postfixed with 2.5% glutaraldehyde in PBS for 10 minutes. The grids were washed with double-distilled water for three times in 15 minutes. Then the 1.4-nm gold particles were silver-enhanced. The developer solution was prepared according to Danscher (1983). The sections were incubated with developer solution in a dark chamber for 20 minutes. The reaction was stopped by washing the samples in double-distilled water. Thereafter, the samples were negatively stained as described in 2.1.6.

Developer solution

A. Protective colloid: 25 g gum arabic is dissolved in 50 ml double-distilled water by stirring, and then the solution is aliquoted and stored at -20°C.
B. Citrate buffer (pH 3.5): 2.35 g dehydrated sodium citrate and 2.55 g citric acid in 10 ml double-distilled water.
C. Reducing agent: 0.85 g hydroquinone in 15 ml double-distilled water.
D. Silver ion supply: 0.11 g silver lactate in 15 ml double-distilled water.

The developer solution was prepared by mixing 60 parts of solution A, 10 parts solution B, 15 parts solution C, and 15 parts solution D. Solution D was protected from light and added immediately just before use (Danscher, 1981a).

***Antibodies***

1) Primary antibodies

Table I listed the used primary antibodies against various proteins and the information about their type, donor animal, and the working concentration as well as the source of the antibodies.

2) Secondary antibodies

The type, donor animal, working concentration and the source of the appropriate secondary antibodies used in this part are listed in Table II. Secondary antibodies conjugated with 10 nm gold particles was used for normal immunostaining, 5 nm and 10 nm gold particles were used for double staining, and the 1.4 nm nanogold was used only for silver enhancement.

**Table I. Primary antibodies for localization of synaptic proteins in hippocampus and neurohypophysis**

| Antigen | Type/Signature | Donor | Dilution | Source |
|---|---|---|---|---|
| VAMP II | mono/ cl 69.1 | mouse | 1:50 | Synaptic Systems, Göttingen, Germany |
| SNAP-25 | mono/ cl SMI 81, IgG1 | mouse | 1:20 | Biotrend, Köln, Germany |
| SV2 | mono/ CKK 10H4 | mouse | 1:10 | Dr.R.B. Kelly, San Francisco, USA |
| Rab3A | mono/ cl 42.2, IgG2b | mouse | 1:20 | Synaptic Systems |
| α/β SNAP | mono/ cl 77.1 IgG2b | mouse | 1:20 | Synaptic Systems |
| NSF | poly/ 733-744aa | rabbit | 1:20 | Synaptic Systems |
| NTCC | poly/ anti-α1B 851-867aa | rabbit | 1:20 | Alamone labs Jerusalem |
| PQTCC | poly/ anti-α1A | rabbit | 1:20 | Alamone labs Jerusalem |
| Bassoon | Poly/ - | rabbit | 1:50 | tom Dieck et al. 1998 |
| Oxytoxin | Poly/ - | rabbit | 1:500 | Prof. F. Nürnberger, Frankfurt, Germany |

**Table II. Secondary antibodies for detection of synaptic proteins in hippocampus and neurohypophysis**

| Name | Type | Donor | Dilution | Source |
|---|---|---|---|---|
| Goat anti-mouse IgG (10 nm gold) | mono | goat | 1:20 | British BioCell International (Cardiff, UK) |
| Goat anti-mouse IgG (5 nm gold) | mono | goat | 1:20 | British BioCell International (Cardiff, UK) |
| Goat anti-mouse Fab (1.4 nm nanogold) | mono | goat | 1:200 | British BioCell International (Cardiff, UK) |
| Goat anti-rabbit IgG (10 nm gold) | Poly | goat | 1:20 | British BioCell International (Cardiff, UK) |
| Goat anti-rabbit IgG (5 nm gold) | Poly | goat | 1:20 | British BioCell International (Cardiff, UK) |

### 2.1.6. Staining and examination of ultrathin sections

A “Positive-Negative” Staining method modified from Griffiths (1984) was used to reveal the ultrastructure of mossy fiber terminals in the hippocampus and neurosecretory endings in the neurohypophysis. After immunolabeling and postfixing, the specimens were rinsed with distilled water to remove the inorganic phosphate. Then the grids were stained by floating on

drops of a mixture of 2% uranyl acetate and 1.5% methylcellulose in the dark on ice for 10 minutes. This mixture was prepared immediately prior to use and kept on ice in the dark at all times. Then the grids were individually taken out using a 3.5 mm-diameter wire loop. The excess solution was drawn off with filter paper so that a thin film was left over grid and sections. Finally, the grids were allowed to dry at room temperature in the air. The methylcellulose was introduced to protect thawed frozen sections against the damage from surface tension caused by air-drying. Together with the initial aldehyde fixation, the treatment with methylcellulose determines the structural preservation of the thawed cryosection. In addition, it was reported that sections with a thickness of approximately 80-110 nm would yield an average thickness of 70 nm after they were thawed and dried under the protection of methyl cellulose (Griffiths et al., 1984). This proved suitable for examining the sections under the transmission electron microscope. With this method a mixture of positive and negative contrast was finally produced. The nucleus and microtubules were usually positively stained, whereas the membranes gave a strong negative contrast.

Specimens were examined under a Zeiss EM 902 electron microscope operated at 80 kV. In order to obtain a higher contrast for the cryosections a small objective aperture (30 μm in diameter) were used.

Stock solution of methylcellulose

2% methyl cellulose (25 centipoise viscosity, Sigma, Germany) was mixed in double distilled water at 4°C. When completely dissolved, the solution was centrifuged at 100,000 g with Beckman ultracentrifuge (Optima™ TLX, rotor TLA45) at 4°C for 1 hour. Then they were stored carefully in the refrigerator without disturbing the insoluble pellet at the bottom of the tube.

Stock solution of uranyl acetate

8% uranyl acetate was fully dissolved in double distilled water under constant stir in the dark, then stored at 4°C in the refrigerator.

The mixture of 1.5% methylcellulose and 2% uranyl acetate

The mixture was freshly prepared by completely mixing three parts of 2% methylcellulose stock solution with one part of 8% uranyl acetate stock solution. The mixture was kept on ice all the time.

### 2.1.7. Quantitative analysis of immunolabeling

The number of gold particles was used as an indicator for evaluating the labeling density of various synaptic proteins. The electron microscopy images were inputted into a computer using a CCD camera and the quantitative analysis was carried out with the image analysis software MCID from Imaging Research (ST. Catharines, Ontario, Canada).

In mossy fiber terminals, the density of the immunolabeling in the active zone area (A.z. area, the selected cytoplasmic part within 100 nm of the active zone membrane) and in the vesicle area (V. area, the other area outside the active zone area) was determined, respectively. Every area of interest was measured and the number of gold particles falling within this area was counted. The density was calculated as the number of gold particles per square micrometer (number of gold particles/$\mu m^2$). For area analysis a total of 15 to 38 random profiles were taken for every synaptic proteins. Then the comparative ratio of the immunolabeling density in these two areas (A.z. area/V. area) was calculated. Similarly, the linear density of gold particles at the plasma membrane of the active zone (p.m. at A.z) and outside the active zone (p.m. outside A.z) was obtained and compared. The length of the selected plasma membrane and the number of the gold particles on it were measured and counted, respectively. The linear density of gold particles was expressed as the number of gold particles per micrometer (number of gold particles/μm). Gold particles situated within a distance of 10 nm (the size of a gold particle) from the plasma membrane were assigned to membrane labeling. Random lengths for different proteins ranging from 16 to 41 samples were analyzed for the linear density. The ratio of the linear density of gold particles at the plasma membrane of the active zone and outside the active zone was calculated (P.m. at A.z./P.m. outside A.z.).

In neurosecretory terminals of the neurohypophysis the immunolabeling density over clustered microvesicles and over the secretory granule population (number of gold particles/$\mu m^2$) were examined and compared. In addition, the linear labeling density of the terminal plasma membrane was determined (number of gold particles/μm). In total 15 to 28 and 16 to 22 independent analyses for various proteins were performed for area and linear density, respectively.

The same quantitative analysis was performed for the related control samples with monoclonal and polyclonal antibodies, respectively. The statistical evaluation was carried out using an unpaired t-test.

## 2.2. Study of synaptic proteins in primary astrocytic culture

The conventional preembedding immunocytochemical technique and the novel LR Gold postembedding method were employed in the investigation of the subcellular localization of synaptic proteins in primary astrocytic cultures. In addition, horseradish peroxidase (HRP) was used as a marker for the study of endocytic structures.

### 2.2.1. Primary culture of astrocytes

***Working rules***

An aseptic technique was followed throughout. All glassware was first sterilized by autoclaving, all metal preparation devices were sterilized by dry heat at 190°C for 4 hours, and all the solutions and reagents for cell culture were subjected to autoclaving or sterile filtration. All manipulations for the cell culture were performed under a sterile hood. The work surface was decontaminated with 70% ethanol before and after manipulation. Bottles and other similar items were wiped with 70% ethanol when they were placed into the hood. All solutions and media were prewarmed to 37°C before use.

***Preparation of astrocyte cultures***

The primary astrocytic culture was prepared according to Queiroz et al. (1997) and Maienschein et al. (1999). Cerebral cortices of four newborn (postnatal day 1) wistar rats were dissected out and placed into ice-cold PBS. Meninges and larger blood vessels were removed under the stereo-microscope. Then the tissue was cut into small pieces in a drop of culture medium and dissociated by trituration in 10 ml same medium. The cell suspension was passed through nylon gauze (50 µm) and then centrifuged at 200 g for 5 minutes (Fa. Hermle ZK 380). The cell pellet was resuspended in 10 ml medium and recentrifuged at 200 g for 5 minutes. This was repeated twice. Then the cell number was determined and cells were plated at a density of 200.000/ml in poly-L-lysine-coated Permanox chamber slides (Nunc, Wiesbaden, Germany). The cell culture was incubated in astrocyte culture medium at 37°C with 5% $CO_2$. The culture medium was changed on the next day.

Astrocyte culture medium

Dulbecco's Modified Eagle Medium (DMEM, GIBCO/ BRL, Germany) containing 4 mM L-alanyl-L-glutamine was supplemented with 10% fetal calf serum (FCS), 100 U/ml penicillin and 100 µg/ml streptomycin, and 10 ng/ml lipopolysaccharid.

***Determination of cell number***

In order to estimate the concentration of the cells, the cell number was determined in a standard manner using a Neubauer hemocytometer and a Trypan blue solution. At first, the cells were resuspended by pipeting up and down to give a uniform cell suspension. Then an aliquot of the cell sample was diluted 1:4 for the counting. A drop of diluted cell suspension was added immediately to either chamber of the hemocytometer and the viable cells were counted using an inverted microscope. Viable cells were remained unstained because of their intact cell membrane, whereas the dead cells were stained blue. Cell counting was completed within 2-3 minutes, since longer observation time led to additional cell death. Each large square on the Neubauer hemocytometer has 16 small squares and gives an area of 1 $mm^2$ and a depth of 0.1 mm. Thus its volume is 0.1 $mm^3$**,** i. e. $10^{-4}$ ml. The cells of four large squares in the chamber were counted and added up. The sum was divided by 4 to obtain the mean number of cells in one large square, then divided by $10^{-4}$ ml (volume of one large squares) and finally multiplied by 4 (the ratio of the dilution) to get the number of the cells per milliliter (cells/ml) in the probe.

## 2.2.2. Preembedding immunocytochemical method

The conventional preembedding immunocytochemical method was first applied in the cultured astrocytes for the study of the subcellular localization of synaptic proteins and the stimulation-induced endocytotic structure using HRP as a marker. The cells were stimulated with different stimuli including 1 mM glutamate, 1 μM brandykinin as well as 500 μM N-methyl-D-aspartate (NMDA) in the presence of HRP (5 mg/ml, sigma, Germany). The HRP reaction was performed after fixation but before immunolabeling. For the immunocytochemical analysis the cells were fixed for 20 minutes with 3% paraformaldehyde and 0.05% glutaraldehyd either in the hypotonic phosphate buffer (5 mM PB) that led to the rupture of the plasma membrane so that the antibodies could get access to the binding sites (Marxen et al., 1999) or in normal PBS buffer and then treated with the bacterial toxin streptolysin-O (1 μg/ml). Streptolysin-O binds cholesterin on the plasma membrane at 0°C. Through a temperature change from 0°C to 37°C the membrane-bound monomeres of streptolysin-O fuse into oligomeres, resulting in the formation of ~30 nm pores in the plasma membrane (Bhakdi et al., 1993). These pores allow the antibodies to diffuse into the cytoplasm. Cultured 4-day-old astrocytic cells were used for the experiments. The experimental procedure is as following:

*Stimulation, fixation and DAB reaction*

- Wash with physiological saline at 37°C for 5 minutes to remove excess medium
- Stimulate the cells at 37°C in the presence of HRP (5 mg/ml) for 1 minute
- Wash twice with physiological saline solution at 37°C
- Fix with 3% paraformaldehyde and 0.05% glutaraldehyde either in hypotonic phosphate buffer (5 mM PB) or in normal buffer (PBS) * for 20 minutes
- Wash with PBS 3 x 5 minutes

  * Cells fixed in normal buffer were treated with the bacterial toxin streptolysin-O (1 µg/ml) at 0 °C for 5 minutes and then at 37°C for 10 minutes.
- Incubate with 0.05% diaminobenzidine (DAB, sigma, Germany) and 0.01% $H_2O_2$ in 60 mM Tris-HCl (PH 7.6) for 20 minutes
- Wash with Tris-buffered saline (TBS) for 5 minutes
- Wash with PBS 2 x 5 minutes

*Immunolabeling, postfixation and embedding*

- Incubate in 5% BSA for 20 minutes to block non-specific binding sites
- Incubate in primary antibody diluted in PBS containing 1% BSA at 4°C for 4 hours
- Wash with PBS 3 x 20 minutes
- Incubate in 10 nm gold-conjugated secondary antibody (1:20) at 4°C overnight
- Wash with PBS 6 x 10 minutes
- Postfix with 2.5% glutaraldehyde in PBS for 30 minutes
- Wash with PBS 3 x 5 minutes
- Fix with 1% osmium tetroxide ($OsO_4$) in PBS for 2 hours
- Wash with PBS 3 x 5 minutes
- Dehydrate in 50% ethanol 2 x 5 minutes
- In 70% ethanol for 5 minutes
- Stain with 2% uranyl acetate in 70% ethanol for 20 minutes in the dark
- Dehydrate in increasing ethanol series 70, 80, 90, 96, 100, 100%, 5 minutes each
- In propylenoxid for 15 min
- Propylenoxid / Epon (1:1) for 1 hour
- Infiltrate in Epon in gelatin capsules overnight and polymerize at 60°C for 24 hours
- Trim and section

Physiological saline

120 mM NaCl, 4.8 mM KCl, 1.22 mM $KH_2PO_4$, 25.5 mM $NaHCO_3$, 14.3 mM glucose, 1.5 mM $MgSO_4$ and 2 mM $CaCl_2$. pH adjusted to 7.4

Composition of the Epon-mixture

| | |
|---|---|
| Epon 812 | 17.44 ml (Fa. Serva, Heidelberg, Germany) |
| DDSA | 16.0 ml |
| MNA | 6.96 ml |
| DMP | 1 ml |

### 2.2.3. LR Gold postembedding immunocytochemical method

A modified LR Gold postembedding immunocytochemical method from Migheli et al. (1992) was used for the localization of synaptic proteins in astrocytic cells. The polar acrylic resin "LR Gold" has been introduced for postembedding immunocytochemistry because its hydrophilic property provides a better penetration for antibodies in aqueous solution (Klinger, 1994). Moreover, optimal preservation of both ultrastructure and antigenicity of the tissue has been obtained by staining with uranyl acetate, total dehydration in acetone and embedding at low temperature (Berryman and Rodewald, 1990).

In the present study, 4-day-old cultured astrocytic cells were used for the experiment. At first, the cells were washed in physiological saline for 5 minutes at 37 °C to remove excess medium. Then they were fixed with 4% paraformaldehyde and 0.05% glutaraldehyde in 0.1 M phosphate buffer (PB) for 2 hours. After washing, the samples were incubated in 50 mM ammonium chloride for 30 minutes to quench the remaining free aldehydes and then treated with 2% uranyl acetate at 0°C for 2 hours. Thereafter they were dehydrated in an acetone series at -20°C and infiltrated with LR Gold resin at -20°C overnight. The cells were polymerized in LR Gold containing 0.5% diberzoylperoxide in gelatin capsules at -20°C for 24 hours. Then the sample blocks were trimmed and sectioned and the ultrathin sections were collected on 200 mesh nickel grids.

Immunolabeling was carried out by floating the grids with ultrathin sections sequentially on droplets of the various solutions on a piece of parafilm at room temperature (see 2.1.5.). After floating on 5% BSA for 20 minutes the sections were incubated with the primary antibody and the corresponding gold-conjugated (10 nm) secondary antibody (1:20) for 3 hours, respectively. After washing with double-distilled water for 6 x 5 minutes the sections were counterstained with lead citrate solution for 2 minutes.

Lead citrate solution (Reynolds, 1963)

Dissolve 1.33 g lead nitrate $Pb(NO_3)_2$ and 1.76 g sodium citrat $Na_3(C_6H_5O_7)\cdot 2H_2O$ in 30 ml freshly prepared double-distilled water ($CO_2$-free), then add 8 ml 1 N NaOH and shake until the solution becomes clear. Fill with the same double-distilled water up to 50 ml. The entire process should be protected from $CO_2$ to avoid the precipitation of lead carbonate.

## 2.3. Expression and localization of synaptic proteins in the astrocytoma cell line U373 MG

The cell line U373 MG was used in this study as a model system to investigate the expression and localization of synaptic proteins in astrocytoma cells. Various recombinant DNAs encoding different synaptic proteins were transfected into the U373 cells and detected by immunocytochemical methods via immunofluorescence and electron microscopy.

### 2.3.1. Constructs

cDNAs encoding VAMP II-, SNAP-25-, syntaxin I- and cellubrevin (generously supplied by Prof. Niemann) were linked to the tags myc (oncogene of myelocytomatosis virus), HA (hemagglutinin), VSVG (the vesiclar stomatitis virus glycoprotein) and flag at their 5´-ends, respectively, and all of the resulting recombinant cDNAs were then cloned into an expression vector pcDNA3 (Invitrogen, Holland) by Dr. Alexander Wilhelm in our laboratory. The tags myc, HA, VSVG and flag, are all small peptides consisting of 8-12 amino acids and are expressed at N-terminus of VAMP II, SNAP-25, syntaxin I and cellubrevin, respectively. The pcDNA3 vector has a high rate of expression for both the cDNAs of interest and the linked tags. By use of a monoclonal antibody raised against the corresponding tag, the detection of these recombinant proteins could be then carried out immunocytochemically.

In addition, by means of the green fluorescent protein (GFP) and the red fluorescent protein (RFP), the expression and localization of the transfected proteins Rab5 and syntaxin I were investigated in the U373 cells. The Rab5-cDNAs in the GFP-containing expression vector pEGFP C3 were kindly provided by prof. Dr. Marino Zerial (Dresden). The syntaxin I-cDNAs were cloned to the RFP-encoding expression vector pDsRed1-N1 (Clontech, Germany) by Friederike Küster in our laboratory. GFP, originally identified in the jellyfish *Aequorea victoria*, displays an inherent green fluorescence (Prasher, 1995; Kendall and Badminton, 1998). RFP has recently been isolated from an Indo Pacific sea anemone-relative, *Discosoma sp*. (Matz et al., 1999). RFP shows homology to GFP and displays an inherent red

fluorescence. The fusion protein with fluorescent GFP or RFP can be directly observed under a fluorescent microscope, without the help of the antibodies. Therefore, the background due to nonspecific binding of either primary or secondary antibodies can be eliminated greatly at the level of light microscopy. GFP and RFP have been reported in many studies to serve as excellent fluorescent markers for analysis of gene expression and protein localization and dynamics.

### 2.3.2. Bacterial culture

The bacteria *Escherichia coli* (*E. coli*) DH5α was used as host strain to propagate plasmid DNA. Small ice pieces of bacteria from a frozen glycerol bacterial stock (stored in -80°C) were picked up using an inoculating loop under sterile conditions and inoculated immediately into 400 ml LB-medium/ampicillin in a 1-liter sterile flask. Under constant, suitable shaking, the inoculated cultures were grown in a 37°C incubator over night. Then the culture was ready for use.

LB-medium

10 g bacto tryptone, 5 g bacto-yeast extract and 10 g NaCl were dissolved in 1 liter double distilled water, pH 7.5 and autoclaved

LB-medium/ampicillin

A sterile stock solution of the antibiotic ampicillin (50 mg/ml) was added into the LB-medium at a final concentration of 0.1 mg/ml.

### 2.3.3. Maxi-preparation of plasmids

The plasmid DNA from *E. coli* was extracted with the Maxi-Prep-kit Nucleobond AX from the company Macherey-Nagel (Germany). The preparation was carried out according to the manufacture's standard protocol for the purification of plasmids. The cartridge AX 500 was applied for the maxi-preparation.

The bacterial culture was harvested by centrifuging at 2100 g, 4°C, for 10 minutes (Kontron Hermle: Centrikon T324, rotor A6.14). The bacterial pellet was then carefully resuspended in 12 ml resuspension buffer S1. After complete resuspension, 12 ml lysis buffer S2 was added and the suspension was mixed gently and thoroughly. Then the mixture was incubated at room temperature for 5 minutes, so that the bacterial cells could be lysed completely by NaOH/SDS in buffer S2. The chromosomal and plasmid DNA were denatured under these alkaline condition. The RNA liberated during the alkaline lysis was digested by

RNase A contained in buffer S1. Thereafter 12 ml neutralization buffer S3 was added and mixed gently. The homogeneous suspension was incubated on ice for 5 minutes. The acidic buffer S3 neutralized the lysate and the high concentration of potassium acetate caused the white precipitate containing chromosomal DNA and other cellular compounds. The plasmid DNA remained in solution and renatured to its supercoiled structure. During the incubation a Necleobond cartridge AX 500 was prepared. The cartridge was equilibrated with 5 ml equilibration buffer N2. The incubated bacterial lysate was loaded onto a prewetted filter to remove completely the precipitated debris from the plasmid samples. The cleared lysate passed directly through the cartridge by gravity flow and the plasmid DNA in the solution was adsorbed by the cartridge. The cartridge was then washed twice with 12 ml wash buffer N3 to remove all contaminating substances. Thereafter, the bound plasmid-DNA in the cartridge matrix was eluted with 12 ml elution buffer N5. The eluate was collected in a centrifuge tube. 8.4 ml isopropanol was added to precipitate the purified plasmid DNA. The plasmid DNA was pelleted by centrifugation at 12,000 rpm and 4°C for 45 minutes (Hermle Z.360K, rotor 22078 V01). The DNA pellet was washed with 5 ml 70% ethanol to remove precipitated salt and centrifuged again for 30 minutes. The DNA pellet was allowed to dry under vacuum at 20 mbar for 15 minutes. Then the DNA was redissolved in 200 µl double distilled water and stored at 4°C.

Buffer solutions

S1: 50 mM Tris/HCl, 10 mM EDTA, 100 µg/ml RNase A, pH 8.0 (stored at 4°C)

S2: 200 mM NaOH, 1% sodium dodecyl sulfate (SDS)

S3: 2.8 M potassium acetate, pH 5.1

N2: 100 mM Tris/$H_3PO_4$, 15% ethanol and 900 mM KCl, 0.15% Triton X-100 pH 6.3

N3: 100 mM Tris/$H_3PO_4$, 15% ethanol and 1150 mM KCl, pH 6.3

N5: 100 mM Tris/$H_3PO_4$, 15% ethanol and 1000 mM KCl, pH 8.5

### 2.3.4. Determination of the DNA concentration

The concentration and the purity of the DNA were determined with a spectrophotometer (Hitachi U2000, Japan). The harvested DNA was first diluted 500 folds with double-distilled water. The optical density (OD) of the DNA solution was measured at the wavelengths of 260 nm and 280 nm in a Quarz curvette (d = 1 cm) and expressed as absorbance units. The concentration of DNA was determined at 260 nm. According to Sambrook et al. (1989) the solution with one absorbance unit of OD at 260 nm contains 50 ng/µl of double chain DNA

($1A_{260nm}$ unit = 50 ng/µl DNA). The purity of DNA was then estimated by the ratio between the measured ODs at 260 and 280 nm. A preparation with acceptable purity has an $OD_{260}/OD_{280}$ value between 1.6 and 2.0.

### 2.3.5. Cell culture

***Cells***

The cell line U373 MG derived from a human astrocytoma was used as a model system for the study of the expression and localization of transfected synaptic proteins. It was kindly provided by Prof. Dr. Frank Fahrenholz from the University of Mainz.

The U373 cell line was maintained in 35-mm-diameter culture dishes with growth medium in a humidified 37°C incubator with 5% $CO_2$. The U373 cell culture grew and proliferated rapidly. Every 2-3 days the cells became 80-90% confluent and were ready for subculture.

An aseptic technique was applied according to the working rules detailed in 2.2.1. The waste of wash buffer and the medium from the transfected cells were inactivated by autoclaving.

Growth medium for the U373 cells

Dulbecco´s modified Eagle medium (DMEM, GIBCO/BRL, Germany) containing 4 mM L-alanyl-L-glutamine was supplemented with 10% fetal calf serum, 100 U/ml penicillin and 100 µg/ml streptomycin.

***Cell splitting***

The culture medium was first aspirated completely with a Pasteur pipette. Then the cells were rinsed twice with prewarmed PBS to remove cell debris and the rest of the medium. 2 ml trypsin/EDTA (ethylenediaminetetraacetic acid) solution (0.05% trypsin and 0.53 mM EDTA in PBS, Gibco BRL, Germany) was added and the dishes were then swirled to make sure that the entire bottom surface of the dish was covered with a thin layer of trypsin/EDTA solution. The proteolytic enzyme trypsin digests the extracellular matrix protein responsible for cell adhesion to the substratum. EDTA was used in combination with trypsin to remove the cultured cells from the bottom of the dish. The cells were incubated in trypsin/EDTA for 2 minutes and then detached mechanically from the bottom by gently tapping the dishes against a solid object. Thereafter, 4 ml growth medium containing natural trypsin-inhibiting factor was added to each dish to inactivate the trypsin. The cells were pipetted off the substratum by

gentle sweeping the dish bottom with growth medium and dispersed by gentle and repeated pipetting to provide a single cell suspension. An aliquot of this cell suspension à 1.5-2 ml depending on the concentration of the cells was distributed directly to the new culture dish containing 20 ml fresh medium. Then the cells were returned to the incubator.

### 2.3.6. Transfection of U373 cells by electroporation

Physical transfection through electroporation was adopted in this study for the expression of synaptic proteins in U373 cells. The cells in suspension were exposed to a pulsed electric field that caused transient formation of pores in the cell membrane and provided a local driving force for transport of the plasmid DNA constructs through these transient pores into the cells. Then the DNA molecules reached the nucleus and were expressed.

Exponentially growing 50-80% confluent cultures of U373 cells were used for electroporation. The cells were harvested using the standard trypsin detachment procedure as described above. The resuspended cells were centrifuged at 200 g for 5 minutes. Then the cell pellet was resuspended in 800 µl of electroporation buffer. 50 µg of plasmid DNA was added carefully to the resuspended cells and mixed gently. The cell-DNA mixture was then transferred into a sterile electroporation cuvette with a 4-mm electrode gap. The cuvette was rocked gently several times to homogenize the mixture and placed immediately into the electroporation chamber. The electroporation was performed at the room temperature with an electroporation apparatus (Electro cell manipulator 600, BTX-Genotronics, San Diego, USA) with the following parameters: 2250 µF capacitance, 500V/capacitance-resistance, 186 Ω resistances and 240V charging voltage. The pulse lasted for 30-40 ms. The transfected cells were transferred to a centrifuge tube containing 20 ml of prewarmed (37°C) recovery culture medium and incubated with the slightly opened cap to allow gas exchange at 37°C with 5% $CO_2$ for 30 minutes, such that the cells could recover from the electroporation shock. Then the cells were centrifuged at 200 g for 5 minutes and resuspended in 2-4 ml culture medium.

Cell number was determined with Trypan blue and the cells were plated immediately as described in 2.2.1. Cells intended for immunofluorescence experiments were plated onto poly-D-lysine coated cover slips in 24-well tissue culture plates at a density ranging from 20,000-30,000 cells/$cm^2$. Each well contained 1 ml prewarmed (37°C) growth medium and one cover slip. For electron microscopy, cells were plated into 35-mm-diameter culture dishes with prewarmed growth medium at a density of 1-5 x $10^6$ cells/dish. The plated cells were allowed to grow and settle in the incubator at 37°C with 5% $CO_2$ for 24 hours.

Electroporation buffer

137 mM NaCl, 5 mM KCl, 0.7 mM $Na_2HPO_4$, 6 mM dextrose and 20 mM Hepes were dissolved in triple-distilled water, pH 7, autoclaved and stored at 4°C.

Recovery-medium

3 mM EGTA in U373 growth medium

***Cotransfection***

For double immunolabeling, the U373 cells were cotransfected with two types of DNA constructs simultaneously to express two different synaptic proteins in the same cell, each type with 50 µg plasmid DNA.

***Control for the transfected proteins***

The pcDNA3 vector alone without any inserts was transfected into U373 cells to control for the expression of the transfected proteins. The process of the electroporation was the same as described above.

## 2.3.7. Preparation of cover slips

Cover slips (1cm in diameter, Fisher) were cleaned and sterilized before use as follows: they were first boiled in 1 N HCl solution for 1 hour. After cooling, the cover slips were rinsed in triple-distilled water to remove the HCl, and then cleaned in 70% ethanol. The 70% ethanol solution was replaced by fresh triple-distilled water. At last, they were dried at 60°C in a dry oven for 1 hour. The dry cover slips were packed in a piece of aluminum foil, avoiding mutual contact. The packets were placed into a cleaned glass Petri dish and sterilized by heating at 190°C for 3 hours.

Then the cover slips were coated with poly-D-lysine under sterile conditions to facilitate the adherence of cells. A long piece of sterilized parafilm was attached onto the surface of the sterile bench. The sterile cover slips were placed orderly onto the hydrophobic parafilm. 100 µl of a poly-D-lysine solution with a concentration of 5 µg/ml was added to each cover slip. After 30 minutes incubation, the cover slips were washed 3 times with sterile distilled water, each for 5 minutes, and then allowed to dry under the sterile flow hood for ~1 hour. Thereafter the coated cover slips were placed individually into a 24-multiwell plate with the coated side up.

## 2.3.8. Immunocytochemical methods

Two methods were used in the immunocytochemical analysis of transfected synaptic proteins in U373 cells. One was immunofluorescence microscopy for detecting the distribution pattern of the transfected protein in the entire cell; the other was the cryo-immunogold technique with electron microscopy for determining the subcellular localization of the proteins. After 24 hours in culture medium at 37°C, the electroporated cells, which still stayed in the transient expression phase, were processed for immunocytochemical analysis. The transfected proteins were detected with the respective primary antibody directed against the corresponding tag, but in some cases also with the antibodies against the proteins themselves. The former recognized only the recombinant proteins, whereas the latter detected both the recombinant and the endogenous proteins. Generally, 10 nm gold-conjugated secondary antibodies were applied for the detection of the various recombinant proteins, unless mentioned otherwise.

### 2.3.8.1. Immunofluorescence microscopy

In the present study, immunofluorescence microscopy was used to reveal the entire distribution of the transfected synaptic proteins at the cellular level. In addition, it was also very helpful for establishing suitable conditions of fixation and antibody binding for a successful labeling of ultrathin sections.

The immunofluorescence labeling was performed in a Petri dish lined with hydrophobic parafilm. The cells were washed twice in prewarmed physiological saline solution to remove the culture medium and fixed either in absolute methanol at –20°C for 7 minutes or in a fixative containing 4% paraformaldehyde and 0.05% glutraraldehyde in PBS for 20 minutes. The methanol was able to permeabilize the cells directly. However, cells fixed with 4% paraformaldehyde and 0.05% glutraraldehyde must be treated with 0.1% Triton X-100 in PBS for 10 minutes, which dissolves lipid membranes and enhances penetration of antibody. Then the cells were washed with PBS three times for 15 minutes and incubated with 5% BSA in PBS for 20 minutes to block nonspecific binding sites. Afterwards the cells were incubated without further washing directly with the primary antibody diluted in 1% BSA for 20 minutes. The unbound primary antibody was drained off and the cells were washed three times in PBS, 5 min each. From then on, the cells were manipulated in the dark and protected from light. The cells were incubated with the corresponding FITC- or Cy3-conjugated goat anti-mouse or anti-rabbit IgG secondary antibody in 1% BSA for 20 minutes. After several washings with

PBS for 20 minutes, the excess wash buffer was withdrawn from the coverslips and the glass coverslips were mounted onto a clean slide with a small drop of anti-fading-medium, cell-side down. At last, the glass coverslips was sealed with nail varnish around the margin to prevent leakage of the mountant and the specimens were stored in the refrigerator avoiding exposure to light.

Fixative

4% paraformaldehyde and 0.05% glutaraldehyde in PBS

Freshly prepared paraformaldehyde (see 2.1.1.) or its frozen aliquot was used.

Anti-fading reagent

6 g glycerol and 2.4 g mowiol were stirred in 6 ml double-distilled water in the dark for 2 hours. 12 ml 0.2 M Tris-buffer (pH 8.5) was added, and the solution was stirred and incubated in 50°C for further 2 hours, then stored at –20°C. Prior to use, the solution should be thawed, 2.5% DABCO (1,1-diazobicyclo-(2,2,2)-octane) added, and then stirred for 20 minutes in the dark.

### *Control experiment*

In control experiments, the primary antibody was omitted to examine if the immunolabeling was specific or merely resulted from nonspecific binding of the secondary antibody.

To control for the expression of transfected proteins, cells transfected only with the empty pcDNA3 vector were incubated with primary antibody raised against the respective tag or protein and the corresponding secondary antibodies, respectively. The other procedure was as described above.

### *Double immunolabeling*

The double labeling method was applied to localize simultaneously two different synaptic proteins in the same cell. Two noncross-reacting immunostainings were performed sequentially on the coverslips. Every time after the incubation with the antibody the cells were intensely washed with PBS for three times. Before application of the secondary primary antibody the cells were blocked again with 5% BSA for 20 minutes. Two corresponding secondary antibodies, goat-anti-mouse and goat-anti-rabbit, were conjugated with the appropriate fluorochromes FITC or Cy3.

***Localization of fluorescent fusion proteins***

Cells transfected with the construct GFP-Rab5 or RFP-syntaxin I displayed an inherent green or red fluorescence of GFP or RFP. No antibody was needed. From the beginning, all handling was performed in the dark to reduce fluorescence bleaching. 24 hours after electroporation, the transfected cells were visualized directly under the fluorescent microscopy. For extended storage, the cells were washed once with physiological saline to remove the remaining culture medium and fixed in absolute methanol at –20°C for 7 minutes. After washing with PBS three times for 15 minutes, the cells on the glass coverslips were mounted with anti-fading-medium onto a glass slide and stored in the refrigerator. For double protein localization, when both constructs containing GFP or RFP were used simultaneously, the cells were treated as described above. However, when a GFP- or RFP-construct and another construct with nonfluorescent tag were transfected simultaneously, the nonfluorescent tag had to be immunolabeled. The specimens were treated as for the single antigen detection in the dark.

***Observation***

The samples were examined under the fluorescence microscope (Zeiss, Germany) equipped with an MCID 4 imaging analysis system (Imaging Research, St. Catharines, Canada). Emission signals were filtered with a Zeiss Axiophot I 450-490 nm filter for FITC excitation and 510-560 nm for Cy3. Confocal images were obtained with a laser assisted confocal scanning microscope (Leica TCS4D, Germany). FITC and GFP were excited with the 480 nm laser; Cy3 and RFP with the 580 nm laser. All micrographs were processed with Adobe Photoshop 6.0.

### 2.3.8.2. Immunoelectron microscopy

The cryo-immunogold technique was applied for the subcellular localization of recombinant synaptic proteins. Transfected U373 cells for use in electron microscopy were grown on 35-mm tissue culture dishes for 24 hours. Thereafter, the cells was rinsed twice with prewarmed physiological saline solution (37°C) to discard floating cells and cell debris, and then fixed directly in the dish at the room temperature by adding fixative containing 4% paraformaldehyde and 0.05% glutaraldehyde in PBS. After 90 minutes, the fixed cells were scraped off the substratum and centrifuged for 15 minutes at 3000 rpm (Hermle Z.360K, rotor 22078 V01). The supernatant was carefully discarded without disturbing the cells. The solid

pellet of the cells was taken out and then treated as for tissue blocks during further processing. Small pieces of the cell pellet were infiltrated with 2.3 M sucrose in PBS or a mixture of 1.8 M sucrose and 20% PVP for 3 hours. During that time the cryoprotectant solution was changed carefully several times. Small pieces of nitrocellulose were used to aid the transport of the cells. Cryo-protected cell pellets were mounted on specimen holders and immediately frozen in liquid nitrogen. The preparation of ultrathin cryosections, immunolabeling and staining of sections was the same as for treatment of tissue blocks **(**see 2.1.4. 2.1.5. and 2.1.6., respectively).

***Control experiments***

Control sections were processed as described above (see Control experiments in 2.1.5.). For double labeling control, goat anti-mouse IgG conjugated with 10 nm colloidal gold and goat anti-rabbit IgG with 20 nm colloidal gold were applied.

In control experiment for the expression of transfected proteins, sections obtained from the cells transfected with the pcDNA3 vector only were incubated with various primary antibodies and the corresponding with 10 nm gold particles conjugated secondary antibodies, respectively. The samples were treated as for the normal immunolabeling procedure described above.

### 2.3.8.3. Antibodies

1) Primary antibodies: Antibodies against the following proteins (Table III) were applied for light and electron microscopy of U373 cells.

**Table III. Primary antibodies for localization of recombinant synaptic proteins in U373 cells**

| Antigen | Type/Signature | Dilution | Donor | Source |
|---|---|---|---|---|
| Myc | mono | 5 µg/ml | mouse | Our laboratory |
| VSVG | mono | 1:100 | mouse | Sigma |
| HA | mono | 1:50 | mouse | Sigma |
| Flag | mono | 1:100 | mouse | Sigma |
| Syntaxin I | mono/78.2 | 1:50 | mouse | Sigma |
| SNAP-25 | mono/SMI 81 | 1:20 | mouse | Biotrend , Köln. |
| cellubrevin | poly | 1:100 | rabbit | Dr. McMahon (Cambridge; UK) |
| GFP | poly | 1:50 | rabbit | Clontech,Heidelberg |

2) Secondary antibodies: The following secondary antibodies were used to detect the recombinant synaptic proteins in U373 cells. Their properties are listed in the Table IV.

**Table IV. Secondary antibodies for detection of recombinant synaptic proteins in U373 cells**

| Name | Type | Dilution | Donor | Source |
|---|---|---|---|---|
| Anti-mouse-FITC | mono | 1:100 | goat | Dianova |
| Anti-rabbit -FITC | poly | 1:100 | goat | Sigma |
| Anti-mouse-Cy3 | mono | 1:800 | goat | Sigma |
| Anti-rabbit-Cy3 | poly | 1:400 | goat | Sigma |
| Goat anti-mouse IgG (5 nm gold) | mono | 1:20 | goat | British BioCell International (Cardiff, UK) |
| Goat anti-mouse IgG (10 nm gold) | mono | 1:20 | goat | British BioCell International (Cardiff, UK) |
| Goat anti-rabbit IgG (10 nm gold) | poly | 1:20 | goat | British BioCell International (Cardiff, UK) |
| Goat anti-rabbit IgG (20 nm gold) | poly | 1:20 | goat | British BioCell International (Cardiff, UK) |

# 3. Results

## 3.1. Localization of synaptic proteins in mossy fiber terminals and neurohypophysial endings

The cryo-immunogold technique was successfully applied in the present study to reveal the distribution of various synaptic proteins in two different types of nerve terminals, the mossy fiber terminals of the CA3 region of the hippocampus and the typical neurosecretory endings in the neurohypophysis. The modified "positive-negative" staining method results in a strong negative contrast for membranes and a positive staining for the nucleus.

### 3.1.1. Morphology of mossy fiber terminals and neurohypophysial endings

**Mossy fiber terminals**

In the hippocampal CA3 field, the distinctive mossy fiber axons arising from the granule cells of the dentate gyrus occupy the narrow stratum lucidum which is located adjacent to the pyramidal cell layer (Blackstad et al., 1970; Gaarskjaer, 1978), as shown in Fig.2A. The pyramidal cells contain thick spiny thorns on their dendrites that extend into the stratum lucidum (Gaarskjaer, 1986; Frotscher, 1988).

Under the electron microscope, the terminals of the mossy fibers in the stratum lucidum were easily recognized by their unique structural characteristics. They appeared as giant, vesicle-rich profiles and made several synaptic contacts with dendritic spines, which were frequently observed to be embedded in the presynaptic terminals (Fig.2B). It has been evidenced that the mossy fibers use glutamate as a primary transmitter substance (Storm-Mathisen et al., 1983; Garthwaite and Brodbelt, 1990). Enormous numbers of densely packed, electron-lucent small vesicles, which measured ~50 nm in diameter, filled the presynaptic terminals of mossy fibers. In addition, a few LDCVs that ranged in size between 100-150 nm were intermingled with clear small vesicles. Mitochondria were usually observed clustered together. Using this technique the presynaptic active zones that are characterized by electron dense material in conventional electron microscopy (Peters et al., 1991) were recognized as negatively-stained thickened presynaptic membranes that made widened contacts with the juxtaposed thickened postsynaptic membranes.

**The neurohypophysis**

The neurohypophysis, the posterior lobe of the pituitary, is mainly composed of nerve endings of magnocellular neurosecretory neurons of the hypothalamus**.** The long axons of the neurons in the supraoptic and paraventricular nuclei terminate on fenestrated capillaries in the neurohypophysis as shown in Fig.2C**.** The secreted neuronal substances are then further transported via blood vessels. The terminal varicosities of the axons were characterized by densely populated neurosecretory granules and microvesicle clusters (Fig.2D). In the present study, axonal terminals were often found to be surrounded by collagen-rich extracellular space or small processes of pituicytes, the specialized astroglial cells of the neurohypophysis. The oxytocin- (OX) or vasopressin- (VP) containing large dense core granules were 150-230 nm in diameter and almost occupied the entire ending. They are assembled in the neuronal perikarya and transported to the neurohypophysis along the hypothalamo-hypophyseal tract (Brownstein et al., 1980). Small electron-lucent microvesicles segregated into a morphological distinct cluster separated from the granules. They were similar to synaptic vesicles in morphology and size. The clustered microvesicles were often seen beneath the plasma membrane, facing the extracellular space or adjacent to the endothelial wall of the fenestrated capillaries. Obviously, active zones comparable to those in the central synapses could not be observed in neurosecretory endings. However, synaptoid contacts between axons and pituicytes were occasionally observed. They differ from interneuronal synaptic contacts in that the axonal presynaptic membrane appears to be slightly thicker than that in neighboring areas, whereas the postsynaptic membrane of the pituicyte showed no post-synaptic specialization (Fig.2E).

### 3.1.2. Immunolabeling of synaptic proteins in mossy fiber terminals of the hippocampus and neurosecretory terminals of the neurohypophysis

Cryosections prepared according to Tokuyasu's method are considered suitable for immunocytochemistry. In the present study, both the ultrastructure and the protein antigenicity were relatively well preserved. For all the investigated synaptic proteins, the immunolabeling was specially allocated to well-contrasted organelles and could be quantified simply by counting the gold particles. Nevertheless, it was obvious that using this procedure not all sites or organelles of interest could be labeled.

**VAMP II**

On the cryosections of the CA3 region, abundant labeling of VAMP II was detected

selectively over the densely packed electron-lucent vesicles in mossy fiber terminals (Fig.3A, B). The gold particles were associated extensively with the synaptic vesicles. At active zones, some gold particles were localized at docked vesicles and in close proximity to the presynaptic membrane, suggesting that VAMP II was integrated into a docking complex. In contrast, mitochondria and dendrites were free of gold particles.

It is worthy mentioning, that with conventional cryo-immunogold technique VAMP II labeling was detected only over part but not over all synaptic vesicles. By comparison, a higher labeling density was obtained in the samples that were labeled with the 1.4 nm nanogold particles and then treated with silver enhancement (Fig.3C, D). Moreover, more gold particles were found at the active zone. The ultrastructural detail in these samples was similar to that observed without silver enhancement. However, the size of particles after silver enhancing was rather irregular and merging of growing silver/gold particles often occurred.

In the neurohypophysis, the immunolabeling of VAMP II was localized specifically at the clustered microvesicles (Fig.4). The gold particles were scattered over the microvesicle populations. These labeled clustered microvesicles were often found near the plasma membrane, facing the interstitial space. Especially, the immunolabeling could be frequently detected at the plasma membrane, where contact between the microvesicles and the membrane was observed (Fig.4A, C, D). This immunolabeling was not restricted to special domains of the membrane, but more or less randomly distributed over the plasma membrane. In contrast, the large granules were mostly unlabeled. Only minor labeling was found in the vicinity of clustered microvesicles which might be mainly derived from closely adjacent microvesicles. Mitochondria and extracellular space showed no apparent labeling.

**SNAP-25**

Labeling of the t-SNARE SNAP-25 was localized at the presynaptic plasma membrane of the active zone (Fig.5A, B) and also at the plasma membrane outside the active zone (Fig.5B). According to the quantitative analysis (Table V), the labeling density of SNAP-25 at the plasma membrane of the active zone (5.8 particles/μm) was about two folds higher than that outside active zone (2.2 particles/μm). In addition, some gold particles were also found to be associated with synaptic vesicles. The labeling close to synaptic vesicles at the active zones implied the association of SNAP-25 with the presynaptic docking complex (Fig.5C). In addition, Golgi complex was labeled in neuronal soma, suggesting that SNAP-25 was first packed at the Golgi apparatus, then transported to the terminals via carrier vesicles (Fig.5D).

In neurosecretory endings, gold particles were found to be associated with the plasma membrane adjacent to the clustered microvesicles (Fig.5E, F). However, no increased membrane labeling related to certain membrane domains was observed. In addition, there was also some microvesicle labeling with a density similar to that observed for synaptic vesicles in mossy fiber terminals. Especially some microvesicles adjacent to the plasma membrane were labeled. The neurosecretory granules and the mitochondria were obviously free of gold particles (Fig.5F).

**SV2**

In mossy fiber terminals, labeling of the integral synaptic vesicle protein SV2 was extensively localized at the synaptic vesicle population including some docked vesicles at the active zone of the plasma membrane as shown in Fig.6A and B. In addition, some labeling was observed at the presynaptic membrane. The labeling was very specific. No binding sites were detected elsewhere such as at dendrites or mitochondria.

The immunolabeling in neurosecretory endings was restricted to the region of the microvesicle clusters (Fig.6C, D). The gold particles were scattered over the microvesicles similar to those over synaptic vesicles. The microvesicles near the plasma membrane were often labeled (Fig.6E). However, few gold particles occurred on the plasma membrane. Granules were evidently devoid of gold particles, although SV2 has been found on the granules of PC12 cells (Marxen et al., 1997; Tanner et al., 1996).

**Rab3A**

In mossy fiber terminals the immunolabeling of the small GTP-binding protein Rab3A was associated mainly with synaptic vesicles including the vesicles near the active zones (Fig.7A, B). Mitochondria and other areas were free of gold particles. In neurosecretory endings of the neurohypophysis the clustered microvesicles were always labeled with a labeling density similar to that of synaptic vesicles (Fig.7C-E). However, two different types of granule populations could be unexpectedly differentiated according to labeling. One was unlabeled, even though the clustered microvesicles in the same terminal carried the gold particles (Fig.7C, D). The other population was intensively labeled but some gold particles were located somewhat in the interior of the granules (Fig.7D, E). These two types of granules were obviously assigned to two different terminals. As shown in Fig.7D, unlabeled granules surrounding labeled microvesicle clusters were situated in one terminal whereas the granules in adjacent terminal carried the gold particles. In Fig.7E, labeled granules and clustered

microvesicles were observed in the same terminal, but granules in the adjacent terminal were free of gold particles. Both examples show that the labeled granules and microvesicles are in a sharp contrast with the unlabeled granule populations. In addition, gold particles were also found at the plasma membrane (Fig.7F) close to the labeled granules. Double labeling suggested that Rab3A labeling was associated with the oxytocin-containing granule population (Fig.7G, H). Two different-sized gold particles, 10 nm for Rab3A and 5 nm for oxytocin, were detected over the same granules. Neither of them was observed on the other granule population in the nearby terminal (Fig.7H).

**α/β-SNAP and NSF**

α-SNAP is the receptor protein for NSF when both of them are recruited to the trimeric 7S SNARE complex to form a 20S particle. Both are essential components for the initiation of vesicle fusion (Sollner et al., 1993b). In the present study, however, there was little labeling of α/β-SNAP at the central synapse, either in the cytoplasm or on synaptic vesicles and plasma membrane (Fig.8A). In the neurohypophysial terminals, microvesicles were not labeled either, as for the synaptic vesicles. However, the gold particles of α/β-SNAP were associated intensely and specifically with neurosecretory granules, forming a sharp contrast to the unlabeled microvesicles (Fig.8B). Some gold particles also occurred in the interior of the granules. Granules located close to the plasma membrane and the plasma membrane itself were labeled too (Fig.8C). Furthermore, gold particles were even associated with the membrane of a granule forming an Ω-like opening at the plasma membrane (Fig.8D). In analogy to the localization of α/β-SNAP, some labeling of NSF was detected on the granules in the neurohypophysis (Fig.9A). But no gold particles were found over the microvesicle area. However, low labeling of NSF was observed on synaptic vesicles (Fig.9B) and some gold particles were seen on the Golgi complex at the central synapse (Fig.9C).

**N-types $Ca^{2+}$ channel**

The N-type $Ca^{2+}$ channel is thought to be located to the plasma membrane and to interact with the SNARE proteins at active zones to assure the exposure of the docking complex to inflowing extracellular calcium ions (Stanley, 1997). In the present study, significant immunolabeling was found at the plasma membrane of active zones and, unexpectedly, also on the synaptic vesicles in mossy fiber terminals (Fig.10A-C). Also some docked vesicles were evidently labeled with gold particles. The labeling density revealed some differences between the various samples. In some terminals the synaptic vesicles were labeled

particularly intensely. In addition, there was also some labeling at the plasma membrane outside the active zone.

In neurosecretory endings, the N-type $Ca^{2+}$ channel was largely confined to the clustered microvesicles (Fig.10D, E). Moreover, the gold particles were also observed at the plasma membrane, especially at sites, where the clustered microvesicles approached the axonal membrane. Mitochondria and interstitial space were obviously devoid of gold particles, demonstrating that the labeling was very specific. No labeling was detected over the granule population, in clear contrast to the labeled microvesicles.

**P/Q-type $Ca^{2+}$ channels**

As N-type $Ca^{2+}$ channels, P/Q-type $Ca^{2+}$ channels have been implicated in neurotransmitter release in presynaptic nerve terminals of a wide variety of neurons (Dunlap et al., 1995; Westenbroek et al., 1995). In the present study, overall, less immunolabeling was detected in central synapse (Fig.11A, B). Few gold particles were present on synaptic vesicles. Nevertheless, some gold particles were found specifically on the plasma membrane at and outside the active zone.

In the neurohypophysis, labeling for P/Q-type $Ca^{2+}$ channels was associated intensively with the granule population (Fig.11C-E). Some gold particles were also found in the interior of the granules. Interestingly, the high density of immunolabeling over the granules occurred apparently only in a subset of terminals. An involvement of P/Q-type $Ca^{2+}$ channels selectively in vasopressin release has been proposed previously (Wang et al., 1997a). Additionally, some gold particles were also observed on the plasma membrane. By contrast, no significant labeling was found over the clustered microvesicles (Fig.11C).

**Bassoon**

In the present study, Bassoon displayed its own special distributive feature in presynaptic terminals. In contrast to the extensive distribution of the other proteins over the entire presynaptic terminal, abundant labeling for Bassoon was mainly concentrated at the active zone region (Fig.12). According to the quantitative analysis, the labeling density was about nine fold higher at the active zone area than that outside the active zone area (Table V). However, although gold particles were exquisitely localized proximal to the active zone, they were barely found directly associated with the presynaptic membrane. The majority of gold particles was concentrated characteristically close to but at a distance (mostly 50-70 nm) from

the active zone plasma membrane. In addition, some particles were also found at vesicles outside the active zone region. No immunolabeling was observed in neurosecretory terminals that lack obvious active zones.

**Controls**

In control experiments primary antibody was omitted. Instead, the sections were incubated with 1% BSA in PBS followed by 10 nm colloidal gold-conjugated secondary antibody, either goat anti-mouse IgG or goat anti-rabbit IgG. Negative results were obtained. No specific labeling was detected on the organelles in the nerve terminal profiles in the control samples from the CA3 region of hippocampus and the neurohypophysis (Fig.13).

**Quantitative analysis of immunolabeling**

The immunolabeling of various synaptic proteins was assessed quantitatively to compare their distribution pattern in the mossy fiber terminals of the hippocampal CA3 region and in the typical neurosecretory terminals of the neurohypophysis. Table V presents the quantitative data for the various proteins at different sites, revealing differences or similarities of labeling density either in a given site among the various proteins or for a certain protein at different sites. The intensity of immunostaining presumably reflects both the abundance of the antigen investigated and the labeling efficiency with the corresponding antibody under the given experimental conditions. The variance results from changes in labeling efficacy for a given antibody between different samples. The respective ratios compare the distribution of a given antigen between two different sites/compartments.

In mossy fiber terminals the immunolabeling density in active zone area (A.z. area) was compared to that in the vesicle area (V. area) outside the active zone. The active zone area included all docked synaptic vesicles and the vesicles located in close proximity to the active zone. The vesicle area relates to the reserve pool of synaptic vesicles. Evidently, the labeling densities for all antigens investigated were higher in the active zone area than in the remainder vesicle area (Fig.14A). For VAMP II, SV2, Rab3A and the N-type $Ca^{2+}$ channel this increase varied between 50% and 80%. The t-SNARE SNAP-25 revealed a near five-fold increase in the active zone area and Bassoon was increased nine fold. Furthermore, a comparison of linear density of gold particles on the plasma membrane at the active zone (P.m. at active zone) and outside the active zone (P.m. outside active zone) revealed a preferential association of these synaptic proteins with the active zone plasma membrane. As shown in Fig.14B, increased immunolabeling, especially for VAMP II, SNAP-25, SV2 and

N-type $Ca^{2+}$ channel, was shown at the active zone membrane. It should be noted, however, that it is difficult to differentiate between endogenous labeling of the plasma membrane and of antigens situated at closely adjacent docking or fusion vesicles. The number of gold particles here might include both of them.

In neurohypophysial terminals, the immunolabeling over the microvesicles for the synaptic proteins VAMP II, SNAP-25, SV2, Rab3A and the N-type $Ca^{2+}$ channel was similar to that over the synaptic vesicles in mossy fiber terminals. The labeling density for VAMP II, SNAP-25, SV2 and the N-type $Ca^{2+}$ channel over microvesicles was by far higher than that over the granules. The granules showed very low labeling for these proteins (Fig.15A). In contrast, the intense labeling for Rab3A on only one subset of granules was not quantified. In addition, these proteins, especially VAMP II, SNAP-25 and the N-type $Ca^{2+}$ channel, were also detected at the plasma membrane of neurohypophysial terminals, but with a clearly lower density than that at the active zone membrane in the presynaptic terminals (Fig.15B). The labeling for α/β-SNAP, NSF and the P/Q-type $Ca^{2+}$ channel was not included in this quantitative analysis because they showed significant labeling density only on the granules and some gold particles were situated in the interior of the granules. Labeling for the secondary antibodies alone in control samples was very low in all cases and not subjected to this evaluation.

Table V. Distribution of synaptic proteins as revealed by colloidal gold labeling in mossy fibber terminals and neurosecretory terminals.

| | *VAMP II* | *SNAP-25* | *SV2* | *Rab3A* | *N-CaCh* | *Bassoon* | *Control-M* | *Control-P* |
|---|---|---|---|---|---|---|---|---|
| Mossy fiber terminals | | | | | | | | |
| Active zone area | 231.4 ± 163.6 | 65.3 ± 32.2 | 69.4 ± 39.1 | 51.2 ± 48.4 | 91.1 ± 62.1 | 140.8 ± 58.6 | 1.5 ± 2.7 | 0 |
| Vesicle area | 128.5 ± 106.3$^{*}$ | 14.0± 14.3$^{***}$ | 43.2 ± 22.0$^{*}$ | 33.1± 17.1 | 59.9 ± 29.4$^{*}$ | 15.1 ± 13.3$^{***}$ | 1.3 ± 2.3 | 1.7 ± 3.4 |
| A.z. area / V. area | 1.8 | 4.7 | 1.6 | 1.6 | 1.5 | 9.3 | - | - |
| P.m. at active zone | 11.9 ± 7.9 | 5.8 ± 4.0 | 5.3 ± 4.1 | 1.3 ± 2.3 | 5.2 ± 4.4 | 1.2 ± 2.3 | 0 | 0 |
| P.m. outside active zone | 2.0 ± 1.7$^{***}$ | 2.2 ± 1.5$^{**}$ | 1.8 ± 2.2$^{**}$ | 0.3 ± 0.6 | 2.1 ± 1.3$^{**}$ | 0.1 ± 0.5$^{**}$ | 0 | 0 |
| P.m. at A.z. / P.m. outside A.z. | 6.0 | 2.6 | 2.9 | 4.3 | 2.5 | 12.0 | - | - |
| Neurosecretory terminals | | | | | | | | |
| Microvesicle area | 179.5± 68.2 | 15.9 ± 5.0 | 95.9 ± 36 | 48.9 ± 11.7 | 62.9 ± 40.2 | n.d. | 1.4 ± 2.9 | 0.9 ± 2.3 |
| Granule area | 4.4 ± 3.2$^{***}$ | 1.2 ± 1.4$^{***}$ | 0.5 ± 0.7$^{***}$ | 1.4 ± 1.4$^{***}$ | 1.4 ± 1.5$^{***}$ | n.d. | 0.1 ± 0.3 | 0.2 ± 0.4 |
| Microvesicle area / Granule area | 40.8 | 13.3 | 191.8 | 34.9 | 44.9 | n.d. | - | - |
| P. m. | 3.7 ± 1.8 | 1.6± 1.1 | 0.6 ± 0.7 | 0.7 ± 1.1 | 1.8 ± 1.2 | n.d. | 0 | 0.1 ± 0.3 |

Values represent the number ± standard deviation of gold particles per unit area ($\mu m^2$) or in the case of the plasma membrane (P.m.) per unit length (μm). The active zone area relates to the cytoplasmic area within 100 nm of the active zone (A.z.). The vesicle area (V. area) is located outside the active zone area. The number of gold particles at the plasma membrane of the active zone (P.m. at active zone) was compared to the number of gold particles of the nerve terminal plasma membrane outside the active zone (P.m. outside active zone). In the neurosecretory terminals the number of gold particles was determined in domains highly enriched in microvesicles (microvesicle area) or granules (granule area) or at the plasma membrane (P.m.). For mossy fiber synapses the number of area and length profiles analyzed was between 15 and 38, and 16 and 41, respectively. For neurosecretory terminals it was between 15 and 28, and 16 and 22, respectively. Control-M and Control-P, controls for secondary antibodies used for the localization of monoclonal and polyclonal antibodies, respectively. N-CaCh, N-type $Ca^{2+}$ channel; n.d. not determined. $^{*}$, $^{**}$, $^{***}$: P values smaller than 0.05, 0.01 and 0.001, respectively when values are compared to those shown in the line above.

## Photographic Plate I

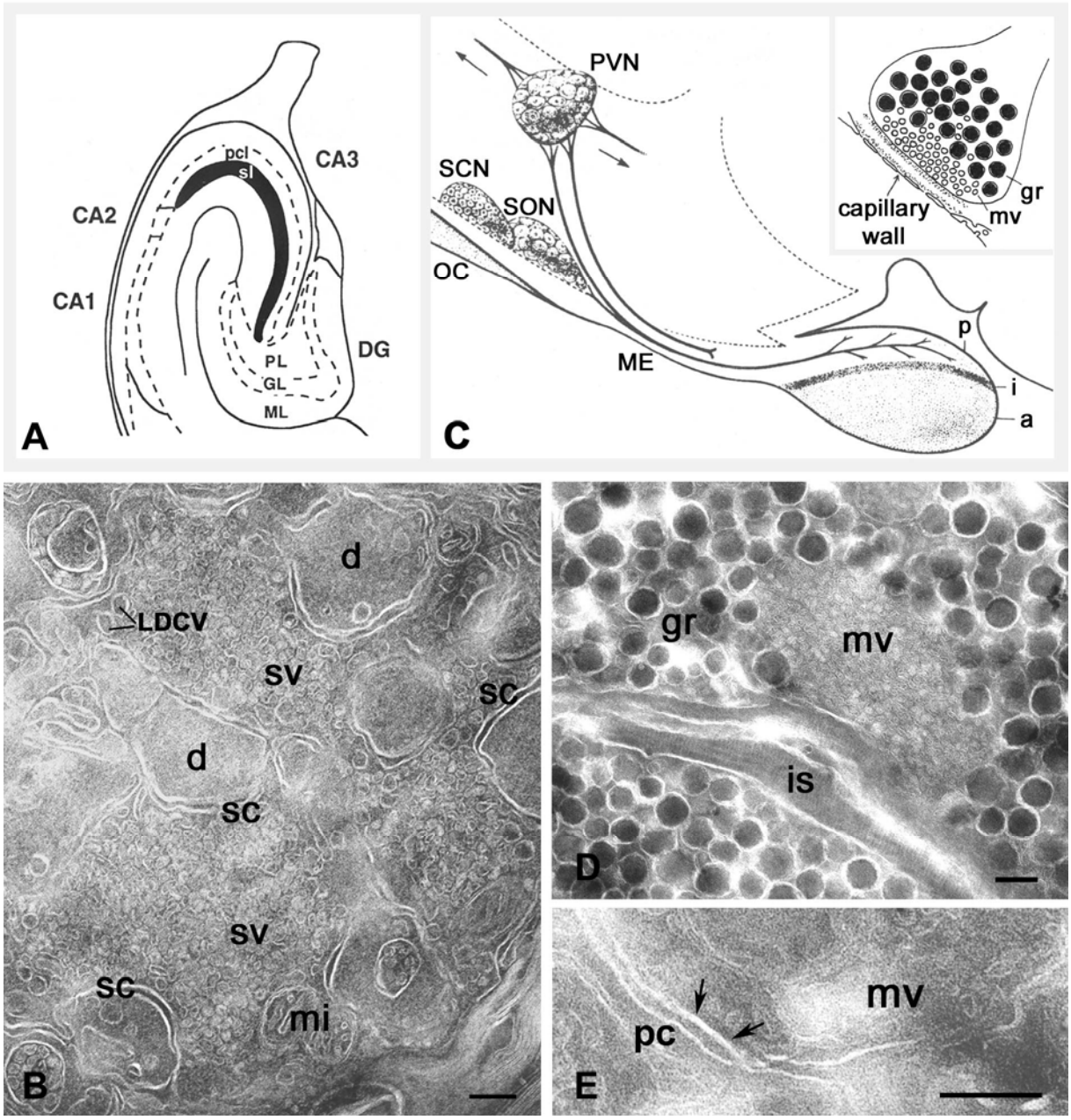


Fig.2. General observation of mossy fiber terminals in the hippocampus and of neurosecretory terminals in the neurohypophysis. (A) Position of mossy fiber terminals in the rat hippocampus. The mossy fiber terminals are located in the narrow stratum lucidum just next to the pyramidal cell layer in CA3 region. (Modified from Anaral and Witter, 1995). (B) Ultrastructure of the mossy fibers terminals in the CA3 region. (C) Neurosecretory system in the rat hypothalamus und neurohypophysis (modified from Brownstein et al., 1980). The insert shows a neurosecretory terminal contacting a blood capillary (modified from Navone et al., 1989). (D) Large dense core neurosecretory granules and clustered electron-lucent microvesicles in axonal terminals. Microvesicles are often clustered beneath the plasma membrane facing the collagen-rich interstitial space. (E) Synaptoid contact (arrows) between nerve terminal and pituicytes. d, dendritic spines; DG, dentate gyrus; GL, granule cell layer; gr, granules; is, interstitial space; LDCV, large dense core vesicles; ME, median eminence; mi, mitochondria; ML, molecular layer; mv, microvesicles; OC, optic chiasma; p, i and a, posterior, intermediate and anterior lobe of the pituitary, respectively; pc, pituicytes; pcl, pyramidal cell layer; PL, polymorphic layer; PVN, paraventricular nuclei; sc, synaptic contact; SCN, suprachiasmatic nuclei; sl, stratum lucidum; SON, supraoptic nuclei; sv, synaptic vesicle. Scale bar = 200 nm

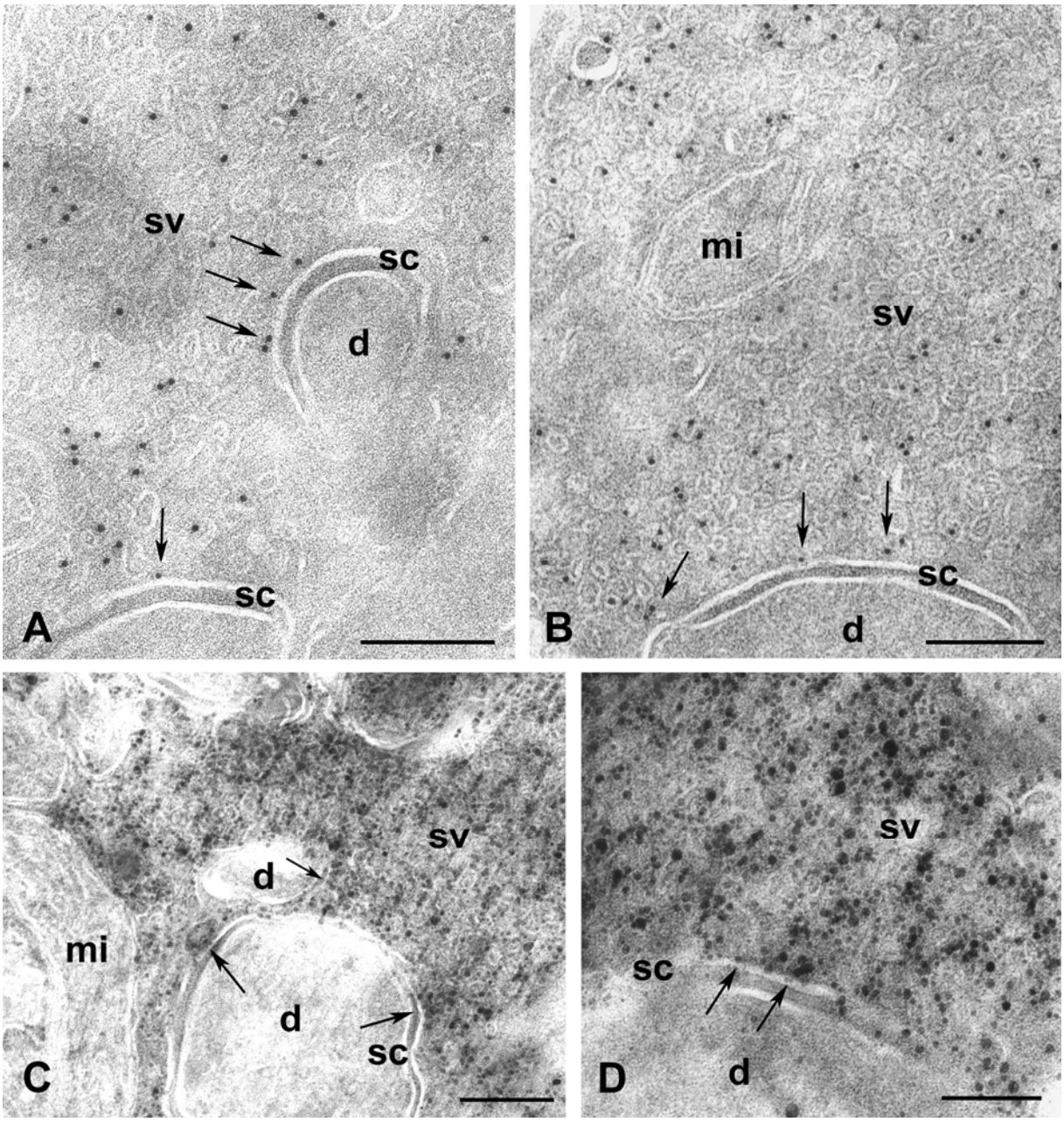


Fig.3. Immunolabeling for VAMP II in mossy fiber terminals of the hippocampal CA3 field. (A, B) Abundant VAMP II gold particles are located selectively over the densely packed electron-lucent vesicles. Some gold particles occur at docked vesicles and in close proximity to the presynaptic membrane at active zones (arrows). No gold particles on dendrites and mitochondria. (C, D) As compared with A and B, higher labeling density in synaptic vesicle area and more gold particles at the active zone (arrows) displayed by the cryo-immunogold technique with the silver enhancement method. d, dendrite; mi, mitochondria; sc, synaptic contacts; sv, synaptic vesicle. Scale bar = 200 nm

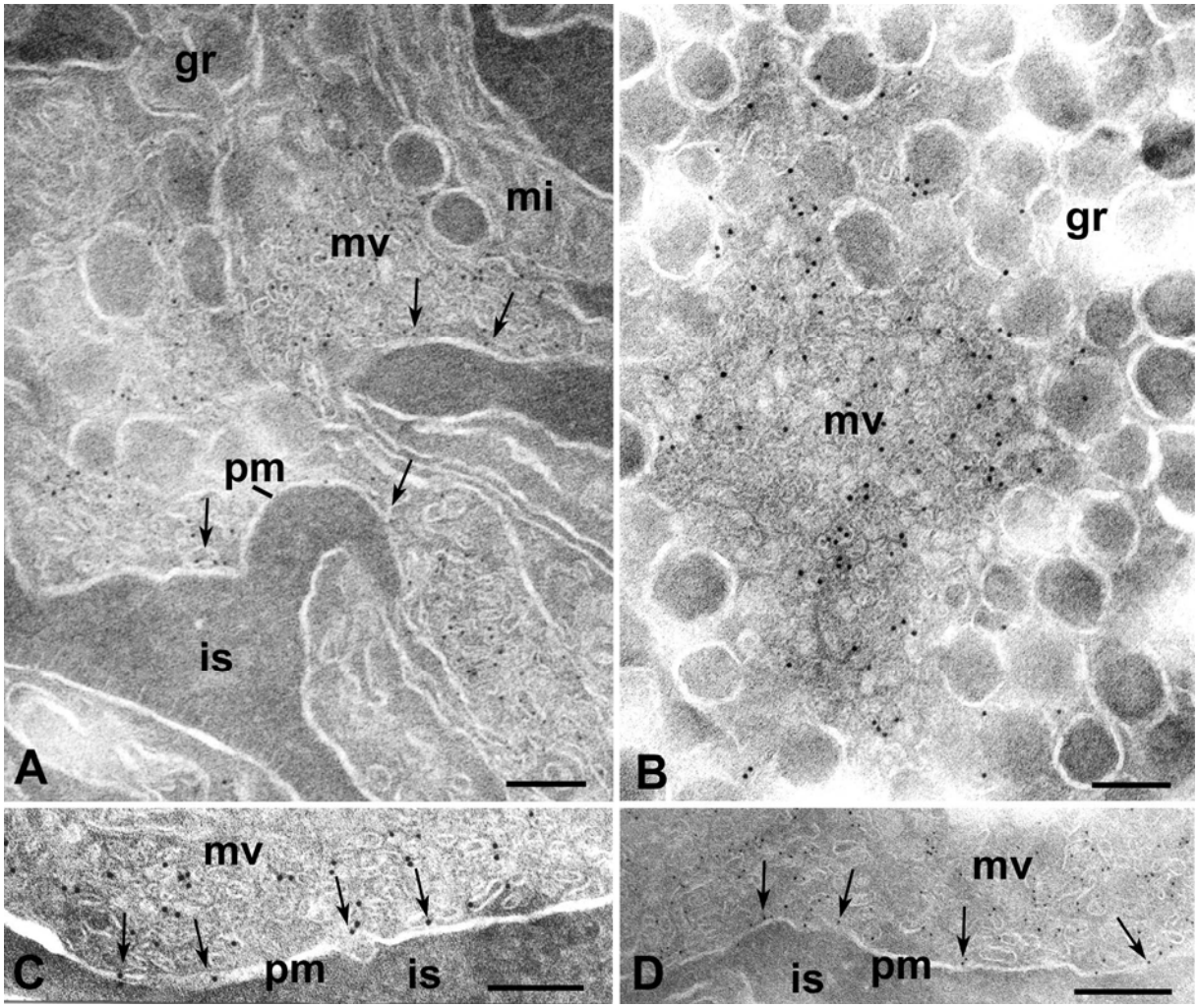


Fig.4. Immunolabeling for VAMP II in neurosecretory terminals of the neurohypophysis. (A) Overview in the area next to the intersititial space. Labeling occurs selectively in the region of the clustered microvesicles and is absent from granules, mitochondria and interstitial space. Some gold particles are present at microvesicles very close to or at the plasma membrane (arrows). (B) Labeled clustered microvesicles and the surrounding unlabeled granules. Sparse labeling also on the granules adjacent to microvesicles. (C, D) Labeled microvesicle cluster near the axonal plasma membrane facing the intersititial space and some labeling on the microvesicles closely adjacent to and on the plasma membrane (arrows). A and D with 5 nm gold particles. gr, granule; is, interstitial space; mi mitochondria; mv, microvesicle; pm, plasma membrane. Scale bar = 200 nm

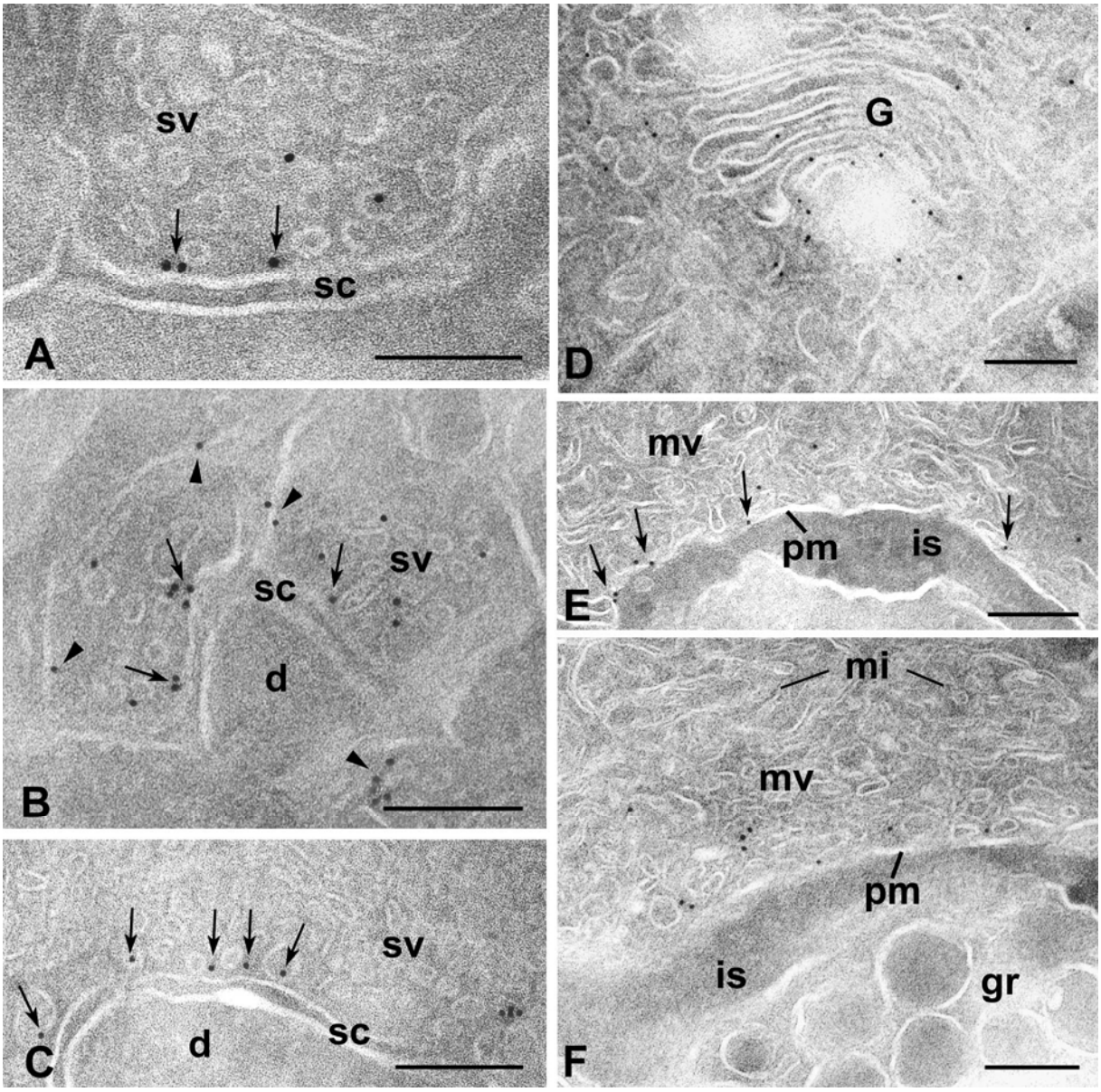


Fig.5. Immunolabeling for the t-SNARE SNAP-25 in hippocampal nerve terminals and neurohypophysial nerve terminals. (A) Immunolabeling is localized at the plasma membrane of the active zone (arrows) and at synaptic vesicles. (B) Gold particles are also found at the plasma membrane outside the active zone (arrowheads) besides the active zone membrane (arrows) and synaptic vesicles in the small nerve terminals of the hippocampus. (C) Gold particles at synaptic vesicles near the active zone of the mossy fiber terminal (arrows) implying the association of SNAP-25 with the presynaptic docking complex. (D) Gold particles are located at the Golgi complex. (E) Dispersely distributed gold particles at the plasma membrane (arrows) of neurosecretory endings. (F) Immunolabeling on microvesicles adjacent to the plasma membrane and at the plasma membrane (arrows). Granules and mitochondria are unlabeled. d, dendrite; G, Golgi complex; gr, granule; is, interstitial space; mi, mitochondria; mv, microvesicle; pm, plasma membrane; sc, synaptic contact; sv, synaptic vesicle. Scale bar = 200 nm

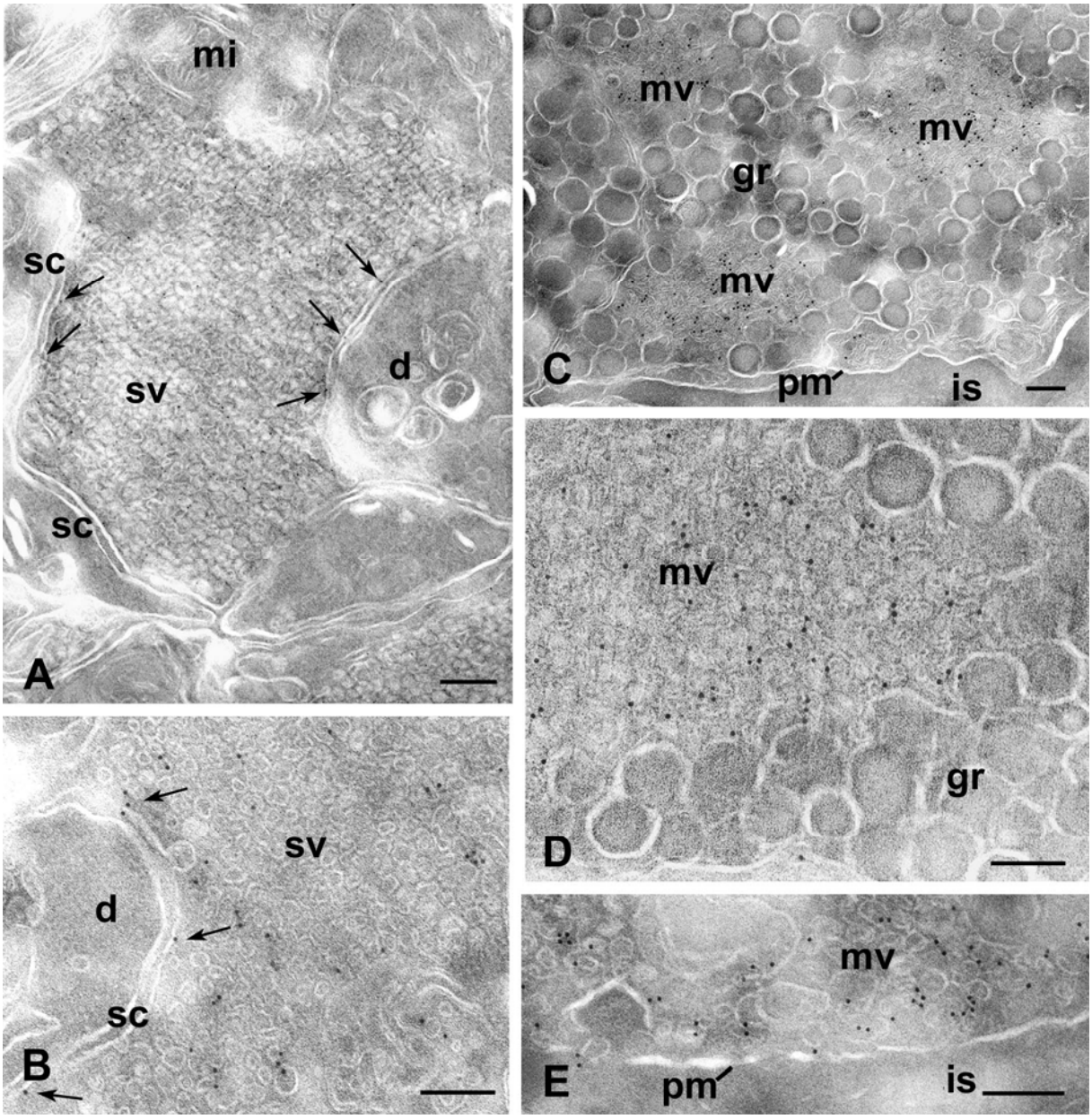


Fig.6. Immunolabeling for SV2 in hippocampal mossy fiber terminals and neurohypophysial nerve terminals. (A, B) Gold particles in mossy fiber terminals are associated extensively with synaptic vesicles. Some of them are located at docked vesicles or at the active zone membrane (arrows). 5 nm gold particles was used in A. Dendrites and mitochondria are free from the gold particles. (C, D) Immunolabeling in neurosecretory endings is restricted only to the clustered microvesicles and absent from granules. (E) Immunolabeling at clustered microvesicles near the plasma membrane. Few gold particles occur at the plasma membrane. d, dendrite; gr, granule; is, interstitial space; mi, mitochondria; mv, microvesicle; pm, plasma membrane; sc, synaptic contacts; sv, synaptic vesicle. Scale bar = 200 nm

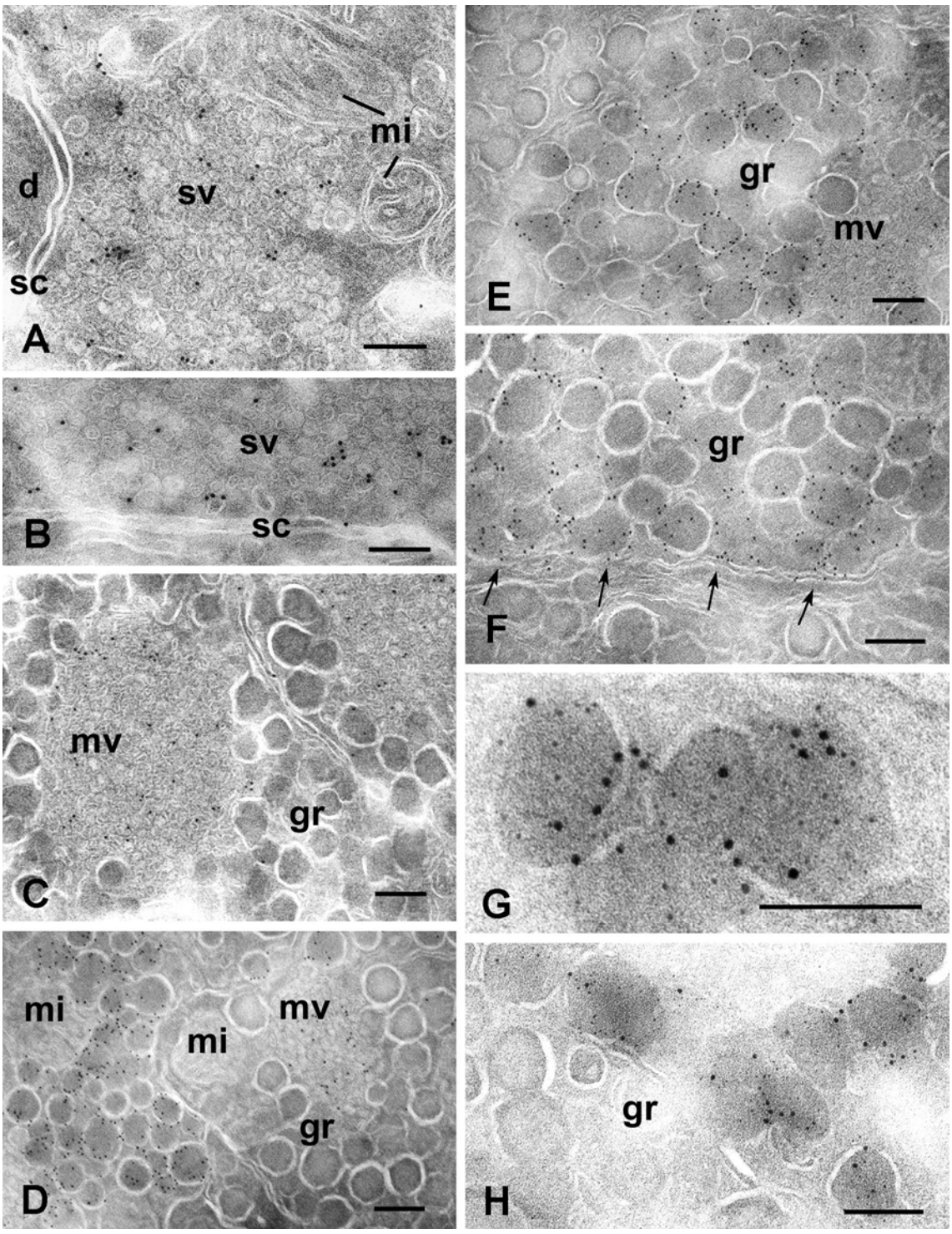


Fig.7. Immunolabeling for Rab3A in mossy fiber terminals of the hippocampus and neurosecretory terminals of the neurohypophysis. (A) Immunolabeling is localized specifically to synaptic vesicles. Mitochondria and dendrite are clearly devoid of gold particles. (B) Randomly distributed immunolabeling near the active zone of a mossy fiber terminal. (C) Clustered microvesicles selectively carry gold particles, whereas granules surrounding the labeled microvesicles in the same terminal have no labeling. (D, E) Two adjacent terminals showing two types of granule populations with or without immunolabeling, respectively. Clustered microvesicles are always labeled. Mitochondria in (D) were obviously free of gold particles. (F) Gold particles are present on granules close to the plasma membrane and some of them on the plasma membrane (arrows). The granules and the plasma membrane in the nearby terminal are devoid of gold particles. (G, H) Double labeling for Rab3A and oxytocin, showing colocalization of these two proteins in the same granules, 10 nm gold particle for Rab3A and 5 nm for oxytocin. Neither of them occurs on the other group of granules in the nearby terminal. d, dendrite; gr, granule; is, interstitial space; mi, mitochondria; mv, microvesicle; sc, synaptic contacts; sv, synaptic vesicle. Scale bar = 200 nm.

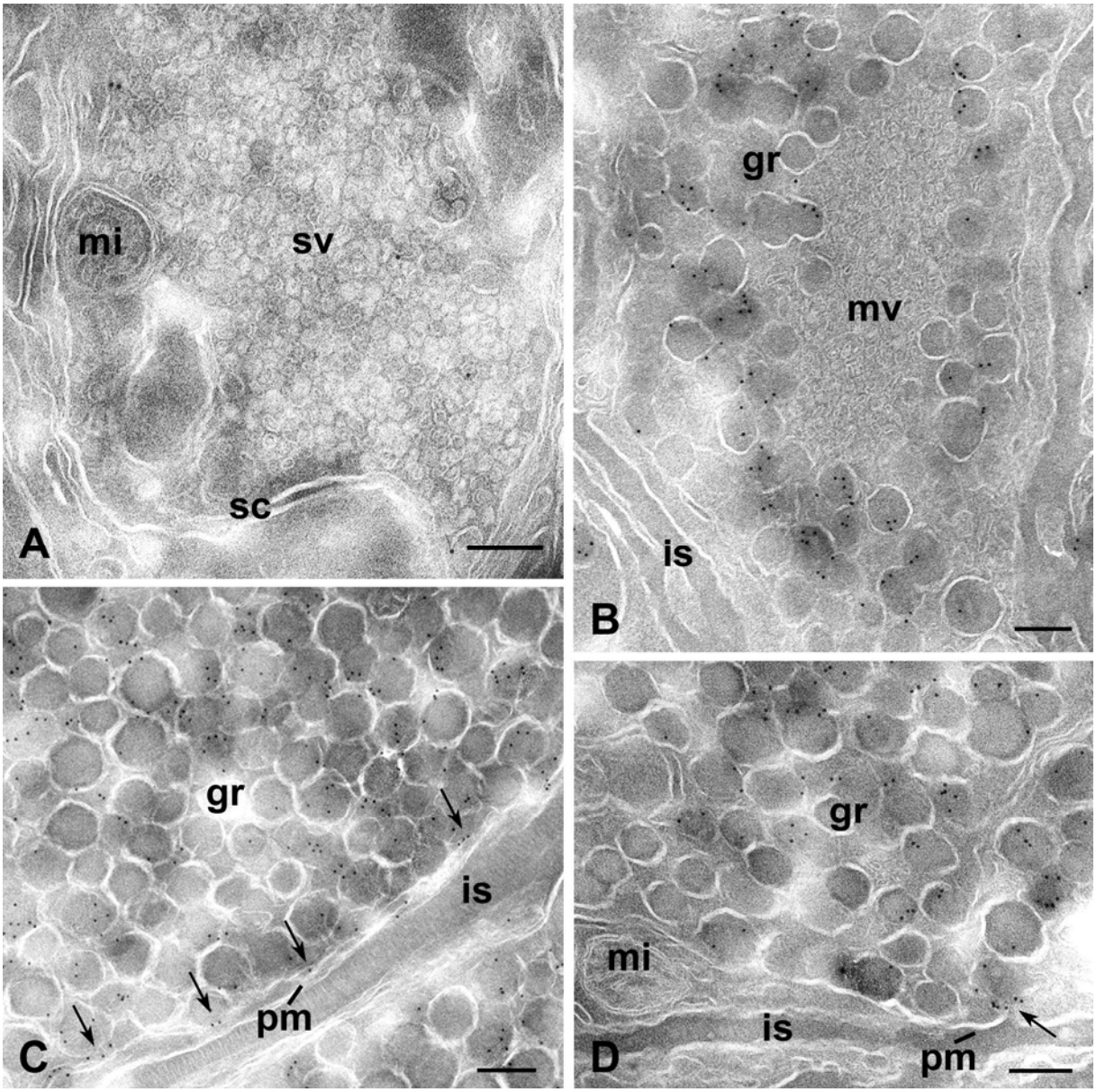


Fig.8. Immunolabeling for α/β SNAP in hippocampal mossy fiber terminals and neurohypophysial nerve terminals**.** (A) Little labeling occurs in the synaptic terminal. (B) Gold particles are associated specifically with neurosecretory granules in the neurohypophysial terminals, forming a clear contrast to the unlabeled microvesicles. (C) Labeled granules close to the plasma membrane, showing the gold particles at docked granules or at the plasma membrane (arrows). (D) Gold particles are associated with the connecting part of a granule that shows an Ω-formation with the plasma membrane (arrow). The interstitial space and mitochondria are free of gold particles. gr, granule; is, interstitial space; mi, mitochondria; mv, microvesicle; pm, plasma membrane; sc, synaptic contacts; sv, synaptic vesicle. Scale bar = 200 nm

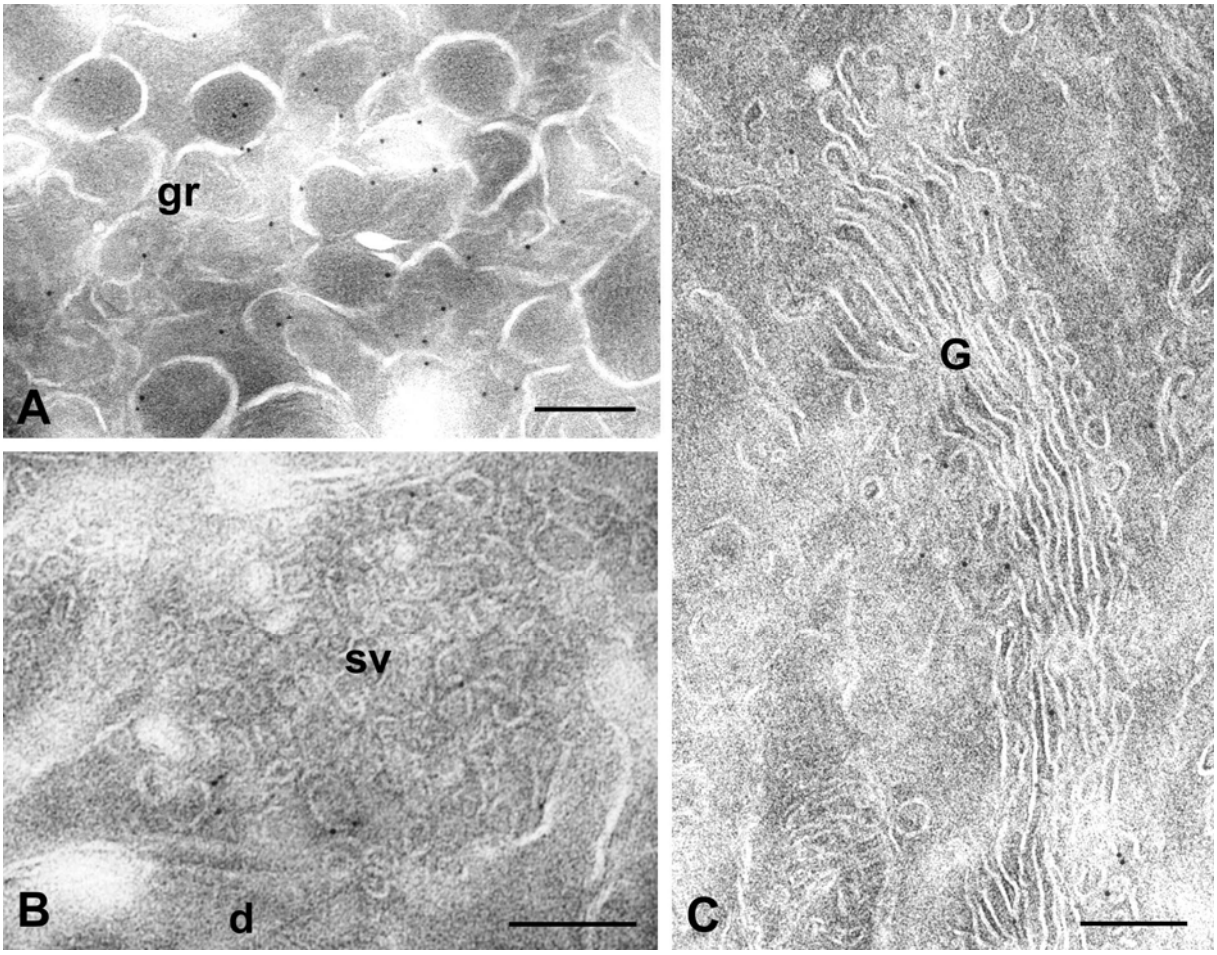


Fig.9. Immunolabeling for NSF. (A) Some labeling is located at the granules in the neurohypophysis. (B) Low labeling with 5 nm gold particles at synaptic vesicles of the central synapse. (C) Some gold particles occur at a Golgi complex in the CA3 region. d, dendrite; G, Golgi complex; gr, granule; sv, synaptic vesicle. Scale bar = 200 nm

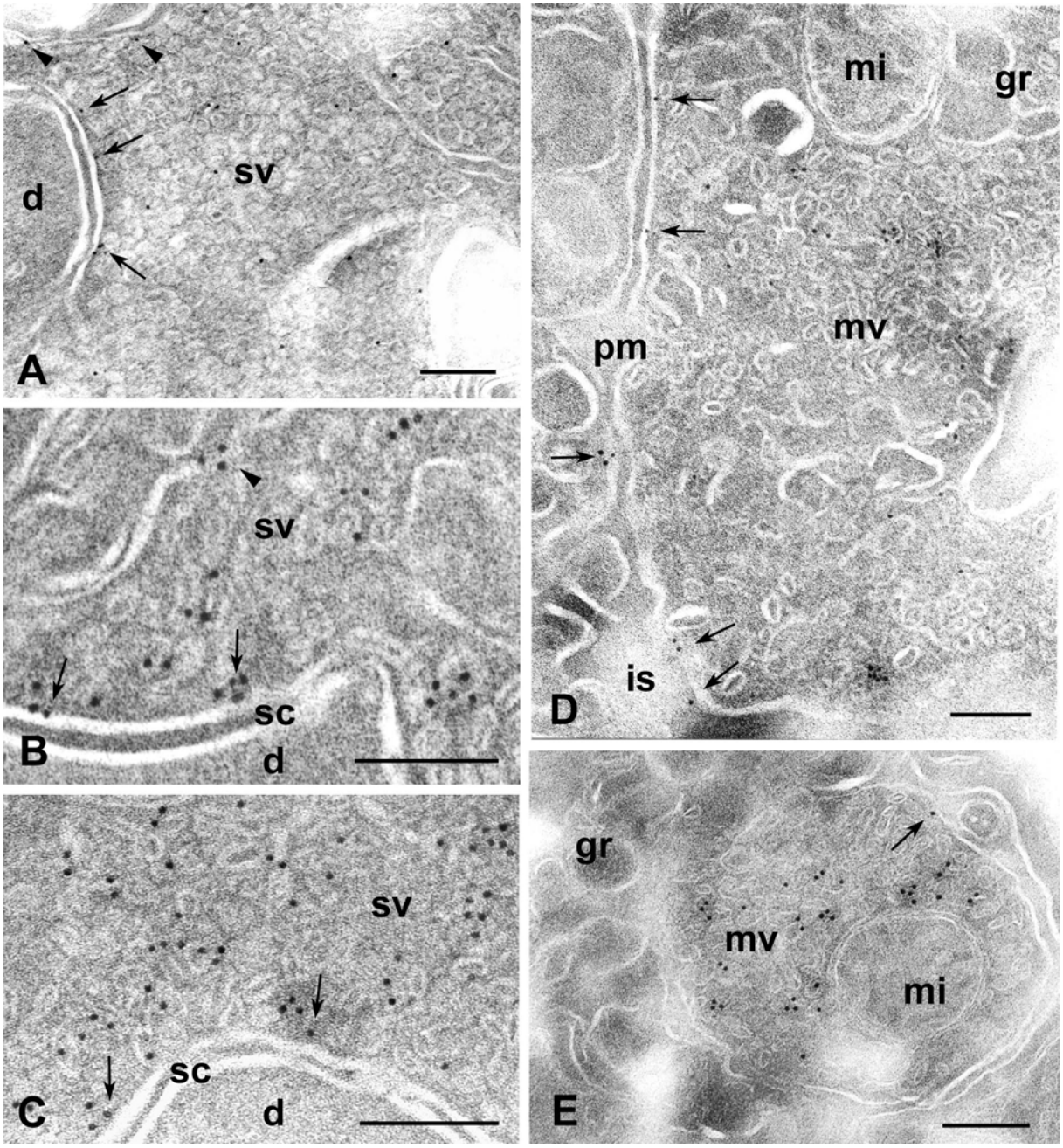


Fig.10. Immunolabeling for the N-type $Ca^{2+}$ channel in the hippocampal mossy fiber terminals and neurohypophysial nerve terminals. (A-C) Immunolabeling in mossy fiber terminals with gold particles located to the synaptic vesicles and the presynaptic membrane at the active zone (arrows) and outside the active zone (arrowhead). (D, E) Immunolabeling in neurosecretory endings is confined to microvesicles and the plasma membrane (arrows). Granules and mitochondria are free of gold particles. d, dendrite; gr, granule; is, interstitial space; mi, mitochondria; mv, microvesicle; pm, plasma membrane; sc, synaptic contacts; sv, synaptic vesicle. Scale bar = 200 nm

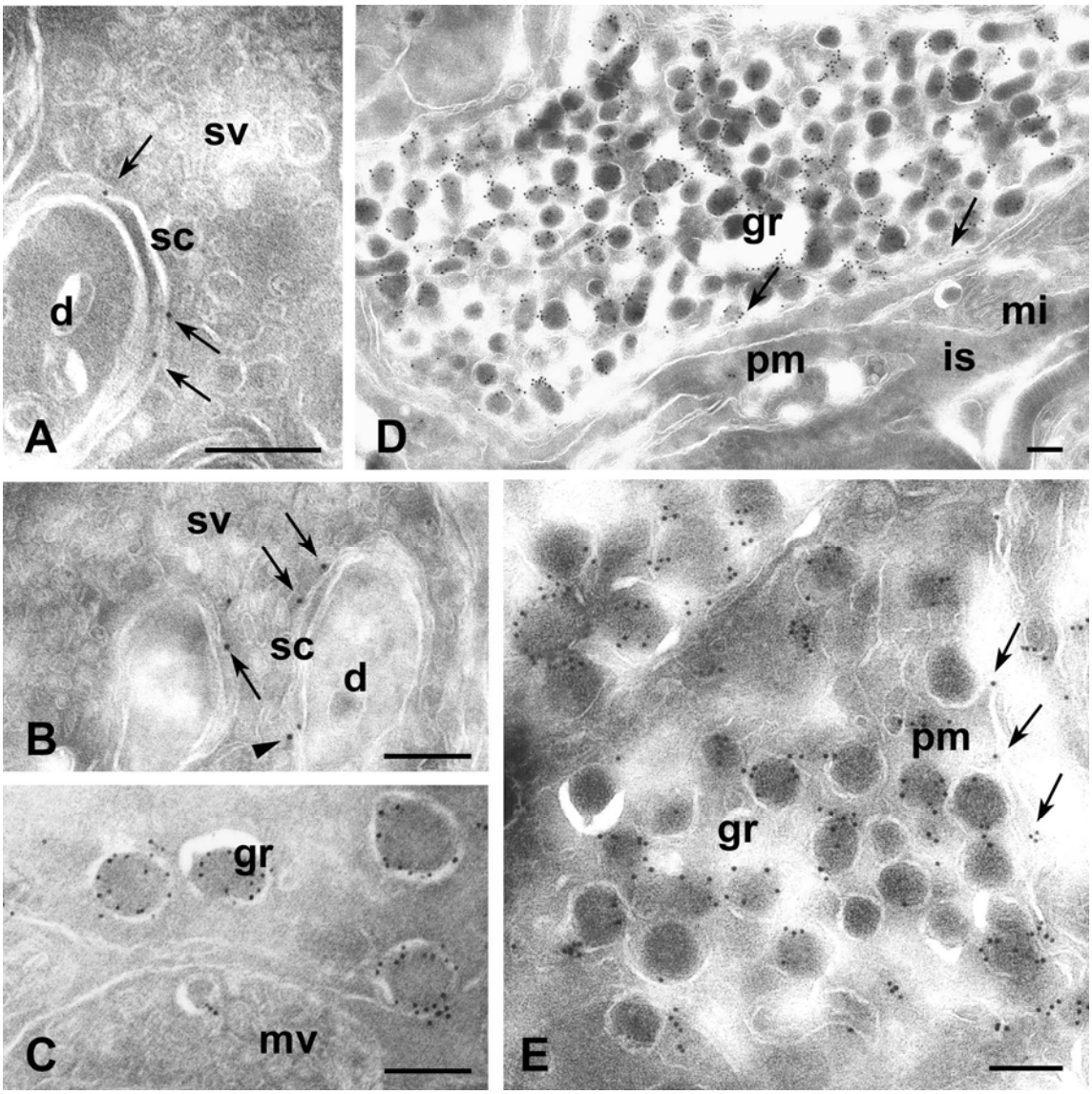


Fig.11. Immunolabeling of P/Q-type $Ca^{2+}$ channels in hippocampal mossy fiber terminals and neurohypophysial nerve terminals. (A, B) Immunolabeling in mossy fiber terminals with a few gold particles specifically at the plasma membrane at the active zone (arrows) and outside the active zone (arrowhead). However, little labeling occurs at the synaptic vesicles. (C-E) Gold particles are associated intensively with a population of granules in some terminals of the neurohypophysis. Some are also present at the plasma membrane (D, E; arrows). No labeling occurs over microvesicles in a sharp contrast to the labeled granules (C). d, dendrite; gr, granule; is, interstitial space; mi, mitochondria; mv, microvesicle; pm, plasma membrane; sc, synaptic contacts; sv, synaptic vesicle. Scale bar = 200 nm

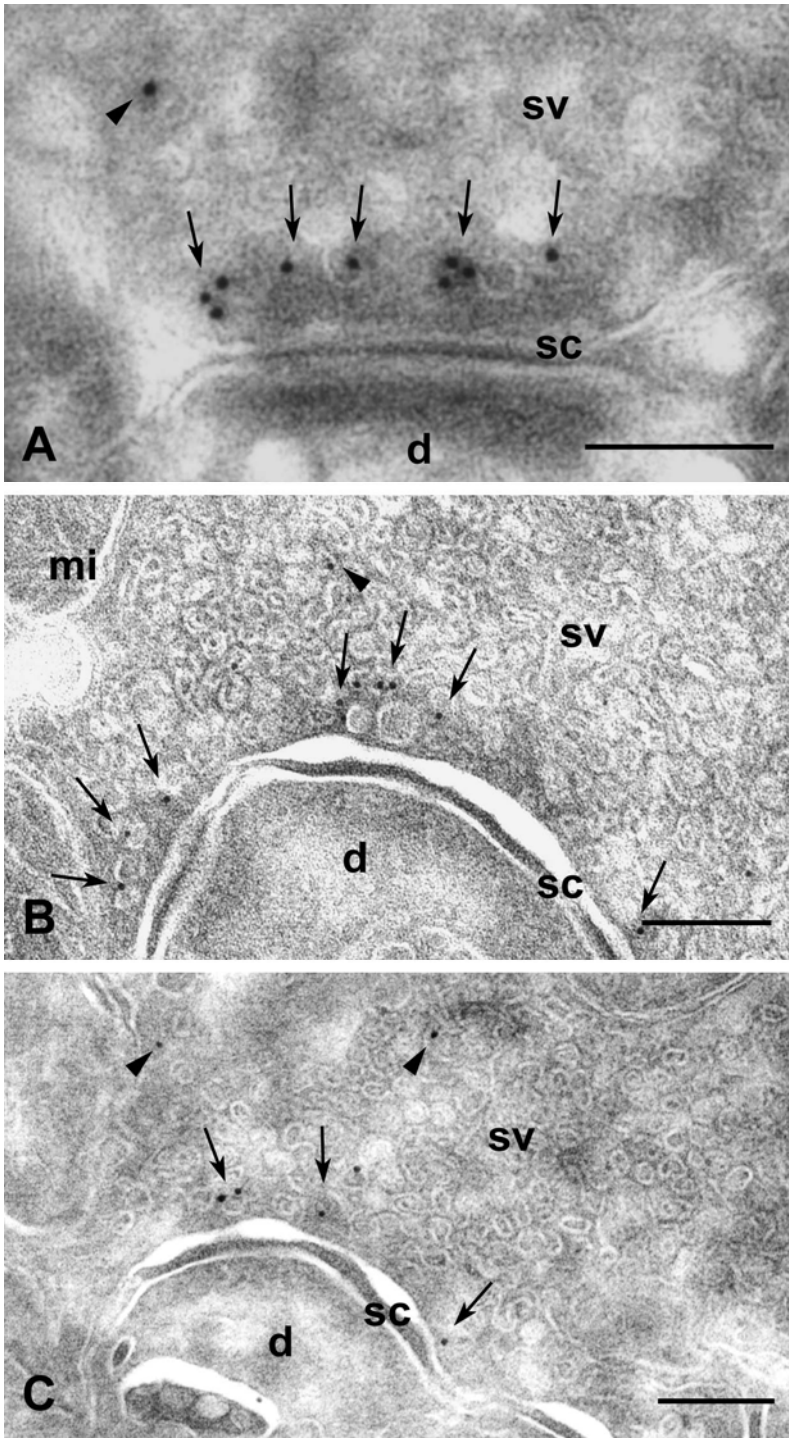


Fig.12. Immunolabeling for Bassoon in the synaptic nerve terminals of the hippocampus. Immunolabeling is localized specifically in proximity to the active zone in a small synaptic nerve terminal (A) and at large mossy fiber terminals (B, C). The majority of the gold particles are characteristically concentrated close to but at a clear distance away from the presynaptic plasma membrane (arrows). Little labeling for Bassoon is observed directly at the plasma membrane. A few particles are also found at vesicles outside the active zone region (arrowheads). d, dendrite; mi, mitochondria; sc, synaptic contacts, sv, synaptic vesicle. Scale bar = 200 nm

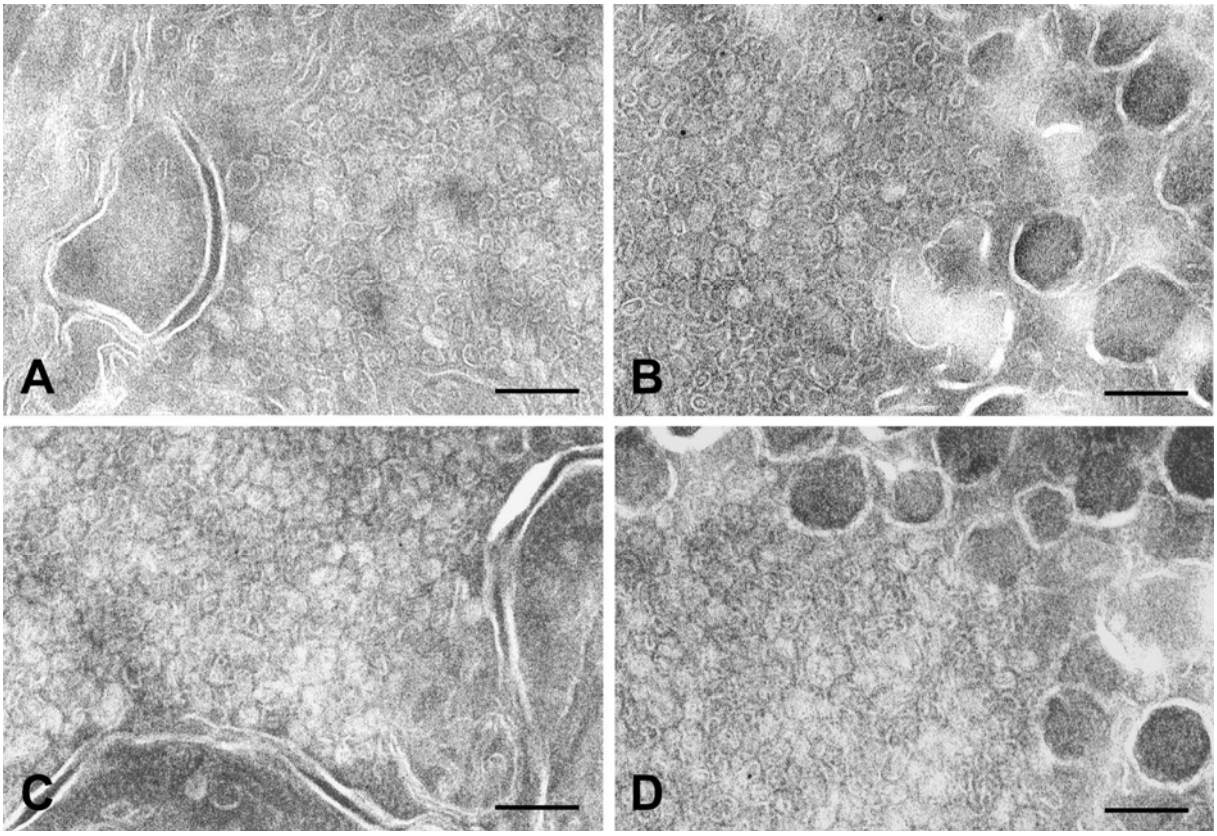


Fig.13. Control experiments with application of goat anti-mouse IgG to mossy fiber terminals (A) and neurosecretory endings (B) or of goat anti-rabbit IgG to mossy fiber terminals (C) and neurosecretory endings (D). No significant labeling is detected. Scale bar = 200 nm

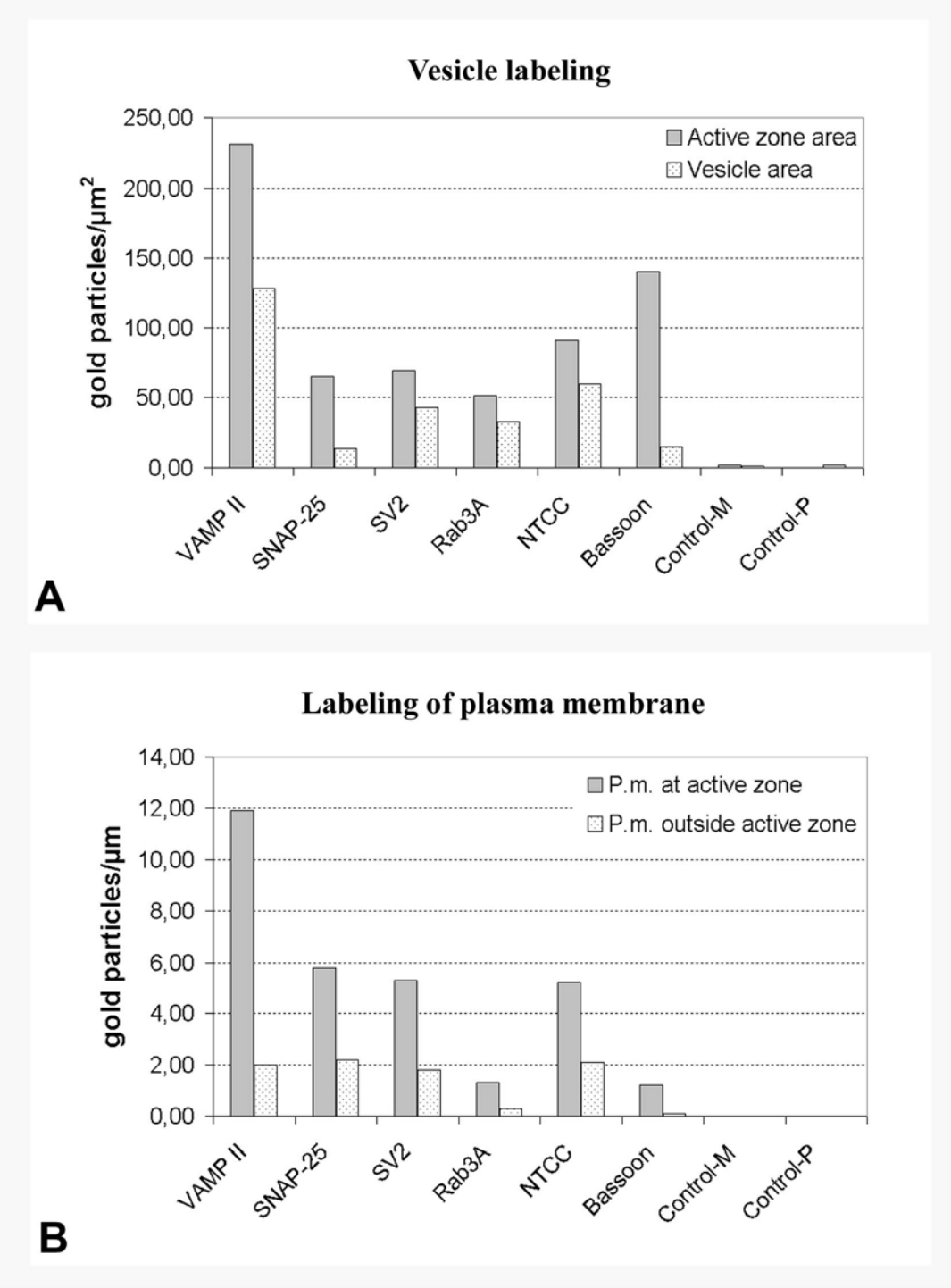


Fig.14. Comparison of the density of immunolabeling of various synaptic proteins in mossy fiber terminals (A) Comparison of vesicle labeling between active zone area and vesicle area outside the active zone. All synaptic proteins investigated display increased labeling in the active zone area. (B) Comparison of labeling of plasma membrane between the active zone (P.m. at active zone) and outside the active zone (P.m. outside active zone). A Higher density of immunolabeling for synaptic proteins occurs at the active zone membrane. Almost no gold particles were detected in controls for both monoclonal (control-M) and polyclonal (control-P) antibodies.

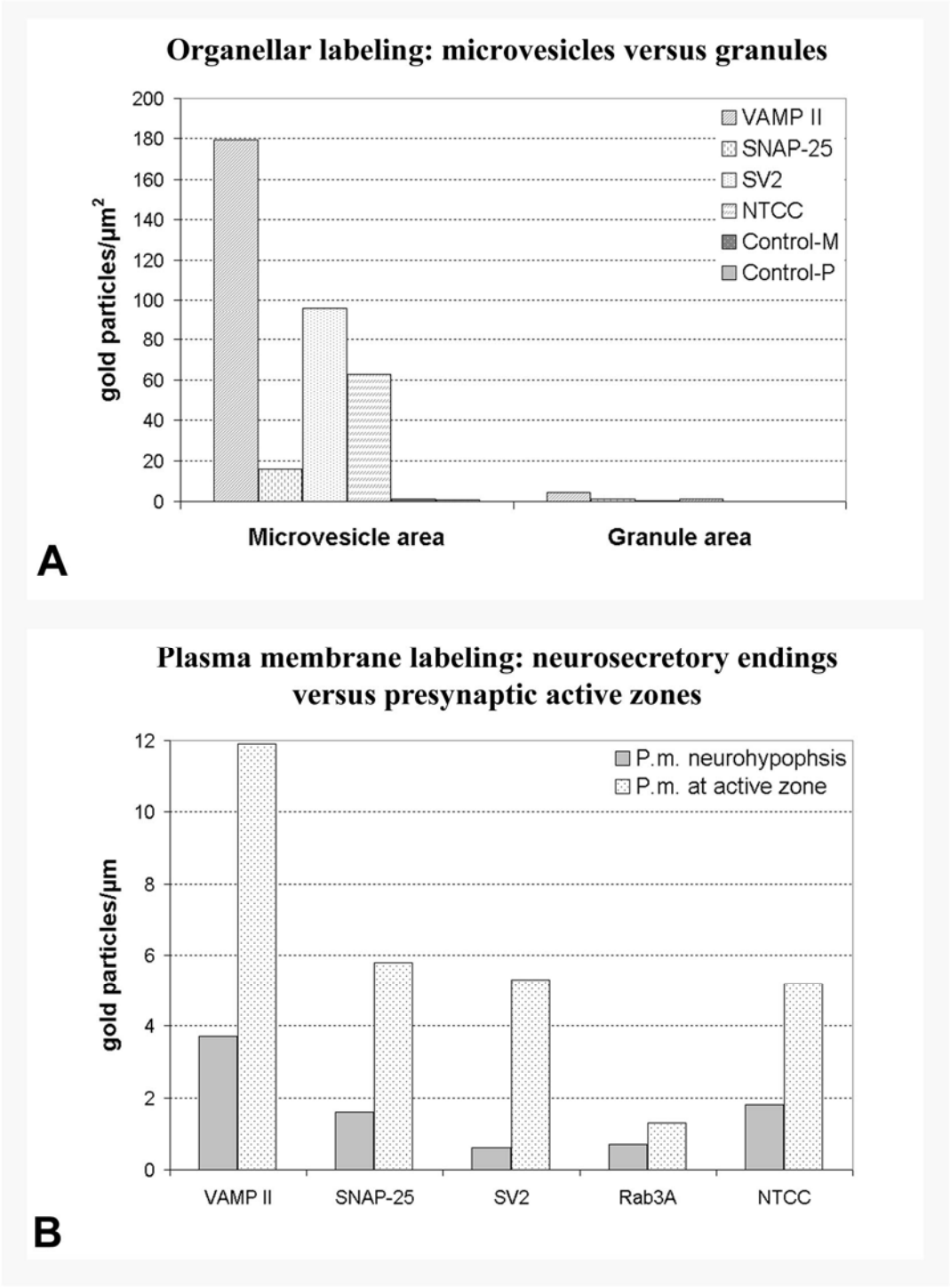


Fig.15. Histogram of immunolabeling densities of various synaptic proteins in the neurohypophysis. (A) Comparison of immunolabeling densities for VAMP II, SV2, SNAP-25 and N-type $Ca^{2+}$ channel in the microvesicle area with those in the granule area. All of the proteins were more highly expressed in the microvesicle area than in the granule area. Immunolabeling in the granule area is very low. Controls for both monoclonal (Control-M) and polyclonal (Control-P) antibodies are almost zero in both areas. (B) Comparison of the immunolabeling densities for various synaptic proteins at the plasma membrane of neurohypophysial terminals with those at the active zone membrane in the presynaptic terminals. Overall, labeling at the former is much lower than that at the latter.

## 3.2. Localization of synaptic proteins in primary astrocyte cultures

A variety of synaptic proteins essential for synaptic transmission have been found in cultured astrocytes and thought to be responsible for astrocytic vesicular exocytosis. In the present study, the conventional preembedding immunocytochemical method was applied to investigate the subcellular localization of these synaptic proteins and to examine whether these synaptic proteins were associated with stimulation-induced endocytotic organelles marked by HRP. However, in the present experiments HRP-filled vacuoles were seen in both stimulated and unstimulated cells, even if great care was taken not to activate cells. Nevertheless, consistent with the results of Maienschein et al. (1999), the vesicle protein VAMP II was localized at vesicular organelles of different size in cells fixed with 3% paraformaldehyde and 0.05% glutaraldehyde in 5 mM hypotonic PB as shown in the Fig.16A. Vesicular organelles and some HRP-filled vacuoles were also labelled in cells that were stimulated with 1 mM glutamate in the presence of HRP and then fixed with the fixative diluted in 5 mM hypotonic PB (Fig.16B). In addition, labelled vesicular organelles were found in the cells treated with the bacterial toxin streptolysin-O (Fig.16C). Streptolysin-O increases the permeability of the cell membrance for the antibodies. The cells treated with streptolysin-O showed fewer vacuolar structures than those fixed in the hypotonic PB.

In order to increase the accessibility of antibodies to antigens, the LR Gold postembedding method, an alternative to cryomicrotomy, was applied to localize the synaptic proteins in the astrocytic cells. The acrylic resin LR Gold has been employed in postembedding immunocytochemistry for the localization of a wide variety of plant and animal antigens (Anaral and Witter, 1995). This method has been considered to improve markedly the immunolabeling efficiency due to the hydrophilic property of LR Gold. Moreover, because the samples can be embedded with LR Gold at low temperature conditions (-20°C), the fine structure and the antigenicity of the proteins are better preserved (Netter and Ingram, 1957; Thorpe, 1999). In agreement with the results obtained with the preembedding immunocytochemical method, vesicular organelles labeled for VAMP II were observed in the cultured astrocytes (Fig.17A), in a clear contrast to the control samples (Fig.17B).

## Photographic Plate II

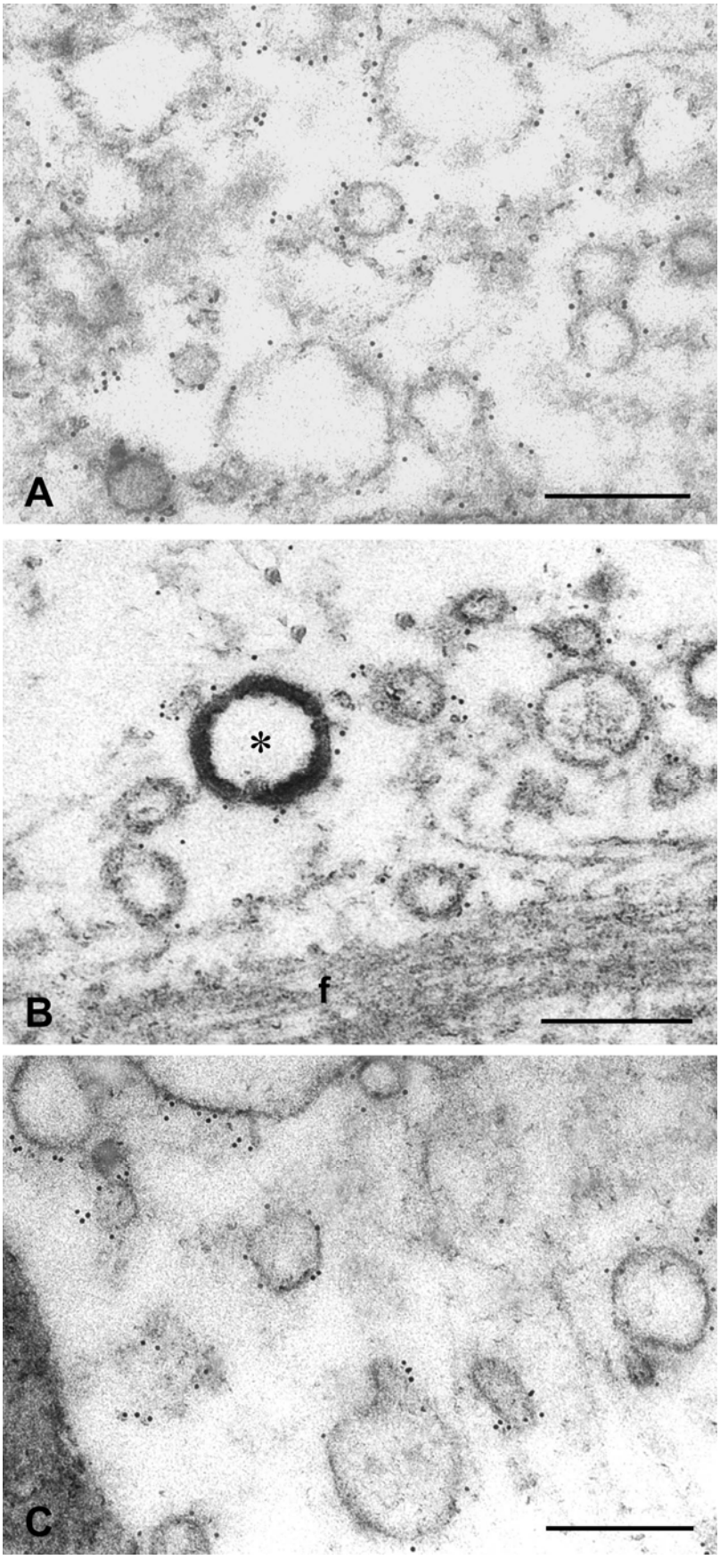


Fig.16. Immunolocalization of VAMP II in the primary astrocyte culture using the preembedding method. (A) Labelled vesicular organelles in cells fixed with 3% paraformaldehyde and 0.05% glutaraldehyde in hypotonic PB (5 mM). (B) VAMP II is localized to vesicular organelles in the cells that were stimulated with 1 mM glutamate in the presence of HRP and then fixed with the same fixative in 5 mM PB. A HRP-filled vacuole is also labelled (asterisk). (C) Labeled vesicular organelles in cells that with the same fixative diluted in PBS and then treated with the bacterial toxin streptolysin-O. f, filaments. Scale bar = 200 nm.

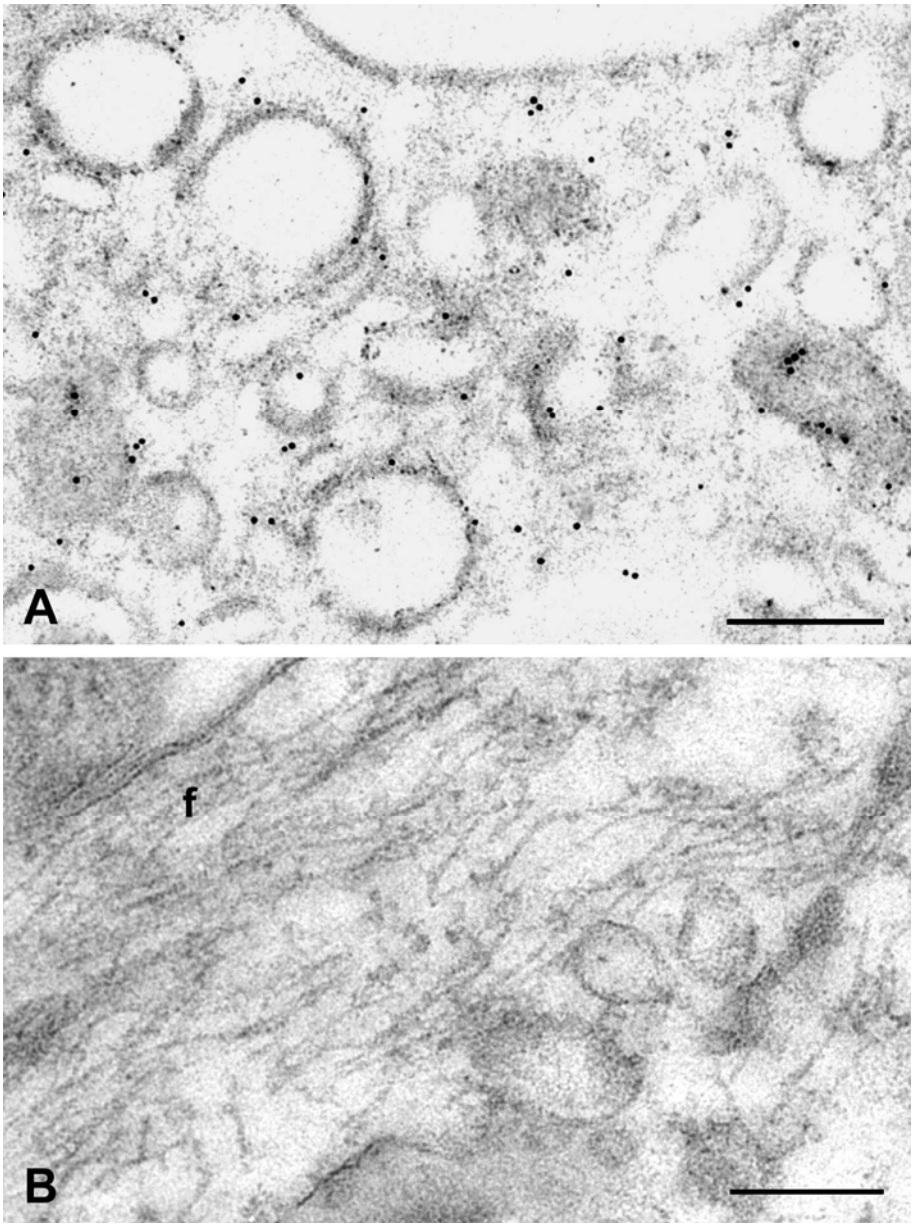


Fig.17. Localization of VAMP II in the primary astrocyte culture using the LR Gold postembedding method. (A) Labeled vesicular organelles of different size. (B) The control sample with application of goat anti-mouse IgG. f, filaments. Scale bar = 200 nm

## 3.3. Expression and localization of transfected proteins in the astrocytoma cell line U373 MG

### 3.3.1. Observation of U373 cells by light and electron microscopy

U373 MG cells generally had very flat shape. Similar to astrocytes in morphology they also showed both protoplasmic and fibrous cellular forms**.** The protoplasmic cells had a large cell body, whereas fibrous cells were provided with relatively small cell body but long processes. Phase-contrast microscopy revealed many dark punctuate organellar structures throughout the cytoplasm.

Under the electron microscope, multiple morphologically distinct intracellular compartments could be distinguished: the nucleus, endoplasmic reticulum, Golgi apparatus, endosomes, mitochondria, heterogeneously sized and shaped electron-lucent vesicular structures, and a few electron dense granules. In particular, U373 MG cells contained a large number of tubules and vesicles throughout the cytoplasm (Fig.18A). Most of the electron-lucent vesicles had a diameter of 40-120 nm. The tubular structures of various lengths were between 40 and 60 nm in diameter. They were intermingled with small vesicles or dispersed individually. In cryo-sections it was difficult to distinguish between cross-sections through the tubules and vesicles. Some vesicular profiles most likely included both tubules and small vesicles. These mixed tubulovesicular structures were often found in close proximity to the TGN areas and endosomes as well as in the peripheral cytoplasm of the cell. Tubular structure in the periphery of the U373 cells could derive from the plasma membrane. They were also observed to be in direct association with the plasma membrane (Fig.18B)**.**

The relatively uniform vesicle populations, consisting mainly of numerous clustered small vesicles with an average diameter of ~50 nm, were often found in the cytoplasm (Fig.19A). In the periphery of the cells some vesicular buds appeared to be budding from tubule-like invaginations of the plasma membrane (Fig.19B). Many clustered small round vesicles were clearly generated from plasma membrane-associated tubulovesicular structures or the endosome-vacuole-like structure in the periphery of the cells (Fig.19C, D) and in the cytoplasm (Fig.19E, F). These structures might therefore represent donor compartments of these small vesicles.

Many endosomes were found to distribute among these vesicular organelles. They were comprised of vacuolar and tubulovesicular subdomains (Fig.25B**)**. The large electron-lucent

endosomal vacuoles were round, oval or oblate in shape. They were empty or contained some material and a few internal vesicles. The tubulovesicular membrane profiles were observed to be in close association with endosomal vacuoles. In addition, multivesicular bodies and lysosomes occurred among clustered tubulovesicles. The spherical multivesicular bodies (300-600 nm) were full of internal small vesicles and enclosed by a limiting membrane (Fig.25A, G, H). The abundant internal vesicles were relatively uniform in size and shape and measured 50-70 nm in diameter. However, the oval or irregularly shaped lysosomes were filled mainly with electron dense material, sometimes together with obscure degraded internal membrane vesicles (Fig.25E, F; Fig.27F)**.**

### 3.3.2. Immunolocalization of recombinant proteins

The very weak immunosignal for the endogenous proteins VAMP II, syntaxin I, SNAP-25 and Rab5 in immunoblots of subcellular fractions obtained in our laboratory implied that endogenous contents of these proteins are very low in U373 cells. Therefore, only the cells that had been transfected with tagged recombinant proteins were used in the present experiments. Transiently transfected cells revealed intense immunoreactivity in immunofluorescent microscopy. All proteins investigated exhibited a punctuate cellular distribution pattern. The differently sized immunopositive dots corresponded largely to the dark punctuate structures in phase contrast optics. To more precisely characterize the subcellular compartments occupied by these recombinant proteins, the cryo-immunogold technique was adopted in the further study. At the ultrastructural level, every protein exhibited its own unique distribution pattern with electron-lucent vesicular organelles. The nucleus and mitochondria were clearly free of the gold particles for all proteins.

**VAMP II**

VAMP II is an essential member of the synaptic SNARE complex. As a v-SNARE, VAMP II is associated mainly with the membrane of vesicular structures. The transfected U373 cells revealed a high expression level of the recombinant myc-VAMP II protein, which was immunolocalized via monoclonal antibody directed against the myc-tag in the present study. The immunoreactivity of myc-VAMP II showed a diffuse punctuate staining pattern throughout the cell body under the immunofluorescent microscope. Myc-VAMP II was associated with large and numerous fine puncta scattered in the cytoplasm and more concentrated in the perinuclear area. Furthermore, the immunolabeling not only occurred in the cell body, but also

in the cellular processes (Fig.20A, B). The immunopositive dots were detected in the long processes of fibrous U373 cells up to their tips.

The immunoelectron microscopy on cryo-sections revealed that the expressed myc-VAMP II was organelle-associated. The labeled clustered vesicles, tubulovesicular organelles, Golgi apparatus, endosomes, multivesicular bodies, and lysosomes are likely to correspond to the various puncta observed with the fluorescence microscopy. Strikingly, the gold particles were predominantly localized at the membrane of the numerous electron-lucent vesicular structures of various sizes and shapes (round, oval and tubular) that were distributed individually or clustered in the cytoplasm (Fig.21A-C). Clearly, it is difficult to distinguish morphologically between VAMP II-carrying vesicles and cross-sectioned tubules in the cryosections. The extensively distributed VAMP II-containing tubulovesicular organelles were often observed in the cell periphery (Fig.21D) and in the vicinity of the nucleus (Fig.21E, F). And particularly, some populations of relatively regular-sized small vesicles with a diameter of 50-70 nm were usually labeled intensively (Fig.22A, B). Furthermore, fragmenting tubules were labelled (Fig.22C). Gold particles were also seen on some smaller vesicular profiles that were budding from tubules in the cytoplasm (Fig.22D-F). This indicated the formation of small vesicles by budding from these tubular structures. In addition, in the perinuclear part of the U373 cells, the endoplasmic reticulum (ER, Fig.23A) and the Golgi apparatus were intensively labeled (Fig.23B, C). Myc-VAMP II was observed to selectively accumulate at TGN vesicles of the Golgi apparatus, but there was only low labeling on the Golgi cisternae. Gold particles were occasionally found on the membrane of the electron dense granules that were dispersed in the cytoplasm (Fig.23D, E). In some overexpressed cells a high density of gold particles was located at the plasma membrane (Fig.24A-D). The clustered or individually distributed tubulovesicular organelles close to the plasma membrane were also clearly labeled. These labeled organelles beneath the plasma membrane possibly correspond to the donor compartments of synaptic-like microvesicles in PC12 cells (Schmidt et al., 1997). Occasionally, gold particles were also detected on omega-shaped structures at the plasma membrane (Fig.24E) and filopodial membrane processes (Fig.24F). In addition, gold particles are observed over presumptive endosomes, multivesicular bodies, and lysosomes (Fig.25). Myc-VAMP II was localized to the membrane of the large, oval or oblate shaped vacuoles and especially to associated tubulovesicles of the endosomes situated in the cell periphery (Fig.25A) and scattered in the cytoplasm (Fig.25B-F). The more regular, round multivesicular bodies were also immunopositive for myc-VAMP II. The gold particles were found on the

membrane of the internal vesicles and some of them on the limiting membrane (Fig.25A, G, H). In addition, the membrane of the electron dense lysosomes was usually labeled, showing partial targeting of VAMP II to the degradative pathway (Fig.25E, F).

**Syntaxin I**

The transfected U373 cells were intensely labeled for the recombinant t-SNARE syntaxin I as revealed by fluorescence microscopy. VSVG-syntaxin I was immunolocalized via monoclonal antibodies raised against either the VSVG-tag or snytaxin I itself. In addition, syntaxin I was also directly visualized under fluorescence microscope by RFP fused to syntaxin I. Immunofluorescent puncta for syntaxin I were revealed throughout the entire cell body and accumulated in the perinuclear region (Fig.26A, C, D). Furthermore, immunolabeling was detected along long processes of the fibrous cells (Fig.26B). Immunoelectron microscopy on the cryo-sections showed that VSVG-syntaxin I was associated mostly with vesicles (40-100 nm in diameter) in the cytoplasm including the area near the plasma membrane (Fig.27A, B). However, no significant gold labeling of the plasma membrane was observed. In addition, the gold particles were visible on the long and thin tubular structures with a diameter of 40-60 nm (Fig.27C, D). Endosomes were also labeled (Fig.27E). Gold particles were located on the membrane of the round endosomal vacuoles and surrounding vesicles around. Electron dense lysosomes containing electron dense material and some obscurely degraded internal vesicles beneath the limiting membrane was virtually devoid of gold particles, whereas the vesicles next to it were clearly labeled (Fig.27F).

**SNAP-25**

In the experiments with the recombinant t-SNARE HA-SNAP-25, the expression of the protein was limited to only a few transfected cells. The majority of U373 cells revealed no immunoreactivity by immunofluorescence microscopy. The transfected small cells were intensely labeled, showing a relatively high expression level. Recombinant HA-SNAP-25 was immunolocalized by monoclonal antibodies directed against the HA-tag or the SNAP-25 protein. Immunofluorescence of HA-SNAP-25 was associated with numerous fine puncta throughout the entire cell and revealed an enhanced perinuclear location, similar to the pattern of immunoreactivity observed for other transfected proteins (Fig.28A-C). No immunofluorescent fibrous cells with long processes were detected. At the ultrastructural level, the labeling of HA-SNAP-25 was observed only on some electron-lucent vesicular organelles of varing size and form (Fig.28G, H). No gold particles were found at the plasma membrane.

**Cellubrevin**

Cellubrevin belongs to the v-SNARE family. It is a synaptobrevin/VAMP-related protein. The recombinant flag-cellubrevin was immunolocalized with fluorescence microscopy by both the anti-flag monoclonal antibody and the anti-cellubrevin polyclonal antibody. However, only the anti-cellubrevin antibody was applied at the ultrastructural level because the anti-flag antibody failed to detect flag-cellubrevin. Immunoreactivity for cellubrevin was present throughout the cytoplasm but was accumulated more in the perinuclear region (Fig.29A-D). The latter probably corresponded to the labeling of the Golgi complex, as indicated in many other cell types (Parpura et al., 1995a; McMahon et al., 1993). Fig.29A shows that the punctuate staining was especially concentrated around the nucleus in some cells. Moreover, the immunostaining extended into the processes of fibrous cells (Fig.29B). Immunofluorescence was enhanced at the ruffling edge of the cell (Fig.29D). As expected, immunoelectron microscopy confirmed the association of the cellubrevin immunoreactivity with the Golgi apparatus in the perinuclear area (Fig.30A-C). The immunogold labeling was detected predominantly at small round vesicles and buds of TGN, but only few gold particles were found directly on the flattened cisternae of Golgi apparatus. In addition, the gold particles were observed at clusters of round vesicles in the cytoplasm (Fig.30D) and the tubulovesicular organelles in the vicinity of the nucleus (Fig.30E). Some dispersed small vesicles and small clusters of tubules and vesicles in the cytoplasm were specifically labeled (Fig.30F, G). No obvious endosomal labeling was found at the ultrastructural level.

**Rab5**

Rab5, a low molecular weight GTP-binding protein, is involved in endocytic vesicle trafficking and endosome fusion. With the aid of GFP-fused Rab5, the distribution of the Rab5 fusion protein could be visualized directly under the fluorescence microscope. GFP-Rab5 was observed in association with numerous fine puncta and especially many larger punctuate structures that appeared as clearly discernible fluorescent spots throughout the cytoplasm (Fig.31A-C). Moreover, immunopositive dots were located more densely in the perinuclear region of some cells that might derive from the overexpression of GFP-Rab5. The immunopositive dots were not confined to the cell body; they were also present in the long processes of the fibrous cells where GFP-Rab5 was allocated to large puncta (Fig.31C). Immunogold studies with the polyclonal anti-GFP primary antibody showed that the GFP-Rab5 fusion protein occurred over clusters of small vesicles (Fig.32A, B) and larger vesicular structures of round, oval and tubular shape (Fig.32.C-E). GFP-Rab5 was also localized to

endosomal structures and the surrounding vesicles (Fig.32F). Probably, the labeled endosomes and clustered vesicular structures corresponded to the large puncta observed under the fluorescence microscope.

**Double labeling**

Double labeling experiments were performed in order to further analyze and compare the distribution pattern of these recombinant proteins and in particular to investigate whether the proteins that exhibited a similar labeling pattern were colocalized on identical organelles. This would be helpful for analyzing their potential functional relations.

***VAMP II and cellubrevin:*** The monoclonal antibody anti-myc and the polyclonal antibody anti-cellubrevin were used for the double labeling of myc-VAMP II and flag-cellubrevin. A partial colocalization of these two recombinant proteins was revealed under the scanning laser confocal microscope (Fig.33A-C). Some yellow or orange puncta of different sizes were scattered throughout the cytoplasm, indicating that myc-VAMP II was colocalized with flag-cellubrevin to some extent (Fig.33C). Increased labeling of flag-cellubrevin (green) was observed in the perinuclear area. Under the immunoelectron microscope the colocalization of these two proteins on clustered vesicular organelles of various sizes was detected, which may correspond to the yellow or orange puncta under the fluorescence microscope. Moreover, differentially sized gold particles were located at the same vesicles (Fig.33D, E).

***VAMP II and syntaxin I:*** Double labeling for the two recombinant SNAREs proteins myc-VAMP II and RFP-syntaxin I was carried out by means of the monoclonal anti-myc antibody and by the inherent red fluorescence of RFP with fluorescence microscopy. Myc-VAMP II and RFP-syntaxin I exhibited very similar labeling patterns (Fig.34A, B). A high level of colocalization was indicated by the large number of yellow staining on punctuate structures in the cell body (Fig.34C). Moreover, myc-VAMP II was colocalized with RFP-syntaxin I even in the cellular processes. It appeared, however, that myc-VAMP II immunoreactivity was more intensely expressed in the peripheral cytoplasm than RFP-syntaxin I. Because only monoclonal antibodies were available for the immunolocalization, double labeling under ultrastructural level was not performed. The single staining of immunoelectron microscopy showed that both myc-VAMP II and RFP-syntaxin I were localized to vesicular organelles (as described above).

***VAMP II and Rab5:*** Double labeling for the recombinant proteins myc-VAMP II and GFP-Rab5 was performed with the aid of the monoclonal anti-myc antibody and the inherent green fluorescence of GFP. A partial colocalization of myc-VAMP II with GFP-Rab5 was revealed

under fluorescence microscope (Fig.35A-C). Many differentially sized yellow or orange puncta were dispersed in the cytoplasm. GFP-Rab5 (green signal) was more intensely expressed in the perinuclear region. However, the red labeling of myc-VAMP II was distributed more extensively and intensively towards the cell periphery. By immunoelectron microscopy myc-VAMP II and GFP-Rab5 were found to colocalize to the same vesicle clusters, but only a small number of vesicles were found to be labeled with both proteins (Fig.35D, E). The labeled vesicle clusters probably corresponded to the yellow or orange puncta observed under the fluorescence microscope. However, no colocalization on the endosomes was found.

**Controls**

In control sections, scarce immunogold particles were seen when the first antibodies were omitted and only the 10 nm gold-conjugated secondary antibody goat anti-mouse IgG (Fig.36A) or goat anti-rabbit IgG (Fig.36B) was applied to the sections. The control sections for double labeling were simultaneously treated with 10 nm gold conjugated goat anti-mouse IgG and 20 nm gold conjugated goat anti-rabbit IgG. Similarly, little labeling was obtained (Fig.36C). This suggests that the immunogold staining is specific for the proteins investigated. The specificity of immunolabeling was further verified in experiments where cells were transfected with the empty pcDNA3 vector alone and incubated with primary antibodies and the corresponding 10 nm gold particles conjugated to secondary antibodies. No significant labeling was detected (Fig.36D). Negative results were also obtained in the control experiments for immunofluorescence microscopy (Photographs were not shown).

## Photographic Plate III

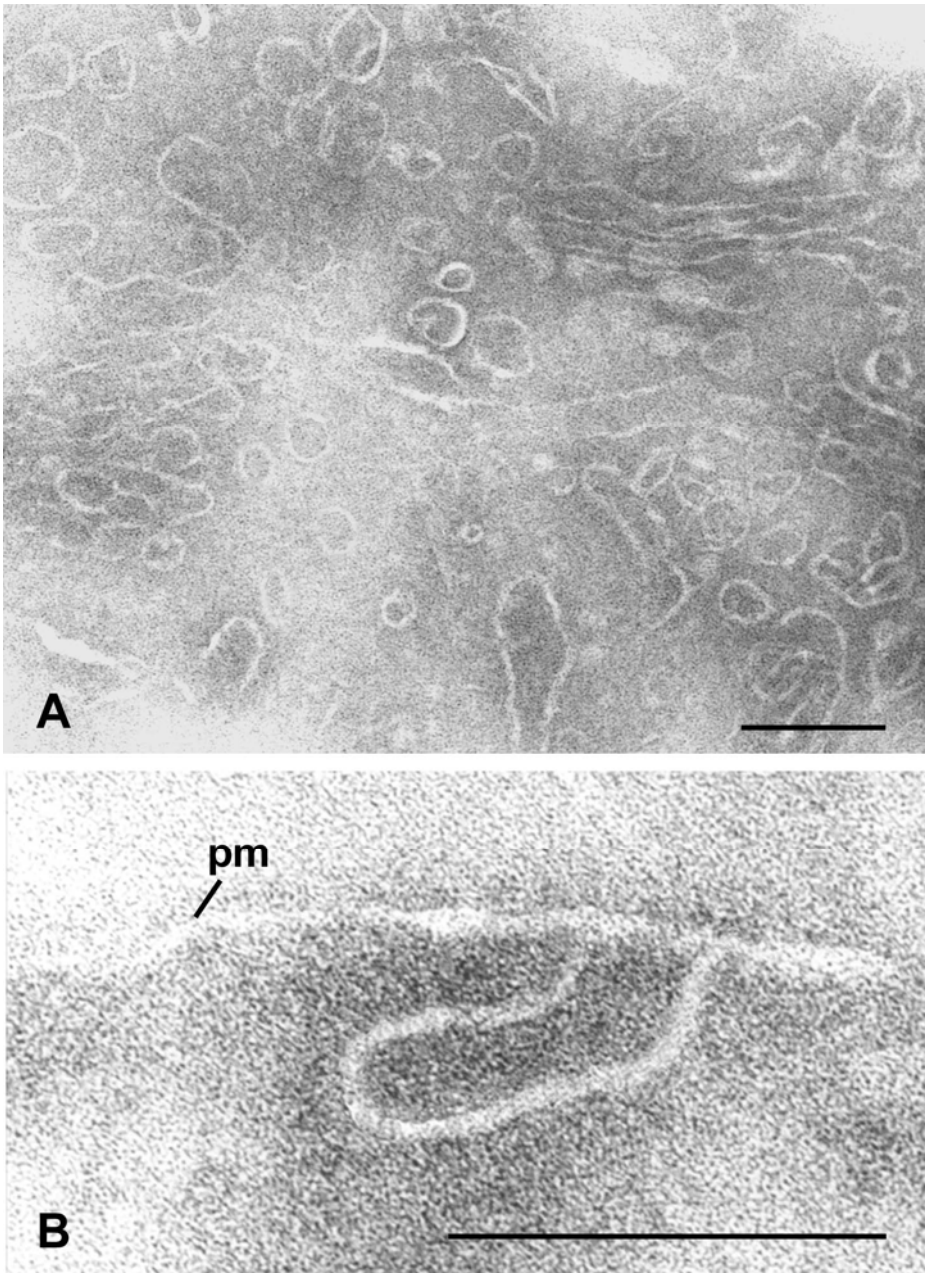


Fig.18. Ultrastructure of vesicles and tubules in U373 cells. (A) Ultrathin cryosections showing abundant vesicles and tubules in the cytoplasm of U373 cells. (B) The tubular structure in the periphery of a U373 cell directly connected to the plasma membrane (pm). Scale bar = 200 nm.

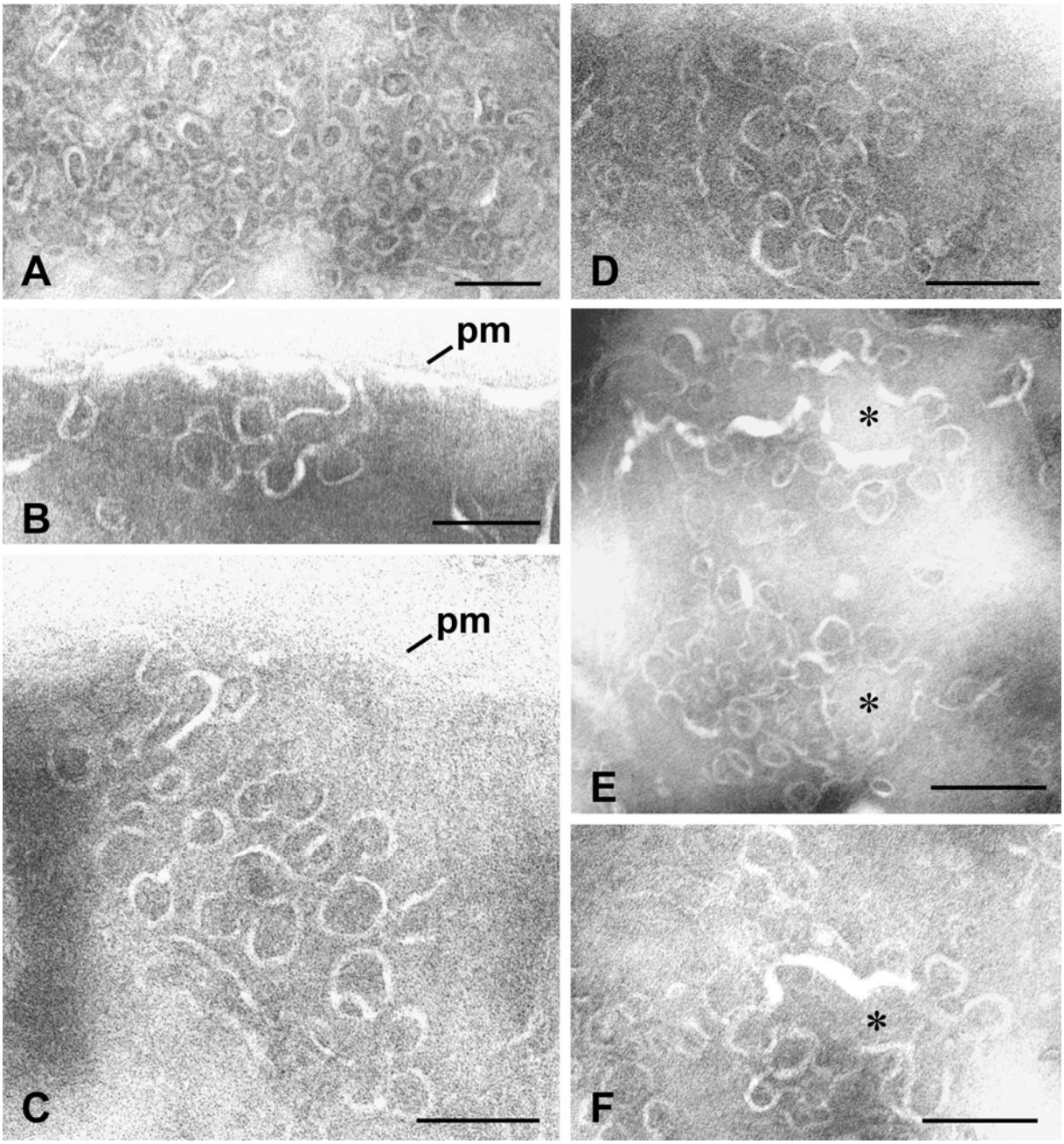


Fig.19. Morphology and the formation of small vesicles in U373 cells. (A) Relatively uniform population of small vesicles with an average diameter of 50-70 nm in the cytoplasm. (B) Some small vesicles are budding from a thick tubule-shaped invagination of the plasma membrane (pm). (C) Many round and clustered vesicles appear to be generated from a plasma membrane-associated tubular structure. (D) Clusters of round small vesicles in the cell periphery. (E, F) Small clustered vesicles are appearantly formed from vacuole-like structures (asterisk) in the cytoplasm. Scale bar = 200 nm.

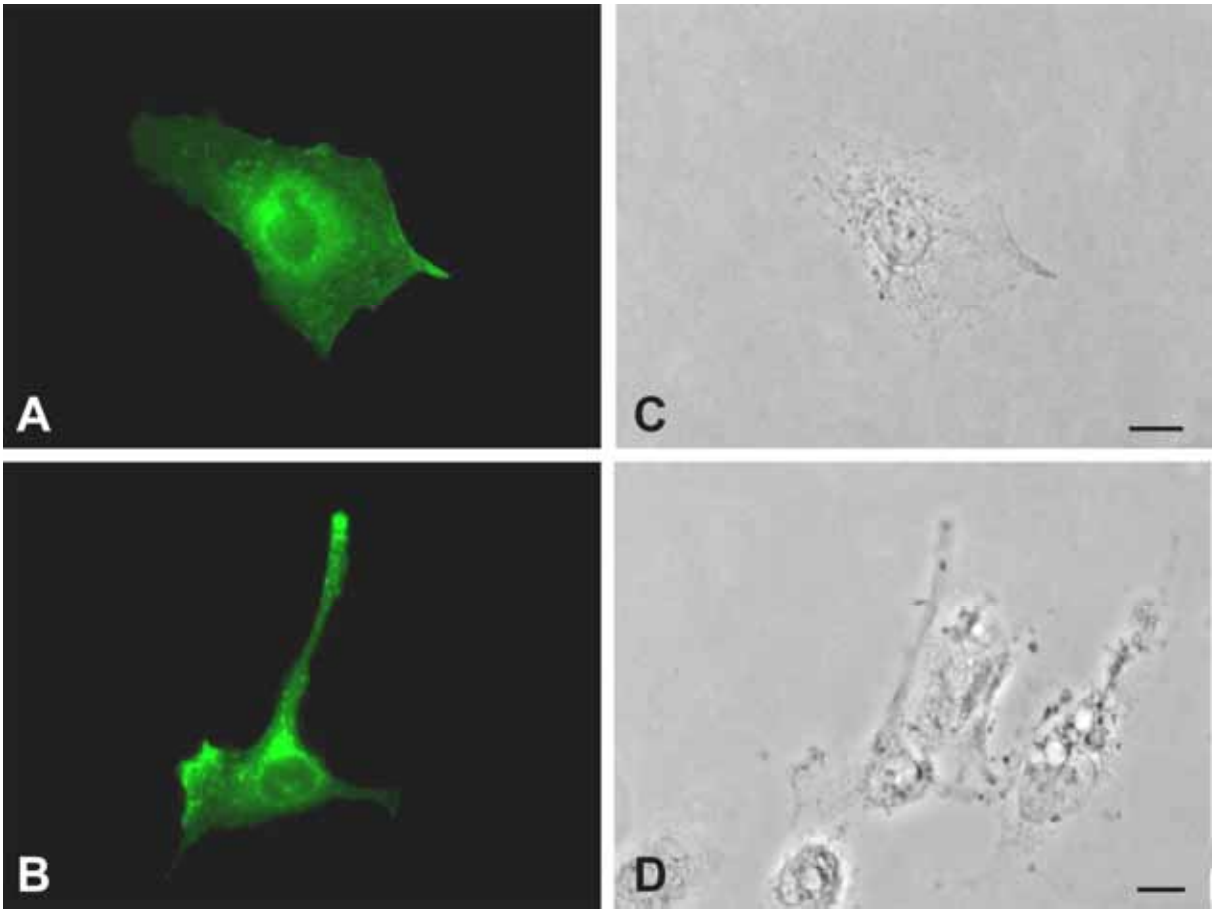


Fig.20. Immunofluorescence localization of myc-VAMP II in U373 cells (A) Localization of myc-VAMP II to numerous fine and larger punctuate structures in the cytoplasm. Immunostaining is more concentrated in the perinuclear region. (B) Labeled fibrous cell exhibiting immunopositive dots in its long cellular process up to the tip. (C, D) Corresponding phase contrast images for A and B. Scale bar = 10 μm.

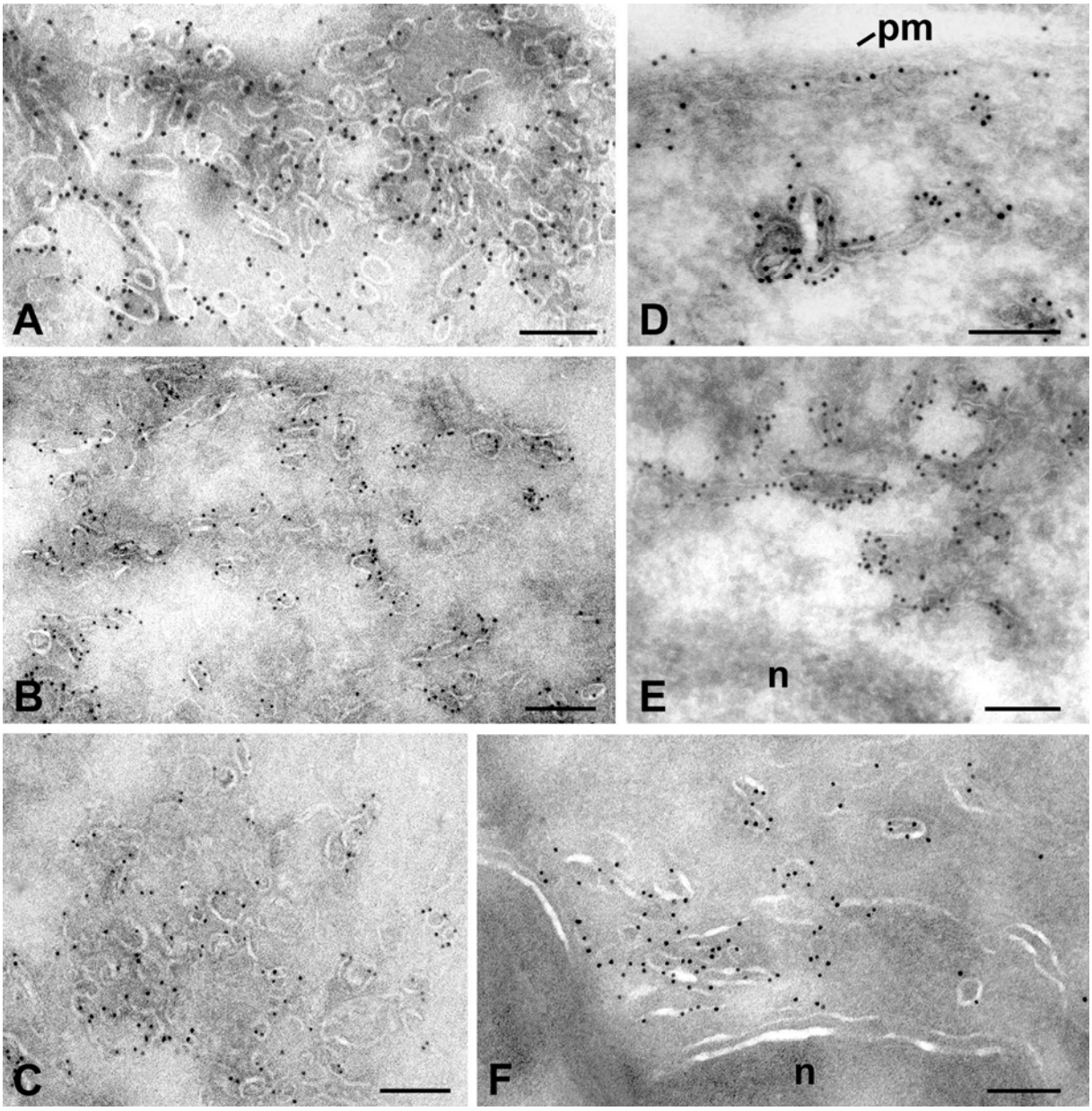


Fig.21. Immunogold labeling for myc-VAMP II at electron-lucent organelles in U373 cells. (A-C) Numerous electron-lucent vesicular structures of various size and shape (round, oval and tubular) are intensely labeled in the cytoplasm. (D) Myc-VAMP II-containing tubulovesicular structures located in the peripherial cytoplasm. (E, F) Immunolabeling of tubulovesicular structures in the vicinity of the nucleus (n). Scale bar = 200 nm.

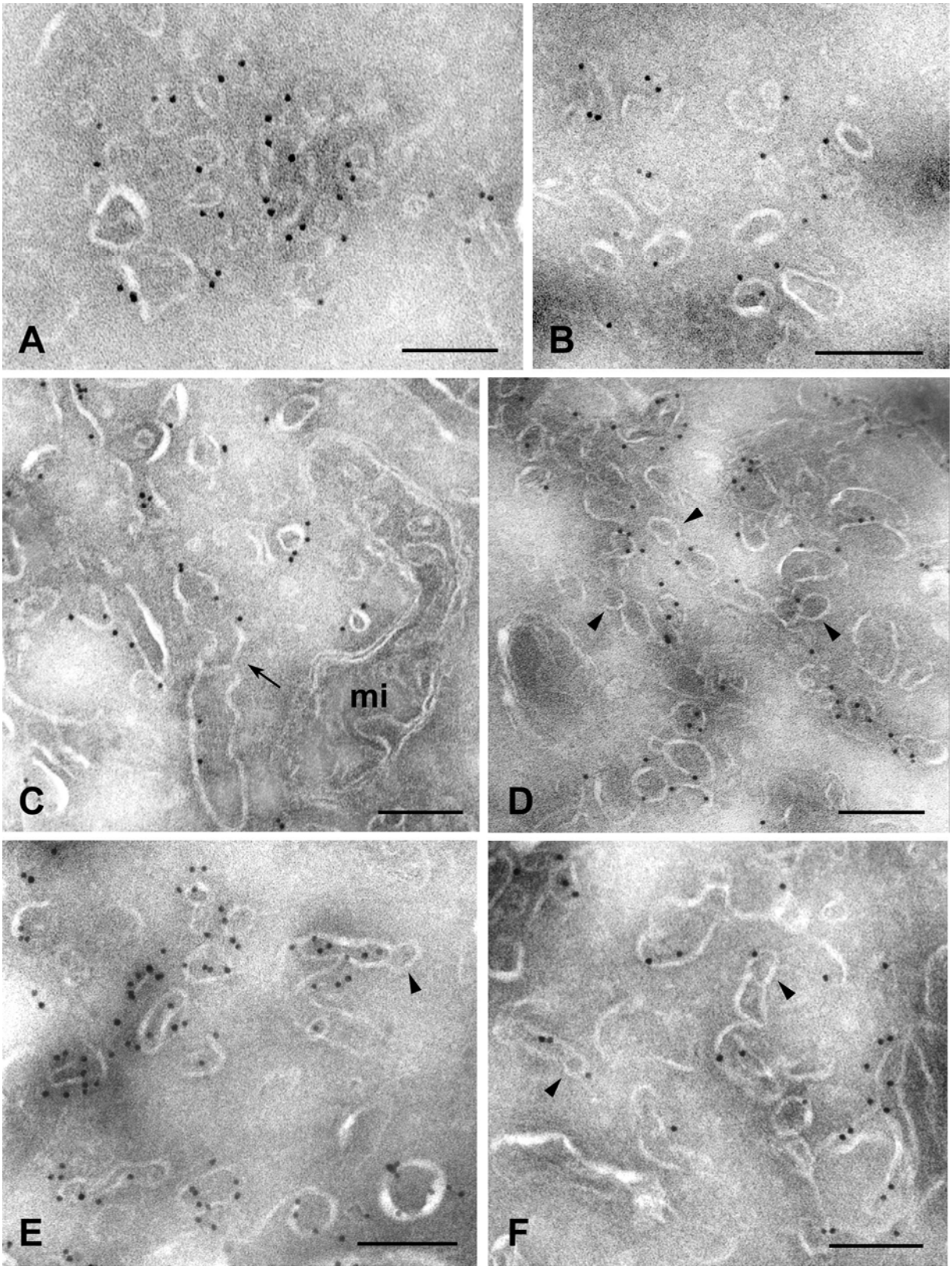


Fig.22. Immunogold labeling for myc-VAMP II of the small vesicles and tubular organelles showing the potential formation of small vesicles in U373 cells. (A, B) The population of relatively regular-sized small vesicles is selectively labeled. (C) Labeling of a long tubule that is exhibiting fragmentation (arrow) and many other vesicular organelles. The large mitochrondium (mi) is free of gold particles. (D-F) A lot of labeled tubules and vesicles in the cytoplasm. Some smaller vesicular profiles (arrowheads) are budding from labeled tubular organelles in the cytoplasm. Note the labeling of buds (arrowheads) from a tubular organelle in F. Scale bar = 200 nm.

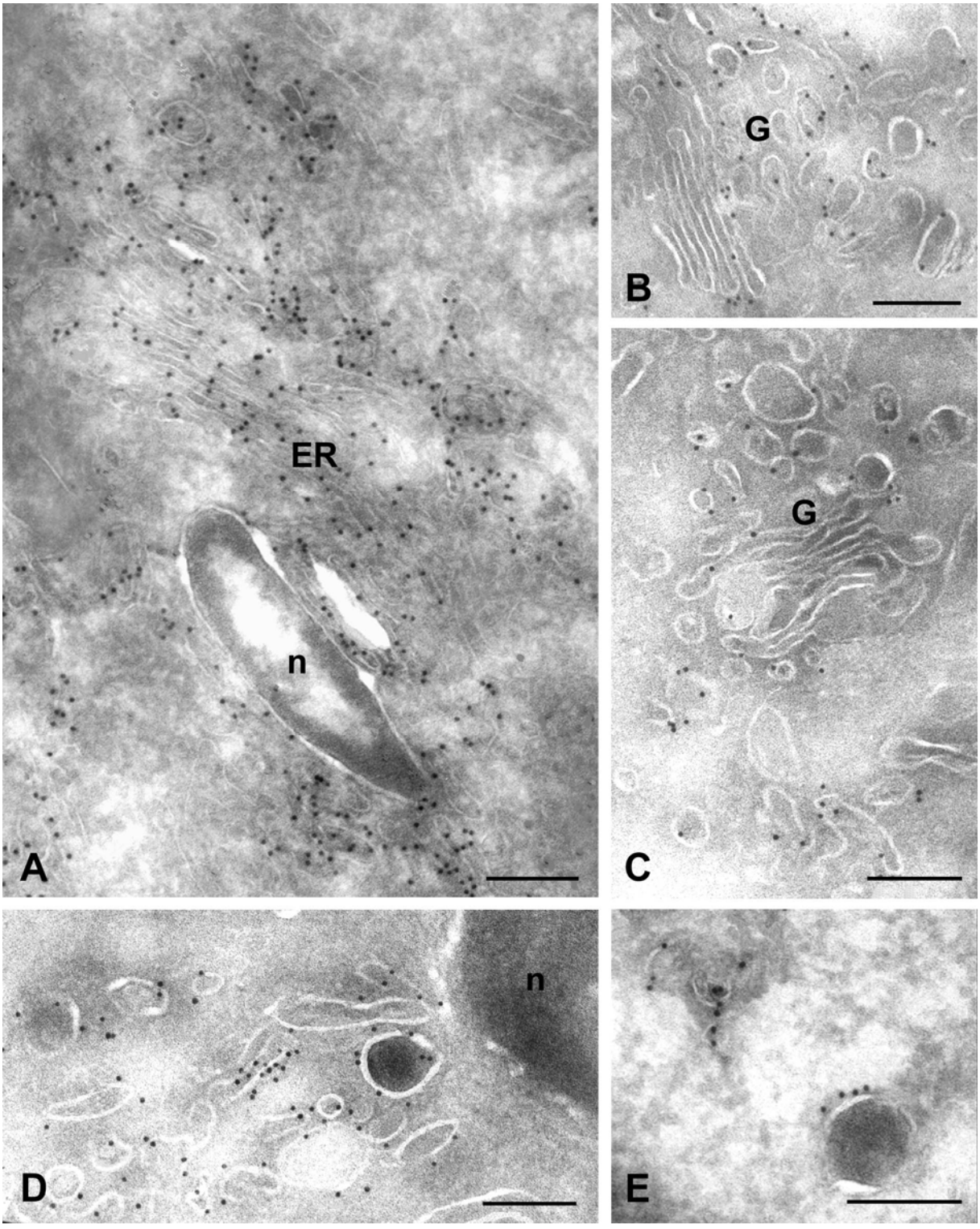


Fig.23. Immunogold labeling for myc-VAMP II of endoplasmic reticulum (ER), Golgi apparatus (G) and granules in U373 cells. (A) Overview of the labeling in the perinuclear area. The endoplasmic reticulum and various vesicular and tubular structures are intensively labeled. (B, C) Gold particles occur selectively at TGN vesicles of the Golgi apparatus. There is only low labeling over the Golgi cisternae. (D, E) Labeling at the membrane of electron dense granules dispersed in the cytoplasm. Myc-VAMP II is also clearly detectable on tubular and vesicular structures in the vicinity of the nucleus (n). Scale bar = 200 nm.

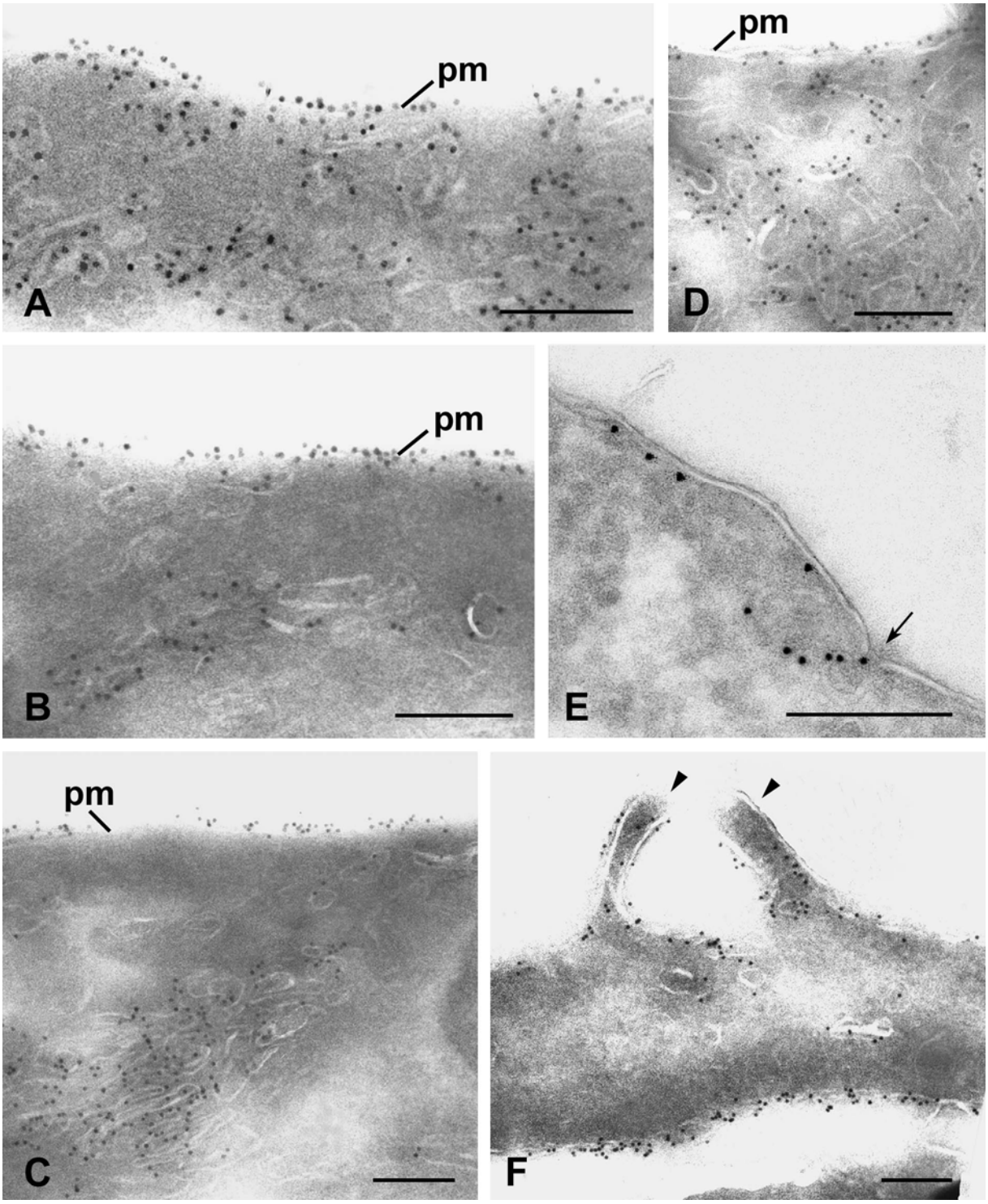


Fig.24. Myc-VAMP II immunolabeling at the plasma membrane (pm) of U373 cells. (A-D) Gold particles are localized at high density to the plasma membrane and the adjacent tubulovesicular structures. B and C show labeled populations of tubulovesicular organelles in the peripheral cytoplasm. (E) Gold particles are occasionally detected at Ω-like structures at the plasma membrane (arrow). (F) Labeling of the membrane of filopodia at a cellular process (arrowheads). Scale bar = 200 nm.

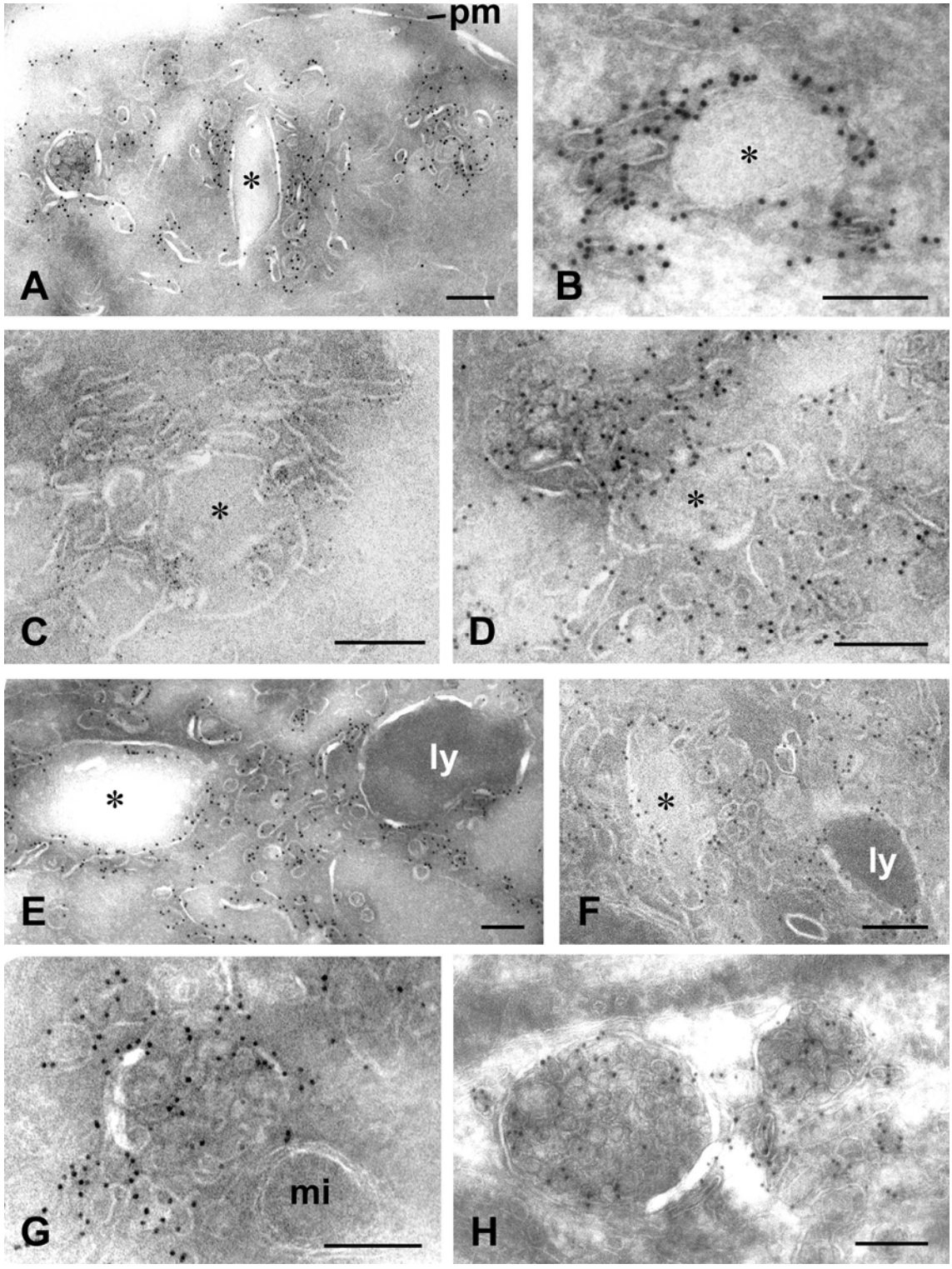


Fig.25. Immunolocalization of myc-VAMP II on endosomal structures, multivesicular bodies and electron dense lysosomes in U373 cells (A) Various immunoreactive organelles in the cell periphery. Gold particles occur on a spherical multivesicular body with many internal small vesicles and the tubulovesicular organelles around, an oblate endosomal vacuole (asterisk) and associated tubulovesicles, and a cluster of vesicles. The plasma membrane (pm) is labeled too. (B-D) Labeled endosomal structures in the cytoplasm. Gold particles are localized to the membrane of large electron-lucent endosomal vacuoles (asterisk) and especially to the associated tubulovesicles. Some internal vesicles situated in the periphery of the vacuoles are also labeled in C and D. (E, F) Next to the immunopositive endosomal vacuoles (asterisk) and the surrounding tubulovesicles, the membrane of electron dense lysosomes (ly) are labeled. (G, H) Labeled regular, round shaped multivesicular bodies. The gold particles are found specifically on internal vesicles and the limiting membrane as well as at the tubulovesicles around, but not on the mitochondrium (mi). Scale bar = 200 nm.

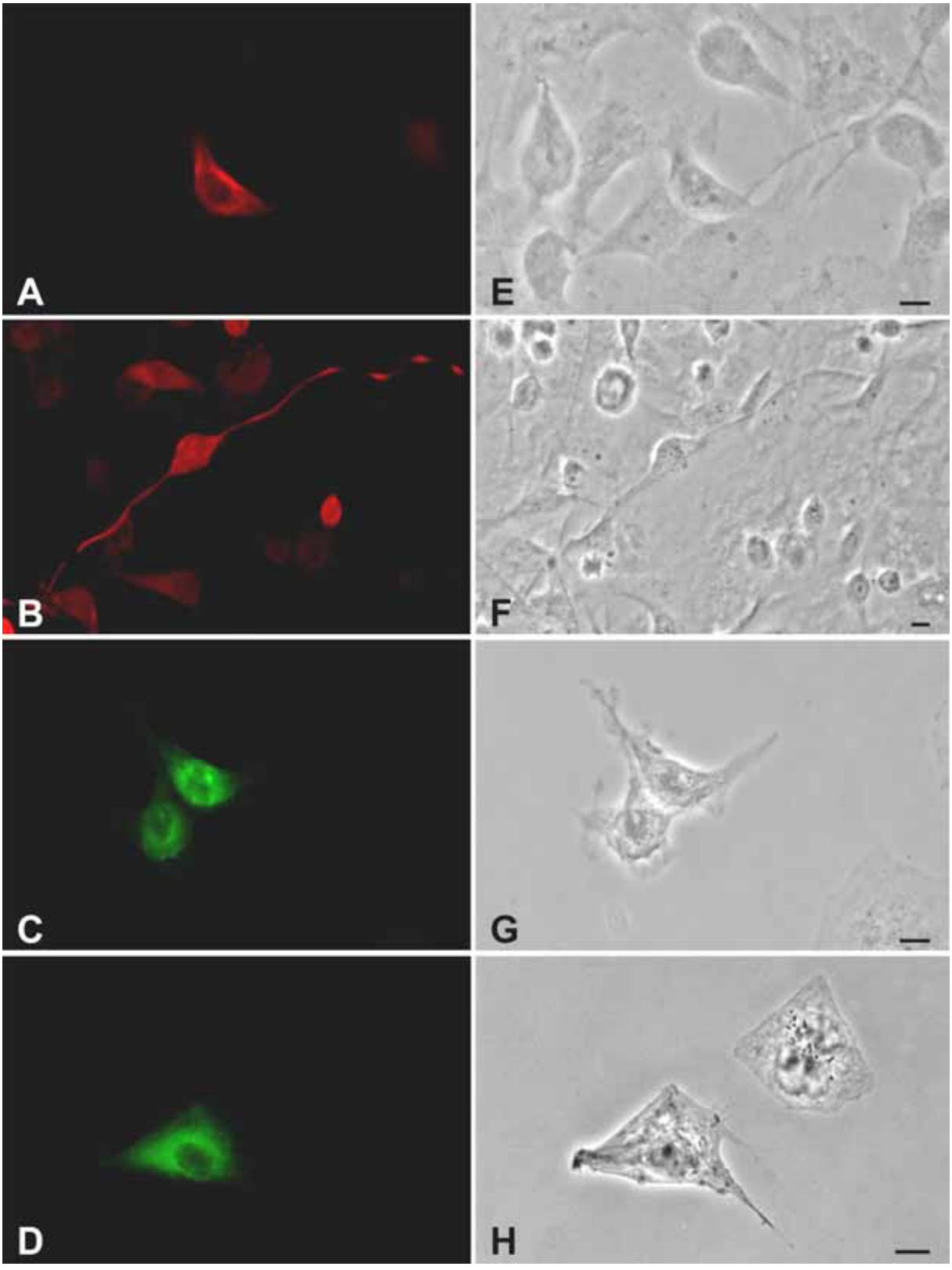


Fig.26. Immunofluorescence labeling for VSVG-syntaxin I in U373 cells (A) VSVG-syntaxin I is labeled with an anti-VSVG monoclonal primary antibody and visualized by a Cy3-conjugated secondary antibody, showing immunofluorescent puncta throughout the entire cell body and more enhanced in the perinuclear region. (B) The same as in A, but the immunofluorescent long processes of a fibrous cell is specially shown. (C, D) The cells are labeled with an anti-syntaxin I monoclonal primary antibody and a FITC-conjugated secondary antibody and display the same labeling pattern as in A. Nevertheless, the immunolabeling is more intense in the perinuclear cytoplasm. (E-H) Corresponding phase-contrast images of A-D, respectively. Scale bar = 10 μm.

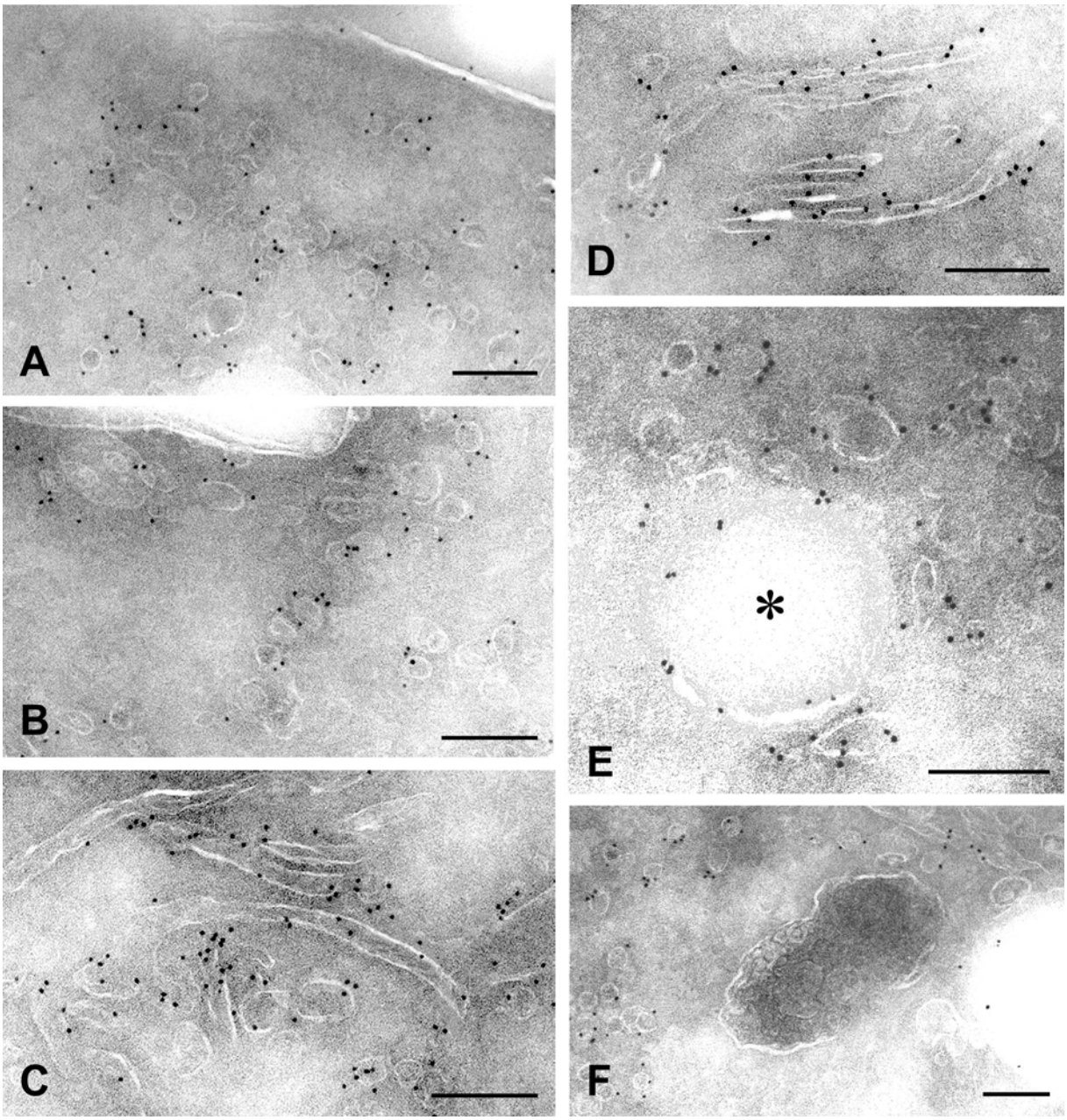


Fig.27. Immunolabeling for VSVG-syntaxin I by electron microscopy in U373 cells. (A, B) VSVG-syntaxin I is associated with the vesicles (40-100 nm) in the peripheral cytoplasm. Few gold particles appear at the plasma membrane itself. (C, D) Immunogold labeling occurs on long and thin tubules (30-50 nm in diameter). The vesicles clustered adjacent to the long tubules are also labeled in C. (E) Gold particles at the membrane of a large round endosomal vacuole and the surrounding vesicles. (F) An electron dense irregular-shaped lysosome with some obscure degraded internal vesicles is devoid of gold particles, whereas the adjacent small vesicles are labeled. Scale bar = 200 nm.

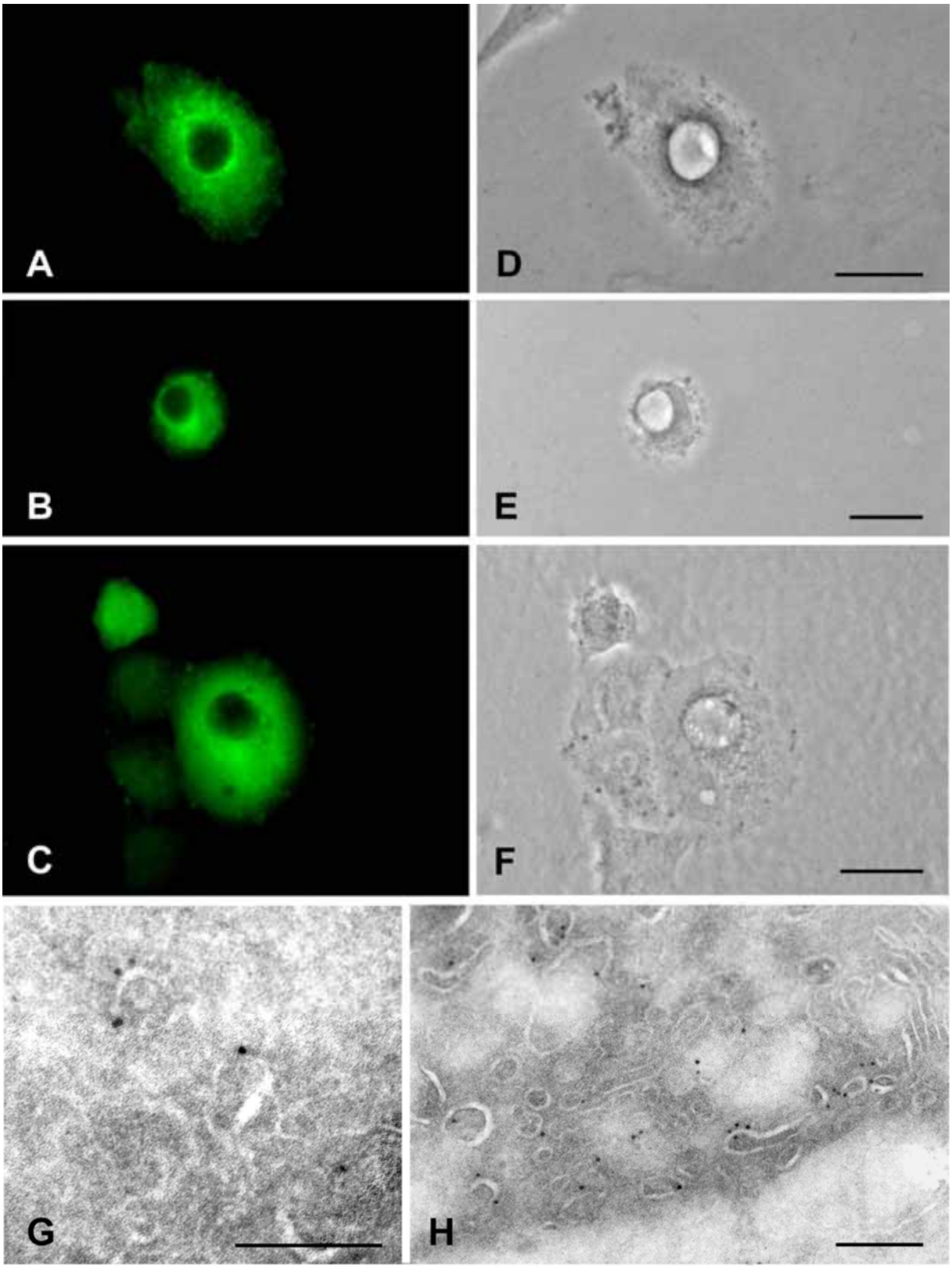


Fig.28. Immunolocalization of HA-SNAP-25 in U373 cells. (A-C) Immunofluorescence of HA-SNAP-25 in small transfected U373 cells. Numerous fine puncta of HA-SNAP-25 are distributed throughout the cell and are concentrated in the perinuclear area. The cells are labeled with the monoclonal primary antibody anti-HA in A and anti-SNAP-25 in B and C. (D-F) Corresponding phase-contrast images of A-C, respectively. (G, H) Immunogold localization of HA-SNAP-25 by electron microscopy. HA-SNAP-25 is localized to electron-lucent vesicular organelles of various sizes. The cells are labeled with the monoclonal antibody anti-HA in G and anti-SNAP-25 in H. Scale bar in A-C = 10 μm, in D and E = 200 nm.

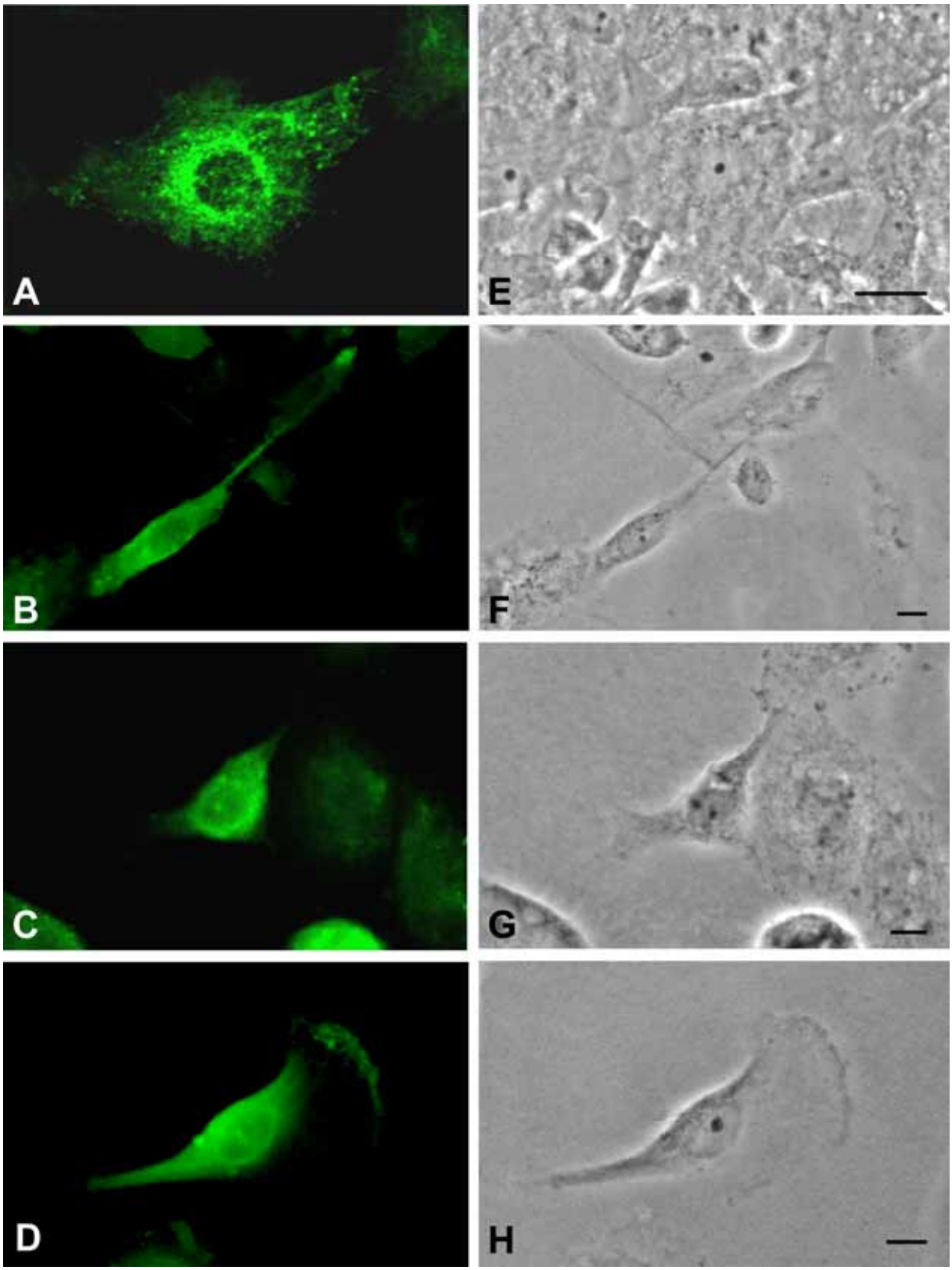


Fig.29. Immunofluorescence localization of flag-cellubrevin in U373 cells. (A) High magnification of an immunopositive cell labeled with the polyclonal anti-cellubrevin antibody, revealing that punctuate staining is concentrated around the nucleus. (B) Cells were treated as same as in A, showing immunofluorescence labeling in a fibrous cell with a long process. (C) Immunofluorescence in cells labeled with the monoclonal anti-flag antibody. (D) The sample was treated as in C, especially revealing immunostaining on the ruffling edge of the cell. (E-H) Corresponding phase contrast images of A-D, respectively. Scale bar = 10 μm.

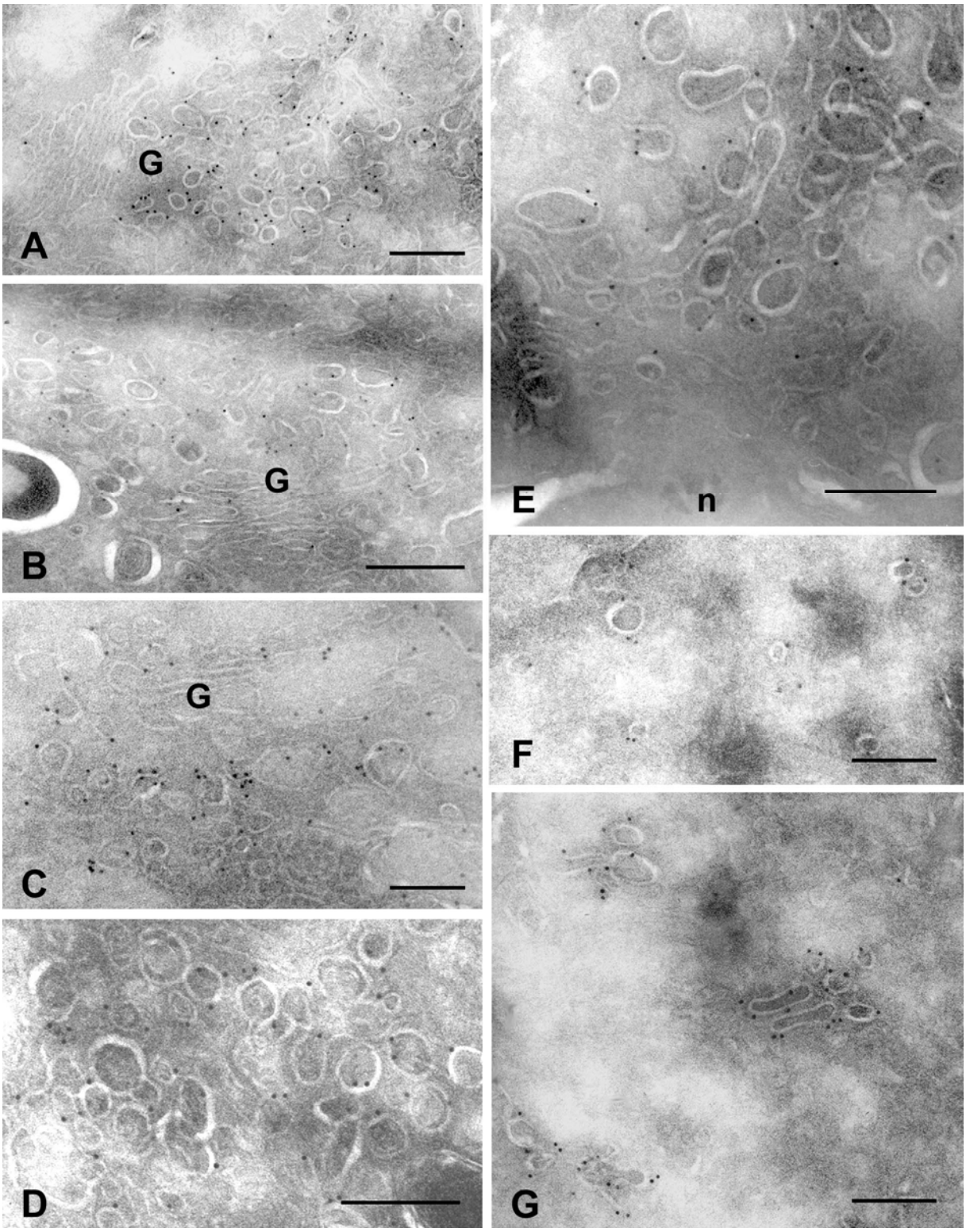


Fig.30. Immunogold labeling for flag-cellubrevin by electron microscopy in U373 cells. (A-C) Gold particles are detected mainly at the small round vesicles in the TGN of the Golgi complex (G). Only few gold particles are associated directly with the flattened Golgi cisternae. (D) Gold particles are present in clustered round vesicles in the cytoplasm. (E) Labeled tubulovesicular organelles in the vicinity of the nucleus (n). (F, G) Labeling on some dispersed and clustered tubules and vesicles in the cytoplasm. Scale bar = 200 nm.

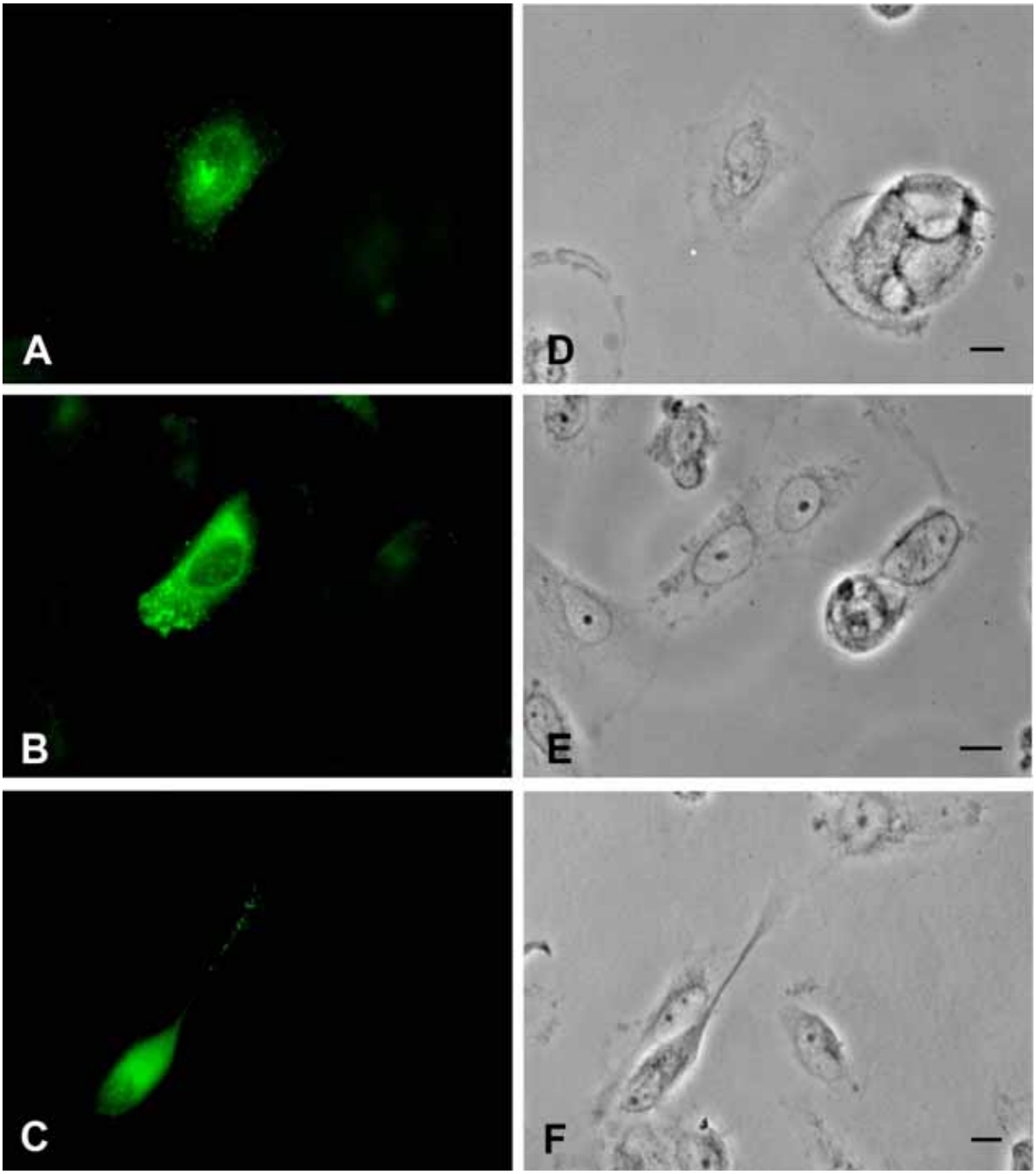


Fig.31. Localization of GFP-Rab5 by means of the inherent fluorescence of GFP in U373 cells. (A, B) GFP-Rab5 in a protoplasmic form of U373 cells. Numerous fine and many larger fluorescent spots occur in the cytoplasm. The fine fluorescent dots are more densely located to the perinuclear region in A. (C) GFP-Rab5 in a fibrous U373 cell. The fluorescent dots are present not only in the cell body but also in the process of the fibrous cell where GFP-Rab5 is allocated to large puncta. (D-F) Corresponding phase contrast images of A-C. Scale bar = 10 μm.

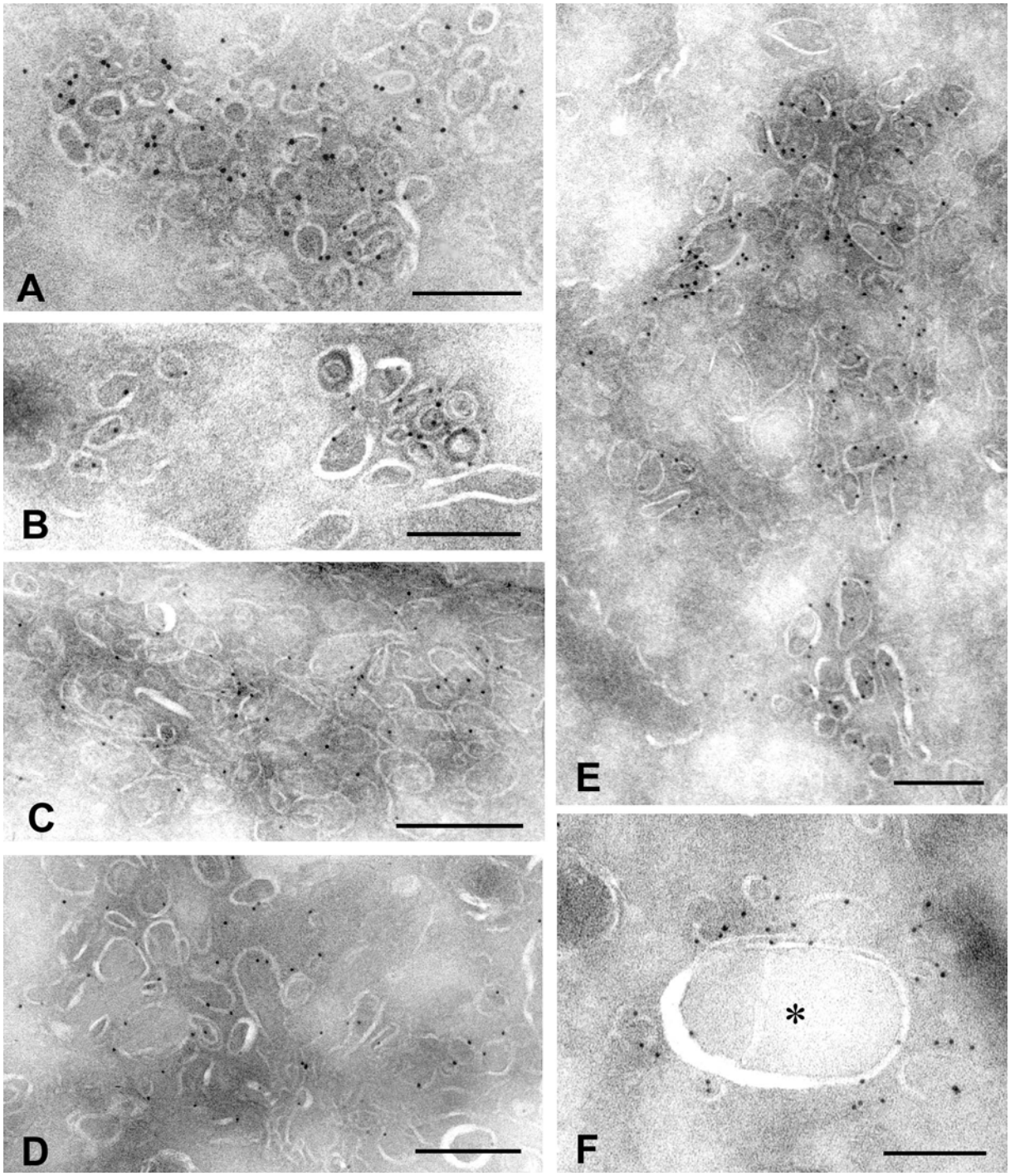


Fig.32. Immunogold localization of GFP-Rab5 by electron microscopy in U373 cells. (A, B) Labeling of clustered vesicles. (C-E) GFP-Rab5 is associated with vesicular structures of various sizes in the cytoplasm. (F) GFP-Rab5 is localized to an endosomal vacuole (asterisk) and the vesicles around. Scale bar = 200 nm.

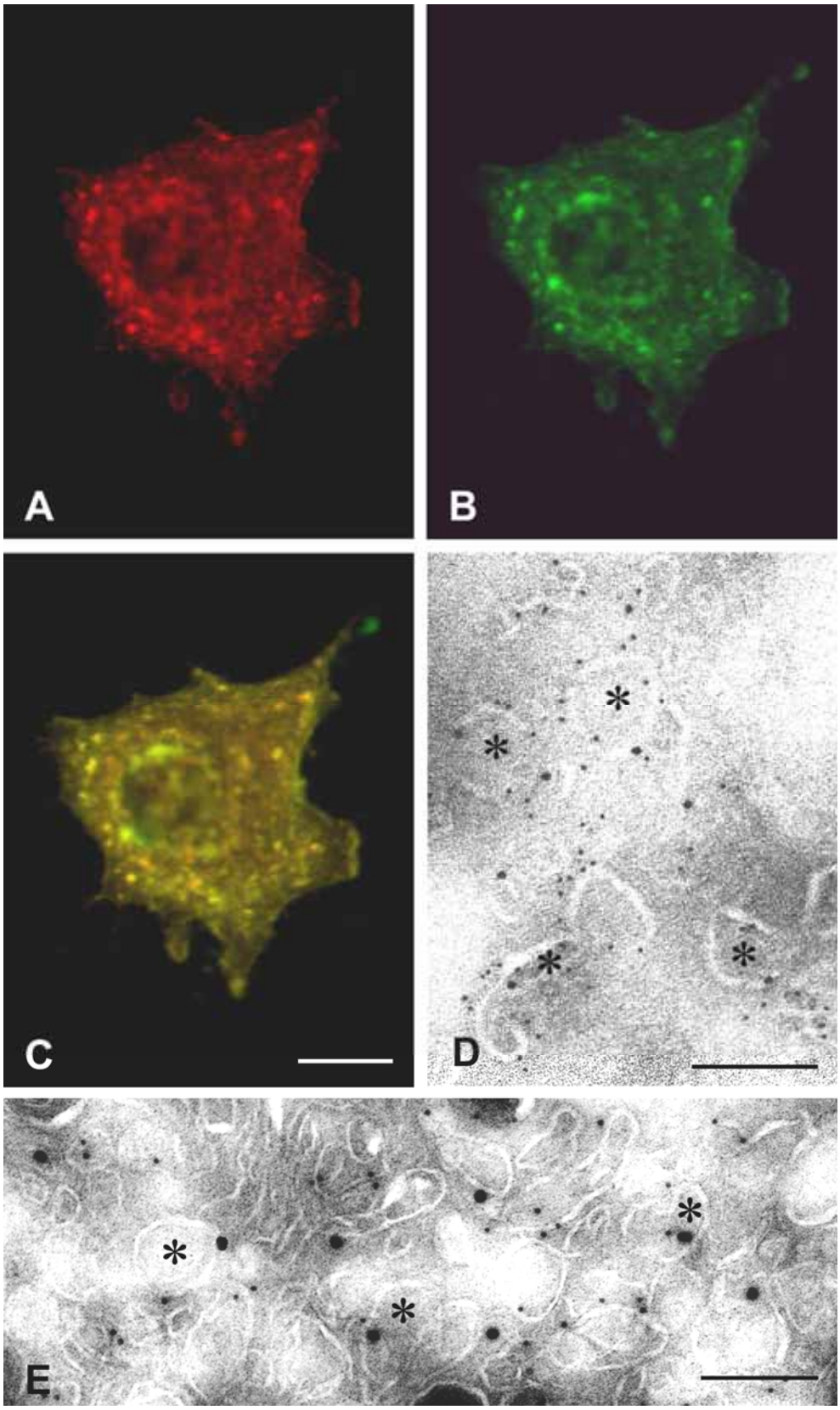


Fig.33. Double immunolabeling for myc-VAMP II and flag-cellubrevin revealed by confocal laser microscopy and cryo-electron microscopy in U373 cells.
(A) Immunoabeling for VAMP II revealed by the anti-myc primary antibody and Cy3-conjugated secondary antibody.
(B) Immunostaining for cellubrevin detected by a cellubrevin specific antibody and FITC-conjugated secondary antibody.
(C) Overlay of A and B, exhibiting a partial colocalization of myc-VAMP II and flag-cellubrevin. Some scattered yellow or orange puncta of different size in the cytoplasm display partial colocalization of myc-VAMP II and flag-cellubrevin. More flag-cellubrevin (green) appears around the nucleus. (D, E) Double immunogold labeling for myc-VAMP II and flag-cellubrevin at the ultrastructural level. Two differently sized gold particles are colocalized to the same vesicle clusters and even to the same vesicles (asterisk). In D, 5 nm gold particles for myc-VAMP II and 10 nm for flag-cellubrevin; In E, 10 nm gold particles for myc-VAMP II and 20 nm for flag-cellubrevin. Scale bar in A-C = 10 μm, in D and E = 200 nm.

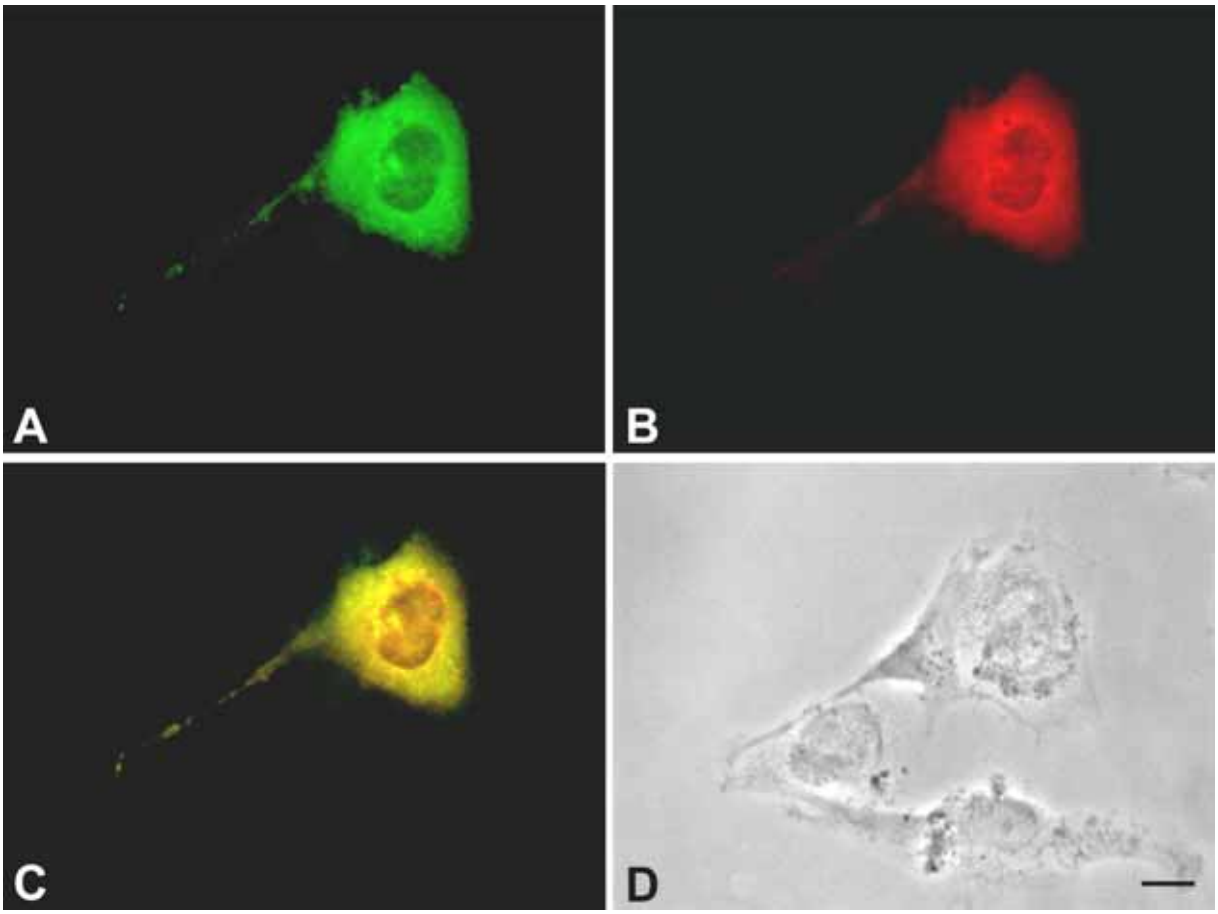


Fig.34. Double immunofluorescence labeling for myc-VAMP II and RFP-syntaxin I in U373 cells. (A) The distribution of myc-VAMP II was detected with the anti-myc primary antibody and visualized with FITC–conjugated anti-mouse IgG (green). (B) The distribution of RFP-syntaxin I was observed directly by means of the RFP fluorescence (red). (C) Overlay of the two images A and B. Myc-VAMP II and RFP-syntaxin I show a high level of colocalization in the cell body and the cell process. Myc-VAMP II was expressed more intensely than RFP-syntaxin I in the peripheral cytoplasm and in the process. (D) Phase-contrast image of the same sample. Scale bar = 10 μm.

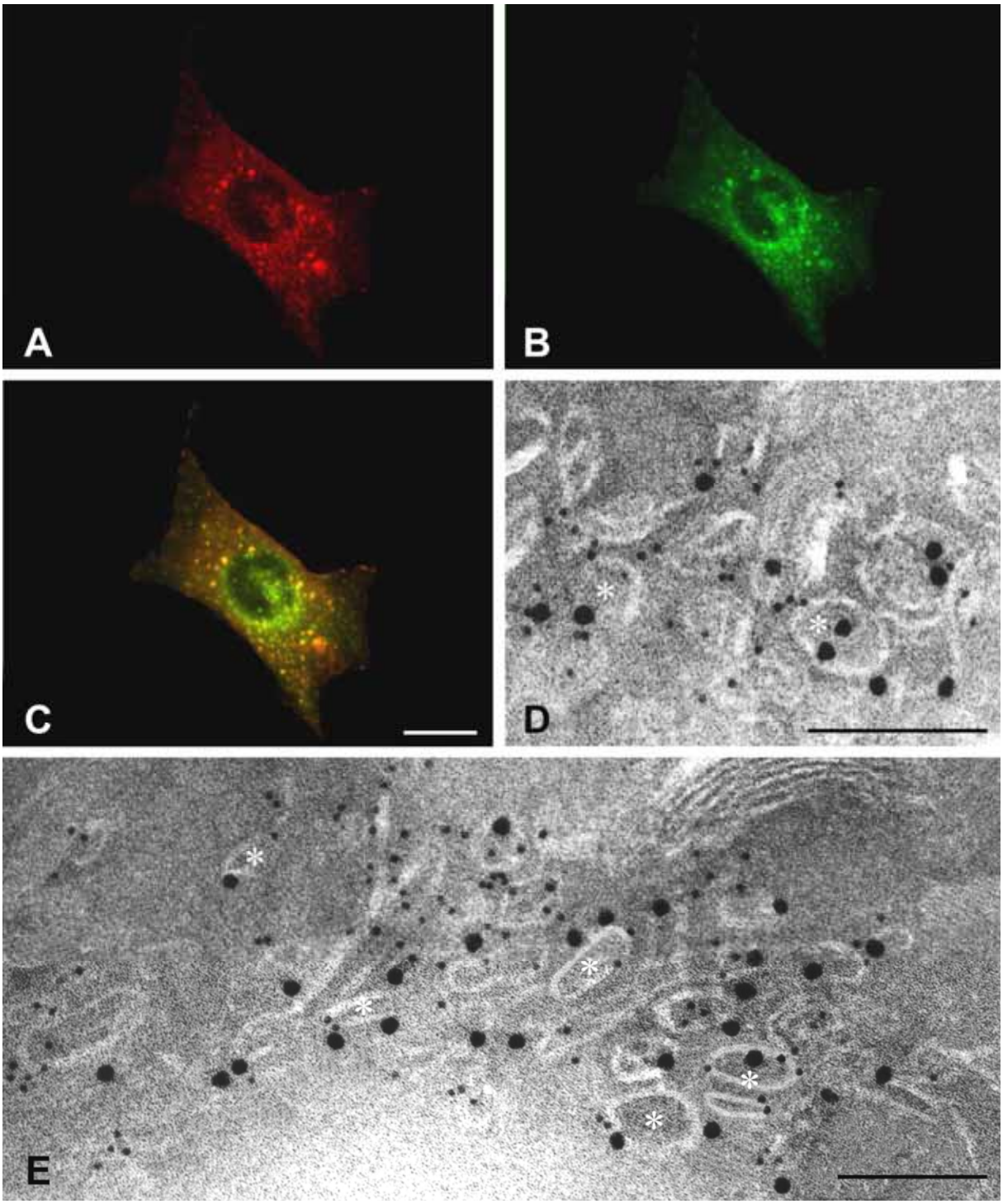


Fig. 35. Double fluorescence and cryo-immunogold labeling for myc-VAMP II and GFP-Rab5 in U373 cells. (A) The distribution of myc-VAMP II was detected with the anti-myc primary antibody and visualized with Cy3–conjugated anti-mouse IgG (red). (B) The distribution of GFP-Rab5 was visualized directly with the GFP fluorescence (green). (C) Overlay of the two images A and B. Myc-VAMP II and GFP-Rab5 reveal partial colocalization shown as many yellow or orange puncta of varous size in the cytoplasm. GFP-Rab5 is expressed more intensely in the perinuclear region than myc-VAMP II. (D, E) Double immunogold labeling for myc-VAMP II and GFP-Rab5. Myc-VAMP II and GFP-Rab5 are colocalized to the same vesicle clusters. Some vesicles are labeled for both proteins (asterisk). 10 nm gold particles for myc-VAMP II and 20 nm gold particles for GFP-Rab5. Scale bar in A-C = 10 μm, in D and E = 200 nm.

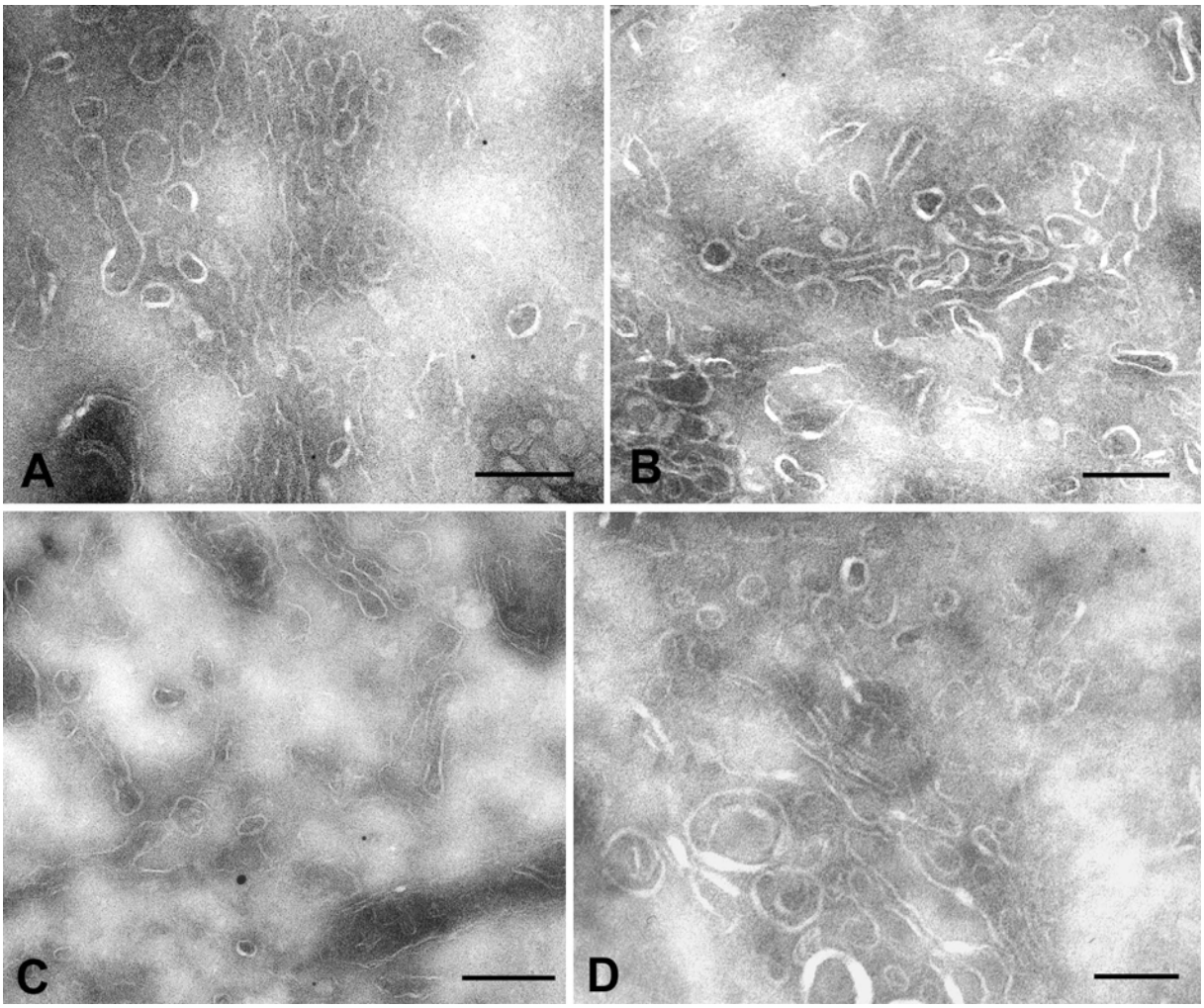


Fig.36. Controls for antibody specifity and tranfection in U373 cells. (A) The primary antibody is omitted and only the colloidal gold-coupled secondary antibody goat anti-mouse IgG is applied. Rare immunogold particles occur in the cytoplasm. (B) Same as in A. However, instead of goat anti-mouse IgG, goat anti-rabbit IgG was used. (C) Identical results are obtained in control sections for double labeling where both secondary antibodies with differently sized gold particles, goat anti-mouse IgG (10 nm) and goat anti-rabbit IgG (20 nm) are used in the same section. (D) Control for the expression of the transfected proteins. The section was obtained from cells that had been transfected with the empty pcDNA3 vector alone and then incubated with the effective primary antibody anti-myc and the corresponding monoclonal secondary antibody. No significant labeling is obtained. Scale bar = 200 nm.

# 4. Discussion

## 4.1. Using the cryo-immunogold technique for the subcellular localization of synaptic proteins

The cryo-immunogold technique has been demonstrated as a suitable method for the immunolocalization of synaptic proteins in both nerve terminals and cultured cells. By comparison, an obvious advantage of this technique lies in the fact that no resin embedding is involved in the entire sample preparation processes. The molecules are not affected by the treatment with organic solvents. Thus, not only the structural integrity but also the peptide antigenicity is better preserved.

Throughout this method, the only potential chemical denaturation step for antigens before labeling is the initial aldehyde fixation. In immunocytochemistry, the choice of fixative always represents a compromise between the preservation of morphology and the retention of antigenicity. The mixture of 4% paraformaldehyde and 0.05% glutaraldehyde in PBS is shown as an ideal fixative in this study which yields a good preservation for both tissue morphology and antigenicity.

In the cryosection method, the cryo-protectant is not only essential for the vitrification of the tissue pieces to minimize cellular destruction by ice crystals during the freezing but it is also a determinant for the plasticity of the samples that is very important in the sectioning (Tokuyasu, 1980). 2.3 M sucrose or a mixture of sucrose and PVP which permits rapid freezing of the samples and provides enough preservation of ultrastructural details (Tokuyasu, 1989) proved to be an excellent cryo-protectant in the present study.

Like all other postembedding immunocytochemical methods, the Tokuyasu cryosection technique offers the advantage that the antibodies can easily get access to antigen epitopes in every cellular compartment at the surface of sections (Griffiths et al., 1984). In this study, as expected, the immunolabeling is especially allocated to defined organelles, verifying previous biochemical results. However, it is obvious that using this procedure, not all vesicles can be labeled, even for VAMP II that has the highest labeling efficiency in this study. Also at the active zone only part of the proteins that are thought to be involved in the docking complex could bind the gold particles. This suggests that not all epitopes in the samples are accessible to the antibodies. Although the cryo-immunogold method is referred to as the most sensitive

postembedding technique for immunolabeling (Griffiths et al., 1983), it has been found that the colloidal gold probably does not penetrate equally into sections for detection of antigens at a distance from the cut surface of ultra-thin cryosection (Takizawa and Robinson, 1994). The immunocytochemical staining is mostly limited to the availability of epitopes exposed to the surface of the thin sections. Labeling efficiency has been known to vary significantly between compartments (Griffiths and Hoppeler, 1986). Thus, one possible explanation would be that the membranes in the present study usually appeared as a "line" on the surface of the thin sections. Some membrane-bound antigenic sites that are not exposed themselves to the surface of the sections cannot be labeled. In addition, recent work has shown that antibody molecules can dissociate from IgG-colloidal gold on storage, leading to reduced immunolabeling (Kramarcy and Sealock, 1991; Vandre and Burry, 1992). It has been demonstrated that the density of gold particles is usually not identical with the biochemically determined concentration of an antigen (Griffiths and Hoppeler, 1986).

There is extensive evidence that labeling efficiency is relative to the size of colloidal gold particles in immunoelectron microscopy (Horisberger, 1981). Differential penetration of the differently sized immunogold particles into ultra-thin cryosection has been reported (Slot and Geuze, 1981). Decreasing diameter of the gold probe results in an increase of labeling efficiency. In addition, the matrix density can affect the labeling efficiency (Slot et al., 1989). The sections with lower matrix density (such as thawed frozen sections) provide a better chance for smaller gold particles to penetrate (Humbel et al., 1995). The smaller 1.4 nm Nanogold particles with Fab' fragments that are only one third the size of a full IgG molecule (Hainfeld and Powell, 2000), have been shown to penetrate further into the low density matrix of the cryosections than any of the larger colloidal gold particles employed (Takizawa and Robinson, 1994). Furthermore, the ultra-small gold particles are more stable than colloid gold immunoprobes, because the secondary antibody molecules are covalently linked to these ultra-small gold particles rather adsorbed as in IgG-colloidal gold (Hainfeld and Furuya, 1992). 1.4 nm immunogold particles with the silver enhanced method have been shown to result in a more intense labeling than colloidal gold. This is verified in the present study with VAMP II immunolabeling. Evidently, these smaller gold particles yielded a higher labeling density in ultra-thin cryosections than 10 nm colloidal gold. However, there are still some problems with silver enhancement, such as the irregular size of the enhanced particles and the merging of growing silver/gold particles. The final effect is dependent on the time of enhancement, the gold particle density and some other factors (Humbel et al., 1995; Burry et

al., 1992). Thus, further improvement is required.

After immunolabeling, the cryosections were treated with the modified "Positive-Negative Staining Method", in which the mixture of methylcellulose and uranyl acetate is used for both good preservation of cryosection ultrastructure and strong negative contrast of the membrane. By comparison, the negative contrast is a better method to delineate membrane structure, especially to show high-resolution detail, than any other methods, such as preembedding with Epon and postembedding with LR Gold. However, the presynaptic dense projection of the active zone, which has been revealed by special staining treatment with phosphotungstic acid (Akert et al., 1971), could not be recognized in this study. A further improvement of the staining method is required to display this structure with the docked vesicles on the cryosections for the analysis of the excytosis mechanism.

Taken together, the cryo-immunogold technique has more advantages in displaying the ultrastructure and in the immunolabeling than the preembedding method with Epon and the postembedding method with LR Gold. In the present study it proved a more suitable method for the localization of the synaptic proteins on the membrane.

## 4.2. Localization of synaptic proteins in hippocampal mossy fiber terminals and neurohypophysial endings

The giant mossy fiber synapses in the hippocampal CA3 subfield possess multiple active zones for neurotransmitter release, whereas the neurosecretory endings of the neurohypophysis are not provided with special release sites. In the present study, by using the immunogold labeling method on frozen ultrathin sections, the localization of SNARE proteins and other exocytosis-related synaptic proteins is investigated in these two different types of nerve terminals. By comparing the distribution of these synaptic proteins in these two neuronal terminals their functional characteristics are discussed.

### 4.2.1. Identities and differences in the distribution of synaptic proteins between two different types of nerve terminals

Some identities and differences in the localization of the synaptic proteins investigated are revealed between the two different types of terminals. In the mossy fiber terminals, the V-SNARE VAMP II and the other vesicle-associated proteins SV2 as well as Rab3A were extensively detected at the numerous small vesicles. The t-SNARE SNAP-25 and the N-type $Ca^{2+}$ channel were observed not only at the plasma membrane, but also at the vesicles in the

central synapses. These proteins were also detected in the neurosecretory endings of the neurohypophysis. However, it is striking that the labeling of all these proteins shows a high preference for microvesicles over granules. Moreover, the immunolabeling intensities of these proteins over microvesicles corresponded to that over synaptic vesicles. In addition, significant labeling of SNAP-25, the N-type $Ca^{2+}$ channel and VAMP II was detected at the plasma membrane near the clustered microvesicles. Similar to their roles in regulating vesicle docking and fusion in presynaptic nerve terminals, they may also participate in exocytic events in neurosecretory nerve endings of the neurohypophysis. These results suggest that these synaptic proteins share an identical association with synaptic vesicles and microvesicles. To the contrary, no significant concentrations of VAMP II, SNAP-25, SV2 and N-type $Ca^{2+}$ channel were present in the membranes of neurosecretory granules. However, α/β-SNAP and some NSF were found to be associated with granules, and so did the P/Q-type $Ca^{2+}$ channels and Rab3A in a subset of the nerve terminals. α/β-SNAP did not revealed significant labeling in the central synapses. P/Q-type $Ca^{2+}$ channels were detected mainly at the active zone plasma membrane. The scarce peptide-storing granules in the central synapses were not included in the investigation. In addition, the novel protein Bassoon was only restricted to central synapses, no immunolabeling of Bassoon was detected in the neurosecretory terminals of the neurohypophysis, where active zones are lacking. Obviously, these clear differences in distribution of these proteins between the two different types of terminals reflect the special functional features of these proteins and are highly consistent with the distinct functional characteristics of the two terminals themselves.

### 4.2.2. Evidence for increased immunolabeling of some exocytosis-related proteins at the active zone of central synapses

Whereas many synaptic proteins including the members of the SNARE family have been strongly implicated in the processes of synaptic vesicle exocytosis by means of genetic, physiological and biochemical approaches (Zheng and Bobich, 1998; Sollner et al., 1993b), there is little morphological evidence available. Especially, evidence is still lacking for a preferential localization of these proteins at the active zone of synapses to demonstrate their association with fast neurotransmitter release in situ. The present study reveals an evidently increased immunolabeling of VAMP II, SNAP-25, Rab3A, SV2 and N-type $Ca^{2+}$ channels at active zones of fast synapses. The quantitative analysis exhibits a more concentrated localization of these proteins both in the active-zone-related vesicle area and at the active

zone plasma membrane. This may reflect both the increase in synaptic vesicle density at release sites and a docking-related accumulation of the proteins. Of all these proteins VAMP II has the highest enrichment at both the vesicle membrane and the plasma membrane. The localization of VAMP II and SNAP-25 on many docked vesicles at the active zone indicates their participation in the docking complex. In addition, P/Q-type $Ca^{2+}$ channels are localized specifically at the active zone plasma membrane and Bassoon is concentrated particularly in the vicinity of the active zone. These results confirm the existence of these proteins in the neurotransmitter release sites and provide strong support for the direct participation of these proteins in synaptic vesicle exocytosis in the fast central synapse (Rizo and Sudhof, 1998; tom et al., 1998; Seagar et al., 1999).

### 4.2.3. Distribution of SNAP-25 at nerve terminals

According to the original SNARE hypothesis, the specificity of vesicle targeting during exocytosis at the presynaptic plasma membrane is assured by complex formation between the v-SNARE VAMP II and the t-SNAREs SNAP-25 and syntaxin I (Rothman, 1994b). The t-SNAREs SNAP-25 and syntaxin I are essential presynaptic membrane components for the specific targeting of synaptic vesicles to the active zone (Sollner et al., 1993a). In this study, labeling for SNAP-25 was localized to the active zone plasma membrane of the central synapse, revealing its participation in synaptic vesicle exocytosis. In mossy fiber terminals, the labeling on the docked synaptic vesicles at the actives zones implies an association of SNAP-25 with the presynaptic docking complex. However, the gold particles do not appear to be restricted to the active zone. They were also found at the plasma membrane outside the active zone. The result is in agreement with the notion that t-SNAREs are not specifically associated with the presynaptic release sites but are located also at the remainder of the axonal membrane (Zimmermann, 1997; Kretzschmar et al., 1996). Labeling for SNAP-25 was also found along the entire axonal plasma membrane (Tao-Cheng et al., 2000; Garcia et al., 1995; Galli et al., 1995). The widespread distribution of this t-SNARE at axonal plasma membranes suggests that it could not be responsible for defining the release site for synaptic vesicles.

Furthermore, in this study, SNAP-25 was also found to be partially associated with synaptic vesicles in the synaptic terminals and with microvesicles in the neurosecretory endings. Although the majority of the t-SNAREs were localized at the plasma membrane, significant amount was reported also on the vesicle membrane. Both SNAP-25 and syntaxin I have been demonstrated in association with synaptic vesicles (Walch-Solimena et al., 1995;

Kretzschmar et al., 1996; Schulze et al., 1995), chromaffin granules (Tagaya et al., 1995; Tagaya et al., 1996; Hohne-Zell and Gratzl, 1996), and the large dense core vesicles of PC12 cells (Marxen et al., 1997). The functional significance of these t-SNAREs on vesicular organelles remains to be explained. It cannot be excluded that some of these vesicles represent constitutive carrier vesicles transporting newly synthesized SNAP-25 from the soma to the plasma membrane of the terminals. Moreover, in agreement with the other reports (Tao-Cheng et al., 2000; Duc and Catsicas, 1995), the Golgi complex was also labeled with SNAP-25 in neuronal soma in the present experiment, suggesting that SNAP-25 is first sorted at the trans-Golgi, then transported to the terminals via carrier vesicles. On the other hand, it has been demonstrated by subcellular fractionation that the major pools of t-SNAREs recycle with synaptic vesicles in the nerve terminals in order to reactivate them (Walch-Solimena et al., 1995). SNAP-25 positive tubulovesicular structures are considered as endosome-related vesicles undergoing recycling between the plasma membrane and the early endosomes (Tao-Cheng et al., 2000). Furthermore, it has been reported that not only all individual SNARE elements but also their complex can be associated with free undocked vesicular organelles (Otto et al., 1997; Hohne-Zell and Gratzl, 1996). SNARE complexes are not exclusively assembled between opposing membranes at the sites of exocytosis, but side by side in the same membrane (Otto et al., 1997). These complexes may even be present during fast axonal transport before reaching the nerve endings. They can be required to properly direct presynaptic membrane proteins to the neuronal ending (Shiff and Morel, 1997; Morel et al., 1998). Before docking, these complexes may be disassembled by NSF and SNAP proteins in an ATP-dependent manner, priming the synaptic vesicles for exocytosis (Otto et al., 1997).

Obviously, the localization of t-SNAREs and the specific v/t-SNARE interaction cannot be the sole determinants for membrane-targeting specificity (Yang et al., 1999). Additional control components are required to define release sites and to restrict SNARE action to the appropriate site (Zhang et al., 2000; Galli et al., 1995; Pelham, 2001).

### 4.2.4. Localization of α/β-SNAP and NSF on granules of the neurohypophysis

The action of SNAPs is tightly associated with that of NSF. Both of them are known to be universally required for membrane fusion events (Sollner et al., 1993a; Hay and Scheller, 1997). It has been thought that SNAPs and NSF interact with their membrane receptors only when vesicles are docked on the target membrane. They bind transiently to the assembled 7S

synaptic SNARE complex to form a so-called large 20S particle. However, it has recently been shown that α-SNAP and NSF exist predominantly in a membrane-bound form. Chromaffin vesicles were found to specifically contain bound α-SNAP and NSF (Banaschewski et al., 1998). NSF was also observed on highly purified synaptic vesicles of rat brain (Hong et al., 1994). And α-SNAP was identified in synaptic vesicles at the neuromuscular junction (Nishiki et al., 2001). In addition, the analysis of the distribution of NSF and α-SNAP in fractionated organelles from the adrenal medulla indicated that NSF and α-SNAP are associated with chromaffin granules (Burgoyne and Williams, 1997). Moreover, immunoreactivity for α-SNAP and NSF has been reported in the rat neurohypophysis by immunofluorescence histochemistry (Jacobsson and Meister, 1996). In the present study, labeling for α/β-SNAP is present neither on synaptic vesicles of fast synapses nor on the microvesicles of the neurohypophysis. Yet, the intensive labeling for α/β-SNAP on the granules and some labeling of NSF on the synaptic vesicles and granules support the idea that vesicular organelles can carry NSF and α-SNAP to the site of exocytosis. These proteins may also exert their function prior to vesicle docking. The α/β-SNAP labeling on the granules near the plasma membrane and the association of gold particles with the connecting stalk of the granules with the plasma membrane further suggest that α/β-SNAP is involved in the regulation of the granule exocytosis.

### 4.2.5. Association of Rab3A with both small clear vesicles and granules

Rab3A, the predominant Rab protein in the brain, has been shown to be exclusively localized to the membrane of synaptic vesicles and function in the regulation of neurotransmitter release (Matteoli et al., 1991; Stahl et al., 1994; Oberhauser et al., 1992). In particular, Rab3A has been implicated in regulating the formation and stability of the SNARE complex (Oberhauser et al., 1992; Stahl et al., 1994). Rab3A has also been revealed to be associated specifically with bovine chromaffin granules and granules in rat PC12 cells (Lin and Scheller, 2000; Weber et al., 1996; Darchen et al., 1995; Darchen et al., 1990). Noticeably, some chromaffin granules remained unstained which is considered to be due to heterogeneity of the granule population (Darchen et al., 1995). In the present study, Rab3A is localized to both types of secretory vesicles. The presence of Rab3A at the membrane of synaptic vesicles in the central synapse and of microvesicles in neurohypophysial terminals reveals that Rab3A has an important role in the secretion of small vesicles. In addition, in the neurohypophysis, Rab3A was also localized by double labeling specifically to the oxytocin-

containing granule population, implicating that the Rab3A protein is involved in the hormone secretory pathway in neurohypophysis. A similar observation has been reported for another Rab3 isoform Rab3B that shares 80% amino acid identity with Rab3A. Co-localization of Rab3B and oxytocin was revealed at electron dense granules of the sheep corpus luteum (Al Matubsi et al., 1999). However, the presence of the gold particles also in the interior of the granules remains to be elucidated. It is still questionable whether Rab3A is specially associated with the core material of the granules.

### 4.2.6. Presence of N-type and P/Q-type $Ca^{2+}$ channels on both plasma membrane and secretory vesicles

Rapid neurotransmitter release requires the localization of both synaptic vesicles and calcium channels at the presynaptic active zone. By specific molecular interactions of syntaxin I, SNAP25 and synaptotagmin I in a multiprotein complex both, N-type and P/Q-type $Ca^{2+}$ channels have been revealed to be coupled to the molecular machinery of exocytosis at presynaptic neurotransmitter release sites (Stanley, 1997; Sheng et al., 1998; Seagar et al., 1999). Consistent with their functional characteristics in regulated exocytosis, N-type and P/Q-type $Ca^{2+}$ channels have been found by light microscopy in a wide variety of presynaptic neural terminals (Westenbroek et al., 1995; Sheng et al., 1998). However, ultrastructural evidence for further defining the subcellular localization of these $Ca^{2+}$ channels is rather scarce. In the present study, the immunolabeling of N-type and P/Q-types $Ca^{2+}$ channels could be allocated to the active zone of mossy fiber terminals, providing further morphological evidence for their participation in the regulation of the rapid neurotransmission and for the hypothesis that these two $Ca^{2+}$ channels can interact with the trimetric SNARE complex. In addition, a few gold particles were also found on the remainder of the plasma membrane of the central synapse. N-type $Ca^{2+}$ channels have been previously reported to be associated not only with presynaptic neuronal terminals but also widely with the plasma membrane along the entire length of dendrites and cell bodies of a wide range of neurons (Westenbroek et al., 1992). Besides initiating neurotransmitter release they also have other functions, such as mediating dendritic calcium transients (Westenbroek et al., 1995). As compared to N-type $Ca^{2+}$ channels, P/Q-type $Ca^{2+}$ channels are considered to have a relatively low density in the membrane of dendrites and cell bodies of most central neurons implying a more prominent role in neurotransmitter release at central synapses (Westenbroek et al., 1995).

In neurohypophysial terminals multiple types of $Ca^{2+}$ channels containing N-, L-, P/Q-. and R-type $Ca^{2+}$ channels have been identified via physiological or biochemical approaches (Fisher and Bourque, 1995; Wang et al., 1999). However, less is known concerning their localization. The present study suggests that N-type $Ca^{2+}$ channel are associated with the plasma membrane of neurohypophysial terminals. The immunolabeling on the plasma membrane near the clustered microvesicles indicates the competence for the microvesicle exocytosis through N-type $Ca^{2+}$ channels. In addition, the presence of gold particles for P/Q-type $Ca^{2+}$ channels on the granules and plasma membrane in some terminals supports physiological and pharmacological evidence that the P/Q-type $Ca^{2+}$ current component exists only in a subset of the neurohypophysial terminals (Wang et al., 1997a). In combination with N- and L-type $Ca^{2+}$ channels, they control vasopressin but not oxytocin peptide release in these terminals. In addition, present observation does not provide evidence for a clustered distribution of N- or P/Q-type $Ca^{2+}$ channels at the plasma membrane. This agrees with the notion that neurohypophysial terminals lack specialized release zones. The release of granules has been proposed to be dependent on a general elevation in sub-membranous $Ca^{2+}$, which is mediated by the summation of $Ca^{2+}$ influx through multiple dispersed $Ca^{2+}$ channels (Fisher and Fernandez, 1999).

An unexpected finding in this study is that N-type $Ca^{2+}$ channels are present in the membrane of both synaptic vesicles in the central synapse and in microvesicles of neurosecretory terminals. In addition, P/Q-type $Ca^{2+}$ channels are specifically associated with neurosecretory granules in some terminals of the neurohypophysis. This suggests that these vesicular organelles might either be involved in the trafficking of $Ca^{2+}$ channels from the soma to the terminal membrane or serve as an internal reserve pool of N- and P/Q-type $Ca^{2+}$ channels. These internally stored $Ca^{2+}$ channels may be rapidly translocated to the plasma membrane to enhance the release of messenger substance when the physiological need is high. Up to now, however, few data are available regarding intracellular trafficking of N- or P/Q-type $Ca^{2+}$ channels in neuronal and endocrine cells. Interestingly, internal storage of N-type $Ca^{2+}$ channels on the chromograin B-containing secretory granules has been demonstrated in neuroblastoma and PC12 cell line. These channels can be inserted into the plasma membrane when the cells are exposed to different secretagogues, such as KCI, ionomycin, and phorbol ester (Passafaro et al., 1996).

### 4.2.7. Involvement of Bassoon in neurotransmitter release

Bassoon is a high molecular weight protein that is considered to be specifically associated with the active zone area (tom et al., 1998; Gundelfinger and tom, 2000). This labeling pattern was confirmed in the mossy fiber terminals and other smaller synaptic endings by the cryo-immunogold technique in the present observation. In sharp contrast with the random distribution of the other proteins in the presynaptic terminals, a preferential localization of Bassoon near the active zone was observed. The quantitative analysis shows that Bassoon, out of all proteins investigated, has the highest increase ratio of the immunolabeling at the active zone area. However, unlike the other proteins, little labeling of Bassoon appeared directly on the plasma membrane. The vast majority of the gold particles were characteristically observed at a distance (50-70 nm) from the active zone plasma membrane. This labeling pattern implies that Bassoon is intimately associated with the tips of presynaptic dense-projection (Zhang et al., 2000). The presynaptic dense projection is thought to function in the guiding of vesicles to their release sites (Zimmermann, 1993). Thus, Bassoon may be involved in the structural and functional organization of the neurotransmitter release site to assure preferential docking and exocytosis of synaptic vesicles at the active zones (tom et al., 1998; Zhang et al., 2000). It perhaps plays an important role in determining the specificity of vesicle docking and fusion. The absence of immunolabeling from neurohypophysial terminals confirms the specific role of Bassoon at the active zone from another angle.

Bassoon has also been reported to be associated with membranous compartments in neurons by biochemical assay and electron microscopy performed on the same biochemical fractions (Sanmarti-Vila et al., 2000). In the present study, scarce immunolabeling was also found at the vesicles outside the active zone region. This might represent the transport of Bassoon to the presynaptic site.

### 4.2.8. Microvesicles and neurosecretory granules in the neurohypophysis

The present study indicates that some proteins essential for the docking and fusion of synaptic vesicles are present in the neurohypophysis. Nevertheless, the distribution pattern reveals that these proteins have obviously a differential association with the population of microvesicles and large granules. The immunolabeling for the synaptic proteins VAMP II, SNAP-25, SV2, Rab3A and the N-type $Ca^{2+}$ channels was found specifically on microvesicles and the labeling intensity of these proteins over the microvesicles was similar to that over the

synaptic vesicles. Using either biochemical analysis or immunocytochemical methods many synaptic proteins including VAMP II, SNAP-25, syntaxin I, SV2, synapsin I, synaptophysin, synaptotagmin, and cysteine string proteins (csps, serving as a regulatory factor for exocytosis) have been found to be associated with microvesicles in the neurohypophysis (Walch-Solimena et al., 1993; Jurgutis et al., 1996; Pupier et al., 1997; Navone et al., 1989; Hayashi et al., 1994b). Thus, these microvesicles contain obviously the entire molecular machinery required for fast and $Ca^{2+}$-dependent exocytosis. The present results support the view that microvesicles have not only a similar size and appearance but also similar characteristics as typical synaptic vesicles (Navone et al., 1989).

By contrast, only synaptotagmin and csps (Jacobsson and Meister, 1996; Pupier et al., 1997; Walch-Solimena et al., 1993; Hayashi et al., 1994b) as well as small amounts of VAMP II (Pupier et al., 1997; Jurgutis et al., 1996) have been reported previously to be associated with neurosecretory granules. Recently, CAPS, $Ca^{2+}$-dependent activator proteins for secretion, have been reported to be essential proteins for LDCV exocytosis and not to be required for the exocytosis of synaptic vesicles (Berwin et al., 1998; Jurgutis et al., 1996). In the present study, little labeling for the synaptic proteins VAMP II, SNAP-25, SV2 and the N-type $Ca^{2+}$ channel was observed at the membrane of the granules, in sharp contrast to the abundant labeling of microvesicles. On the other hand, α/β-SNAP and some NSF were found on the granules, and in some terminals also Rab3A and the P/Q-type $Ca^{2+}$ channels. The identification of P/Q-type $Ca^{2+}$ channels and Rab3A only in a subset of terminals in the present study reveals that there are probably some differences in the regulation of exocytosis even between granule subpopulations. Correspondingly, physiological and pharmacological experiments have indicated that P/Q-type $Ca^{2+}$ channels and R-type $Ca^{2+}$ channels selectively exist in vasopressin (Wang et al., 1997a) or oxytocin releasing nerve terminals (Wang et al., 1999) and function only in controlling vasopressin or oxytocin release, respectively. However, the labeling of these proteins in the interior of the granules remains elusive. Whether the results from the experimental procedure or whether the antibodies against these proteins associate with the internal material of the granules is unknown. In any case, the lower contents of multiple exocytosis-related synaptic proteins on neurosecretory granules indicated that the molecular basis for the exocytosis between synaptic vesicles and granules is different. This is consistent with the view that synaptic vesicles and secretory granules possess distinct regulatory protein components and are organelles related to two different secretory pathways. Although both types of organelles undergo $Ca^{2+}$- dependent exocytosis, it

is quite likely that they have differential mechanisms for the regulation of exocytosis (Zimmermann, 1997; De Camilli and Jahn, 1990). In addition, the differential distribution of the various synaptic proteins investigated in the present study demonstrates that there are distinct differences in membrane composition between microvesicles and neurosecretory granules in the nerve terminals of the neurohypophysis. This agrees with the notion that microvesicles represent organelles different from granules (Navone et al., 1989; Meeker et al., 1991). Recently, it has been revealed by capacitance measurement the that the exocytosis of these two vesicle types is differently mediated (Klyachko and Jackson, 2002).

### 4.2.9. Exocytosis of microvesicles in the neurohypophysis

The similarity in morphology and membrane composition of microvesicles to synaptic vesicles suggests that microvesicles are involved in the secretion of messenger substances (Meeker et al., 1991; Navone et al., 1989; Hayashi et al., 1994b). The present observation provides further support for this hypothesis. An accumulation of small clear vesicles was found along the membrane and some vesicles beneath the plasma membrane appeared to be in contact with the plasma membrane (Meeker et al., 1991; Hayashi et al., 1994b). The presence of VAMP II, SNAP-25, and N-type $Ca^{2+}$ channels at the plasma membrane facing the clustered vesicles indicates in particular the competence of microvesicles for docking and exocytosis along the extended plasma membrane in the absence of active zones. Physiologically, by measuring the capacitance of the microvesicles, microvesicles have recently been demonstrated to have similar functional capabilities as synaptic vesicles and to undergo $Ca^{2+}$-triggered exocytosis in response to membrane depolarization (Klyachko and Jackson, 2002).

However, the physiological significance of the exocytotic release of messenger substances from microvesicles for the neurohypophysis is still unclear. Generally, the secretion from neurosecretory terminals of the neurohypophysis is considered to function in the direct release of peptide hormones from the granules into the blood stream and this release of neurohormones is restricted to the terminals lining the pericapillary space. However, neurosecretory axons have frequently been observed to actually terminate near pituicytes, the specialized astrocytes of the neurohypophysis (Tweedle and Hatton, 1982). Synaptoid contacts have been observed between neurosecretory axons and pituicytes as well as between axonal terminals themselves (Castel et al., 1996; Boersma et al., 1993; Van Leeuwen et al., 1983). Furthermore, it has been reported that pituicyte enclosure may be involved in the

inhibition of hormone release and there is a dynamic relationship between the neurosecretory processes and pituicytes. When the hormones are at high demand, synaptoid contacts with pituicytes are increased and pituicytes apparently retract their processes from the neurosecretory terminals, allowing greater access for nerve terminals to the basal lamina surrounding the fenestrated capillaries (Boersma et al., 1993). Therefore, there are probably direct cellular interactions between them. The messengers released from microvesicles may be used as local regulatory factors such as to coordinate the secretion of the neurohypophysial terminal. Thus, messenger substance release from neurohypophysial nerve endings includes not only exocytosis from secretory granules but also from microvesicles. Evidently, further studies on the microvesicle secretion will be very important for a thorough understanding of the physiological function of the neurohypophysis.

## 4.3. Expression and localization of transfected proteins in the astrocytoma cell line U373 MG

The astrocytoma-derived U373 MG cell line can express GFAP and release NGF, glutamate and GABA (Emmett et al., 1997; Ye and Sontheimer, 1999; Soria-Jasso and Arias-Montano, 1996). Therefore, it is a potential cell line for the study of the astrocytic messenger release mechanism. In the present study, the expression and localization of some essential proteins responsible for regulated exocytosis and intercellular membrane fusion was investigated and compared to that in astrocytes and neurons

### 4.3.1. Expression of transfected proteins

Using transient transfection and immunocytochemistry techniques, the expression and distribution of a variety of recombinant proteins were examined in U373 MG cells in order to investigate the potential release characteristics of the messenger substances. The results reveal that U373 MG cells are capable of expressing all three members of the synaptic SNARE complex (the v-SNARE VAMP II, the t-SNAREs syntaxin I and SNAP-25*)*, the ubiquitous v-SNARE cellubrevin and the small GTP-binding protein Rab5. The synaptic SNARE complex has been demonstrated to play a crucial role in regulated exocytosis at synaptic terminals (Sollner et al., 1993a; Jahn and Sudhof, 1999). Cellubrevin, a synaptobrevin (VAMP II) homologue, has been thought to be involved in both constitutive and regulated exocytosis in many different tissues (McMahon et al., 1993). Rab5 is an endosome-associated GTP-binding

protein. It has been known to serve critical regulatory roles in endosome fusion and was found also on synaptic vesicles (Jahn and Sudhof, 1999; Fischer et al., 1994b).

A large body of experimental evidence indicates that the fundamental mechanism involved in membrane trafficking from yeast to neuron is very similar (Morgan, 1995; Ferro-Novick and Jahn, 1994; Bennett and Scheller, 1993). This evolutionary conservation in all eukaryotic cells implies that similar proteins can be used for controlling membrane fusion in neurons and the other non-neural cells. Moreover, recent data have shown that proteins originally thought to be specific for synaptic neurotransmitter release might also occur in non-neural cells. In particular, cultured astrocytes have been shown to express some members of the SNARE proteins, such as VAMP II and syntaxin I (Parpura et al., 1995a). Furthermore, the t-SNARE SNAP-25 and the synaptic vesicle proteins SV2, Rab3A, synaptotagmin I, synaptophysin, and synapsin I have been identified in primary astrocyte cultures from cerebral cortices of newborn rats (Maienschein et al., 1999). Consistent with the results of Maienschein et al. (1999) VAMP II was localized in the present experiment to vesicular organelles of different size at the ultrastructural level. These experiments were performed with primary astrocytes cultured from cerebral cortices of newborn rats. All of the above proteins have been implicated in astrocytic messenger release (Parpura et al., 1995a; Jeftinija et al., 1997). The astrocytoma cell line U373 has been shown to secrete neurotransmitters such as glutamate and GABA (Soria-Jasso and Arias-Montano, 1996; Ye and Sontheimer, 1999). In view of the functional generality of these membrane fusion-related proteins, it is reasonable to expect that the proteins expressed in U373 cells also serve similar functions as in neurons and astrocytes. The present results suggest that U373 are competent to carry out regulated exocytosis by means of the classical vesicular SNARE mechanism.

### 4.3.2. Association of expressed proteins with vesicular organelles

All recombinant synaptic proteins investigated in U373 cells reveal a very similar punctuate cellular distribution under the fluorescence microscope. This implies that all of them are mainly associated with intracellular compartments. Furthermore, the punctuate staining patterns of these transfected proteins are essentially equivalent to those of their corresponding endogenous counterparts (Volknandt et al., 2002), indicating that the transfected proteins were appropriately targeted in U373 cells. The distribution of the v-SNAREs VAMP II and cellubrevin as well as the t-SNAREs syntaxin I and SNAP-25 is also

consistent with their labeling pattern in cultured astrocytes (Maienschein et al., 1999; Parpura et al., 1995a).

Under electron microscope U373 cells reveal abundant vesicular organelles. The organellar association of the proteins investigated was further confirmed by cryo-immunoelectron microscopic analysis. All proteins including the v-SNAREs VAMP II, cellubrevin, the t-SNAREs syntaxin I, SNAP-25 and the small GTPase Rab5 were found to be selectively localized at the membrane of vesicular organelles of low electron density. This direct morphologic evidence reveals their participation in the trafficking of these vesicular organelles, probably including vesicle exocytosis in U373 cells. However, every protein has its own distribution characteristics, indicating that all of these proteins serve own specific functions in the particular cycling stages.

***VAMP II:*** VAMP II was identified as a membrane protein of synaptic vesicles first in the rat brain (Baumert et al., 1989) and has been known to play a critical role as v-SNARE in synaptic vesicle fusion of nerve terminals (Rizo and Sudhof, 1998). In addition, it is also expressed in astrocytes and in a variety of other nonneuronal cells (Rossetto et al., 1996). The cryo-electron microscopy showed that the recombinant myc-VAMP II was expressed in U373 cells at a higher level than the other investigated proteins. It was associated with various types of vesicular organelles throughout the entire cell body. In particular, myc-VAMP II was localized to numerous small vesicles and tubulovesicular organelles, suggesting that myc-VAMP II is involved in the trafficking of these vesicles in U373 cells as it is in neurons and astrocytes. The observation that myc-VAMP II was present especially at the TGN vesicles of the Golgi apparatus and at tubulovesicular compartments of endosomes indicates that myc-VAMP II could be sorted into small vesicles from the dynamic TGN and possibly also from endosomes. In addition, the occasional labeling on granules in the cytoplasm is in agreement with subcellular fractionation experiments demonstrating a small pool of VAMP II in association with granules in U373 cells (Volknandt et al., 2002). However, the high expression of myc-VAMP II at multivesicular bodies and lysosomes most likely resulted from the overexpression of this recombinant protein, resulting in its targeting to the ultimately degradative pathway. In addition, the dense arrangement of gold particles for myc-VAMP II over the plasma membrane in some cells might also result from the overexpression of this transfected protein. A similar observation was made at the plasma membrane of the PC12 cells when very high expression levels of the transfected VAMP II occurred (Grote and Kelly,

1996). Nevertheless, it has been reported recently that VAMP II is associated with the plasma membrane of nerve terminals of the Torpedo electric organ (Taubenblatt et al., 1999), and VAMP II can also be sorted into small vesicles directly from the plasma membrane (Shi et al., 1998). This broad distribution of VAMP II indicates that VAMP II is involved in various stages of vesicular cycling in U373 cells. Double labeling of myc-VAMP II with flag-cellubrevin and myc-VAMP II with GFP-Rab5 revealed a partial colocalization. By comparison, myc-VAMP II was located more extensively and intensively in the peripheral cytoplasm than flag-cellubrevin and GFP-Rab5, where more myc-VAMP II was probably associated with vesicles of various form and size.

***SNAP-25 and syntaxin I:*** Both t-SNAREs of the neuronal fusion complex SNAP-25 and syntaxin I were expressed in U373 cells. Many previous studies have failed to demonstrate the presence of SNAP-25 in cultured astrocytes. It seems that the expression of SNAP-25 is restricted to neurons and neuroendocrine cells. By contrast, its homologue SNAP-23 was found to be widely distributed in astrocytes and other glial cell types (Hepp et al., 1999). However, in primary cultures from cerebral cortices of newborn rats the expression of SNAP-25 has recently been demonstrated to be time-dependent. It declines with prolonged culture time (Maienschein et al., 1999). In the present study, the expression of transfected HA-SNAP-25 was limited to only a minority of small cells, but with a relatively high expression level. It appears that the transfection with HA-SNAP-25 itself inhibits the growth of the transfected cells. However, the immunofluorescence of the HA-SNAP-25 in the transfected cells exhibited a similar pattern of immunoreactivity as for the other transfected protein. By contrast, another transfected t-SNARE, syntaxin I, was intensively expressed in a large number of U373 cells. Syntaxin I has been identified in astrocytes in many previous studies (Maienschein et al., 1999; Hepp et al., 1999; Parpura et al., 1995a). The labeling pattern of syntaxin I in U373 cells is consistent with that in cultured astrocytes.

It is noteworthy that, in accordance with results obtained from astrocytes, the immunolabeling of both presumptive t-SNAREs syntaxin I and SNAP-25 in U373 cells was confined to the vesicular organelles. No significant labeling was found on the plasma membrane of U373 MG cells by immunofluorescence microscopy and electron microscopy. In neurons, although SNAP-25 and syntaxin I are localized primarily to the plasma membrane, these proteins have also been observed on synaptic vesicles or granules (Walch-Solimena et al., 1995; Kretzschmar et al., 1996). The precise function of these t-SNAREs in U373 cells

remains to be elucidated. The high level of fluorescent colocalization of the recombinant proteins RFP-syntaxin I and myc-VAMP II in the cell body and in cell processes suggests that the two proteins were mostly sorted into identical vesicular organelles. It is possible that these syntaxin I- or SNAP-25-containing vesicles are used as a reserve pool of these t-SNAREs. However, it cannot be excluded that these t-SNARE proteins may also be involved in other functions, in addition to their participation in the formation of SNARE fusion complex.

***Cellubrevin:*** Cellubrevin, a ubiquitously expressed small (14 kDa) integral membrane protein, is 97% identical to VAMP II (McMahon et al., 1993). It has a wide tissue distribution in non-neural cells and is selectively cleaved by tetanus toxin (Yamasaki et al., 1994; McMahon et al., 1993). This toxin cleavage has been indicated to impair exocytosis of transferrin receptor-containing recycling vesicles in CHO cells (Galli et al., 1994). In the nervous system cellubrevin is expressed at significant levels primarily in glial cells (Chilcote et al., 1995). In cultured astrocytes, cellubrevin was localized throughout the cytoplasm and accumulated primarily in the area occupied by the Golgi complex (Parpura et al., 1995a). Furthermore, cellubrevin has been revealed to interact with the t-SNAREs syntaxin I and SNAP-23 (Hepp et al., 1999) and also be a substrate for the proteolytic action of tetanus toxin and botulinum toxins in astrocytes (Verderio et al., 1999; Parpura et al., 1995a). In U373 cells, the recombinant flag-cellubrevin was found throughout the cytoplasm and to be concentrated in the perinuclear area, consistent with the results from cultured astrocytes. Correspondingly, the gold particles for flag-cellubrevin were observed by electron microscopy at small vesicles dispersed in the cytoplasm and particularly at the TGN vesicles of the Golgi complex**.** Cellubrevin has been targeted to synaptic vesicle-like microvesicles when expressed in PC12 cells (Chilcote et al., 1995; Grote et al., 1995) and thought to have similar function as its homologue VAMP II because of their similar subcellular localization and biochemical properties (Chilcote et al., 1995). In U373 cells, though the overall distribution pattern of these two proteins was similar, double labeling of flag-cellubrevin with myc-VAMP II revealed only a partial colocalization in the cytoplasm as revealed by fluorescence microscopy. The yellow staining was confined to the differentially sized puncta dispersed in the cytoplasm. Under the electron microscopy, differentially sized gold particles for both proteins were visualized only over electron-lucent vesicles. The partial colocalization of these two proteins implies a similar function as v-SNARE.

***Rab5:*** The low molecular weight GTP-binding protein Rab5 has been known to regulate membrane traffic in the early endocytic pathway. It is responsible for the delivery of material from the plasma membrane to early endosomes (Bucci et al., 1992; Trischler et al., 1999) and functions as an important regulator of endosome fusion (Barbieri et al., 1998; Gorvel et al., 1991; Stenmark et al., 1994). In addition, it has also been proposed that Rab5 is involved in membrane transport, motility and intracellular distribution of early endosomes by regulating the endosome interaction with microtubules (Nielsen et al., 1999). Rab5 has been localized to endosomes (Sonnichsen et al., 2000; Novick and Zerial, 1997) and also to synaptic vesicles in rat brain (Fischer et al., 1994b). The Rab5-dependent trafficking pathway has been demonstrated to play an important role in synaptic neurotransmitter release. Rab5 overexpression increases the release efficacy (Wucherpfennig et al., 2003). In primary astrocyte cultures Rab5 is found in the cytoplasm and over the membrane of the endosomes (Megias et al., 2000). In U373 cells, GFP-Rab5 was observed at clustered vesicular organelles and endosomes. This suggests that Rab5 is involved in the vesicle cycle and in endosome fusion of U373 cells. Double labeling for GFP-Rab5 and myc-VAMP II by fluorescent microscopy showed a partial colocalization in the cytoplasm. GFP-Rab5 was obviously more intensely expressed in the perinuclear area. A colocalization of these two proteins at the ultrastructural level was only found on some clustered vesicles. Partial colocalization of Rab5 with VAMP II in U373 cells suggested that the endosomal protein Rab5 is associated with VAMP II-containing organelles during some stages of their life cycle. The potential functional relations between these two proteins require further study.

### 4.3.3. Formation of small vesicles in U373 cells

Numerous small vesicles (40-60 nm in diameter) occur in clusters or are dispersed individually in the cytoplasm of U373 cells. They represent potential organelles for the secretion of low molecule weight messengers in the cells. It has been known that early endosomes can act not only as an acceptor for membrane-derived endocytic vesicles but also as a sorting station for vesicle proteins in the vesicle recycling pathway (Grote and Kelly, 1996). In PC12 cells, the recombinant protein VAMP II has been found to recycle through the vacuolar part of early endosomes to the associated tubules (emanating from vacuole). Moreover, endosome tubules have been demonstrated to bud off to yield a population of transport vesicles (de Wit et al., 1999; Geuze et al., 1987). On the other hand, a second pathway for the formation of small vesicles has recently been demonstrated, whereby the

plasma membrane is the direct precursor of synaptic vesicles (Schmidt et al., 1997; Shi et al., 1998; Takei et al., 1996). The proteins of small vesicles are sorted directly from plasma membrane, without passing through an endosomal intermediate. Schmidt et al. (1997) described a novel compartment, from which small vesicles originate. This compartment was connected to the plasma membrane via narrow membrane continuity, forming the so-called sub-plasmalemmal tubulo-cisternal membrane system.

In the present experiment, tubular structures were observed to be connected directly with the plasma membrane. Furthermore, some small round vesicles appeared to be budding from thick and deep tubulovesicular invaginations of the plasma membrane**.** Many vesicle clusters were found to be generated from plasma membrane-deriving tubulovesicular structures or vacuoles in the periphery of the cells. Moreover, the wide tubulovesicular structures beneath the plasma membrane which were similar to the donor compartments of synaptic-like microvesicles in PC12 cells (Schmidt et al., 1997) were labeled by VAMP II. These observations provide direct morphological evidence for the existence of a plasma membrane-derived pathway of vesicle formation in U373 cells. In addition, a high level of the vesicle protein VAMP II was localized to both the endosomal vacuoles and the associated tubulovesicular structures. Interestingly, also tubules that were fragmenting into small vesicular profiles were observed in the cytoplasm. These tubules are likely candidates for the intracellular donor compartment of small vesicles in U373 cells. VAMP II has been demonstrated to be sorted into small vesicles from both endosomes and the plasma membrane in PC12 cells (Shi et al., 1998). The results from U373 cells support the notion that two pathways of small vesicle formation coexist in the same cell.

### 4.3.4. Similarities between U373 cells and cultured astrocytes in exocytosis

The subcellular fractionation experiments in our laboratory revealed that U373 cells contain two pools of vesicular organelles with clearly different density. The organelles of lower density carry the majority of myc-VAMP II and the granule pool of high density contains mainly secretogranin II and a small amount of myc-VAMP II. Thus, U373 MG cells may also use two types of vesicular organelles to release messenger substances by the regulated pathway (Volknandt et al., 2002). In line with these findings the present study indicates that U373 MG cells can express many essential proteins that are involved in regulated exocytosis. Furthermore, the cryo-electron microscopy provides direct evidence for

the association of all these expressed proteins with electron-lucent vesicular organelles, indicating the potential of U373 MG cells to release low molecular weight messengers by vesicular secreting pathway similar or identical to that in neurons or cultured astrocytes. In addition, the labeling of myc-VAMP II on the granules exhibits that VAMP II may participate in the release of the granules in U373 cells. The release of secretogranin II from granules by means of bradykinin and ATP as well as the calcium ionophore calcimycin has been shown in U373 cells, suggesting that U373 cells can secrete proteins or peptides via a regulated release pathway similar to astrocytes (Volknandt et al., 2002).

Similar to cultured astrocytes, U373 cells do not form axons and lack synapses. While clustered small vesicles or tubulovesicular structures were extensively observed in the cytoplasm or even close to plasma membrane, neither a distinct release region, such as “the active zone” nor docked small vesicles in specialized areas of the cells were found. In addition, the expression pattern of the investigated proteins in U373 cells shares similarities with that in long term cultured astrocytes. VAMP II, cellubrevin, syntaxin I, SNAP-25 and SNAP-23 were demonstrated to be the essential members of SNARE proteins in U373 cells (Volknandt et al., 2002). Moreover, unlike in neurons, syntaxin I and SNAP-25 in U373 cells were found to be associated only with intracellular vesicular organelles showing a similar organellar association as in cultured astrocytes. Obviously, the GFAP-expressed astrocytoma cell line U373 MG is equipped with many representative astrocytic release characteristics. The cells release their messenger substances probably via a similar secretory mechanism as astrocytes.

## 4.4. Perspectives

The present study reveals that the cryo-immunogold technique has strong advantages in preserving both structural integrity and peptide antigenicity. The negative contrast is excellent to delineate membrane structure. This technique is expected to be applied in the further studies for the localization of the synaptic proteins and/or the other membrane proteins.

As expected, in the present study, an evidently increased immunolabeling for VAMP II, SNAP-25, Rab3A, SV2 and N-type $Ca^{2+}$ channels is revealed at active zones of fast synapses. However, the widespread distribution of the t-SNAREs along the axonal plasma membranes reveals that the specific SNARE interactions cannot be the sole targeting determinants. The presumptive role of SNARE proteins in docking and exocytosis of the synaptic vesicles must

be complemented by other factors. The presynaptic dense projections of the active zone have been thought to serve as structures for guiding vesicle to release sites (Zimmermann, 1993). However, these could not be recognized in the present experiment because they are only revealed by staining with phosphotungstic acid. The improvement of the staining method for displaying this structure together with the docked vesicles and the immunolabeling of the synaptic proteins on the cryosections should be helpful for a further functional analysis of these synaptic proteins at the action zone and in the study of the mechanism of exocytosis.

Although the immunolabeling was specifically allocated to defined organelles, not all of them could be labeled. At the active zone, only part of the proteins involved in the docking complex bound the gold particles. A possible explanation is that the immunolabeling is mostly limited to the available epitopes exposed at the surface of the cryosections. The small 1.4 nm Nanogold proved to be able to penetrate farther into the low-density matrix of the cryosections. In the present experiments, 1.4 nm immunogold particles together with silver enhancement gave rise to a higher labeling density than colloidal gold. However, there are still some problems with the irregular size of the enhanced particles and the merging of growing silver/gold particles. An improvement of the present procedure with more suitable experimental conditions would provide a more effective approach for the further studies.

Dense gold particles for α/β-SNAP, as well as for Rab3A and P/Q-type $Ca^{2+}$ channels were found selectively on the granules in some specific terminals. However, the presence of the labeling of these proteins in the interior of the granules is very elusive. Whether the selective labeling of the interior of the granules implies a specific association with the core material of the granules or an artifactual association requires further study. The investigation of the function of these proteins in the granules might provide important data for the study of the granule secretory mechanism.

Microvesicles have a similar morphology and membrane composition as synaptic vesicles and also store neurotransmitters. Their secretion competence is demonstrated again in the present study. The study of messenger substance release from neurohypophysial nerve endings should include not only exocytosis from secretory granules but also from microvesicles. Further investigatios on the release mechanism and the physiological function of microvesicles will be very important for understanding thoroughly the properties of neurosecretion in the neurohypophysis.

Like neurons and astrocytes, U373 MG cells may also use two types of vesicular organelles to release messenger substance via regulated pathway (Volknandt et al., 2002). The present results demonstrated that U373 MG cells are capable of expressing all three members of the synaptic SNARE complex (v-SNARE VAMP II, t-SNAREs syntaxin I and SNAP25*)* and the ubiquitous v-SNARE cellubrevin. However, similar to cultured astrocytes, the immunolabeling of both presumptive t-SNAREs syntaxin I and SNAP-25 was confined to the intracellular vesicular organelles. No significant labeling was identified by electron microscopy at the plasma membrane of U373 MG cells. The high level of fluorescent colocalization of syntaxin I and VAMP II in the cell body and in processes suggests that syntaxin I is mostly sorted into identical vesicular organelles as VAMP II. The exact function of these presumptive t-SNARE proteins in this astrocytic cell line requires further study. On the other hand, if syntaxin I and SNAP-25 are not present at the plasma membrane, which proteins would then take over the t-SNARE function for exocytosis in U373 cells? Isoforms of these t-SNARE proteins seem to be potential candidates. The identification of the possible t-SNARE proteins by means of the biochemical and/or immunochemical methods will be very significant for the clarification of the release mechanism in astrocytic cells.

# 5. Summary / Zusammenfassung

**SUMMARY:** In the present study the cryo-immunogold technique was used and optimized for investigating the ultrastructure and immunolabeling of synaptic proteins. It is evidently a suitable method for the localization of membrane proteins since the antigens are not treated with any chemical denaturation before immunolabeling except for the fixation and since the antigens are directly exposed to the surface of the cryo-ultrasections.

The v-SNARE VAMP II and the vesicle-associated proteins SV2 and Rab3A were detected extensively at small vesicles in the mossy fiber terminals. The t-SNARE SNAP-25, and N-type and P/Q type $Ca^{2+}$ channels were allocated to the plasma membrane both at the active zone and outside the active zone. SNAP-25 and N-type $Ca^{2+}$ channels appeared also at synaptic vesicles. A significantly increased immunolabeling of VAMP II, SV2, Rab3A, SNAP-25 and N-type $Ca^{2+}$ channels was found at the active zones of fast synapses, indicating a concentration of these proteins at sites of exocytosis.

The widespread distribution of the t-SNARE SNAP-25 at the axonal plasma membrane reveals that membrane-targeting specificity cannot be determined solely by v/t-SNARE interactions. Additional control components are required to assure the docking and exocytosis of the synaptic vesicles at active zones.

The novel protein Bassoon was only found at active zones of central synapses and showed the highest specific labeling among all proteins investigated. Its labeling pattern implies an association of Bassoon with the presynaptic dense projections, the structural guide for vesicle exocytosis. The involvement of Bassoon in the organization of the neurotransmitter release site suggests that Bassoon may play an important role in determining the specificity of vesicle docking and fusion.

In the neurosecretory endings of neurohypophysis the synaptic proteins VAMP II, SNAP-25, SV2, Rab3A, and the N-type $Ca^{2+}$ channels showed a preferential labeling over microvesicles. Moreover, the immunolabeling intensity of these proteins over microvesicles corresponded closely to that over synaptic vesicles. This suggests that these synaptic proteins share an identical association with synaptic vesicle and microvesicles. A significant labeling of SNAP-25, the N-type $Ca^{2+}$ channels and VAMP II was also detected at the plasma

membrane near the clustered microvesicles, indicating the competence of microvesicles for docking and exocytosis along the plasma membrane in the absence of active zones.

No significant labeling of VAMP II, SNAP-25, SV2 and N-type $Ca^{2+}$ channel was observed at the membrane of neurosecretory granules. This is in agreement with the notion that synaptic vesicles and microvesicles possess regulatory mechanisms for exocytosis different from those of granules. In contrast, α/β-SNAP and NSF were found on the granules, and Rab3A and the P/Q-type $Ca^{2+}$ channels on granules in a subset of terminals. Rab3A is associated specifically with the oxytocin-containing granule population.

Interestingly, some plasma membrane proteins, such as SNAP-25 and even N-type $Ca^{2+}$ channels and P/Q-type $Ca^{2+}$ channels, were observed not only at the plasma membrane but also at the vesicular organelles. This suggests that these vesicular organelles may be involved in transporting newly synthesized proteins from the soma to the plasma membrane of the terminal. Furthermore, the vesicular pool of the $Ca^{2+}$ channels may serve in the stimulation-induced translocation into the plasma membrane when required.

Using the conventional preembedding method with Epon and the post-embedding method with LR Gold, VAMP II was localized at vesicular organelles of varying size and on horseradish peroxidase filled endocytic organelles in cultured astrocytes, with and without stimulation in the presence of the horseradish peroxidase. This indicates that VAMP II is involved in the cycle of vesicular exocytosis and endocytosis in astrocytes.

U373 cells are capable of expressing all three members of the synaptic SNARE complex (v-SNARE VAMP II, t-SNARE syntaxin I and SNAP25). This indicates the competence of U373 to carry out regulated exocytosis by means of the classical SNARE mechanism. In addition, the ubiquitous v-SNARE cellubrevin and the endosome-associated small GTP-binding protein Rab5 could be expressed in U373 cells.

All recombinant synaptic proteins investigated in U373 cells revealed a punctuate cellular distribution under the fluorescence microscope, suggesting that they are mainly associated with intracellular compartments. The cryo-electron microscopy provided direct evidence for the association of all expressed proteins with electron-lucent vesicular organelles. It further supports the potential of U373 MG cells to release low molecular weight messengers by a regulated exocytosis mechanism. In addition, myc-VAMP II was found on dispersed granules. Probably, VAMP II also participates in the exocytosis event of granules in U373 cells.

Gold labeling for the two presumptive t-SNAREs syntaxin I and SNAP-25 in U373 cells was confined to the vesicular organelles. At the ultrastructural level no significant labeling was identified at the plasma membrane.

The high level of colocalization of the two SNARE proteins VAMP II and syntaxin I in the cell body and in cell processes suggests that the two proteins are mostly sorted into identical vesicular organelles. A partial colocalization of VAMP II and cellubrevin as well as of VAMP II and Rab5 was observed under the fluorescence microscope. At the ultrastructural level, a colocalization of VAMP II and cellubrevin as well as of VAMP II and Rab5 was found on some clustered vesicles. The partial colocalization of VAMP II and cellubrevin implies that they similarly function as v-SNAREs. The partial colocalization of Rab5 with VAMP II in U373 cells suggests that the endosomal protein Rab5 is associated with VAMP II-containing organelles during some stages of their life cycle.

**ZUSAMMENFASSUNG:** Die Freisetzung von Neurotransmittern aus kleinen synaptischen Vesikeln schneller Synapsen hängt von dem koordinierten Zusammenwirken spezifischer Vesikelproteine ab. Genetische, physiologische und biochemische Untersuchungen legen nahe, dass sich viele synaptische Proteine - einschließlich der Mitglieder der SNARE-Familie - an den Exozytose-Prozessen der synaptischen Vesikel beteiligen. Die genauen molekularen Mechanismen der Vesikel-Exozytose sind jedoch weitgehend unbekannt. Es fehlen außerdem eindeutige morphologische Nachweise der bevorzugten Lokalisation dieser Proteine an den aktiven Zonen des Synapsen, die ihre Assoziation mit der schnellen Neurotransmitter-Freisetzung in situ zeigen könnten. Die fundamentalen Mechanismen des „membrane traffic" gelten bei allen eukaryotischen Zellen als phylogenetisch konserviert. Dies bedeutet, dass ähnliche Proteine für die Kontrolle der Membranfusion sowohl bei Neuronen als auch bei anderen nicht-neuralen Zellen benutzt werden können. Wie zahlreiche jüngere Untersuchungen zeigen, können Astrozyten ihre Botenstoffe mittels eines Neuronen-ähnlichen sekretorischen Prozesses freisetzen. Dabei wird vermutlich eine regulierte Vesikel-Exozytose und besonders der klassische SNARE-Mechanismus in den Sekretionsprozess miteinbezogen. Allerdings gibt es für den Vesikelzyklus bei Astrozyten kaum morphologische Nachweise für die Funktion der Exozytose-relevanten Proteine.

In der vorliegenden Arbeit wurden daher die Lokalisation von SNARE-Proteinen sowie anderen Vesikel-relevanten Proteinen an zwei unterschiedlichen Nerventerminalen sowie bei astrozytären Zellen mittels Immunfluoreszenz und Elektronenmikroskopie untersucht. Ziel dieser Arbeit ist es, ein besseres Verständnis der Funktion dieser Proteine bei der Freisetzung der Botenstoffe zu erhalten.

**1. Lokalisation der synaptischen Proteine an zwei unterschiedlichen Typen von Nervenendigungen**

Zum morphologischen Nachweis der verschiedenen synaptischen Proteine wurde die Methode der Immungoldmarkierung an ultradünnen Kryoschnitten angewendet. Untersucht und analysiert wurden die Lokalisation und die Verteilung dieser synaptischen Proteine an (1) den großen Moosfaserendigungen mit vielen aktiven Zonen in der hippocampalen CA3 Region, und an (2) den neurosekretorischen Terminalen ohne spezielle Freisetzungsstellen in Neurohypophyse. Hier war besonders von Interesse, ob SNARE-Proteine vorzugsweise mit aktiven Zonen in den schnellen Synapsen verbunden sind, und inwieweit die Lokalisation

dieser Proteine in solchen Endigungen, die keine definierten Freisetzungsstellen besitzen, von denjenigen in den synaptischen Terminalen verschieden sind.

In den hippokampalen Moosfaserendigungen wurden das v-SNARE VAMP II und die weiteren Vesikel-gebundenen Proteine SV2 und Rab3A umfassend an den synaptischen Vesikeln lokalisiert. Das t-SNARE SNAP-25, und N- und P/Q-Typ $Ca^{2+}$-Kanäle ließen sich an der Plasmamembran in und außerhalb der aktiven Zone nachweisen. SNAP-25 und N-Typ $Ca^{2+}$-Kanäle wurden auch an synaptischen Vesikeln gefunden. Die quantitative Analyse zeigte eine deutlich erhöhte Immunmarkierung von VAMP II, SV2, Rab3A, SNAP-25, und N-Typ $Ca^{2+}$-Kanäle an den aktiven Zonen. Dies deutet auf eine direkte Teilnahme solcher Proteine an der Exozytose von synaptischen Vesikeln in den schnellen zentralen Synapsen. Besonders die Markierung von VAMP II und SNAP-25 dicht an den angedockten synaptischen Vesikeln und an der Plasmamembran in aktiven Zonen weist auf eine Assoziation von diesen Proteinen mit dem präsynaptischen Docking-Komplex hin. Der Nachweis von N-Typ und P/Q-Typ $Ca^{2+}$-Kanäle an den aktiven Zonen liefert einen morphologischen Beleg für ihre Beteiligung an der Regulierung der schnellen Neurotransmission. Er unterstützt auch die Hypothese, dass diese beiden $Ca^{2+}$-Kanäle mit dem SNARE-Komplex interagieren können.

Die breite Verteilung von SNAP-25 an der axonalen Plasmamembran weist darauf hin, dass seine Funktion nicht wesentlich für die Positionierung der Freisetzungsstelle von synaptischen Vesikeln sein dürfte. Die Docking-Spezifität der Vesikel wird nicht nur durch die v/t-SNARE-Interaktion definiert. Zusätzliche kontrollierende Faktoren sind folglich erforderlich, um „docking“ und Exozytose der synaptische Vesikel an der aktiven Zone zu gewährleisten.

Das hochmolekulare Protein Bassoon war hauptsächlich an den aktiven Zonen der zentralen Synapsen zu finden. Direkt auf der Plasmamembran waren jedoch keine Markierungen nachzuweisen. Das Verteilungsmuster deutet auf eine Assoziation von Bassoon mit den „presynaptic dense projections“ hin. Die Einbeziehung von Bassoon in die Organisation des Freisetzungsortes von Neurotransmittern verdeutlicht, dass dieses Protein eine wichtige Rolle bei der Definition der Spezifität für „docking“ und Fusion der synaptischen Vesikeln spielt.

In den neurosekretorischen Endigungen der Neurohypophyse zeigten die synaptischen Proteine VAMP II, SV2, Rab3A, SNAP-25, und die N-Typ $Ca^{2+}$-Kanäle eine bevorzugte Markierung auf Mikrovesikeln. Die Intensität der Immunmarkierung dieser Proteine auf den Mikrovesikeln entspricht derjenigen von synaptischen Vesikeln. Dieses deutet darauf hin,

dass diese synaptischen Proteine eine identische funktionelle Bedeutung auf synaptischen Vesikeln und Mikrovesikeln besitzen. Die vorliegende Untersuchung stützt damit die Hypothese, dass die Mikrovesikel nicht nur bezüglich ihrer Größe und ihrer Morphologie denen typischer synaptischer Vesikel ähnlich sind, sondern auch ähnliche Eigenschaften wie diese haben. Eine starke Markierung von SNAP-25, N-Typ $Ca^{2+}$-Kanäle sowie von VAMP II ließ sich auch an der Plasmamembran nahe der Mikrovesikel-Cluster nachweisen. Dies läßt vermuten, dass Mikrovesikel die Kompetenz zum „docking“ und zur Exozytose entlang der Plasmamembran besitzen, auch wenn eine aktive Zone fehlt. Die aus den Mikrovesikeln freigesetzten Botenstoffe könnten als lokale regulierende Faktoren verwendet werden, um die Sekretion an neurohypophysären Endigungen zu koordinieren.

An den neurosekretorischen Granula konnten Markierungen von VAMP II, SV2, SNAP-25, und N-Typ $Ca^{2+}$-Kanäle nicht nachgewiesen werden. Dies entspricht der Vorstellung, dass Granula, verglichen mit Mikrovesikeln und synaptischen Vesikeln, unterschiedliche Mechanismen für die Exozytose besitzen. Allerdings wurden α/β-SNAP und NSF auf den Granula nachgewiesen, und ebenso Rab3A und P/Q-Typ $Ca^{2+}$-Kanäle auf den Granula einer Subpopulation von neurohypophysären Terminalen. Rab3A war mit Oxytocin-Granula spezifisch assoziiert, wie durch die Doppelmarkierung gezeigt werden konnte. Die Markierungen von α/β-SNAP an der Plasmamembran und am Verbindungsstiel des Granulums mit der Plasmamembran lassen vermuten, dass α/β-SNAP an die Regulierung der Exozytose der neurohypophysärer Granula mitbeteiligt ist. Die Markierungen für α/β-SNAP und NSF auf den Granula unterstützen die Hypothese, dass vesikuläre Organellen beide Proteine zum Exozytoseort transportieren können. Möglicherweise können diese Proteine ihre Funktion bereits vor dem Vesikeldocking ausüben. Außerdem zeigte keine der untersuchten Proteine eine konzentrierte Markierung an spezifischen Domänen der Plasmamembran der neurohypophysären Endigungen. Auch diese Ergebnisse machen deutlich, dass in den neurohypophysären Endigungen ein definierter Freisetzungsort fehlt. Offensichtlich entsprechen die Unterschiede bezüglich der Verteilung der untersuchten Proteine in den beiden Nerventerminalen auch den spezifischen Funktionseigenschaften dieser Proteine, was wiederum in hohem Maße mit den spezifischen Funktionseigenschaften der beiden Nerventerminalen selbst korrespondiert.

Interessanterweise konnten einige Plasmamembranproteine, wie SNAP-25, sogar N- und P/Q-Typ $Ca^{2+}$-Kanäle, nicht nur auf der Plasmamembran sondern auch auf vesikulären Organellen

lokalisiert werden. Vermutlich sind diese vesikulären Organellen am Transport von neu synthetisierten Proteinen vom Soma bis zur Plasmamembran in den Nervenendigungen beteiligt. Weiterhin wurde vorgeschlagen, dass SNAP-25 zusammen mit den synaptischen Vesikeln in den Terminalen rezirkuliert wird, um sie dann zu reaktivieren. Der vesikuläre Vorrat an $Ca^{2+}$-Kanälen könnte wiederum der stimulationsabhängigen Translokation in die Plasmamembran dienen.

**2. Lokalisation der Vesikel-relevanten Proteine in astrozytären Zellen**

Um die Funktion von synaptischen Proteinen in astrocytären Zellen zu verstehen, wurde die subzelluläre Lokalisation von den Proteinen auf vesikulären Organellen sowie auf den durch Stimulation induzierten endozytotischen Kompartimenten an kultivierten kortikalen Astrozyten von neonatalen Ratten nachgewiesen. Zusätzlich wurden die Expression und die Lokalisation vieler Proteine, die für eine regulierte Exozytose und die interzelluläre Membranfusion verantwortlich sind, an Zellen aus einer permanenten Astrozytoma-Zellinie (U373 MG) untersucht. Verschiedene Konstrukte, die für die Proteine und die relevanten zusätzlichen Tags kodieren, wurden transient in diese Zellen transfiziert. Die Lokalisation der exprimierten rekombinanten Proteine wurde anschließend mittels Immunfluoreszenz und Kryo-Immunelektronmikroskopie nachgewiesen. Das Ziel war es, die sekretorischen Charakteristika der U373 MG Zellen aufzuklären sowie zu prüfen, ob diese Zell-Linie als effektives experimentelles Modell zur weiteren Studie des astrozytären Exozytose-Mechanismus genutzt werden kann.

In kultivierten Astrozyten konnte VAMP II an elektronenlichten vesikulären Organellen variierender Größe sowie an mit Meerrettich-Peroxidase (HRP) gefüllten endozytotischen Organellen - mit oder ohne Stimulation in Anwesenheit von HRP - sowohl mittels der Präembedding-Methode als auch mittels der LR Gold Postembedding-Methode nachgewiesen werden. Daraus folgt, dass in Astrozyten VAMP II am Zyklus der vesikulären Exo- und Endozytose beteiligt wird.

U373 MG Zellen konnten alle drei Mitglieder des synaptischen SNARE-Komplexes (v-SNARE VAMP II, t-SNARE Syntaxin I, und SNAP-25) exprimieren. U373 MG Zellen sind folglich fähig, eine regulierte Exozytose mittels des klassischen vesikulären SNARE-Mechanismus durchzuführen. Zusätzlich konnten auch das ubiquitär vorhandene v-SNARE Cellubrevin und das Endosomen-assoziierte kleine GTP-bindende Protein Rab5 in den U373 MG Zellen exprimiert werden.

Alle exprimierten rekombinanten Proteine zeigten in den U373 MG Zellen fluoreszenzmikroskopisch eine punktuelle zelluläre Verteilung. Vermutlich sind diese Proteine vor allem mit intrazellulären Kompartimenten assoziiert. Elektronenmikroskopisch zeigten sich in U373 MG Zellen zahlreiche vesikuläre Organellen. Den direkten Nachweis für eine Assoziation dieser Proteine mit den hellen Vesikeln lieferte der immunzytochemische Nachweis aller exprimierten Proteine an ultradünnen Kryoschnitten. Diese Daten weisen vor allem auf das Potential der U373 MG Zellen hin, niedermolekulare Botenstoffe mittels einer regulierten Exozytose freizusetzen.

Die Kryoelektronen-Mikroskopie zeigte außerdem, dass myc-VAMP II in größerer Menge als die anderen untersuchten Proteine in U373 MG Zellen exprimiert wurden. Verschiedene Typen vesikulärer Organellen wurden intensiv mit myc-VAMP II markiert. Besonders auffallend sind dichte Markierungen auf zahlreichen kleinen Vesikeln, tubulovesikulären Organellen sowie der Plasmamembran. Vermutlich ist myc-VAMP II am Recycling von hellen vesikulären Organellen mitbeteiligt. Auch Granula sind mit myc-VAMP II markiert. Dies bedeutet, dass sich dieses Protein in den U373 MG Zellen auch an der Exozytose der Granula beteiligen kann. Die massive Expression von myc-VAMP II an multivesikulären Körpern und Lysosomen läßt sich wahrscheinlich auf überexprimiertes rekombinantes Protein zurückführen, das schließlich degradiert wird. Diese vielfältige VAMP II Markierung in U373 MG Zellen weist darauf hin, dass dieses Protein an den verschiedenen Stadien des Vesikelrecyclings beteiligt ist. Die hohe Kolokalisation der zwei SNARE-Proteine VAMP II und Syntaxin I im Zellkörper und in den Zellfortsätzen weist darauf hin, dass beide Proteine in der Regel in identische vesikuläre Organellen sortiert werden. Die teilweise Kolokalisation von VAMP II mit Cellubrevin an den hellen Vesikeln deutet auf eine ähnliche Funktion der beiden v-SNAREs hin.

GFP-Rab5 ließ sich an hellen Vesikeln und Endosomen nachweisen. Vermutlich ist Rab5 sowohl in das Vesikelrecycling als auch in die Endosomenfusion der U373 MG Zellen involviert. Die teilweise Kolokalisation von Rab5 mit VAMP II an den hellen Vesikeln weist darauf hin, dass das endosomale Protein Rab5 während einiger Stadien seines Lebenszyklus mit den VAMP II-enthaltenen Organellen verbunden ist.

Ähnlich wie bei den kultivierten Astrozyten konnten bei U373 MG Zellen keine eindeutigen Freisetzungsorte, wie eine neuronale aktive Zone, nachgewiesen werden. Auch kleine gedockte Vesikel sind in definierten Zellbereichen nicht zu finden. Überdies ähnelt das

Expressionsmuster der untersuchten Proteine dem über lange Zeit kultivierter primärer Astrozyten. Die Markierung für die beiden mutmaßlichen t-SNARE Syntaxin I und SNAP-25 fand sich auf vesikulären Organellen. Die Plasmamembran der U373 MG Zellen zeigte keine signifikante Markierung. Diese Befunde legen nahe, dass U373 MG Zellen ihre Botenstoffe über einen ähnlichen Sekretionsmechanismus wie Astrozyten freisetzen. Sie können daher als geeignetes Model für weitere Untersuchungen des astrozytären Exozytosemechanismus eingesetzt werden.

# 6. References

Ahnert-Hilger,G. and Bigalke,H. (1995). Molecular aspects of tetanus and botulinum neurotoxin poisoning. Prog. Neurobiol. *46*, 83-96.

Akert,K. (1972). [The ultrastructure of synapses]. Arkh. Anat. Gistol. Embriol. *62*, 5-8.

Akert,K., Moor,H., and Pfenninger,K. (1971). Synaptic fine structure. Adv. Cytopharmacol. *1*, 273-290.

Al Matubsi,H.Y., Breed,W., Jenkin,G., and Fairclough,R.J. (1999). Co-localization of Rab3B and oxytocin to electron dense granules of the sheep corpus luteum during the estrous cycle. Anat. Rec. *254*, 214-221.

Anaral,D.G. and Witter,M.P. (1995). Hippocampal Formation. In The Rat Nervous System, G.Paxinos, ed. (New York, London: Academic Press), pp. 443-593.

Araque,A., Carmignoto,G., and Haydon,P.G. (2001). Dynamic signaling between astrocytes and neurons. Annu. Rev. Physiol *63*, 795-813.

Araque,A., Li,N., Doyle,R.T., and Haydon,P.G. (2000). SNARE protein-dependent glutamate release from astrocytes. J. Neurosci. *20*, 666-673.

Bajjalieh,S.M., Frantz,G.D., Weimann,J.M., McConnell,S.K., and Scheller,R.H. (1994). Differential expression of synaptic vesicle protein 2 (SV2) isoforms. J. Neurosci. *14*, 5223-5235.

Bajjalieh,S.M., Peterson,K., Shinghal,R., and Scheller,R.H. (1992). SV2, a brain synaptic vesicle protein homologous to bacterial transporters. Science *257*, 1271-1273.

Banaschewski,C., Hohne-Zell,B., Ovtscharoff,W., and Gratzl,M. (1998). Characterization of vesicular membrane-bound alpha-SNAP and NSF in adrenal chromaffin cells. Biochemistry *37*, 16719-16727.

Barbieri,M.A., Hoffenberg,S., Roberts,R., Mukhopadhyay,A., Pomrehn,A., Dickey,B.F., and Stahl,P.D. (1998). Evidence for a symmetrical requirement for Rab5-GTP in in vitro endosome-endosome fusion. J. Biol. Chem. *273*, 25850-25855.

Barnard,R.J., Morgan,A., and Burgoyne,R.D. (1997). Stimulation of NSF ATPase activity by alpha-SNAP is required for SNARE complex disassembly and exocytosis. J. Cell Biol. *139*, 875-883.

Bauerfeind,R. and Huttner,W.B. (1993). Biogenesis of constitutive secretory vesicles, secretory granules and synaptic vesicles. Curr. Opin. Cell Biol. *5*, 628-635.

Baumert,M., Maycox,P.R., Navone,F., De Camilli,P., and Jahn,R. (1989). Synaptobrevin: an integral membrane protein of 18,000 daltons present in small synaptic vesicles of rat brain. EMBO J. *8*, 379-384.

Bean,A.J. and Scheller,R.H. (1997). Better late than never: a role for rabs late in exocytosis. Neuron *19*, 751-754.

Bean,A.J., Seifert,R., Chen,Y.A., Sacks,R., and Scheller,R.H. (1997). Hrs-2 is an ATPase implicated in calcium-regulated secretion. Nature *385*, 826-829.

Benfenati,F., Onofri,F., and Giovedi,S. (1999). Protein-protein interactions and protein modules in the control of neurotransmitter release. Philos. Trans. R. Soc. Lond B Biol. Sci. *354*, 243-257.

Bennett,M.K. and Scheller,R.H. (1993). The molecular machinery for secretion is conserved from yeast to neurons. Proc. Natl. Acad. Sci. U. S. A *90*, 2559-2563.

Berryman,M.A. and Rodewald,R.D. (1990). An enhanced method for post-embedding immunocytochemical staining which preserves cell membranes. J. Histochem. Cytochem. *38*, 159-170.

Berwin,B., Floor,E., and Martin,T.F. (1998). CAPS (mammalian UNC-31) protein localizes to membranes involved in dense-core vesicle exocytosis. Neuron *21*, 137-145.

Betz,A., Okamoto,M., Benseler,F., and Brose,N. (1997). Direct interaction of the rat unc-13 homologue Munc13-1 with the N terminus of syntaxin. J. Biol. Chem. *272*, 2520-2526.

Betz,W.J. and Angleson,J.K. (1998). The synaptic vesicle cycle. Annu. Rev. Physiol *60*, 347-363.

Bezzi,P., Carmignoto,G., Pasti,L., Vesce,S., Rossi,D., Rizzini,B.L., Pozzan,T., and Volterra,A. (1998). Prostaglandins stimulate calcium-dependent glutamate release in astrocytes. Nature *391*, 281-285.

Bezzi,P. and Volterra,A. (2001). A neuron-glia signalling network in the active brain. Curr. Opin. Neurobiol. *11*, 387-394.

Bhakdi,S., Weller,U., Walev,I., Martin,E., Jonas,D., and Palmer,M. (1993). A guide to the use of pore-forming toxins for controlled permeabilization of cell membranes. Med. Microbiol. Immunol. (Berl) *182*, 167-175.

Blackstad,T.W., Brink,K., Hem,J., and Jeune,B. (1970). Distribution of hippocampal mossy fibers in the rat. An experimental study with silver impregnation methods. J. Comp Neurol. *138*, 433-449.

Boersma,C.J., Sonnemans,M.A., and Van Leeuwen,F.W. (1993). Immunoelectron microscopic demonstration of oxytocin and vasopressin in pituicytes and in nerve terminals forming synaptoid contacts with pituicytes in the rat neural lobe. Brain Res. *611*, 117-129.

Brownstein,M.J., Russell,J.T., and Gainer,H. (1980). Synthesis, transport, and release of posterior pituitary hormones. Science *207*, 373-378.

Bucci,C., Parton,R.G., Mather,I.H., Stunnenberg,H., Simons,K., Hoflack,B., and Zerial,M. (1992). The small GTPase rab5 functions as a regulatory factor in the early endocytic pathway. Cell *70*, 715-728.

Burgess,T.L. and Kelly,R.B. (1987). Constitutive and regulated secretion of proteins. Annu. Rev. Cell Biol. *3*, 243-293.

Burgoyne,R.D. (1991). Control of exocytosis in adrenal chromaffin cells. Biochim. Biophys. Acta *1071*, 174-202.

Burgoyne,R.D. and Williams,G. (1997). NSF and SNAP are present on adrenal chromaffin granules. FEBS Lett. *414*, 349-352.

Burns,M.E. and Augustine,G.J. (1995). Synaptic structure and function: dynamic organization yields architectural precision. Cell *83*, 187-194.

Burry,R.W., Vandre,D.D., and Hayes,D.M. (1992). Silver enhancement of gold antibody probes in pre-embedding electron microscopic immunocytochemistry. J. Histochem. Cytochem. *40*, 1849-1856.

Calegari,F., Coco,S., Taverna,E., Bassetti,M., Verderio,C., Corradi,N., Matteoli,M., and Rosa,P. (1999). A regulated secretory pathway in cultured hippocampal astrocytes. J. Biol. Chem. *274*, 22539-22547.

Carmignoto,G. (2000). Reciprocal communication systems between astrocytes and neurones. Prog. Neurobiol. *62*, 561-581.

Castel,M., Morris,J., and Belenky,M. (1996). Non-synaptic and dendritic exocytosis from dense-cored vesicles in the suprachiasmatic nucleus. Neuroreport *7*, 543-547.

Chapman,E.R., An,S., Barton,N., and Jahn,R. (1994). SNAP-25, a t-SNARE which binds to both syntaxin and synaptobrevin via domains that may form coiled coils. J. Biol. Chem. *269*, 27427-27432.

Chen,X., Tomchick,D.R., Kovrigin,E., Arac,D., Machius,M., Sudhof,T.C., and Rizo,J. (2002). Three-dimensional structure of the complexin/SNARE complex. Neuron *33*, 397-409.

Chilcote,T.J., Galli,T., Mundigl,O., Edelmann,L., McPherson,P.S., Takei,K., and De Camilli,P. (1995). Cellubrevin and synaptobrevins: similar subcellular localization and biochemical properties in PC12 cells. J. Cell Biol. *129*, 219-231.

Chou,J.H. and Jahn,R. (2000). Binding of Rab3A to synaptic vesicles. J. Biol. Chem. *275*, 9433-9440.

Chung,S.H., Takai,Y., and Holz,R.W. (1995). Evidence that the Rab3a-binding protein, rabphilin3a, enhances regulated secretion. Studies in adrenal chromaffin cells. J. Biol. Chem. *270*, 16714-16718.

Cotrina,M.L., Lin,J.H., and Nedergaard,M. (1998). Cytoskeletal assembly and ATP release regulate astrocytic calcium signaling. J. Neurosci. *18*, 8794-8804.

Danscher,G. (1981a). Histochemical demonstration of heavy metals. A revised version of the sulphide silver method suitable for both light and electronmicroscopy. Histochemistry *71*, 1-16.

Danscher,G. (1981b). Light and electron microscopic localization of silver in biological tissue. Histochemistry *71*, 177-186.

Danscher,G. (1981c). Localization of gold in biological tissue. A photochemical method for light and electronmicroscopy. Histochemistry *71*, 81-88.

Danscher,G. (1983). A silver method for counterstaining plastic embedded tissue. Stain Technol. *58*, 365-372.

Darchen,F., Senyshyn,J., Brondyk,W.H., Taatjes,D.J., Holz,R.W., Henry,J.P., Denizot,J.P., and Macara,I.G. (1995). The GTPase Rab3a is associated with large dense core vesicles in bovine chromaffin cells and rat PC12 cells. J. Cell Sci. *108 ( Pt 4)*, 1639-1649.

Darchen,F., Zahraoui,A., Hammel,F., Monteils,M.P., Tavitian,A., and Scherman,D. (1990). Association of the GTP-binding protein Rab3A with bovine adrenal chromaffin granules. Proc. Natl. Acad. Sci. U. S. A *87*, 5692-5696.

De Camilli,P. and Jahn,R. (1990). Pathways to regulated exocytosis in neurons. Annu. Rev. Physiol *52*, 625-645.

de Wit,H., Lichtenstein,Y., Geuze,H.J., Kelly,R.B., van der,S.P., and Klumperman,J. (1999). Synaptic vesicles form by budding from tubular extensions of sorting endosomes in PC12 cells. Mol. Biol. Cell *10*, 4163-4176.

Douglas,W.W., Nagasawa,J., and Schulz,R.A. (1971). Coated microvesicles in neuro-secretory terminals of posterior pituitary glands shed their coats to become smooth "synaptic" vesicles. Nature *232*, 340-341.

Dresbach,T., Qualmann,B., Kessels,M.M., Garner,C.C., and Gundelfinger,E.D. (2001). The presynaptic cytomatrix of brain synapses. Cell Mol. Life Sci. *58*, 94-116.

Duc,C. and Catsicas,S. (1995). Ultrastructural localization of SNAP-25 within the rat spinal cord and peripheral nervous system. J. Comp Neurol. *356*, 152-163.

Dunlap,K., Luebke,J.I., and Turner,T.J. (1995). Exocytotic Ca2+ channels in mammalian central neurons. Trends Neurosci. *18*, 89-98.

Edelmann,L., Hanson,P.I., Chapman,E.R., and Jahn,R. (1995). Synaptobrevin binding to synaptophysin: a potential mechanism for controlling the exocytotic fusion machine. EMBO J. *14*, 224-231.

Ellinor,P.T., Zhang,J.F., Horne,W.A., and Tsien,R.W. (1994). Structural determinants of the blockade of N-type calcium channels by a peptide neurotoxin. Nature *372*, 272-275.

Elliott,E.M., Malouf,A.T., and Catterall,W.A. (1995). Role of calcium channel subtypes in calcium transients in hippocampal CA3 neurons. J. Neurosci. *15*, 6433-6444.

Emmett,C.J., McNeeley,P.A., and Johnson,R.M. (1997). Evaluation of human astrocytoma and glioblastoma cell lines for nerve growth factor release. Neurochem. Int. *30*, 465-474.

Fasshauer,D., Antonin,W., Subramaniam,V., and Jahn,R. (2002). SNARE assembly and disassembly exhibit a pronounced hysteresis. Nat. Struct. Biol. *9*, 144-151.

Fasshauer,D., Bruns,D., Shen,B., Jahn,R., and Brunger,A.T. (1997a). A structural change occurs upon binding of syntaxin to SNAP-25. J. Biol. Chem. *272*, 4582-4590.

Fasshauer,D., Eliason,W.K., Brunger,A.T., and Jahn,R. (1998). Identification of a minimal core of the synaptic SNARE complex sufficient for reversible assembly and disassembly. Biochemistry *37*, 10354-10362.

Fasshauer,D., Otto,H., Eliason,W.K., Jahn,R., and Brunger,A.T. (1997b). Structural changes are associated with soluble N-ethylmaleimide-sensitive fusion protein attachment protein receptor complex formation. J. Biol. Chem. *272*, 28036-28041.

Feany,M.B., Lee,S., Edwards,R.H., and Buckley,K.M. (1992). The synaptic vesicle protein SV2 is a novel type of transmembrane transporter. Cell *70*, 861-867.

Ferro-Novick,S. and Jahn,R. (1994). Vesicle fusion from yeast to man. Nature *370*, 191-193.

Fischer,v.M., Mignery,G.A., Baumert,M., Perin,M.S., Hanson,T.J., Burger,P.M., Jahn,R., and Sudhof,T.C. (1990). rab3 is a small GTP-binding protein exclusively localized to synaptic vesicles. Proc. Natl. Acad. Sci. U. S. A *87*, 1988-1992.

Fischer,v.M., Stahl,B., Li,C., Sudhof,T.C., and Jahn,R. (1994a). Rab proteins in regulated exocytosis. Trends Biochem. Sci. *19*, 164-168.

Fischer,v.M., Stahl,B., Walch-Solimena,C., Takei,K., Daniels,L., Khoklatchev,A., De Camilli,P., Sudhof,T.C., and Jahn,R. (1994b). Localization of Rab5 to synaptic vesicles identifies endosomal intermediate in synaptic vesicle recycling pathway. Eur. J. Cell Biol. *65*, 319-326.

Fischer,v.M., Sudhof,T.C., and Jahn,R. (1991). A small GTP-binding protein dissociates from synaptic vesicles during exocytosis. Nature *349*, 79-81.

Fisher,T.E. and Bourque,C.W. (1995). Distinct omega-agatoxin-sensitive calcium currents in somata and axon terminals of rat supraoptic neurones. J. Physiol *489 ( Pt 2)*, 383-388.

Fisher,T.E. and Fernandez,J.M. (1999). Pulsed laser imaging of Ca(2+) influx in a neuroendocrine terminal. J. Neurosci. *19*, 7450-7457.

Frotscher,M. (1988). Neuronal Elements in the Hippocampus and Their Synaptic Connections. In Embryology and Cell Biology 111: Neurotransmission in the Hippocampus, M.Frotscher, P.Kugler, U.Misgeld, and K.Zilles, eds. (Heidelberger, Germany: Springer), pp. 2-19.

Gaarskjaer,F.B. (1978). Organization of the mossy fiber system of the rat studied in extended hippocampi. I. Terminal area related to number of granule and pyramidal cells. J. Comp Neurol. *178*, 49-72.

Gaarskjaer,F.B. (1986). The organization and development of the hippocampal mossy fiber system. Brain Res. *396*, 335-357.

Galli,T., Chilcote,T., Mundigl,O., Binz,T., Niemann,H., and De Camilli,P. (1994). Tetanus toxin-mediated cleavage of cellubrevin impairs exocytosis of transferrin receptor-containing vesicles in CHO cells. J. Cell Biol. *125*, 1015-1024.

Galli,T., Garcia,E.P., Mundigl,O., Chilcote,T.J., and De Camilli,P. (1995). v- and t-SNAREs in neuronal exocytosis: a need for additional components to define sites of release. Neuropharmacology *34*, 1351-1360.

Gallwitz,D. and Jahn,R. (2003). The riddle of the Sec1/Munc-18 proteins - new twists added to their interactions with SNAREs. Trends Biochem. Sci. *28*, 113-116.

Garcia,E.P., McPherson,P.S., Chilcote,T.J., Takei,K., and De Camilli,P. (1995). rbSec1A and B colocalize with syntaxin 1 and SNAP-25 throughout the axon, but are not in a stable complex with syntaxin. J. Cell Biol. *129*, 105-120.

Garthwaite,J. and Brodbelt,A.R. (1990). Glutamate as the Principal Mossy Fibre Transmitter in Rat Cerebellum: pharmacological evidence. Eur. J. Neurosci. *2*, 177-180.

Geppert,M., Bolshakov,V.Y., Siegelbaum,S.A., Takei,K., De Camilli,P., Hammer,R.E., and Sudhof,T.C. (1994). The role of Rab3A in neurotransmitter release. Nature *369*, 493-497.

Geppert,M., Goda,Y., Stevens,C.F., and Sudhof,T.C. (1997). The small GTP-binding protein Rab3A regulates a late step in synaptic vesicle fusion. Nature *387*, 810-814.

Geppert,M. and Sudhof,T.C. (1998). RAB3 and synaptotagmin: the yin and yang of synaptic membrane fusion. Annu. Rev. Neurosci. *21*, 75-95.

Geuze,H.J., Slot,J.W., and Schwartz,A.L. (1987). Membranes of sorting organelles display lateral heterogeneity in receptor distribution. J. Cell Biol. *104*, 1715-1723.

Goda,Y. and Sudhof,T.C. (1997). Calcium regulation of neurotransmitter release: reliably unreliable? Curr. Opin. Cell Biol. *9*, 513-518.

Gorvel,J.P., Chavrier,P., Zerial,M., and Gruenberg,J. (1991). rab5 controls early endosome fusion in vitro. Cell *64*, 915-925.

Gray,E.G. and Guillery,R.W. (1966). Synaptic morphology in the normal and degenerating nervous system. Int. Rev. Cytol. *19*, 111-182.

Griffiths,G. (1993). Fine Structure Immunocytochemistry. (Berlin: Springer).

Griffiths,G. and Hoppeler,H. (1986). Quantitation in immunocytochemistry: correlation of immunogold labeling to absolute number of membrane antigens. J. Histochem. Cytochem. *34*, 1389-1398.

Griffiths,G., McDowall,A., Back,R., and Dubochet,J. (1984). On the preparation of cryosections for immunocytochemistry. J. Ultrastruct. Res. *89*, 65-78.

Griffiths,G., Simons,K., Warren,G., and Tokuyasu,K.T. (1983). Immunoelectron microscopy using thin, frozen sections: application to studies of the intracellular transport of Semliki Forest virus spike glycoproteins. Methods Enzymol. *96*, 466-485.

Grote,E., Hao,J.C., Bennett,M.K., and Kelly,R.B. (1995). A targeting signal in VAMP regulating transport to synaptic vesicles. Cell *81*, 581-589.

Grote,E. and Kelly,R.B. (1996). Endocytosis of VAMP is facilitated by a synaptic vesicle targeting signal. J. Cell Biol. *132*, 537-547.

Gundelfinger,E.D. and tom,D.S. (2000). Molecular organization of excitatory chemical synapses in the mammalian brain. Naturwissenschaften *87*, 513-523.

Guthrie,P.B., Knappenberger,J., Segal,M., Bennett,M.V., Charles,A.C., and Kater,S.B. (1999). ATP released from astrocytes mediates glial calcium waves. J. Neurosci. *19*, 520-528.

Hainfeld,J.F. and Furuya,F.R. (1992). A 1.4-nm gold cluster covalently attached to antibodies improves immunolabeling. J. Histochem. Cytochem. *40*, 177-184.

Hainfeld,J.F. and Powell,R.D. (2000). New frontiers in gold labeling. J. Histochem. Cytochem. *48*, 471-480.

Hanson,P.I., Roth,R., Morisaki,H., Jahn,R., and Heuser,J.E. (1997). Structure and conformational changes in NSF and its membrane receptor complexes visualized by quick-freeze/deep-etch electron microscopy. Cell *90*, 523-535.

Harlow,M.L., Ress,D., Stoschek,A., Marshall,R.M., and McMahan,U.J. (2001). The architecture of active zone material at the frog's neuromuscular junction. Nature *409*, 479-484.

Hata,Y., Slaughter,C.A., and Sudhof,T.C. (1993). Synaptic vesicle fusion complex contains unc-18 homologue bound to syntaxin. Nature *366*, 347-351.

Hay,J.C. and Scheller,R.H. (1997). SNAREs and NSF in targeted membrane fusion. Curr. Opin. Cell Biol. *9*, 505-512.

Hayashi,T., McMahon,H., Yamasaki,S., Binz,T., Hata,Y., Sudhof,T.C., and Niemann,H. (1994a). Synaptic vesicle membrane fusion complex: action of clostridial neurotoxins on assembly. EMBO J. *13*, 5051-5061.

Hayashi,T., Soulie,F., Nakata,T., and Hirokawa,N. (1994b). Redistribution of synapsin I and synaptophysin in response to electrical stimulation in the rat neurohypophysial nerve endings. Cell Struct. Funct. *19*, 253-262.

Hayashi,T., Yamasaki,S., Nauenburg,S., Binz,T., and Niemann,H. (1995). Disassembly of the reconstituted synaptic vesicle membrane fusion complex in vitro. EMBO J. *14*, 2317-2325.

Haydon,P.G. (2001). GLIA: listening and talking to the synapse. Nat. Rev. Neurosci. *2*, 185-193.

Hepp,R., Perraut,M., Chasserot-Golaz,S., Galli,T., Aunis,D., Langley,K., and Grant,N.J. (1999). Cultured glial cells express the SNAP-25 analogue SNAP-23. Glia *27*, 181-187.

Hirokawa,N., Sobue,K., Kanda,K., Harada,A., and Yorifuji,H. (1989). The cytoskeletal architecture of the presynaptic terminal and molecular structure of synapsin 1. J. Cell Biol. *108*, 111-126.

Hohne-Zell,B. and Gratzl,M. (1996). Adrenal chromaffin cells contain functionally different SNAP-25 monomers and SNAP-25/syntaxin heterodimers. FEBS Lett. *394*, 109-116.

Holz,R.W., Brondyk,W.H., Senter,R.A., Kuizon,L., and Macara,I.G. (1994). Evidence for the involvement of Rab3A in Ca(2+)-dependent exocytosis from adrenal chromaffin cells. J. Biol. Chem. *269*, 10229-10234.

Hong,R.M., Mori,H., Fukui,T., Moriyama,Y., Futai,M., Yamamoto,A., Tashiro,Y., and Tagaya,M. (1994). Association of N-ethylmaleimide-sensitive factor with synaptic vesicles. FEBS Lett. *350*, 253-257.

Horisberger,M. (1981). Colloidal gold : a cytochemical marker for light and fluorescent microscopy and for transmission and scanning electron microscopy. Scan Electron Microsc. 9-31.

Humbel,B.M., Sibon,O.C., Stierhof,Y.D., and Schwarz,H. (1995). Ultra-small gold particles and silver enhancement as a detection system in immunolabeling and in situ hybridization experiments. J. Histochem. Cytochem. *43*, 735-737.

Jacobsson,G. and Meister,B. (1996). Molecular components of the exocytotic machinery in the rat pituitary gland. Endocrinology *137*, 5344-5356.

Jahn,R., Hell,J., and Maycox,P.R. (1990). Synaptic vesicles: key organelles involved in neurotransmission. J. Physiol (Paris) *84*, 128-133.

Jahn,R., Lang,T., and Sudhof,T.C. (2003). Membrane fusion. Cell *112*, 519-533.

Jahn,R. and Sudhof,T.C. (1999). Membrane fusion and exocytosis. Annu. Rev. Biochem. *68*, 863-911.

Janz,R., Goda,Y., Geppert,M., Missler,M., and Sudhof,T.C. (1999). SV2A and SV2B function as redundant Ca2+ regulators in neurotransmitter release. Neuron *24*, 1003-1016.

Janz,R. and Sudhof,T.C. (1999). SV2C is a synaptic vesicle protein with an unusually restricted localization: anatomy of a synaptic vesicle protein family. Neuroscience *94*, 1279-1290.

Jeftinija,S.D., Jeftinija,K.V., and Stefanovic,G. (1997). Cultured astrocytes express proteins involved in vesicular glutamate release. Brain Res. *750*, 41-47.

Jeftinija,S.D., Jeftinija,K.V., Stefanovic,G., and Liu,F. (1996). Neuroligand-evoked calcium-dependent release of excitatory amino acids from cultured astrocytes. J. Neurochem. *66*, 676-684.

Johannes,L., Doussau,F., Clabecq,A., Henry,J.P., Darchen,F., and Poulain,B. (1996). Evidence for a functional link between Rab3 and the SNARE complex. J. Cell Sci. *109 ( Pt 12)*, 2875-2884.

Johannes,L., Lledo,P.M., Roa,M., Vincent,J.D., Henry,J.P., and Darchen,F. (1994). The GTPase Rab3a negatively controls calcium-dependent exocytosis in neuroendocrine cells. EMBO J. *13*, 2029-2037.

Jurgutis,P., Shuang,R., Fletcher,A., and Stuenkel,E.L. (1996). Characterization and distribution of SNARE proteins at neuroendocrine nerve endings. Neuroendocrinology *64*, 379-392.

Kang,J., Jiang,L., Goldman,S.A., and Nedergaard,M. (1998). Astrocyte-mediated potentiation of inhibitory synaptic transmission. Nat. Neurosci. *1*, 683-692.

Kendall,J.M. and Badminton,M.N. (1998). Aequorea victoria bioluminescence moves into an exciting new era. Trends Biotechnol. *16*, 216-224.

Kim,D.K. and Catterall,W.A. (1997). Ca2+-dependent and -independent interactions of the isoforms of the alpha1A subunit of brain Ca2+ channels with presynaptic SNARE proteins. Proc. Natl. Acad. Sci. U. S. A *94*, 14782-14786.

Klinger,M. (1994). Post-embedding immunocytochemistry for adhesive proteins and clathrin in LR White- and LR Gold-embedded human platelets. Anat. Anz. *176*, 67-73.

Klyachko,V.A. and Jackson,M.B. (2002). Capacitance steps and fusion pores of small and large-dense-core vesicles in nerve terminals. Nature *418*, 89-92.

Kramarcy,N.R. and Sealock,R. (1991). Commercial preparations of colloidal gold-antibody complexes frequently contain free active antibody. J. Histochem. Cytochem. *39*, 37-39.

Kretzschmar,S., Volknandt,W., and Zimmermann,H. (1996). Colocalization on the same synaptic vesicles of syntaxin and SNAP-25 with synaptic vesicle proteins: a re-evaluation of functional models required? Neurosci. Res. *26*, 141-148.

Kuromi,H. and Kidokoro,Y. (1998). Two distinct pools of synaptic vesicles in single presynaptic boutons in a temperature-sensitive Drosophila mutant, shibire. Neuron *20*, 917-925.

Landis,D.M., Hall,A.K., Weinstein,L.A., and Reese,T.S. (1988). The organization of cytoplasm at the presynaptic active zone of a central nervous system synapse. Neuron *1*, 201-209.

Latour,I., Hamid,J., Beedle,A.M., Zamponi,G.W., and MacVicar,B.A. (2003). Expression of voltage-gated Ca2+ channel subtypes in cultured astrocytes. Glia *41*, 347-353.

Leenders,A.G., Hengst,P., Lopes da Silva,F.H., and Ghijsen,W.E. (2002). A biochemical approach to study sub-second endogenous release of diverse neurotransmitters from central nerve terminals. J. Neurosci. Methods *113*, 27-36.

Leenders,A.G., Lopes da Silva,F.H., Ghijsen,W.E., and Verhage,M. (2001). Rab3a is involved in transport of synaptic vesicles to the active zone in mouse brain nerve terminals. Mol. Biol. Cell *12*, 3095-3102.

Leenders,A.G., Scholten,G., Wiegant,V.M., Da Silva,F.H., and Ghijsen,W.E. (1999). Activity-dependent neurotransmitter release kinetics: correlation with changes in morphological distributions of small and large vesicles in central nerve terminals. Eur. J. Neurosci. *11*, 4269-4277.

Legendre,P. and Poulain,D.A. (1992). Intrinsic mechanisms involved in the electrophysiological properties of the vasopressin-releasing neurons of the hypothalamus. Prog. Neurobiol. *38*, 1-17.

Leica. Leica EM FCS: Gebrauchsanweisung. 1997. Wien, Austria, Leica Aktiengesellschaft.

Ref Type: Pamphlet

Li,C., Takei,K., Geppert,M., Daniell,L., Stenius,K., Chapman,E.R., Jahn,R., De Camilli,P., and Sudhof,T.C. (1994). Synaptic targeting of rabphilin-3A, a synaptic vesicle Ca2+/phospholipid-binding protein, depends on rab3A/3C. Neuron *13*, 885-898.

Lin,R.C. and Scheller,R.H. (1997). Structural organization of the synaptic exocytosis core complex. Neuron *19*, 1087-1094.

Lin,R.C. and Scheller,R.H. (2000). Mechanisms of synaptic vesicle exocytosis. Annu. Rev. Cell Dev. Biol. *16*, 19-49.

Lindo,L., Iborra,F.J., Azorin,I., Guerri,C., and Renau-Piqueras,J. (1993). Analysis of the endocytic-lysosomal system (vacuolar apparatus) in astrocytes during proliferation and differentiation in primary culture. Int. J. Dev. Biol. *37*, 565-572.

Link,E., Blasi,J., Chapman,E.R., Edelmann,L., Baumeister,A., Binz,T., Yamasaki,S., Niemann,H., and Jahn,R. (1994). Tetanus and botulinal neurotoxins. Tools to understand exocytosis in neurons. Adv. Second Messenger Phosphoprotein Res. *29*, 47-58.

Liou,W., Geuze,H.J., and Slot,J.W. (1996). Improving structural integrity of cryosections for immunogold labeling. Histochem. Cell Biol. *106*, 41-58.

Lledo,P.M., Johannes,L., Vernier,P., Zorec,R., Darchen,F., Vincent,J.D., Henry,J.P., and Mason,W.T. (1994). Rab3 proteins: key players in the control of exocytosis. Trends Neurosci. *17*, 426-432.

Llinas,R., Sugimori,M., and Silver,R.B. (1992). Microdomains of high calcium concentration in a presynaptic terminal. Science *256*, 677-679.

Maienschein,V., Marxen,M., Volknandt,W., and Zimmermann,H. (1999). A plethora of presynaptic proteins associated with ATP-storing organelles in cultured astrocytes. Glia *26*, 233-244.

Margittai,M., Fasshauer,D., Jahn,R., and Langen,R. (2003). The Habc domain and the SNARE core complex are connected by a highly flexible linker. Biochemistry *42*, 4009-4014.

Martin,T.F. (1994). The molecular machinery for fast and slow neurosecretion. Curr. Opin. Neurobiol. *4*, 626-632.

Martin-Moutot,N., Charvin,N., Leveque,C., Sato,K., Nishiki,T., Kozaki,S., Takahashi,M., and Seagar,M. (1996). Interaction of SNARE complexes with P/Q-type calcium channels in rat cerebellar synaptosomes. J. Biol. Chem. *271*, 6567-6570.

Marxen,M., Maienschein,V., Volknandt,W., and Zimmermann,H. (1997). Immunocytochemical localization of synaptic proteins at vesicular organelles in PC12 cells. Neurochem. Res. *22*, 941-950.

Marxen,M., Volknandt,W., and Zimmermann,H. (1999). Endocytic vacuoles formed following a short pulse of K+ -stimulation contain a plethora of presynaptic membrane proteins. Neuroscience *94*, 985-996.

Matteoli,M., Takei,K., Cameron,R., Hurlbut,P., Johnston,P.A., Sudhof,T.C., Jahn,R., and De Camilli,P. (1991). Association of Rab3A with synaptic vesicles at late stages of the secretory pathway. J. Cell Biol. *115*, 625-633.

Matz,M.V., Fradkov,A.F., Labas,Y.A., Savitsky,A.P., Zaraisky,A.G., Markelov,M.L., and Lukyanov,S.A. (1999). Fluorescent proteins from nonbioluminescent Anthozoa species. Nat. Biotechnol. *17*, 969-973.

McKiernan,C.J., Stabila,P.F., and Macara,I.G. (1996). Role of the Rab3A-binding domain in targeting of rabphilin-3A to vesicle membranes of PC12 cells. Mol. Cell Biol. *16*, 4985-4995.

McMahon,H.T., Missler,M., Li,C., and Sudhof,T.C. (1995). Complexins: cytosolic proteins that regulate SNAP receptor function. Cell *83*, 111-119.

McMahon,H.T. and Sudhof,T.C. (1995). Synaptic core complex of synaptobrevin, syntaxin, and SNAP25 forms high affinity alpha-SNAP binding site. J. Biol. Chem. *270*, 2213-2217.

McMahon,H.T., Ushkaryov,Y.A., Edelmann,L., Link,E., Binz,T., Niemann,H., Jahn,R., and Sudhof,T.C. (1993). Cellubrevin is a ubiquitous tetanus-toxin substrate homologous to a putative synaptic vesicle fusion protein. Nature *364*, 346-349.

Meeker,R.B., Swanson,D.J., Greenwood,R.S., and Hayward,J.N. (1991). Ultrastructural distribution of glutamate immunoreactivity within neurosecretory endings and pituicytes of the rat neurohypophysis. Brain Res. *564*, 181-193.

Megias,L., Guerri,C., Fornas,E., Azorin,I., Bendala,E., Sancho-Tello,M., Duran,J.M., Tomas,M., Gomez-Lechon,M.J., and Renau-Piqueras,J. (2000). Endocytosis and transcytosis in growing astrocytes in primary culture. Possible implications in neural development. Int. J. Dev. Biol. *44*, 209-221.

Migheli,A., Attanasio,A., and Schiffer,D. (1992). LR Gold embedding of nervous tissue for immunoelectron microscopy studies. Histochemistry *97*, 413-419.

Mizoguchi,A., Yano,Y., Hamaguchi,H., Yanagida,H., Ide,C., Zahraoui,A., Shirataki,H., Sasaki,T., and Takai,Y. (1994). Localization of Rabphilin-3A on the synaptic vesicle. Biochem. Biophys. Res. Commun. *202*, 1235-1243.

Mochida,S. (2000). Protein-protein interactions in neurotransmitter release. Neurosci. Res. *36*, 175-182.

Mochida,S., Yokoyama,C.T., Kim,D.K., Itoh,K., and Catterall,W.A. (1998). Evidence for a voltage-dependent enhancement of neurotransmitter release mediated via the synaptic protein interaction site of N-type Ca2+ channels. Proc. Natl. Acad. Sci. U. S. A *95*, 14523-14528.

Montecucco,C., Papini,E., and Schiavo,G. (1996). Bacterial protein toxins and cell vesicle trafficking. Experientia *52*, 1026-1032.

Montecucco,C. and Schiavo,G. (1995). Structure and function of tetanus and botulinum neurotoxins. Q. Rev. Biophys. *28*, 423-472.

Morel,N., Taubenblatt,P., Synguelakis,M., and Shiff,G. (1998). A syntaxin-SNAP 25-VAMP complex is formed without docking of synaptic vesicles. J. Physiol Paris *92*, 389-392.

Morgan,A. (1995). Exocytosis. Essays Biochem. *30*, 77-95.

Morris,J.F. and Nordmann,J.J. (1980). Membrane recapture after hormone release from nerve endings in the neural lobe of the rat pituitary gland. Neuroscience *5*, 639-659.

Morris,J.F., Nordmann,J.J., and Dyball,R.E. (1978). Structure-function correlation in mammalian neurosecretion. Int. Rev. Exp. Pathol. *18*, 1-95.

Morris,J.F. and Pow,D.V. (1988). Capturing and quantifying the exocytotic event. J. Exp. Biol. *139*, 81-103.

Nagasawa,J., Douglas,W.W., and Schulz,R.A. (1971). Micropinocytotic origin of coated and smooth microvesicles ("synaptic vesicles") in neurosecretory terminals of posterior pituitary glands demonstrated by incorporation of horseradish peroxidase. Nature *232*, 341-342.

Navone,F., Di Gioia,G., Jahn,R., Browning,M., Greengard,P., and De Camilli,P. (1989). Microvesicles of the neurohypophysis are biochemically related to small synaptic vesicles of presynaptic nerve terminals. J. Cell Biol. *109*, 3425-3433.

Netter,F.H. and Ingram,W.R. (1957). A compilation of Paintings on the Anatomy and Functional Relations of the Hypothalamus. In The CIBA collection of medical illustrations, Supplement to Volume I: Nervous system, E.Oppenheimer, ed. (Iowa, USA: CIBA Pharmaceutical Company), pp. 157-165.

Nielsen,E., Severin,F., Backer,J.M., Hyman,A.A., and Zerial,M. (1999). Rab5 regulates motility of early endosomes on microtubules. Nat. Cell Biol. *1*, 376-382.

Nishiki,T., Nihonmatsu,I., Tsuhara,Y., Kawasaki,M., Sekiguchi,M., Sato,K., Mizoguchi,A., and Takahashi,M. (2001). Distribution of soluble N-ethylmaleimide fusion protein attachment proteins (SNAPs) in the rat nervous system. Neuroscience *107*, 363-371.

Novick,P. and Zerial,M. (1997). The diversity of Rab proteins in vesicle transport. Curr. Opin. Cell Biol. *9*, 496-504.

Obaid,A.L., Flores,R., and Salzberg,B.M. (1989). Calcium channels that are required for secretion from intact nerve terminals of vertebrates are sensitive to omega-conotoxin and relatively insensitive to dihydropyridines. Optical studies with and without voltage-sensitive dyes. J. Gen. Physiol *93*, 715-729.

Oberhauser,A.F., Monck,J.R., Balch,W.E., and Fernandez,J.M. (1992). Exocytotic fusion is activated by Rab3a peptides. Nature *360*, 270-273.

Olkkonen,V.M. and Stenmark,H. (1997). Role of Rab GTPases in membrane traffic. Int. Rev. Cytol. *176*, 1-85.

Otto,H., Hanson,P.I., and Jahn,R. (1997). Assembly and disassembly of a ternary complex of synaptobrevin, syntaxin, and SNAP-25 in the membrane of synaptic vesicles. Proc. Natl. Acad. Sci. U. S. A *94*, 6197-6201.

Pabst,S., Hazzard,J.W., Antonin,W., Sudhof,T.C., Jahn,R., Rizo,J., and Fasshauer,D. (2000). Selective interaction of complexin with the neuronal SNARE complex. Determination of the binding regions. J. Biol. Chem. *275*, 19808-19818.

Pabst,S., Margittai,M., Vainius,D., Langen,R., Jahn,R., and Fasshauer,D. (2002). Rapid and selective binding to the synaptic SNARE complex suggests a modulatory role of complexins in neuroexocytosis. J. Biol. Chem. *277*, 7838-7848.

Pallanck,L., Ordway,R.W., and Ganetzky,B. (1995). A Drosophila NSF mutant. Nature *376*, 25.

Parpura,V., Basarsky,T.A., Liu,F., Jeftinija,K., Jeftinija,S., and Haydon,P.G. (1994). Glutamate-mediated astrocyte-neuron signalling. Nature *369*, 744-747.

Parpura,V., Fang,Y., Basarsky,T., Jahn,R., and Haydon,P.G. (1995a). Expression of synaptobrevin II, cellubrevin and syntaxin but not SNAP-25 in cultured astrocytes. FEBS Lett. *377*, 489-492.

Parpura,V. and Haydon,P.G. (2000). Physiological astrocytic calcium levels stimulate glutamate release to modulate adjacent neurons. Proc. Natl. Acad. Sci. U. S. A *97*, 8629-8634.

Parpura,V., Liu,F., Brethorst,S., Jeftinija,K., Jeftinija,S., and Haydon,P.G. (1995b). Alpha-latrotoxin stimulates glutamate release from cortical astrocytes in cell culture. FEBS Lett. *360*, 266-270.

Passafaro,M., Rosa,P., Sala,C., Clementi,F., and Sher,E. (1996). N-type Ca2+ channels are present in secretory granules and are transiently translocated to the plasma membrane during regulated exocytosis. J. Biol. Chem. *271*, 30096-30104.

Pelham,H.R. (2001). SNAREs and the specificity of membrane fusion. Trends Cell Biol. *11*, 99-101.

Pellegrini,L.L., O'Connor,V., and Betz,H. (1994). Fusion complex formation protects synaptobrevin against proteolysis by tetanus toxin light chain. FEBS Lett. *353*, 319-323.

Pellegrini,L.L., O'Connor,V., Lottspeich,F., and Betz,H. (1995). Clostridial neurotoxins compromise the stability of a low energy SNARE complex mediating NSF activation of synaptic vesicle fusion. EMBO J. *14*, 4705-4713.

Peters,A., Palay,S.L., and Webster,H.D. (1991). The Fine Structure of the Nervous System. Neurons and Their Supporting Cells. (New York: Oxford University Press).

Petrenko,A.G., Perin,M.S., Davletov,B.A., Ushkaryov,Y.A., Geppert,M., and Sudhof,T.C. (1991). Binding of synaptotagmin to the alpha-latrotoxin receptor implicates both in synaptic vesicle exocytosis. Nature *353*, 65-68.

Pfeffer,S.R. (1994). Rab GTPases: master regulators of membrane trafficking. Curr. Opin. Cell Biol. *6*, 522-526.

Pfenninger,K., Akert,K., Moor,H., and Sandri,C. (1972). The fine structure of freeze-fractured presynaptic membranes. J. Neurocytol. *1*, 129-149.

Pfenninger,K., Sandri,C., Akert,K., and Eugster,C.H. (1969). Contribution to the problem of structural organization of the presynaptic area. Brain Res. *12*, 10-18.

Pieribone,V.A., Shupliakov,O., Brodin,L., Hilfiker-Rothenfluh,S., Czernik,A.J., and Greengard,P. (1995). Distinct pools of synaptic vesicles in neurotransmitter release. Nature *375*, 493-497.

Poirier,M.A., Xiao,W., Macosko,J.C., Chan,C., Shin,Y.K., and Bennett,M.K. (1998). The synaptic SNARE complex is a parallel four-stranded helical bundle. Nat. Struct. Biol. *5*, 765-769.

Porter,J.T. and McCarthy,K.D. (1997). Astrocytic neurotransmitter receptors in situ and in vivo. Prog. Neurobiol. *51*, 439-455.

Prasher,D.C. (1995). Using GFP to see the light. Trends Genet. *11*, 320-323.

Pupier,S., Leveque,C., Marqueze,B., Kataoka,M., Takahashi,M., and Seagar,M.J. (1997). Cysteine string proteins associated with secretory granules of the rat neurohypophysis. J. Neurosci. *17*, 2722-2727.

Queiroz,G., Gebicke-Haerter,P.J., Schobert,A., Starke,K., and von,K., I (1997). Release of ATP from cultured rat astrocytes elicited by glutamate receptor activation. Neuroscience *78*, 1203-1208.

Queiroz,G., Meyer,D.K., Meyer,A., Starke,K., and von,K., I (1999). A study of the mechanism of the release of ATP from rat cortical astroglial cells evoked by activation of glutamate receptors. Neuroscience *91*, 1171-1181.

Regnier-Vigouroux,A. and Huttner,W.B. (1993). Biogenesis of small synaptic vesicles and synaptic-like microvesicles. Neurochem. Res. *18*, 59-64.

Rettig,J., Sheng,Z.H., Kim,D.K., Hodson,C.D., Snutch,T.P., and Catterall,W.A. (1996). Isoform-specific interaction of the alpha1A subunits of brain Ca2+ channels with the presynaptic proteins syntaxin and SNAP-25. Proc. Natl. Acad. Sci. U. S. A *93*, 7363-7368.

Reynolds,E.S. (1963). The use of lead citrate at high pH as an electron-opaque stain in electron microscopy. J. Cell Biol. *17*, 208-212.

Richter,K., Langnaese,K., Kreutz,M.R., Olias,G., Zhai,R., Scheich,H., Garner,C.C., and Gundelfinger,E.D. (1999). Presynaptic cytomatrix protein bassoon is localized at both excitatory and inhibitory synapses of rat brain. J. Comp Neurol. *408*, 437-448.

Rizo,J. and Sudhof,T.C. (1998). Mechanics of membrane fusion. Nat. Struct. Biol. *5*, 839-842.

Rizo,J. and Sudhof,T.C. (2002). Snares and Munc18 in synaptic vesicle fusion. Nat. Rev. Neurosci. *3*, 641-653.

Robinson,L.J. and Martin,T.F. (1998). Docking and fusion in neurosecretion. Curr. Opin. Cell Biol. *10*, 483-492.

Rossetto,O., Gorza,L., Schiavo,G., Schiavo,N., Scheller,R.H., and Montecucco,C. (1996). VAMP/synaptobrevin isoforms 1 and 2 are widely and differentially expressed in nonneuronal tissues. J. Cell Biol. *132*, 167-179.

Rossetto,O., Seveso,M., Caccin,P., Schiavo,G., and Montecucco,C. (2001). Tetanus and botulinum neurotoxins: turning bad guys into good by research. Toxicon *39*, 27-41.

Rothman,J.E. (1994a). Intracellular membrane fusion. Adv. Second Messenger Phosphoprotein Res. *29*, 81-96.

Rothman,J.E. (1994b). Mechanisms of intracellular protein transport. Nature *372*, 55-63.

Russell,J.T. (1981). The isolation of purified neurosecretory vesicles from bovine neurohypophysis using isoosmolar density gradients. Anal. Biochem. *113*, 229-238.

Sabatini,B.L. and Regehr,W.G. (1996). Timing of neurotransmission at fast synapses in the mammalian brain. Nature *384*, 170-172.

Sambrook,J., Fritsch,E.F., and Maniatis,T. (1989). Molecular cloning, a laboratory manual., J.Sambrook, E.F.Fritsch, and T.Maniatis, eds. (New York: Cold Spring Harbor Laboratory Press).

Sanmarti-Vila,L., tom,D.S., Richter,K., Altrock,W., Zhang,L., Volknandt,W., Zimmermann,H., Garner,C.C., Gundelfinger,E.D., and Dresbach,T. (2000). Membrane association of presynaptic cytomatrix protein bassoon. Biochem. Biophys. Res. Commun. *275*, 43-46.

Sather,W.A., Tanabe,T., Zhang,J.F., Mori,Y., Adams,M.E., and Tsien,R.W. (1993). Distinctive biophysical and pharmacological properties of class A (BI) calcium channel alpha 1 subunits. Neuron *11*, 291-303.

Schiavo,G., Matteoli,M., and Montecucco,C. (2000). Neurotoxins affecting neuroexocytosis. Physiol Rev. *80*, 717-766.

Schimmoller,F., Simon,I., and Pfeffer,S.R. (1998). Rab GTPases, directors of vesicle docking. J. Biol. Chem. *273*, 22161-22164.

Schivell,A.E., Batchelor,R.H., and Bajjalieh,S.M. (1996). Isoform-specific, calcium-regulated interaction of the synaptic vesicle proteins SV2 and synaptotagmin. J. Biol. Chem. *271*, 27770-27775.

Schluter,O.M., Khvotchev,M.V., Jahn,R., and Sudhof,T.C. (2002). Localization versus function of Rab3 proteins: Evidence for a common regulatory role in controlling fusion. J. Biol. Chem.

Schmidt,A., Hannah,M.J., and Huttner,W.B. (1997). Synaptic-like microvesicles of neuroendocrine cells originate from a novel compartment that is continuous with the plasma membrane and devoid of transferrin receptor. J. Cell Biol. *137*, 445-458.

Schulze,K.L., Broadie,K., Perin,M.S., and Bellen,H.J. (1995). Genetic and electrophysiological studies of Drosophila syntaxin-1A demonstrate its role in nonneuronal secretion and neurotransmission. Cell *80*, 311-320.

Seagar,M., Leveque,C., Charvin,N., Marqueze,B., Martin-Moutot,N., Boudier,J.A., Boudier,J.L., Shoji-Kasai,Y., Sato,K., and Takahashi,M. (1999). Interactions between

proteins implicated in exocytosis and voltage-gated calcium channels. Philos. Trans. R. Soc. Lond B Biol. Sci. *354*, 289-297.

Seagar,M. and Takahashi,M. (1998). Interactions between presynaptic calcium channels and proteins implicated in synaptic vesicle trafficking and exocytosis. J. Bioenerg. Biomembr. *30*, 347-356.

Sheng,Z.H., Rettig,J., Takahashi,M., and Catterall,W.A. (1994). Identification of a syntaxin-binding site on N-type calcium channels. Neuron *13*, 1303-1313.

Sheng,Z.H., Westenbroek,R.E., and Catterall,W.A. (1998). Physical link and functional coupling of presynaptic calcium channels and the synaptic vesicle docking/fusion machinery. J. Bioenerg. Biomembr. *30*, 335-345.

Shi,G., Faundez,V., Roos,J., Dell'Angelica,E.C., and Kelly,R.B. (1998). Neuroendocrine synaptic vesicles are formed in vitro by both clathrin-dependent and clathrin-independent pathways. J. Cell Biol. *143*, 947-955.

Shiff,G. and Morel,N. (1997). Association of syntaxin with SNAP-25 and VAMP (synaptobrevin) during axonal transport. J. Neurosci. Res. *48*, 313-323.

Simons,K. and Zerial,M. (1993). Rab proteins and the road maps for intracellular transport. Neuron *11*, 789-799.

Slot,J.W. and Geuze,H.J. (1981). Sizing of protein A-colloidal gold probes for immunoelectron microscopy. J. Cell Biol. *90*, 533-536.

Slot,J.W., Posthuma,G., Chang,L.Y., Crapo,J.D., and Geuze,H.J. (1989). Quantitative aspects of immunogold labeling in embedded and in nonembedded sections. Am. J. Anat. *185*, 271-281.

Sogaard,M., Tani,K., Ye,R.R., Geromanos,S., Tempst,P., Kirchhausen,T., Rothman,J.E., and Sollner,T. (1994). A rab protein is required for the assembly of SNARE complexes in the docking of transport vesicles. Cell *78*, 937-948.

Sollner,T., Bennett,M.K., Whiteheart,S.W., Scheller,R.H., and Rothman,J.E. (1993a). A protein assembly-disassembly pathway in vitro that may correspond to sequential steps of synaptic vesicle docking, activation, and fusion. Cell *75*, 409-418.

Sollner,T., Whiteheart,S.W., Brunner,M., Erdjument-Bromage,H., Geromanos,S., Tempst,P., and Rothman,J.E. (1993b). SNAP receptors implicated in vesicle targeting and fusion. Nature *362*, 318-324.

Sonnichsen,B., de Renzis,S., Nielsen,E., Rietdorf,J., and Zerial,M. (2000). Distinct membrane domains on endosomes in the recycling pathway visualized by multicolor imaging of Rab4, Rab5, and Rab11. J. Cell Biol. *149*, 901-914.

Soria-Jasso,L.E. and Arias-Montano,J.A. (1996). Histamine H1 receptor activation stimulates [3H]GABA release from human astrocytoma U373 MG cells. Eur. J. Pharmacol. *318*, 185-192.

Stahl,B., Chou,J.H., Li,C., Sudhof,T.C., and Jahn,R. (1996). Rab3 reversibly recruits rabphilin to synaptic vesicles by a mechanism analogous to raf recruitment by ras. EMBO J. *15*, 1799-1809.

Stahl,B., von Mollard,G.F., Walch-Solimena,C., and Jahn,R. (1994). GTP cleavage by the small GTP-binding protein Rab3A is associated with exocytosis of synaptic vesicles induced by alpha-latrotoxin. J. Biol. Chem. *269*, 24770-24776.

Stanley,E.F. (1997). The calcium channel and the organization of the presynaptic transmitter release face. Trends Neurosci. *20*, 404-409.

Stea,A., Tomlinson,W.J., Soong,T.W., Bourinet,E., Dubel,S.J., Vincent,S.R., and Snutch,T.P. (1994). Localization and functional properties of a rat brain alpha 1A calcium channel reflect similarities to neuronal Q- and P-type channels. Proc. Natl. Acad. Sci. U. S. A *91*, 10576-10580.

Stenmark,H., Parton,R.G., Steele-Mortimer,O., Lutcke,A., Gruenberg,J., and Zerial,M. (1994). Inhibition of rab5 GTPase activity stimulates membrane fusion in endocytosis. EMBO J. *13*, 1287-1296.

Storm-Mathisen,J., Leknes,A.K., Bore,A.T., Vaaland,J.L., Edminson,P., Haug,F.M., and Ottersen,O.P. (1983). First visualization of glutamate and GABA in neurones by immunocytochemistry. Nature *301*, 517-520.

Sudhof,T.C. (1995). The synaptic vesicle cycle: a cascade of protein-protein interactions. Nature *375*, 645-653.

Sun,X.J., Tolbert,L.P., and Hildebrand,J.G. (1995). Using laser scanning confocal microscopy as a guide for electron microscopic study: a simple method for correlation of light and electron microscopy. J. Histochem. Cytochem. *43*, 329-335.

Sutton,R.B., Fasshauer,D., Jahn,R., and Brunger,A.T. (1998). Crystal structure of a SNARE complex involved in synaptic exocytosis at 2.4 A resolution. Nature *395*, 347-353.

Tagaya,M., Genma,T., Yamamoto,A., Kozaki,S., and Mizushima,S. (1996). SNAP-25 is present on chromaffin granules and acts as a SNAP receptor. FEBS Lett. *394*, 83-86.

Tagaya,M., Toyonaga,S., Takahashi,M., Yamamoto,A., Fujiwara,T., Akagawa,K., Moriyama,Y., and Mizushima,S. (1995). Syntaxin 1 (HPC-1) is associated with chromaffin granules. J. Biol. Chem. *270*, 15930-15933.

Takahashi,T. and Momiyama,A. (1993). Different types of calcium channels mediate central synaptic transmission. Nature *366*, 156-158.

Takei,K., Mundigl,O., Daniell,L., and De Camilli,P. (1996). The synaptic vesicle cycle: a single vesicle budding step involving clathrin and dynamin. J. Cell Biol. *133*, 1237-1250.

Takizawa,T. and Robinson,J.M. (1994). Use of 1.4-nm immunogold particles for immunocytochemistry on ultra-thin cryosections. J. Histochem. Cytochem. *42*, 1615-1623.

Tanner,V.A., Ploug,T., and Tao-Cheng,J.H. (1996). Subcellular localization of SV2 and other secretory vesicle components in PC12 cells by an efficient method of preembedding EM immunocytochemistry for cell cultures. J. Histochem. Cytochem. *44*, 1481-1488.

Tao-Cheng,J.H., Du,J., and McBain,C.J. (2000). Snap-25 is polarized to axons and abundant along the axolemma: an immunogold study of intact neurons. J. Neurocytol. *29*, 67-77.

Taubenblatt,P., Dedieu,J.C., Gulik-Krzywicki,T., and Morel,N. (1999). VAMP (synaptobrevin) is present in the plasma membrane of nerve terminals. J. Cell Sci. *112 ( Pt 20)*, 3559-3567.

Thomas,P., Wong,J.G., Lee,A.K., and Almers,W. (1993). A low affinity Ca2+ receptor controls the final steps in peptide secretion from pituitary melanotrophs. Neuron *11*, 93-104.

Thorpe,J.R. (1999). The application of LR gold resin for immunogold labeling. Methods Mol. Biol. *117*, 99-110.

Thureson-Klein,A., Klein,R.L., and Zhu,P.C. (1986). Exocytosis from large dense cored vesicles as a mechanism for neuropeptide release in the peripheral and central nervous system. Scan Electron Microsc. 179-187.

Thureson-Klein,A.K. and Klein,R.L. (1990). Exocytosis from neuronal large dense-cored vesicles. Int. Rev. Cytol. *121*, 67-126.

Tokuyasu,K.T. (1973). A technique for ultracryotomy of cell suspensions and tissues. J. Cell Biol. *57*, 551-565.

Tokuyasu,K.T. (1980). Immunochemistry on ultrathin frozen sections. Histochem. J. *12*, 381-403.

Tokuyasu,K.T. (1989). Use of poly(vinylpyrrolidone) and poly(vinyl alcohol) for cryoultramicrotomy. Histochem. J. *21*, 163-171.

Tokuyasu,K.T. and Singer,S.J. (1976). Improved procedures for immunoferritin labeling of ultrathin frozen sections. J. Cell Biol. *71*, 894-906.

tom,D.S., Sanmarti-Vila,L., Langnaese,K., Richter,K., Kindler,S., Soyke,A., Wex,H., Smalla,K.H., Kampf,U., Franzer,J.T., Stumm,M., Garner,C.C., and Gundelfinger,E.D. (1998). Bassoon, a novel zinc-finger CAG/glutamine-repeat protein selectively localized at the active zone of presynaptic nerve terminals. J. Cell Biol. *142*, 499-509.

Toonen,R.F. and Verhage,M. (2003). Vesicle trafficking: pleasure and pain from SM genes. Trends Cell Biol. *13*, 177-186.

Trimble,W.S., Linial,M., and Scheller,R.H. (1991). Cellular and molecular biology of the presynaptic nerve terminal. Annu. Rev. Neurosci. *14*, 93-122.

Trischler,M., Stoorvogel,W., and Ullrich,O. (1999). Biochemical analysis of distinct Rab5- and Rab11-positive endosomes along the transferrin pathway. J. Cell Sci. *112 ( Pt 24)*, 4773-4783.

Tsujimoto,S. and Bean,A.J. (2000). Distinct protein domains are responsible for the interaction of Hrs-2 with SNAP-25. The role of Hrs-2 in 7 S complex formation. J. Biol. Chem. *275*, 2938-2942.

Turner,T.J., Adams,M.E., and Dunlap,K. (1993). Multiple Ca2+ channel types coexist to regulate synaptosomal neurotransmitter release. Proc. Natl. Acad. Sci. U. S. A *90*, 9518-9522.

Tweedle,C.D. (1983). Ultrastructural manifestations of increased hormone release in the neurohypophysis. Prog. Brain Res. *60*, 259-272.

Tweedle,C.D. and Hatton,G.I. (1982). Magnocellular neuropeptidergic terminals in neurohypophysis: rapid glial release of enclosed axons during parturition. Brain Res. Bull. *8*, 205-209.

Ullrich,O., Stenmark,H., Alexandrov,K., Huber,L.A., Kaibuchi,K., Sasaki,T., Takai,Y., and Zerial,M. (1993). Rab GDP dissociation inhibitor as a general regulator for the membrane association of rab proteins. J. Biol. Chem. *268*, 18143-18150.

Van Leeuwen,F.W., Pool,C.W., and Sluiter,A.A. (1983). Enkephalin immunoreactivity in synaptoid elements on glial cells in the rat neural lobe. Neuroscience *8*, 229-241.

Van Leeuwen,F.W. and Swaab,D.F. (1977). Specific immunoelectronmicroscopic localization of vasopressin and oxytocin in the neurohypophysis of the rat. Cell Tissue Res. *177*, 493-501.

Vandre,D.D. and Burry,R.W. (1992). Immunoelectron microscopic localization of phosphoproteins associated with the mitotic spindle. J. Histochem. Cytochem. *40*, 1837-1847.

Verderio,C., Coco,S., Rossetto,O., Montecucco,C., and Matteoli,M. (1999). Internalization and proteolytic action of botulinum toxins in CNS neurons and astrocytes. J. Neurochem. *73*, 372-379.

Verhage,M., McMahon,H.T., Ghijsen,W.E., Boomsma,F., Scholten,G., Wiegant,V.M., and Nicholls,D.G. (1991). Differential release of amino acids, neuropeptides, and catecholamines from isolated nerve terminals. Neuron *6*, 517-524.

Vesce,S., Bezzi,P., and Volterra,A. (1999). The active role of astrocytes in synaptic transmission. Cell Mol. Life Sci. *56*, 991-1000.

Volknandt,W. (1995). The synaptic vesicle and its targets. Neuroscience *64*, 277-300.

Volknandt,W. (2002). Vesicular release mechanisms in astrocytic signalling. Neurochem. Int. *41*, 301.

Volknandt,W., Kuster,F., Wilhelm,A., Obermuller,E., Steinmann,A., Zhang,L., and Zimmermann,H. (2002). Expression and allocation of proteins of the exo-endocytotic machinery in U373 glioma cells: similarities to long-term cultured astrocytes. Cell Mol. Neurobiol. *22*, 153-169.

Walch-Solimena,C., Blasi,J., Edelmann,L., Chapman,E.R., von Mollard,G.F., and Jahn,R. (1995). The t-SNAREs syntaxin 1 and SNAP-25 are present on organelles that participate in synaptic vesicle recycling. J. Cell Biol. *128*, 637-645.

Walch-Solimena,C., Takei,K., Marek,K.L., Midyett,K., Sudhof,T.C., De Camilli,P., and Jahn,R. (1993). Synaptotagmin: a membrane constituent of neuropeptide-containing large dense-core vesicles. J. Neurosci. *13*, 3895-3903.

Wang,G., Dayanithi,G., Kim,S., Hom,D., Nadasdi,L., Kristipati,R., Ramachandran,J., Stuenkel,E.L., Nordmann,J.J., Newcomb,R., and Lemos,J.R. (1997a). Role of Q-type Ca2+ channels in vasopressin secretion from neurohypophysial terminals of the rat. J. Physiol *502 ( Pt 2)*, 351-363.

Wang,G., Dayanithi,G., Newcomb,R., and Lemos,J.R. (1999). An R-type Ca(2+) current in neurohypophysial terminals preferentially regulates oxytocin secretion. J. Neurosci. *19*, 9235-9241.

Wang,X., Treistman,S.N., and Lemos,J.R. (1993). Single channel recordings of Nt- and L-type Ca2+ currents in rat neurohypophysial terminals. J. Neurophysiol. *70*, 1617-1628.

Wang,Y., Okamoto,M., Schmitz,F., Hofmann,K., and Sudhof,T.C. (1997b). Rim is a putative Rab3 effector in regulating synaptic-vesicle fusion. Nature *388*, 593-598.

Weber,E., Jilling,T., and Kirk,K.L. (1996). Distinct functional properties of Rab3A and Rab3B in PC12 neuroendocrine cells. J. Biol. Chem. *271*, 6963-6971.

Westenbroek,R.E., Sakurai,T., Elliott,E.M., Hell,J.W., Starr,T.V., Snutch,T.P., and Catterall,W.A. (1995). Immunochemical identification and subcellular distribution of the alpha 1A subunits of brain calcium channels. J. Neurosci. *15*, 6403-6418.

Woppmann,A., Ramachandran,J., and Miljanich,G.P. (1994). Calcium channel subtypes in rat brain: biochemical characterization of the high-affinity receptors for omega-conopeptides SNX-230 (synthetic MVIIC), SNX-183 (SVIB), and SNX-111 (MVIIA). Mol. Cell Neurosci. *5*, 350-357.

Wucherpfennig,T., Wilsch-Brauninger,M., and Gonzalez-Gaitan,M. (2003). Role of Drosophila Rab5 during endosomal trafficking at the synapse and evoked neurotransmitter release. J. Cell Biol. *161*, 609-624.

Xu,T. and Bajjalieh,S.M. (2001). SV2 modulates the size of the readily releasable pool of secretory vesicles. Nat. Cell Biol. *3*, 691-698.

Yamasaki,S., Baumeister,A., Binz,T., Blasi,J., Link,E., Cornille,F., Roques,B., Fykse,E.M., Sudhof,T.C., Jahn,R., and . (1994). Cleavage of members of the synaptobrevin/VAMP family by types D and F botulinal neurotoxins and tetanus toxin. J. Biol. Chem. *269*, 12764-12772.

Yang,B., Gonzalez,L., Jr., Prekeris,R., Steegmaier,M., Advani,R.J., and Scheller,R.H. (1999). SNARE interactions are not selective. Implications for membrane fusion specificity. J. Biol. Chem. *274*, 5649-5653.

Yang,B., Steegmaier,M., Gonzalez,L.C., Jr., and Scheller,R.H. (2000). nSec1 binds a closed conformation of syntaxin1A. J. Cell Biol. *148*, 247-252.

Ye,Z.C. and Sontheimer,H. (1999). Glioma cells release excitotoxic concentrations of glutamate. Cancer Res. *59*, 4383-4391.

Zerial,M. and McBride,H. (2001). Rab proteins as membrane organizers. Nat. Rev. Mol. Cell Biol. *2*, 107-117.

Zhai,R.G., Vardinon-Friedman,H., Cases-Langhoff,C., Becker,B., Gundelfinger,E.D., Ziv,N.E., and Garner,C.C. (2001). Assembling the presynaptic active zone: a characterization of an active one precursor vesicle. Neuron *29*, 131-143.

Zhang,L., Volknandt,W., Gundelfinger,E.D., and Zimmermann,H. (2000). A comparison of synaptic protein localization in hippocampal mossy fiber terminals and neurosecretory endings of the neurohypophysis using the cryo-immunogold technique. J. Neurocytol. *29*, 19-30.

Zheng,X. and Bobich,J.A. (1998). A sequential view of neurotransmitter release. Brain Res. Bull. *47*, 117-128.

Zhu,P.C., Thureson-Klein,A., and Klein,R.L. (1986). Exocytosis from large dense cored vesicles outside the active synaptic zones of terminals within the trigeminal subnucleus caudalis: a possible mechanism for neuropeptide release. Neuroscience *19*, 43-54.

Zimmermann,H. (1990). Neurotransmitter release. FEBS Lett. *268*, 394-399.

Zimmermann,H. (1993). Synaptic Transmission. Cellular and Molecular Basis., H.Zimmermann, ed. Stuttgart, New York: Thieme/Oxford).

Zimmermann,H. (1997). Are mechanisms of exocytosis neurotransmitter specific? Neurochem. Int. *31*, 759-761.

# List of publications

Zhang,L., Volknandt,W., Gundelfinger,E.D., and Zimmermann,H. (2000). A comparison of synaptic protein localization in hippocampal mossy fiber terminals and neurosecretory endings of the neurohypophysis using the cryo-immunogold technique. J. Neurocytol. *29*, 19-30.

Sanmarti-Vila,L., tom,D.S., Richter,K., Altrock,W., Zhang,L., Volknandt,W., Zimmermann,H., Garner,C.C., Gundelfinger,E.D., and Dresbach,T. (2000). Membrane association of presynaptic cytomatrix protein bassoon. Biochem. Biophys. Res. Commun. *275*, 43-46.

Volknandt,W., Kuster,F., Wilhelm,A., Obermuller,E., Steinmann,A., Zhang,L., and Zimmermann,H. (2002). Expression and allocation of proteins of the exo-endocytotic machinery in U373 glioma cells: similarities to long-term cultured astrocytes. Cell Mol. Neurobiol. *22*, 153-169.

Volknandt,W., Wilhelm,A., Obermüller,E., Steinmann,A., Zhang,L., Zimmermann,H. (2000). Expression and subcellular localization of SNARE proteins in astrocytoma cells. Biol. Chem. *381*, Suppl., pS98.

Volknandt,W., Zhang,L., Gundelfinger,E.D., Zimmermann,H. (2000). Localization of synaptic proteins in hippocampal mossy fiber terminals and neurosecretory endings of the neurohypophysis using the cryo-immunogold technique. Eur. J. Neurosci. *12*, suppl. 11, 165.12.

Volknandt,W., Wilhelm,A., Zhang,L., Küster,F., Zimmermann,H. (2001). Synaptic proteins in cultured astrocytes. J. Neurochem. *78*, Suppl. 1. p24, AP10-12.

Volknandt,W., Wilhelm,A., Zhang,L., Küster,F., Zimmermann,H. (2001). Do astrocytes have a vesicular release mechanism? In: The Neurosciences at the Turn of the Century (N. Elsner and G. W. Kreutzber, eds.) Thieme, Stuttgart, New York, 282.

Volknandt,W., Wilhelm,A., Zhang,L., Küster,F., Zimmermann,H. (2001). Do astrocytes have a vesicular release mechanism? In: The Neurosciences at the Turn of the Century (N. Elsner and G. W. Kreutzber, eds.) Thieme, Stuttgart, New York, vol. I, 290.

# *Curriculum vitae*

**Name:** Lixia ZHANG
**Date of Birth:** August 9, 1963
**Place of Birth:** Neimenggu, P. R. China
**Nationality:** Chinese
**Family Status:** Married, with two children

**Education:**

| | |
|---|---|
| 1970-1976 | Primary school in Qingdao, P. R. China |
| 1976-1981 | Middle school in Qingdao, P. R. China |
| 1981-1985 | Undergraduate studies in Qingdao Ocean University, P. R. China<br>Major: Biology<br>Thesis: "Determination of auditory threshold of Pacific herring *Clupea pallasi* " |
| July 1985 | Awarded **"Bachelor of Science"** |
| 1987-1990 | Postgraduate studies in Qingdao Ocean University<br>Major: Hydrobiology<br>Thesis: "Morphology and development of a new species *Eoleptestheria sangziensis* sp. nov. (Crustacea: Conchostraca, Leptestheriidae)" |
| July 1990 | Awarded **"Master of Science"** |
| Since 1998 | Promotion at the Department of Neurochemistry, Institute of Zoology, Biological and Computer Science Division of J. W. Goethe University, Frankfurt am Main, Germany, under the guidance of Prof. Dr. H. Zimmermann. |

**working experience:**

| | |
|---|---|
| 1985-1991 | Assistant at the Department of Aquaculture of Qingdao Ocean University, P. R. China. |

**Other experience:**

| | |
|---|---|
| 1991-1992 | Living in Helgoland, Germany. |
| 1993-1994 | Taking German courses in Bonn University, Germany. |
| 1994-1997 | Upbringing of my daughter in Bonn. |
| 1997 | Practical training in Institute of Zoophysiology of Bonn University under the guidance of Prof. Dr. H. Dircksen. |

## Declaration

Hierwith I declare that I have prepared and written this dissertation on my own without using any other aids and sources than those I have mentioned in the text.

(Lixia Zhang)